Unraveling of the major genetic defects in prostate cancer

Karin Hermans

The studies described in this thesis were performed at the Department of Pathology of the Josephine Nefkens Institute, Erasmus MC, Rotterdam, The Netherlands

Layout and printing by Optima Grafische Communicatie, Rotterdam

Publication of this thesis was financially supported by the Department of Pathology of the Erasmus MC, Novartis, and the Erasmus University Rotterdam

Cover: 3D culture of immortalized benign prostate epithelial cells (PNT2C2) infected with lentivirus expressing green fluorescent protein.

© 2008 K.G.L. Hermans
No part of this thesis may be reproduced, stored in a retrieval system or transmitted in any form or by means, electronical,mechanical, photocopying, recording or otherwise, without written permission of the author. Several chapters are based on published papers, which were reproduced with permission of the co-authors. Copyright of these papers remains with the publisher.

Unraveling of the major genetic defects in prostate cancer

Ontrafelen van de meest belangrijke genetische defecten in prostaatkanker

Proefschrift

Ter verkrijging van de graad van doctor aan de
Erasmus Universiteit Rotterdam
op gezag van de rector magnificus
Prof. Dr. S.W.J. Lamberts
en volgens besluit van het College voor Promoties

De openbare verdediging zal plaatsvinden op
woensdag 28 januari 2009
om 11.45 uur

door

Karin Gertruda Louisa Hermans

Geboren te Boxmeer

PROMOTIECOMMISSIE

Promotor:

Prof.dr.ir. J. Trapman

Overige leden:

Dr.ir. G. Jenster
Prof.dr. A. Geurts van Kessel
Prof.dr. J.W. Oosterhuis

Contents

List of abbreviations		6
Chapter 1	General introduction	7
Chapter 2	Array-based comparative genomic hybridization guides identification of *N-COR* as a novel tumor suppressor gene in prostate cancer	33
Chapter 3	Loss of a small region around the PTEN locus is a major chromosome 10 alteration in prostate cancer xenografts and cell lines	59
Chapter 4	TMPRSS2:ERG fusion by translocation or interstitial deletion is highly relevant in androgen-dependent prostate cancer, but is bypassed in late stage androgen receptor negative prostate cancer	83
Chapter 5	Overexpression of prostate-specific TMPRSS2(exon 0)-ERG fusion transcripts corresponds with favorable prognosis of prostate cancer	99
Chapter 6	Two unique prostate-specific and androgen-regulated fusion partners of ETV4 in prostate cancer	115
Chapter 7	Truncated ETV1, fused to novel tissue-specific genes, and full length ETV1 in prostate cancer	129
Chapter 8	General discussion	153
Summary		167
Samenvatting		169
Curriculum Vitae		171
List of publications		173
Dankwoord		175

List of abbreviations

AR	androgen receptor
BAC	bacterial artificial chromosome
BPH	benign prostatic hyperplasia
CANT1	calcium activated nucleotidase 1
CGH	comparative genomic hybridization
COPA	cancer outlier profile analysis
DHT	dihydrotestosterone
ERG	ETS Related Gene
ETS	E26 Transforming Sequence
ETV1	ETS variant gene 1
ETV4	ETS variant gene 4
ETV5	ETS variant gene 5
EST	expressed sequence tag
FISH	fluorescent *in situ* hybridization
FOXA1	forkhead box A1
FOXP1	forkhead box P1
GFP	green fluorescent protein
HD	homozygous deletion
HERV	human endogenous retrovirus
KLK2	kallikrein 2
LOH	loss of heterozygosity
LTR	long terminal repeat
MIPOL1	miror-image polydactyly 1
MKK4	mitogen-activated protein kinase kinase 4
MMP	matrix metalloproteinase
N-COR	nuclear corepressor
NP	normal prostate
PBGD	porphobilinogen deaminase
PCR	polymerase chain reaction
PI3K	phosphatidylinositol 3-kinase
PIN	prostate inter-epithelial neoplasia
PTEN	phosphatase and tensin homologue deleted on chromosome 10
PSA	prostate specific antigen
QPCR	quantitative polymerase chain reaction
RLM-RACE	RNA ligase mediated rapid amplification of cDNA ends
RP	radical prostatectomy
RT-PCR	reverse transcriptase polymerase chain reaction
TAD	transactivation domain
TMPRSS2	transmembrane protease, serine 2
TURP	transuretheral resection of the prostate
siRNA	small interfering RNA
SNP	single nucleotide polymorphism

Chapter 1

General Introduction

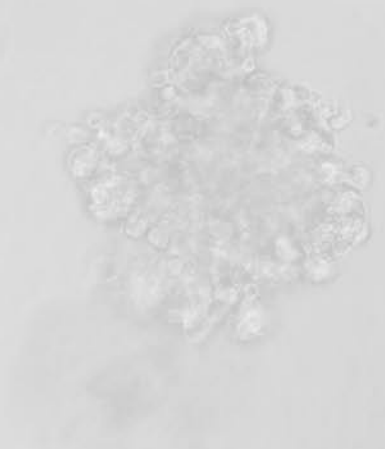

PROSTATE CANCER

In developed countries, prostate cancer is the most common malignancy in men and a major cause of cancer-related death (1). In The Netherlands 93 new cases per 100,000 men were detected in 2003 (The Netherlands Cancer Registry). Prostate cancer incidence varies between different ethnic groups. African-American men have the highest incidence rates, followed by Caucasian-American men and men in Western Europe and Australia. The lowest incidence rates are observed in the Asian population. These differences may be explained by environmental and dietary factors. However, genetic factors, i.e. polymorphisms in genes that can predispose to cancer, may also play a role in prostate cancer development. A major risk factor of prostate cancer is age, since it is predominantly a disease of the senior adult (i.e. men over the age of 65 years). Below the age of 55 the incidence of prostate cancer is very low (2, 3).

During recent years our knowledge of the molecular mechanism underlying prostate cancer development and progression has rapidly increased. However, there are still many gaps in our knowledge that remain to be filled. Genetic analyses of different stages of prostate cancer will increase our knowledge of the molecular background of the development and progression of prostate cancer. The identification of novel biomarkers will help to predict the clinical course of the disease. Furthermore, a better understanding of the molecular mechanism of prostate tumorigenesis is essential for development of novel targeted therapies.

Androgen signalling mediated by the androgen receptor (AR) is essential for development and maintenance of the normal prostate (4). The majority of prostate cancers also depend on a functional AR. The AR is a member of the steroid hormone receptor transcription factor family. It is activated by binding of androgens (testosterone or dihydrotestosterone (DHT)). The AR regulates the transcription of many target genes by binding to androgen response elements in the promoter or enhancer regions. The AR recruits specific cofactors to either activate or repress a specific target gene. In the normal prostate there is a balance of expression of androgen-regulated genes involved in differentiation, proliferation, function and survival. This balance is moved towards proliferation and survival in prostate cancer cells (Figure 1).

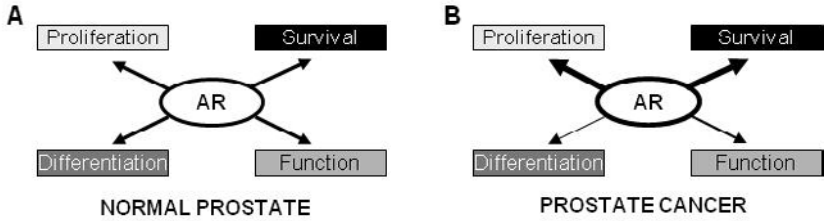

Figure 1. Model of androgen receptor function in the normal adult prostate (A) and in prostate cancer (B)

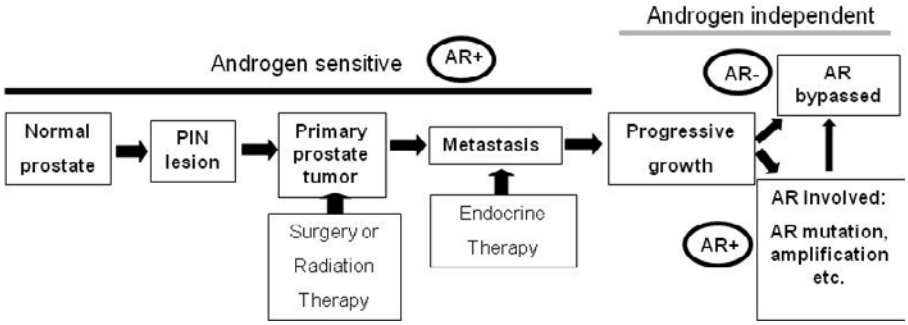

Figure 2. Overview of prostate cancer development and progression.

A well-known androgen-regulated and prostate-specific gene is Prostate Specific Antigen (*PSA*). The PSA protein is secreted by the prostate. In prostate cancer patients PSA levels can be measured in serum. Elevated serum PSA levels are a first indication of prostate cancer, however, elevated PSA might also be caused by benign prostatic hyperplasia (BPH) or prostatitis. Introduction of the PSA test in the 1980's has increased prostate cancer incidence considerably. However, a proportion of the detected cancers will never become life threatening. Consecutive procedures currently used for prostate cancer diagnosis include: serum PSA detection, digital rectal examination, transrectal ultrasonography and histopathological examination of biopsy specimens (5). The histological grade, the tumour stage and PSA level at diagnosis are used to predict prostate cancer progression. Yet, at present, it is impossible to accurately discriminate between patients with clinically significant and more indolent disease (6).

In Figure 2, a schematic representation of the different stages of prostate cancer development and progression is depicted. Prostatic intra-epithelial neoplasia (PIN) is considered to represent the precursor lesion of prostate cancer, because similar genetic alterations are found both in PIN and in primary prostate cancer.

Tumours confined to the prostate can either be treated by surgical removal of the prostate or by local radiation therapy. A third option is active surveillance, i.e. a patient is not treated, but instead is closely monitored for disease progression. Because the AR plays a critical role in overall function of the normal prostate as well as in growth and survival of malignant prostate cells, primary therapy of metastatic disease is androgen-deprivation (endocrine therapy). This therapy is based on inhibition of AR transcriptional activity, by either inhibiting androgen production or by blocking AR function with anti-androgens, such as hydroxy-flutamide or bicalutamide. Initially endocrine therapy results in regression of the tumour. However, eventually all tumours become resistant to hormonal ablation therapy and progress to androgen-independent disease. In most (> 80%) hormone refractory tumours the AR is still expressed and still plays a role in the disease (7). In

part of these tumours the *AR* gene is amplified and the protein over expressed (8). In a small percentage the AR is mutated (9), turning antagonists into agonists. Other factors that may contribute to an active AR in endocrine resistant prostate cancers are over expression of cofactors or inhibition of corepressors (10). Recently, evidence has been provided that expression of enzymes that convert adrenal androgens to DHT or even synthesize DHT from cholesterol, is induced in prostate cancer (11). In a small proportion of prostate cancers the AR is bypassed (7). In these tumours other pathways have taken over the function of the AR pathway. Currently, there are no curative therapies for endocrine therapy resistant disease.

PROSTATE CANCER GENETICS

It is generally accepted that tumours develop from a single cell that acquires a genetic or epigenetic alteration, however, the process from a normal cell to a cancer cell involves a multi-step model, which is driven by the accumulation of genetic and epigenetic changes (12).

Like in many other tumours, a small proportion (5-10%) of prostate cancer is thought to be of hereditary origin (13, 14). Hereditary prostate cancer is associated with an early onset (younger than 55 years) of the disease and family history of prostate cancer prevalence. For identifying genes involved in hereditary cancer high-throughput genotyping techniques and linkage analysis of cancer-prone families are being used to fine map the location of familial cancer genes.

Genome-wide linkage analyses of prostate cancer families have implicated many loci, however, no definitive gene that causes a significant proportion of the familial prostate cancers has been identified. Identified susceptibility loci, which are associated with hereditary prostate cancer are: hereditary prostate cancer 1 (HPC1) on chromosome 1q24-q25 (15), predisposing to prostate cancer (PCaP) on chromosome 1q42.2-q43 (16), CAPB on chromosome 1p36 (17), a locus on chromosome 8p22-23 (18), HPC2 on chromosome 17p11 (19), HPC20 on chromosome 20q13 (20), and HPCX on chromosome Xq27-q28 (21). For these loci only a few candidate genes have been identified so far. Ribonuclease L (*RNASEL*) has been identified as the candidate gene of the HPC1 locus (22). *RNASEL* mediates the antiviral and apoptotic activities of interferons. Inactivating mutations have been detected in a few prostate cancer families. For the HPC2 locus *ELAC2* has been identified as the candidate gene (19). In two families mutations affecting the coding region have been detected.

More recently, genome-wide SNP association studies of individuals with familial prostate cancer and a study on 23,000 Icelanders identified multiple prostate cancer susceptibility loci. These loci include regions on chromosome 8q24, 2p15, Xp11.22 and

17q (23-25). Proposed susceptibility genes, based on genetic variations, are *MSR1* (26), *BRCA2* (27, 28), *PALB2* (29), *CHEK2* (30), and more recently *HNF1B*, *CTBP2*, *MSMB*, *LMTK2* and *JAZF1* (23, 25). So, to date multiple loci and genes with moderate effects associated with susceptibility to prostate cancer have been identified, but none account for a large proportion of susceptibility to the disease.

A standard genetic strategy to identify novel tumour suppressor genes and oncogenes involved in sporadic tumours starts with a genome-wide screen of tumour samples for DNA loss (possible location of a tumour suppressor gene) or DNA gain (possible location of an oncogene). Next, the genes in the lost or gained chromosomal regions are identified. This is followed by mRNA expression analysis, mutation analysis of candidate genes and functional analysis of selected candidate gene(s).

Molecular techniques used to identify genome-wide genomic alterations over the last decades are: karyotyping, multicolour spectral karyotyping (SKY), allelotype analysis, fluorescence *in situ* hybridisation (FISH), chromosome comparative genomic hybridisation (CGH), and more recently genome-wide array CGH.

A powerful tool for detailed genome-wide screening is CGH. In CGH, labelled tumour and reference (normal) DNAs are hybridised to normal human metaphase chromosomes to detect DNA gains and losses (31). The resolution of chromosome CGH is limited (~5-10 Mbp) therefore more sophisticated hybridisation targets have been developed (32). DNA sequences (BACs, oligonucleotides or oligonucleotides containing SNPs) are spotted in an array on slides to which the labelled tumour and/or reference DNA can be hybridised (array CGH). Depending on the distance between the DNA sequences a very high resolution can be obtained. Other advantages of this technique are that it maps losses and gains more precisely and homozygous deletions and high level amplifications can be identified (33, 34). Oligo arrays containing SNPs have an extra advantage in that they also provide allelotypic information. These SNP arrays are nowadays used to identify detailed genome-wide genetic alterations in tumour samples (35, 36).

Genome-wide search for chromosomal alterations in sporadic prostate cancer resulted in the identification of several common regions of DNA loss or DNA gain. In sporadic prostate cancer most frequent regions of DNA loss are part of chromosome arm 6q, 8p, 13q and 16q, and less frequently lost regions are 2q, 5q, 10q, 17p, and 18q. Most frequent regions of DNA gain are on chromosomes 7 and 8q, less frequently gained regions involve: 3q, 17q and Xq (37, 38). However, no clear classical tumour suppressor genes or oncogenes have been identified to date for most of these regions. A small region of loss is frequently found on chromosome 10q23 (see also Chapters 2 and 3). In this region the tumour suppressor gene *PTEN* (39, 40) is located, which will be described in more detail in the next section. Furthermore, we identified *N-COR* as a novel tumour suppressor gene located on chromosome 17p (Chapter 2). More recently, a small region of loss on

chromosome 21q was described. This interstitial deletion results in the recurrent gene fusion of *TMPRSS2* to *ERG* (41), which will be described in more detail below.

PTEN IN CANCER

Germ line mutations of *PTEN* are found in Cowden syndrome, Lhermitte-Duclos disease and Bannayan-Zonana syndrome (42, 43). These rare diseases are autosomal dominant, familial cancer predisposition syndromes. They are characterized by multiple hamartomas and predisposition to neoplasms of thyroid, breast and skin.

PTEN is most frequently inactivated in several sporadic human cancers including, gliobastomas, endometrial cancer, and prostate cancer, either by mutation, homozygous deletion or promoter methylation (44, 45).

Loss of one *PTEN* allele without inactivation of the second allele is also found in prostate cancer. This suggests that *PTEN* haplo-insufficiency plays a role in tumorigenesis. Loss of *PTEN* is detected, in 39-68% of primary prostate cancer samples and in 23% of PIN lesions (46, 47). Loss of one copy of the 10q region, where *PTEN* maps, might also be explained by the presence of a second tumour suppressor gene located nearby *PTEN*. We have screened 14 genes mapping in a ~3 Mbp region around *PTEN* for mRNA expression alterations in prostate cancer xenografts and cell lines (Chapter 3) (48).

The frequency of complete *PTEN* inactivation reported in clinical prostate cancer is highly variable (49-55). This might partially be due to the different techniques used to detect complete inactivation of *PTEN* and to the different stages of disease analysed. The major mechanism of complete *PTEN* inactivation is by homozygous deletion. Most common point mutations produce a premature stop codon. Other frequent mutations are point mutations in the active site of the phosphatase domain of PTEN. Complete inactivation of *PTEN* is most often detected in metastatic prostate cancer, up to 60%, and less frequently in primary tumours, in ~15%. In prostate cancer *PTEN* is the most frequently mutated tumour suppressor gene found to date.

Function of PTEN

PTEN consists of nine exons encoding a 403 amino acid protein that functions as a lipid phosphatase and as a dual specific protein phosphatase. PTEN is a negative regulator of the phosphatidylinositol 3-kinase (PI3K)/AKT pathway, by dephosphorylating phosphatidylinositol (3,4,5)-trisphosphate (PIP3). In this way PTEN counteracts PI3K (Figure 3). The PI3K/AKT pathway regulates signalling of multiple biological processes including cell survival, cell proliferation, cell growth, metabolism and migration. Activation of the PI3K/AKT pathway results in phosphorylation of AKT. AKT on its turn phosphorylates many substrates, including the pro-apoptotic proteins BAD and caspase-9, forkhead

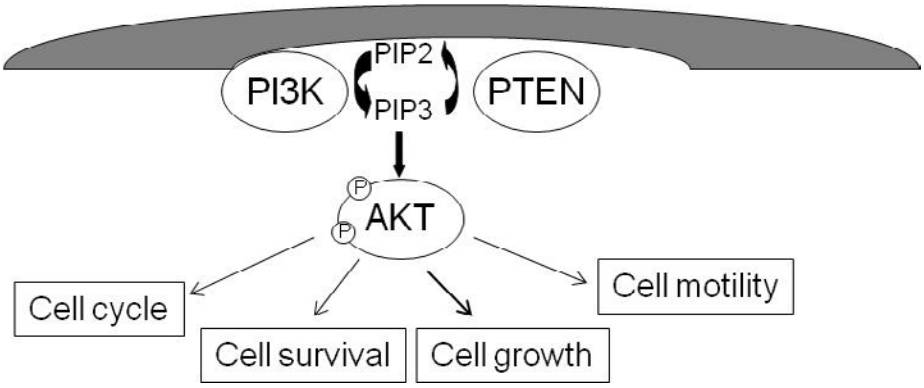

Figure 3. PI3K/AKT signalling activates multiple pathways relevant to cancer.

transcription factors FOXO1, FOXO3A and FOXO4, cell cycle regulator MDM2, glycogen synthase kinase 3 (GSK-3), and mTOR (56, 57).

Hyper-activation of AKT can not only be due to PTEN inactivation, but also be the result of oncogenic point mutations in PI3K (58). These mutations occur frequently in the kinase domain, the adjoining helical domain of the p110α subunit and the PH domain. Mutations are frequently detected in ovarian, breast, endometrial and colon cancer (59), however no mutations have been detected in prostate cancer (60). At low frequency, AKT1 is activated by mutation (E17K) (61) or overexpression. AKT1 mutations are detected in breast, colon, ovarian, lung and prostate cancer (61-64).

PTEN mouse cancer models

Several groups have analysed PTEN function *in vivo* by constitutive *Pten* inactivation or by generation of conditional Pten-deficient mice, using the Cre-LoxP system (65-70). *Pten* null mice are embryonically lethal and die at embryonal day 7-9.5. *Pten*$^{+/-}$ mice develop a broad range of tumours, including thyroid, mammary, endometrial and prostate cancers and T-cell lymphomas. This spectrum closely resembles the neoplasias developed in humans with *PTEN* mutations.

To elucidate the role of PTEN in specific tumours, a series of conditional knock-out (Cre-LoxP system) mice have been generated, by using tissue-specific promoters to express the Cre-recombinase. For prostate tumorigenesis either the probasin promoter, the *PSA* promoter or the *MMTV* promoter have been used for prostate-specific knock-out of *Pten*. Complete loss of *Pten* results in invasive prostate cancer, however, tumour latency differed between different mouse models, from 9-29 weeks to 10-14 months. This can be due to the different genetic background of mouse strains used or the different promoters used to transcribe the Cre-recombinase. Depending on the mouse model used, homozygous deletion of *Pten* leads to metastatic prostate cancer. Heterozygous

loss of *Pten* results in the development of hyperplasia and mPIN, with a latency of 12-16 months. Progression to invasive cancer has not been detected in these mice. However, mono-allelic inactivation of *Pten*, in combination with *Tp53* inactivation can induce prostate cancer (Korsten *et al*, unpublished).

RECURRENT ETS GENE FUSIONS IN PROSTATE CANCER

In 2005 Petrovics *et al* (71) reported frequent overexpression of the ETS transcription factor *ERG* mRNA in clinical prostate cancer (62% of 114 prostate cancer samples). They associated high levels of *ERG* expression with a favourable prognosis, based on longer PSA recurrence-free survival, lower pathological stage, well and moderately differentiated grade, and negative surgical margins status. Later that year, Tomlins *et al* (41) showed that *ERG* overexpression in prostate cancer was caused by a recurrent gene fusion of the *TMPRSS2* gene to the *ERG* gene. In their first experiments they detected overexpression of *ERG* by a novel bioinformatics approach, denoted cancer outlier profile analysis (COPA). COPA was used to identify outlier profiles in gene-expression data sets, to search for genes with marked overexpression in a subset of samples. It successfully identified outlier profiles for genes in specific tumour types in which high-level gene amplification or gene rearrangement was known to occur, like *ERBB2* in breast cancer and *RUNX1T1* in leukaemia. *ERG* was scored as high outlier gene in several independent prostate cancer-profiling studies. Actually, *ERG* is not a standard outlier, because it is overexpressed in a large proportion of prostate cancers.

An exon-walking quantitative PCR (QPCR) strategy of samples with *ERG* overexpression revealed overexpression of the last exons of *ERG* and not the first exons, suggestive for gene rearrangement. To characterize the 5′ end of the *ERG* transcripts, 5′ RNA ligase rapid amplification of cDNA ends (RLM-RACE) was performed. This led to the discovery of fusion of the first exon(s) of *TMPRSS2* (transmembrane protease, serine 2) to *ERG*. *TMPRSS2* is a prostate-specific and androgen-regulated gene (72) and *ERG* is a well-known oncogene. Thus, as a result of this fusion *TMPRSS2* donates the prostate-specific and androgen-regulated transcription regulating sequences to the coding sequences of *ERG*, leading to altered overexpression of *ERG*.

TMPRSS2 and *ERG* are located in the same orientation on chromosome band 21q22, ~3 Mbp apart (Figure 4). Array CGH and FISH analysis have shown that there are two mechanisms for this gene fusion. In approximately 60% of tumour samples with *TMPRSS2-ERG* fusion transcripts the region between *ERG* and *TMPRSS2* is lost. In the other samples with *TMPRSS2-ERG* fusion transcripts this region is retained, here the mechanism is a more complex genomic reallocation (73, 74).

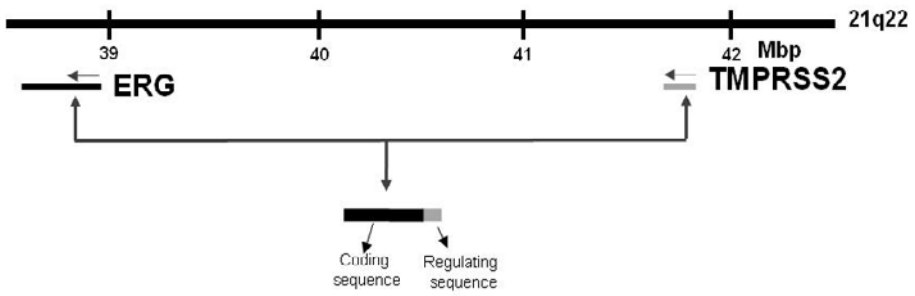

Figure 4. Schematic representation of chromosome 21q region. *ERG* and *TMPRSS2* are indicated, the distance is in Mbp.

Using COPA, *ETV1* (41) and later, two other ETS family members, namely *ETV4* (75) and *ETV5* (76), have been discovered as outliers in prostate cancer samples. Further characterization showed that *ETV1*, *ETV4* and *ETV5* all are involved in gene fusions with *TMPRSS2*, but also with other genes. Overexpression of the ETS genes is mutually exclusive.

ETS transcription factors

The founding member of the ETS family, v-*ets*, was originally discovered as part of gag-myb-ets fusion protein of the avian transforming retrovirus E26. This v-ets oncogene induces both erythroblastic and myeloblastic leukaemias *in vivo*. The ETS transcription factor family consists of ~30 family members, which is one of the largest families of transcriptional regulators (77, 78). All ETS proteins share an evolutionary conserved ETS domain. This 85 amino acid region forms the helix-turn-helix DNA binding domain, which recognises a central GGAA/T core consensus sequence (ETS binding site) in promoter regions of target genes. A second conserved domain is the pointed domain that is present in a subset of ETS genes. This 65-85 amino acid helix-loop-helix domain functions in protein-protein interactions. Based on their structural composition and their homology in the ETS domain, ETS genes are divided into several subfamilies (Table 1).

Besides the ETS domains and PNT domains, also activation and repression domains have been postulated in most ETS factors. For example the PEA3 subfamily has an N-terminal transactivation domain (79).

ETS proteins can function as transcription activators or repressors. They are known to play crucial roles in cellular proliferation, differentiation, apoptosis, tissue remodelling, angiogenesis, metastasis and transformation. To date, over 400 ETS target genes have been defined based upon the presence of ETS binding sites in their regulatory regions. Well-known ETS target genes are matrix metalloproteinases (*MMP*s) and *uPA*/*uPAR*.

Deregulated expression patterns of ETS genes have been observed in leukaemias and solid tumours. Overexpression of wild type ETS genes, most commonly *ETS1*, *ETS2*, *ETV4*,

Table 1. Overview of ETS subfamilies with schematic protein structure of the members. Pointed domains (PNT) and ETS domains are indicated.

ETS (ETS1, ETS2)	
ERG (ERG, FLI1)	
FEV	
TEL (ETV6 (TEL), TEL2)	
GABPα	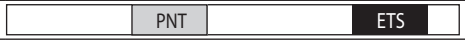
PEA3 (PEA3 (ETV4), ETV1 (ER81), ETV5 (ERM), ER71)	
ELF (ELF1, ELF2, ELF4)	
ESE (ELF3, ESE2/3)	
PDEF	
SPI (PU.1, Spi-B, Spi-C)	
ERF (METS, ERF)	
TCF (ELK1, SAP1, NET, Netb)	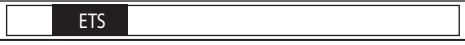

and *ETV1*, is found in breast, colon, lung and prostate cancer. In general, overexpression of wild type ETS genes is associated with advanced stages of disease.

Also, ETS genes are frequently involved in chromosomal translocations, resulting in fusion proteins or in altered expression of the ETS gene. These ETS fusion genes have been detected in Ewing's sarcoma and leukaemia, and more recently in prostate cancer. *FLI1*, *ERG*, *ETV1*, *ETV4* and *FEV* are known to be involved in gene fusion in Ewing's sarcomas (80). Fusion of the 5' part of Ewing sarcoma breakpoint region 1 (*EWSR1*) to the 3' part of an ETS family member (*FLI1*/*ERG*/*ETV1*/*ETV4*/*FEV*) is a hallmark of Ewing's sarcoma. These gene fusions lead to the production of a fusion protein, linking the N-terminal region of EWSR1 to the ETS domain. The most frequent translocation is a fusion of *EWSR1* to *FLI1*, detected in 90-95% of cases, followed by *EWSR1-ERG* (~5%). The other fusions are detected in less than 1% of cases. *EWSR1*-ETS fusions are mutually exclusive. *EWSR1* is a ubiquitously expressed gene and the first exons of EWSR1 encode for a strong transactivation domain. The fusion proteins modulate the expression of target genes in a sequence-specific manner that is determined by the ETS component.

In leukaemias many different fusion genes involving the ETS gene *TEL* have been described (81). Three types of *TEL* rearrangements can be discriminated. 1) *TEL* is juxtaposed to several tyrosine kinase genes, resulting in chimeric proteins. These proteins often possess the N-terminal PNT domain of TEL and the intact protein tyrosine kinase domains from the partner proteins. 2) The N-terminal PNT domain and the central repressor domain of TEL is linked to the nearly complete AML1 protein (82). 3) In MN1-TEL fusions, the N-terminal region of MN1 is juxtaposed to the C-terminal region, including the ETS domain, of TEL (83, 84). In several types of myeloid leukaemia fusion of *TLS/FUS*

to *ERG* has been found. Here, the weakened transcriptional activity, compared to wild type *ERG*, is believed to play a role in transformation of cells (85, 86).

ETS gene fusions in prostate cancer

Besides the initial discovery of *TMPRSS2-ERG* fusion gene in prostate cancer, several other ETS fusion genes have been detected, as stated above. Table 2 shows an overview of all ETS fusion genes known in prostate cancer to date. *TMPRSS2* is not only rearranged with *ERG*, but also with *ETV1*, *ETV4* and *ETV5*. Moreover, whereas *ERG* is exclusively rearranged with *TMPRSS2*, *ETV1*, *ETV4* and *ETV5* all have multiple fusion partners (Table 2) (41, 75, 76, 87-91). The most likely explanation for the high frequency of *ERG* to *TMPRSS2* fusion is that both *TMPRSS2* and *ERG* are located on chromosome 21q in close proximity (Figure 3), whereas *ETV1* is located on 7p, *ETV4* on 17q and *ETV5* on 3q. The fusion partners of *ETV1*, *ETV4* and *ETV5* are located on different chromosomes (Table 2). As shown in Table 2, none of the other fusion genes is detected as frequently as the *TMPRSS2-ERG* fusion gene. The *TMPRSS2-ERG* fusion gene is detected in 40-70% of clinical prostate cancer samples and in ~20% of high-grade PIN lesions (HGPIN) (92, 93).

Table 2. Overview of 5' and 3' fusion partners in prostate cancer

5' fusion partner	Prostate-specific	Androgen-regulated	3' fusion partner	Present
TMPRSS2 (chr 21q)	+	+	ERG (chr 21q)	~60%
TMPRSS2 (chr 21q)	+	+	ETV1 (chr 7p)	<1%
FOXP1 (chr 3p)	ND	ND		<1%
EST14 (chr 14q)	+	+		<1%
HERVK17 (chr 17p)	+	+		<1%
SLC45A3 (chr 1q)	+	+		<1%
HERV-K_22q11.23	+	+		<1%
C15orf21 (chr 15q)	+	+ (down)		<1%
HNRPA2B1 (chr 7p)	-	-		<1%
ACSL3 (chr 2q)	ND	+		<1%
Chr 14q13.3-q21.1*	+	+	ETV1 (chr 7p)	<1%
TMPRSS2 (chr 21q)	+	+	ETV4 (chr 17q)	<1%
KLK2 (chr 19p)	+	+		<1%
CANT1 (chr 17q)	+	+		<1%
DDX5 (chr 17q)	-	-		<1%
TMPRSS2 (chr 21q)	+	+	ETV5 (chr 3q)	<1%
SLC45A3 (chr 1q)	+	+		<1%

* Full length ETV1

ND: not determined

Like *TMPRSS2*, most other fusion partners (*EST14*, *HERVK17*, *SLC45A3*, *HERV-K_22q11.23*, *KLK2*, and *CANT1*) have a prostate-specific and androgen-upregulated expression pattern. One gene (*C15orf21*) has a prostate-specific and androgen-downregulated expression pattern, *HNRPA2B1* and *DDX5* have a ubiquitously expression pattern and are not regulated by androgens. The recently identified *ETV1* fusion partner *ACSL3* is also a strongly androgen-upregulated gene (89). Tissue-specificity of this gene has not been determined yet.

Noteworthy, two of the *ETV1* fusion partners involve endogenous retroviral repeat sequences of the HERVK subfamily (*HERVK17* and *HERV-K_22q11.23*). Retroviral repeat sequences comprise ~8% of the human genome. They are divided over many subfamilies, one of these subfamilies is the HERVK family (94, 95). Some members of the HERVK retroviral subfamily possess active promoters, and previously one similar gene fusion, *HERVK19-FGFR1*, has been reported in a myeloproliferative disorder (96). This makes the finding of particular interest for further investigations of the role of apparent defective retroviral sequences in prostate tumorigenesis.

Two prostate cancer cell lines, LNCaP and MDA Pca 2b, have a rearrangement of the whole *ETV1* locus to the same region on chromosome 14q13.3-q21.1. In this region two known genes are located, *MIPOL1* and *FOXA1*. *FOXA1* has a prostate-specific expression pattern, and *MIPOL1* is ubiquitously expressed. Whether these genes are androgen-regulated is less clear. In LNCaP cells the whole *ETV1* locus is integrated in the last intron of *MIPOL1*. MDA Pca 2b cell line harbours a (7;14) chromosomal translocation. FISH analysis using probes on *ETV1* and on the chromosome 14q13.3-q21.1 region showed a fusion of these loci in the MDA Pca 2b cell line. Interestingly, the *ETV1* fusion partner *EST14* is located in the same region. *EST14* is a two-exon gene that flanks *MIPOL1* (Figure 5). Like *FOXA1*, *EST14* also has a prostate-specific expression pattern. Moreover, *EST14* is weakly androgen-regulated. Thus, this unique region is both involved in *ETV1* gene fusions and in integrations and rearrangements of full length *ETV1*. Further investigation of the chromatin structure of this region may help to elucidate the mechanism of gene rearrangements in prostate cancer.

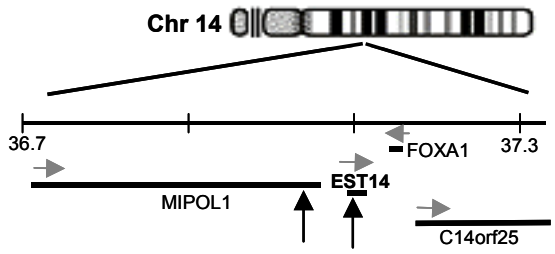

Figure 5. Schematic representation of genomic region on chromosome 14q13.3-q21.1. Distance from the top of chromosome is indicated in Mbp. Grey arrows indicate direction of transcription, black arrows indicate positions of *ETV1* integrations.

Clinical association with *TMPRSS2-ERG* fusion status

TMPRSS2-ERG fusion transcripts are the most frequently, up to 70%, detected fusion transcripts in clinical prostate cancer. To date, many different splice variants of the *TMPRSS2-ERG* fusion gene have been described. Almost all of these fusion transcripts encode N-truncated ERG proteins, however, sometimes a small part of TMPRSS2 is present in a TMPRSS2-ERG chimeric protein. The most frequently detected splice variant is a fusion of *TMPRRS2* exon 1 to *ERG* exon 4, followed by a fusion of *TMPRSS2* exon 0, an alternative first exon of *TMPRSS2*, located 4 kbp upstream of exon 1, to *ERG* exon 4 and *TMPRSS2* exon 1 and 2 to *ERG* exon 4. Other splice variants were identified at low frequency. Most splice variants involve multiple exons of *TMPRSS2* fused to exon 4 of *ERG* or *TMPRSS2* exon 1 fused to different exons of *ERG*. Of note, multiple splice variants can be detected in a single sample.

Several groups have tried to associate *TMPRSS2-ERG* fusion status with clinical data. The most relevant studies are listed in Table 3. Demichelis *et al* (97) observed in 15%

Table 3. Studies that reported on the correlation between *TMPRRS2-ERG* fusion gene and clinical outcome of prostate cancer.

A. Cancer-specific (CSS) and overall survival (OS)						
Reference	**N**	**Samples**	**Technique**	***TMPRSS2-ERG***	**Follow-up (median)**	**Fusion-positive versus fusion-negative cases**
Attard et al (104)	445	TUR-P / Biopsies	FISH	30%	7.5 yr	Shorter CSS and OS (multivariate level)
Demichelis et al (96)	111	TUR-P / prostatectomy	FISH	15%	9.1 yr	Shorter CSS (univariate level)
B. Biochemical progression-free survival (BFS)						
Petrovics et al (71)	114	RP	Q-PCR	62%*	n.s.	Longer BFS (univariate level)
Saramäki et al (102)	150	RP	FISH	33%	5.5 yr	Longer BFS (multivariate level)
Nam et al (97)	165	RP	RT-PCR	42%	1.7 yr	Shorter BFS (multivariate level)
Perner et al (74)	118	RP	FISH	49%	n.s.	**
Wang et al (105)	59	RP	RT-PCR	59%	n.s.	***
Hermans et al (chapter 5)	67	RP	Q-PCR	66%	10.2 yr	No difference in BFS ****

***** ERG overexpression

****** Higher recurrence rate, no survival analysis

******* More early recurrences in patients with variant *TMPRSS2-ERG* fusion**,** no survival analysis

******** Longer BFS for *TMPRSS2(exon0)-ERG* (multivariate level)

N: number of patients

n.s.: not specified

of the tumours from a watchful waiting cohort of 111 men with localized prostate cancer *TMPRSS2-ERG* fusion by FISH analysis. They associate *TMPRSS2-ERG* fusion with a higher frequency of metastasis and cancer-specific death. However, genefusion-positive samples have higher Gleason scores, and after adjusting for Gleason score, the outcome is no longer significant. Nam *et al* showed, in a cohort of 165 patients, association of *TMPRSS2-ERG* fusion with earlier biochemical recurrence after radical prostatectomy (98). This was independent of stage and grade, however median follow-up was short (20 months).

Most groups do not find a strong association with prognostic factors (Gleason score, pathological stage, surgical margins) or clinical outcome (99-102). Initially, before the discovery of the *TMPRSS2-ERG* gene fusions, Petrovics *et al* (71) associated prostate cancers overexpressing *ERG* mRNA with a favourable prognosis (longer PSA recurrence-free survival, negative surgical margins, lower pathological stage and well and moderate differentiation grade). Two other groups recently made similar observations for *TMPRSS2-ERG* fusion positive cancers (103, 104).

Other studies reported on the association of clinical data with specific characteristics of *TMPRSS2-ERG* gene rearrangements or *TMPRSS2-ERG* fusion transcript splice variants. In a study of a watchful waiting cohort of 445 patients, a small subset of the cancers shows a duplication of *TMPRSS2-ERG* in combination with deletion of 5′ *ERG* (2+Edel) (105). This genomic alteration is associated with poor cancer-specific survival and worse overall survival. In this study, two+Edel seems a predictor of poor clinical outcome, independent of Gleason score, baseline PSA and age as determined by multivariate analysis. No difference in survival was observed between patients with fusion gene negative tumours and patients with tumours containing *TMPRSS2-ERG* fusion with translocation as mechanism of rearrangement. In a high-risk cohort of 118 patients (50% Gleason score >7, 49% pT3b tumours, 72% positive surgical margins and 56% node-positive disease), Perner *et al* (74), report presence of *TMPRSS2-ERG* fusion in 49% of the samples as detected by FISH. For patients with *TMPRSS2-ERG* fusion by interstitial deletion a trend for higher PSA recurrence rate was observed as compared to patients without gene fusion. In a cohort of 59 patients, Wang *et al* (106) observe that presence of *TMPRSS2(exon 2)-ERG(exon 4)* fusion transcripts was associated with aggressive disease. Also, they describe that splice variants of *TMPRSS2* exon 1 to either *ERG* exon 2 or exon 3 are associated with seminal vesicle invasion, which is correlated with poor clinical outcome after radical prostatectomy. All these splice variants contain a native translation initiation codon (in *TMPRSS2* exon 2 or *ERG* exon 3) as translation start codon. In our study (chapter 5) we observed no association of prognostic factors with *TMPRSS2-ERG* gene fusion. Recently, a novel *TMPRSS2-ERG* fusion transcript, starting at *TMPRSS2* exon 0, has been described (99). We have separated the fusion gene-positive group in samples with expression of

TMPRSS2(exon 0)-ERG transcripts or without expression of these transcripts. This results in an association of longer time to biochemical recurrence in the group with *TMPRSS2(exon 0)-ERG* expression. Moreover, multivariate analysis identifies expression of *TMPRSS2(exon 0)-ERG* as an independent predictor of longer biochemical recurrence-free survival after radical prostatectomy. More extensive studies, with larger patient cohorts and long clinical follow up, are needed to help resolve the specific prognostic association with gene fusion status.

Recently, Yoshimoto *et al* (107) reported that presence of both *TMPRSS2-ERG* gene fusion and *PTEN* deletion is associated with earlier biochemical recurrence. Three groups of differential patient outcome were discriminated: (1) a poor prognosis group when both *TMPRSS2-ERG* fusion gene and *PTEN* deletion are present, (2) an intermediate group with either *TMPRSS2-ERG* fusion gene or *PTEN* deletion and (3) a favourable prognosis group with neither *TMPRSS2-ERG* fusion gene nor *PTEN* deletion.

Specific morphological features have been identified in most *TMPRSS2-ERG* fusion positive prostate tumour samples, these are blue-tinged mucin, cibriform growth pattern, macronuclei, intraductal tumour spread, and signet-ring cell (108, 109). Most of these characteristics are indications of more aggressive disease.

Prostate cancer is a molecular and histological heterogeneous disease, which can be composed of multiple foci within the same gland (110, 111). Analysis of *TMPRSS2-ERG* gene rearrangements in multifocal prostate cancer samples showed that individual foci can have different rearrangements (112-115). Mehra *et al.* (116) reported that *TMPRSS2-ERG* rearrangement at metastatic sites always occurs through interstitial deletion. Moreover, all metastatic sites in an individual patient display an identical ETS rearrangement status (fusion gene positive or fusion gene negative), pointing to clonal expansion of tumour cells from the same primary focus.

Two studies have applied array CGH analysis on prostate cancer samples and searched for common genomic alterations in ETS fusion-positive and ETS fusion-negative cancers (117, 118). Lapointe *et al* (118) divided their samples in three subtypes based on expression profiling. Subtype two and three tumours showed a more aggressive phenotype compared to tumours of subtype one. Subtype two harbours tumours with *TMPRSS2-ERG* fusion, whereas in subtype one, an ETS fusion-gene negative group, loss of chromosome band 6q15 was detected. Subtype three was also a *TMPRSS2-ERG* fusion-negative group. This group had in general more chromosomal alterations. Kim *et al* (117) distinguished a subgroup with low expression of ETS mRNAs with loss of chromosome band 6q21. Moreover, Tomlins *et al* detected distinct expression signatures for ETS-positive and ETS-negative tumours, including a relative underexpression of genes located on 6q21 in the ETS-negative group (119).

Recently, it has been reported that in ~10% of the ETS fusion gene negative tumours overexpression of *SPINK1* was associated with a shorter time to biochemical recurrence (120).

TMPRSS2-ERG fusion and prostate cancer diagnosis

The serum PSA test is currently used as a first step in prostate cancer diagnosis. Although it is a sensitive and simple test, it lacks specificity, because elevated serum PSA levels can also be measured in case of benign alterations of the prostate. Therefore, there is need for a sensitive and more specific prostate cancer-screening test, preferentially using non-invasive conditions, like a blood or urine test.

For this reason presence of *TMPRSS2-ERG* fusion transcripts in urine sediments, obtained after digital rectal examination (DRE) of prostate cancer patients, was evaluated (121-123). A PCR-based assay resulted in a sensitive and specific detection of *TMPRSS2-ERG* fusion transcripts in urine sediments. However, not all prostate cancer samples harbour *TMPRSS2-ERG* fusion genes, therefore additional biomarkers, *PCA3*, *GOLPH2* and *SPINK1*, were analysed. Although, the combination provided a promising high sensitivity and specificity, data are still preliminary and cannot replace the currently used PSA test. Further refinement and testing of large patient cohorts are needed before routine clinical application, supplementary to or instead of serum PSA detection.

Recently, it has been reported that the *TMPRSS2-ERG* fusion gene can be detected in circulating tumour cells isolated from blood for its potential to monitor tumour metastasis (124). Although *TMPRSS2-ERG* fusion was detected at the genomic level, this was not possible at transcript level. This might be due to the limiting sensitivity of the test or by downregulation of fusion gene expression in circulating cells.

Functional studies of ETS fusion genes in prostate cancer

To characterize the functional role of ETS fusion genes in prostate cancer several *in vitro* and *in vivo* studies have been performed. First the role of ETS fusion genes in prostate cancer cell lines was investigated. The VCaP prostate cancer cell line, that expresses the *TMPRSS2-ERG* fusion gene, has been used to downregulate *ERG* expression by siRNA. The effect on cell biological and tumorigenic properties was evaluated. Tomlins *et al*. (125) showed that *ERG* downregulation inhibited cell invasion, but did not affect cell proliferation. Sun *et al.* (126) reported that *ERG* downregulation resulted in cell morphological changes, slow growing and clumped cells, after 6-8 days. Injection of VCaP cells, transfected with *ERG* siRNA, in severe combined immune-deficient (SCID) mice, showed that these cells were less tumorigenic than parental VCaP cells (126). Both studies also indicated that *ERG* knockdown induced a transcriptional program consistent with prostate differentiation.

The prostate cancer cell line LNCaP overexpresses *ETV1*. In this cell line the complete *ETV1* locus is inserted in the last intron of *MIPOL1*, as described above. Downregulation of *ETV1* expression by siRNA resulted in inhibition of invasive properties of the LNCaP cells (88, 127). Moreover, *ETV1* downregulation reduced the expression of *MMPs*, which are known to be involved in cell invasion. In addition, Cai *et al* (127) reported that downregulation of ETV1 protein inhibited cell proliferation.

Another approach that has been used to determine the role of the ETS fusion genes in prostate cells, was infection of non-tumorigenic, immortalized, benign prostate epithelial cells with viruses expressing ETS factors (N-truncated ERG and ETV1, and full length ETV1 and ETV5) (76, 88, 91, 125) or nucleoporation of immortal, non-tumorigenic BPH1 cells with N-truncated ERG expression constructs (128). The full length forms of these ETS transcription factors have an N-terminal transactivation domain (TAD). In case of gene fusion this N-terminal part is lost. Most studies showed that transient or stable overexpression of these ETS genes have no effect on cell proliferation, although Klezovitch *et al* (128) detected increased rates of cell accumulation. In all studies, ETS overexpression increased cell invasion. Klezovitch *et al* (128) detected little effect on cell migration in BPH1 cells over expressing N-truncated ERG. In contrast, we found that both full length and N-truncated ETV1 stimulated cell migration in PNT2C2 cells (91). Interestingly, over expression of full length ETV1 stimulated anchorage-independent growth, whereas over expression of N-truncated ETV1 or ERG had no effect (88, 91, 125). Moreover, we have shown that N-truncated and full length ETV1 possesses different transcription regulation functions in an ETS reporter assay. Both N-truncated and full length ETS factors induce an invasion-associated transcriptional program, including induction of *MMPs* and *uPAR/uPA*, but comparing full length and truncated ETV1 we found a difference in stimulation of genes involved in integrin-signaling (*ITGB3* and *ITGAV*).

To elucidate the functional properties of the ETS fusion genes in prostate epithelium *in vivo*, transgenic mouse models overexpressing N-truncated ERG or N-truncated ETV1 have been generated, under control of a modified prostate-specific and androgen-regulated probasin (*PB*) promoter (88, 125, 128). The transgenic mice, *PB-ERG* and *PB-ETV1*, do not develop prostate tumours. However, most *PB-ETV1* mice do develop mPIN foci by 12-14 weeks in all three prostate lobes (anterior, ventral and dorsolateral) (88). In *PB-ERG* mice mPIN lesions were found in the ventral lobe after 12-14 weeks (125) or 5-6 months (128).

In vitro and *in vivo* studies indicate that the N-truncated ETS factors are important in earlier stages of prostate cancer, but this might not be sufficient for development of prostate tumours. Additional genetic alterations, like loss or mutation of a tumour suppressor gene like *PTEN*, seem needed to develop prostate cancer. Moreover, we have shown that in prostate cancer xenografts, overexpression of wild type ETS factors is found in AR negative, late stage disease, whereas expression of *TMPRSS2-ERG* fusion

genes is downregulated (73). This points to different roles of N-truncated and full length ETS factors in prostate cancer.

OUTLINE OF THIS THESIS

The aim of this thesis is to characterize the major genetic defects underlying prostate cancer development and progression. In **Chapter 2**, a genome-wide screen for genomic alterations by array CGH is performed in DNA from eleven human prostate cancer xenografts. Our focus was on identification of homozygous deleted regions, because these are reliable landmarks of tumour suppressor genes. Homozygous deletions were confirmed by PCR analysis and genes within these regions were tested on mRNA expression. Most interesting regions were subjected to further structural and functional analysis. In **Chapter 3**, we studied chromosome 10 alterations in more detail in the same xenograft DNAs. *PTEN* and surrounding genes were subjected to expression and structural analysis.

Chapter 4 describes the identification and characterization of the *TMPRSS2-ERG* and *TMPRSS2-ETV1* fusion genes in human prostate cancer xenografts. By array CGH, FISH and QPCR analysis we detected *TMPRSS2-ERG* fusion transcripts in five AR positive xenografts. However, these transcripts were absent in late stage AR negative prostate cancer, although the fusion gene was present.

TMPRSS2 transcription can start at two alternative first exons, exon 0 and 1. In **Chapter 5** we determined the specific characteristics of transcripts starting at these two alternative first exons of *TMPRSS2* in normal tissues, and in prostate cancer xenografts and cell lines. Next, we investigated presence of *TMPRSS2(exon 0)-ERG* and *TMPRSS2(exon 1)-ERG* fusion transcripts in prostate cancer xenografts and in clinical prostate cancer samples. In addition, we correlated expression of *TMPRSS2(exon 0)-ERG* with clinical outcome in a cohort of primary prostate cancers to investigate whether it was of prognostic value.

Besides the initial discovery of *TMPRSS2* to ETS fusion genes, other ETS fusion partners have been described. In **Chapter 6** the identification of two novel unique *ETV4* fusion genes in clinical prostate cancer samples is described. Moreover, we determined the specific characteristics of these novel *ETV4* fusion genes and of both fusion partners. In **Chapter 7**, we investigated overexpression of *ETV1* in clinical prostate cancer specimens by QPCR analysis. We identified overexpression of novel *ETV1* fusion genes and of full length *ETV1*. First, we determined specific characteristics of these novel fusion partners. Next, we assessed the biological properties of both full length and N-truncated ETV1 proteins. Finally, in **Chapter 8** the results described in this thesis are discussed and suggestions for further research are offered.

REFERENCES

1. Jemal A, Siegel R, Ward E, *et al.* Cancer statistics, 2008. CA Cancer J Clin 2008;58(2):71-96.
2. Pienta KJ, Esper PS. Risk factors for prostate cancer. Ann Intern Med 1993;118(10):793-803.
3. Rubin MA, De Marzo AM. Molecular genetics of human prostate cancer. Mod Pathol 2004;17(3):380-8.
4. Dehm SM, Tindall DJ. Molecular regulation of androgen action in prostate cancer. J Cell Biochem 2006;99(2):333-44.
5. Damber JE, Aus G. Prostate cancer. Lancet 2008;371(9625):1710-21.
6. Joniau S, Van Poppel H. Localized prostate cancer: can we better define who is at risk of unfavourable outcome? BJU Int 2008;101 Suppl 2:5-10.
7. van der Kwast TH, Schalken J, Ruizeveld de Winter JA, *et al.* Androgen receptors in endocrine-therapy-resistant human prostate cancer. Int J Cancer 1991;48(2):189-93.
8. Visakorpi T, Hyytinen E, Koivisto P, *et al.* In vivo amplification of the androgen receptor gene and progression of human prostate cancer. Nat Genet 1995;9(4):401-6.
9. Taplin ME, Rajeshkumar B, Halabi S, *et al.* Androgen receptor mutations in androgen-independent prostate cancer: Cancer and Leukemia Group B Study 9663. J Clin Oncol 2003;21(14):2673-8.
10. Chmelar R, Buchanan G, Need EF, Tilley W, Greenberg NM. Androgen receptor coregulators and their involvement in the development and progression of prostate cancer. Int J Cancer 2007;120(4):719-33.
11. Page ST, Lin DW, Mostaghel EA, *et al.* Persistent intraprostatic androgen concentrations after medical castration in healthy men. J Clin Endocrinol Metab 2006;91(10):3850-6.
12. Hanahan D, Weinberg RA. The hallmarks of cancer. Cell 2000;100(1):57-70.
13. Shand RL, Gelmann EP. Molecular biology of prostate-cancer pathogenesis. Curr Opin Urol 2006;16(3):123-31.
14. Verhage BA, Kiemeney LA. Genetic susceptibility to prostate cancer: a review. Fam Cancer 2003;2(1):57-67.
15. Smith JR, Freije D, Carpten JD, *et al.* Major susceptibility locus for prostate cancer on chromosome 1 suggested by a genome-wide search. Science 1996;274(5291):1371-4.
16. Gibbs M, Chakrabarti L, Stanford JL, *et al.* Analysis of chromosome 1q42.2-43 in 152 families with high risk of prostate cancer. Am J Hum Genet 1999;64(4):1087-95.
17. Gibbs M, Stanford JL, McIndoe RA, *et al.* Evidence for a rare prostate cancer-susceptibility locus at chromosome 1p36. Am J Hum Genet 1999;64(3):776-87.
18. Xu J, Zheng SL, Hawkins GA, *et al.* Linkage and association studies of prostate cancer susceptibility: evidence for linkage at 8p22-23. Am J Hum Genet 2001;69(2):341-50.
19. Tavtigian SV, Simard J, Teng DH, *et al.* A candidate prostate cancer susceptibility gene at chromosome 17p. Nat Genet 2001;27(2):172-80.
20. Berry R, Schroeder JJ, French AJ, *et al.* Evidence for a prostate cancer-susceptibility locus on chromosome 20. Am J Hum Genet 2000;67(1):82-91.
21. Xu J, Meyers D, Freije D, *et al.* Evidence for a prostate cancer susceptibility locus on the X chromosome. Nat Genet 1998;20(2):175-9.
22. Rokman A, Ikonen T, Seppala EH, *et al.* Germline alterations of the RNASEL gene, a candidate HPC1 gene at 1q25, in patients and families with prostate cancer. Am J Hum Genet 2002;70(5):1299-304.
23. Eeles RA, Kote-Jarai Z, Giles GG, *et al.* Multiple newly identified loci associated with prostate cancer susceptibility. Nat Genet 2008;40(3):316-21.

24. Gudmundsson J, Sulem P, Rafnar T, *et al.* Common sequence variants on 2p15 and Xp11.22 confer susceptibility to prostate cancer. Nat Genet 2008;40(3):281-3.
25. Thomas G, Jacobs KB, Yeager M, *et al.* Multiple loci identified in a genome-wide association study of prostate cancer. Nat Genet 2008;40(3):310-5.
26. Xu J, Zheng SL, Komiya A, *et al.* Germline mutations and sequence variants of the macrophage scavenger receptor 1 gene are associated with prostate cancer risk. Nat Genet 2002;32(2):321-5.
27. Agalliu I, Karlins E, Kwon EM, *et al.* Rare germline mutations in the BRCA2 gene are associated with early-onset prostate cancer. Br J Cancer 2007;97(6):826-31.
28. Edwards SM, Kote-Jarai Z, Meitz J, *et al.* Two percent of men with early-onset prostate cancer harbor germline mutations in the BRCA2 gene. Am J Hum Genet 2003;72(1):1-12.
29. Erkko H, Xia B, Nikkila J, *et al.* A recurrent mutation in PALB2 in Finnish cancer families. Nature 2007;446(7133):316-9.
30. Seppala EH, Ikonen T, Mononen N, *et al.* CHEK2 variants associate with hereditary prostate cancer. Br J Cancer 2003;89(10):1966-70.
31. Kallioniemi A, Kallioniemi OP, Sudar D, *et al.* Comparative genomic hybridization for molecular cytogenetic analysis of solid tumors. Science 1992;258(5083):818-21.
32. Pinkel D, Segraves R, Sudar D, *et al.* High resolution analysis of DNA copy number variation using comparative genomic hybridization to microarrays. Nat Genet 1998;20(2):207-11.
33. Albertson DG, Pinkel D. Genomic microarrays in human genetic disease and cancer. Hum Mol Genet 2003;12 Spec No 2:R145-52.
34. Inazawa J, Inoue J, Imoto I. Comparative genomic hybridization (CGH)-arrays pave the way for identification of novel cancer-related genes. Cancer Sci 2004;95(7):559-63.
35. Dutt A, Beroukhim R. Single nucleotide polymorphism array analysis of cancer. Curr Opin Oncol 2007;19(1):43-9.
36. Heinrichs S, Look AT. Identification of structural aberrations in cancer by SNP array analysis. Genome Biol 2007;8(7):219.
37. Sun J, Liu W, Adams TS, *et al.* DNA copy number alterations in prostate cancers: a combined analysis of published CGH studies. Prostate 2007;67(7):692-700.
38. Saramaki OR, Porkka KP, Vessella RL, Visakorpi T. Genetic aberrations in prostate cancer by microarray analysis. Int J Cancer 2006;119(6):1322-9.
39. Li J, Yen C, Liaw D, *et al.* PTEN, a putative protein tyrosine phosphatase gene mutated in human brain, breast, and prostate cancer. Science 1997;275(5308):1943-7.
40. Steck PA, Pershouse MA, Jasser SA, *et al.* Identification of a candidate tumour suppressor gene, MMAC1, at chromosome 10q23.3 that is mutated in multiple advanced cancers. Nat Genet 1997;15(4):356-62.
41. Tomlins SA, Rhodes DR, Perner S, *et al.* Recurrent fusion of TMPRSS2 and ETS transcription factor genes in prostate cancer. Science 2005;310(5748):644-8.
42. Liaw D, Marsh DJ, Li J, *et al.* Germline mutations of the PTEN gene in Cowden disease, an inherited breast and thyroid cancer syndrome. Nat Genet 1997;16(1):64-7.
43. Marsh DJ, Dahia PL, Zheng Z, *et al.* Germline mutations in PTEN are present in Bannayan-Zonana syndrome. Nat Genet 1997;16(4):333-4.
44. Sansal I, Sellers WR. The biology and clinical relevance of the PTEN tumor suppressor pathway. J Clin Oncol 2004;22(14):2954-63.
45. Parsons R. Human cancer, PTEN and the PI-3 kinase pathway. Semin Cell Dev Biol 2004;15(2):171-6.

46. Yoshimoto M, Cunha IW, Coudry RA, *et al.* FISH analysis of 107 prostate cancers shows that PTEN genomic deletion is associated with poor clinical outcome. Br J Cancer 2007;97(5):678-85.
47. Yoshimoto M, Cutz JC, Nuin PA, *et al.* Interphase FISH analysis of PTEN in histologic sections shows genomic deletions in 68% of primary prostate cancer and 23% of high-grade prostatic intra-epithelial neoplasias. Cancer Genet Cytogenet 2006;169(2):128-37.
48. Hermans KG, van Alewijk DC, Veltman JA, van Weerden W, van Kessel AG, Trapman J. Loss of a small region around the PTEN locus is a major chromosome 10 alteration in prostate cancer xenografts and cell lines. Genes Chromosomes Cancer 2004;39(3):171-84.
49. Cairns P, Okami K, Halachmi S, *et al.* Frequent inactivation of PTEN/MMAC1 in primary prostate cancer. Cancer Res 1997;57(22):4997-5000.
50. Dong JT, Li CL, Sipe TW, Frierson HF, Jr. Mutations of PTEN/MMAC1 in primary prostate cancers from Chinese patients. Clin Cancer Res 2001;7(2):304-8.
51. Dong JT, Sipe TW, Hyytinen ER, *et al.* PTEN/MMAC1 is infrequently mutated in pT2 and pT3 carcinomas of the prostate. Oncogene 1998;17(15):1979-82.
52. Feilotter HE, Nagai MA, Boag AH, Eng C, Mulligan LM. Analysis of PTEN and the 10q23 region in primary prostate carcinomas. Oncogene 1998;16(13):1743-8.
53. Pesche S, Latil A, Muzeau F, *et al.* PTEN/MMAC1/TEP1 involvement in primary prostate cancers. Oncogene 1998;16(22):2879-83.
54. Verhagen PC, van Duijn PW, Hermans KG, *et al.* The PTEN gene in locally progressive prostate cancer is preferentially inactivated by bi-allelic gene deletion. J Pathol 2006;208(5):699-707.
55. Wang SI, Parsons R, Ittmann M. Homozygous deletion of the PTEN tumor suppressor gene in a subset of prostate adenocarcinomas. Clin Cancer Res 1998;4(3):811-5.
56. Salmena L, Carracedo A, Pandolfi PP. Tenets of PTEN tumor suppression. Cell 2008;133(3):403-14.
57. Cully M, You H, Levine AJ, Mak TW. Beyond PTEN mutations: the PI3K pathway as an integrator of multiple inputs during tumorigenesis. Nat Rev Cancer 2006;6(3):184-92.
58. Samuels Y, Wang Z, Bardelli A, *et al.* High frequency of mutations of the PIK3CA gene in human cancers. Science 2004;304(5670):554.
59. Samuels Y, Velculescu VE. Oncogenic mutations of PIK3CA in human cancers. Cell Cycle 2004;3(10):1221-4.
60. Muller CI, Miller CW, Hofmann WK, *et al.* Rare mutations of the PIK3CA gene in malignancies of the hematopoietic system as well as endometrium, ovary, prostate and osteosarcomas, and discovery of a PIK3CA pseudogene. Leuk Res 2007;31(1):27-32.
61. Carpten JD, Faber AL, Horn C, *et al.* A transforming mutation in the pleckstrin homology domain of AKT1 in cancer. Nature 2007;448(7152):439-44.
62. Bleeker FE, Felicioni L, Buttitta F, *et al.* AKT1(E17K) in human solid tumours. Oncogene 2008.
63. Malanga D, Scrima M, De Marco C, *et al.* Activating E17K mutation in the gene encoding the protein kinase AKT1 in a subset of squamous cell carcinoma of the lung. Cell Cycle 2008;7(5):665-9.
64. Boormans JL, Hermans KG, van Leenders GJ, Trapman J, Verhagen PC. An activating mutation in AKT1 in human prostate cancer. Int J Cancer 2008; *in press*.
65. Backman SA, Ghazarian D, So K, *et al.* Early onset of neoplasia in the prostate and skin of mice with tissue-specific deletion of Pten. Proc Natl Acad Sci U S A 2004;101(6):1725-30.
66. Di Cristofano A, De Acetis M, Koff A, Cordon-Cardo C, Pandolfi PP. Pten and p27KIP1 cooperate in prostate cancer tumor suppression in the mouse. Nat Genet 2001;27(2):222-4.
67. Ma X, Ziel-van der Made AC, Autar B, *et al.* Targeted biallelic inactivation of Pten in the mouse prostate leads to prostate cancer accompanied by increased epithelial cell proliferation but not by reduced apoptosis. Cancer Res 2005;65(13):5730-9.

68. Suzuki A, de la Pompa JL, Stambolic V, *et al.* High cancer susceptibility and embryonic lethality associated with mutation of the PTEN tumor suppressor gene in mice. Curr Biol 1998;8(21):1169-78.
69. Wang S, Gao J, Lei Q, *et al.* Prostate-specific deletion of the murine Pten tumor suppressor gene leads to metastatic prostate cancer. Cancer Cell 2003;4(3):209-21.
70. Trotman LC, Niki M, Dotan ZA, *et al.* Pten dose dictates cancer progression in the prostate. PLoS Biol 2003;1(3):E59.
71. Petrovics G, Liu A, Shaheduzzaman S, *et al.* Frequent overexpression of ETS-related gene-1 (ERG1) in prostate cancer transcriptome. Oncogene 2005;24(23):3847-52.
72. Lin B, Ferguson C, White JT, *et al.* Prostate-localized and androgen-regulated expression of the membrane-bound serine protease TMPRSS2. Cancer Res 1999;59(17):4180-4.
73. Hermans KG, van Marion R, van Dekken H, Jenster G, van Weerden WM, Trapman J. TMPRSS2: ERG fusion by translocation or interstitial deletion is highly relevant in androgen-dependent prostate cancer, but is bypassed in late-stage androgen receptor-negative prostate cancer. Cancer Research 2006;66(22):10658-63.
74. Perner S, Demichelis F, Beroukhim R, *et al.* TMPRSS2:ERG Fusion-Associated Deletions Provide Insight into the Heterogeneity of Prostate Cancer. Cancer Res 2006;66(17):8337-41.
75. Tomlins SA, Mehra R, Rhodes DR, *et al.* TMPRSS2:ETV4 gene fusions define a third molecular subtype of prostate cancer. Cancer Res 2006;66(7):3396-400.
76. Helgeson BE, Tomlins SA, Shah N, *et al.* Characterization of TMPRSS2:ETV5 and SLC45A3:ETV5 gene fusions in prostate cancer. Cancer Res 2008;68(1):73-80.
77. Oikawa T, Yamada T. Molecular biology of the Ets family of transcription factors. Gene 2003;303:11-34.
78. Seth A, Watson DK. ETS transcription factors and their emerging roles in human cancer. Eur J Cancer 2005;41(16):2462-78.
79. Kurpios NA, Sabolic NA, Shepherd TG, Fidalgo GM, Hassell JA. Function of PEA3 Ets transcription factors in mammary gland development and oncogenesis. J Mammary Gland Biol Neoplasia 2003;8(2):177-90.
80. Khoury JD. Ewing sarcoma family of tumors. Adv Anat Pathol 2005;12(4):212-20.
81. Bohlander SK. ETV6: a versatile player in leukemogenesis. Semin Cancer Biol 2005;15(3):162-74.
82. Cayuela JM, Baruchel A, Orange C, *et al.* TEL-AML1 fusion RNA as a new target to detect minimal residual disease in pediatric B-cell precursor acute lymphoblastic leukemia. Blood 1996;88(1):302-8.
83. Kawagoe H, Grosveld GC. MN1-TEL myeloid oncoprotein expressed in multipotent progenitors perturbs both myeloid and lymphoid growth and causes T-lymphoid tumors in mice. Blood 2005;106(13):4278-86.
84. Buijs A, van Rompaey L, Molijn AC, *et al.* The MN1-TEL fusion protein, encoded by the translocation (12;22)(p13;q11) in myeloid leukemia, is a transcription factor with transforming activity. Mol Cell Biol 2000;20(24):9281-93.
85. Pan J, Zou J, Wu DY, *et al.* TLS-ERG leukemia fusion protein deregulates cyclin-dependent kinase 1 and blocks terminal differentiation of myeloid progenitor cells. Mol Cancer Res 2008;6(5):862-72.
86. Prasad DD, Ouchida M, Lee L, Rao VN, Reddy ES. TLS/FUS fusion domain of TLS/FUS-erg chimeric protein resulting from the t(16;21) chromosomal translocation in human myeloid leukemia functions as a transcriptional activation domain. Oncogene 1994;9(12):3717-29.

87. Hermans KG, Bressers AA, van der Korput HA, Dits NF, Jenster G, Trapman J. Two unique novel prostate-specific and androgen-regulated fusion partners of ETV4 in prostate cancer. Cancer Res 2008;68(9):3094-8.
88. Tomlins SA, Laxman B, Dhanasekaran SM, *et al.* Distinct classes of chromosomal rearrangements create oncogenic ETS gene fusions in prostate cancer. Nature 2007;448(7153):595-9.
89. Attard G, Clark J, Ambroisine L, *et al.* Heterogeneity and clinical significance of ETV1 translocations in human prostate cancer. Br J Cancer 2008;99(2):314-20.
90. Han B, Mehra R, Dhanasekaran SM, *et al.* A fluorescence in situ hybridization screen for E26 transformation-specific aberrations: identification of DDX5-ETV4 fusion protein in prostate cancer. Cancer Res 2008;68(18):7629-37.
91. Hermans KG, van der Korput HA, van Marion R, *et al*. Truncated ETV1, fused to novel tissue-specific genes, and full length ETV1 in prostate cancer. Cancer Res 2008;68(18):7541-9.
92. Cerveira N, Ribeiro FR, Peixoto A, *et al.* TMPRSS2-ERG gene fusion causing ERG overexpression precedes chromosome copy number changes in prostate carcinomas and paired HGPIN lesions. Neoplasia 2006;8(10):826-32.
93. Mosquera JM, Perner S, Genega EM, *et al.* Characterization of TMPRSS2-ERG Fusion High-Grade Prostatic Intraepithelial Neoplasia and Potential Clinical Implications. Clin Cancer Res 2008;14(11):3380-5.
94. Buzdin A, Kovalskaya-Alexandrova E, Gogvadze E, Sverdlov E. At least 50% of human-specific HERV-K (HML-2) long terminal repeats serve in vivo as active promoters for host nonrepetitive DNA transcription. J Virol 2006;80(21):10752-62.
95. Stauffer Y, Theiler G, Sperisen P, Lebedev Y, Jongeneel CV. Digital expression profiles of human endogenous retroviral families in normal and cancerous tissues. Cancer Immun 2004;4:2.
96. Guasch G, Popovici C, Mugneret F, *et al.* Endogenous retroviral sequence is fused to FGFR1 kinase in the 8p12 stem-cell myeloproliferative disorder with t(8;19)(p12;q13.3). Blood 2003;101(1):286-8.
97. Demichelis F, Fall K, Perner S, *et al.* TMPRSS2:ERG gene fusion associated with lethal prostate cancer in a watchful waiting cohort. Oncogene 2007;26(31):4596-9.
98. Nam RK, Sugar L, Yang W, *et al.* Expression of the TMPRSS2:ERG fusion gene predicts cancer recurrence after surgery for localised prostate cancer. Br J Cancer 2007;97(12):1690-5.
99. Lapointe J, Kim YH, Miller MA, *et al.* A variant TMPRSS2 isoform and ERG fusion product in prostate cancer with implications for molecular diagnosis. Mod Pathol 2007;20(4):467-73.
100. Rouzier C, Haudebourg J, Carpentier X, *et al.* Detection of the TMPRSS2-ETS fusion gene in prostate carcinomas: retrospective analysis of 55 formalin-fixed and paraffin-embedded samples with clinical data. Cancer Genet Cytogenet 2008;183(1):21-7.
101. Yoshimoto M, Joshua AM, Chilton-Macneill S, *et al.* Three-color FISH analysis of TMPRSS2/ERG fusions in prostate cancer indicates that genomic microdeletion of chromosome 21 is associated with rearrangement. Neoplasia 2006;8(6):465-9.
102. Mehra R, Tomlins SA, Shen R, *et al.* Comprehensive assessment of TMPRSS2 and ETS family gene aberrations in clinically localized prostate cancer. Mod Pathol 2007;20(5):538-44.
103. Saramaki OR, Harjula AE, Martikainen PM, Vessella RL, Tammela TL, Visakorpi T. TMPRSS2:ERG Fusion Identifies a Subgroup of Prostate Cancers with a Favorable Prognosis. Clin Cancer Res 2008;14(11):3395-400.
104. Winnes M, Lissbrant E, Damber JE, Stenman G. Molecular genetic analyses of the TMPRSS2-ERG and TMPRSS2-ETV1 gene fusions in 50 cases of prostate cancer. Oncol Rep 2007;17(5):1033-6.

105. Attard G, Clark J, Ambroisine L, *et al.* Duplication of the fusion of TMPRSS2 to ERG sequences identifies fatal human prostate cancer. Oncogene 2008;27(3):253-63.
106. Wang J, Cai Y, Ren C, Ittmann M. Expression of Variant TMPRSS2/ERG Fusion Messenger RNAs Is Associated with Aggressive Prostate Cancer. Cancer Res 2006;66(17):8347-51.
107. Yoshimoto M, Joshua AM, Cunha IW, *et al.* Absence of TMPRSS2:ERG fusions and PTEN losses in prostate cancer is associated with a favorable outcome. Mod Pathol 2008.
108. Mosquera JM, Perner S, Demichelis F, *et al.* Morphological features of TMPRSS2-ERG gene fusion prostate cancer. J Pathol 2007;212(1):91-101.
109. Tu JJ, Rohan S, Kao J, Kitabayashi N, Mathew S, Chen YT. Gene fusions between TMPRSS2 and ETS family genes in prostate cancer: frequency and transcript variant analysis by RT-PCR and FISH on paraffin-embedded tissues. Mod Pathol 2007;20(9):921-8.
110. Akhavan A, Keith JD, Bastacky SI, Cai C, Wang Y, Nelson JB. The proportion of cores with high-grade prostatic intraepithelial neoplasia on extended-pattern needle biopsy is significantly associated with prostate cancer on site-directed repeat biopsy. BJU Int 2007;99(4):765-9.
111. Arora R, Koch MO, Eble JN, Ulbright TM, Li L, Cheng L. Heterogeneity of Gleason grade in multifocal adenocarcinoma of the prostate. Cancer 2004;100(11):2362-6.
112. Barry M, Perner S, Demichelis F, Rubin MA. TMPRSS2-ERG fusion heterogeneity in multifocal prostate cancer: clinical and biologic implications. Urology 2007;70(4):630-3.
113. Clark J, Attard G, Jhavar S, *et al.* Complex patterns of ETS gene alteration arise during cancer development in the human prostate. Oncogene 2008;27(14):1993-2003.
114. Furusato B, Gao CL, Ravindranath L, *et al.* Mapping of TMPRSS2-ERG fusions in the context of multi-focal prostate cancer. Mod Pathol 2008;21(2):67-75.
115. Mehra R, Han B, Tomlins SA, *et al.* Heterogeneity of TMPRSS2 gene rearrangements in multifocal prostate adenocarcinoma: molecular evidence for an independent group of diseases. Cancer Res 2007;67(17):7991-5.
116. Mehra R, Tomlins SA, Yu J, *et al.* Characterization of TMPRSS2-ETS gene aberrations in androgen-independent metastatic prostate cancer. Cancer Res 2008;68(10):3584-90.
117. Kim JH, Dhanasekaran SM, Mehra R, *et al.* Integrative analysis of genomic aberrations associated with prostate cancer progression. Cancer Res 2007;67(17):8229-39.
118. Lapointe J, Li C, Giacomini CP, *et al.* Genomic profiling reveals alternative genetic pathways of prostate tumorigenesis. Cancer Res 2007;67(18):8504-10.
119. Tomlins SA, Mehra R, Rhodes DR, *et al.* Integrative molecular concept modeling of prostate cancer progression. Nat Genet 2007;39(1):41-51.
120. Tomlins SA, Rhodes DR, Yu J, *et al.* The role of SPINK1 in ETS rearrangement-negative prostate cancers. Cancer Cell 2008;13(6):519-28.
121. Hessels D, Smit FP, Verhaegh GW, Witjes JA, Cornel EB, Schalken JA. Detection of TMPRSS2-ERG fusion transcripts and prostate cancer antigen 3 in urinary sediments may improve diagnosis of prostate cancer. Clin Cancer Res 2007;13(17):5103-8.
122. Laxman B, Morris DS, Yu J, *et al.* A first-generation multiplex biomarker analysis of urine for the early detection of prostate cancer. Cancer Res 2008;68(3):645-9.
123. Laxman B, Tomlins SA, Mehra R, *et al.* Noninvasive detection of TMPRSS2:ERG fusion transcripts in the urine of men with prostate cancer. Neoplasia 2006;8(10):885-8.
124. Mao X, Shaw G, James SY, *et al.* Detection of TMPRSS2:ERG fusion gene in circulating prostate cancer cells. Asian J Androl 2008;10(3):467-73.
125. Tomlins SA, Laxman B, Varambally S, *et al.* Role of the TMPRSS2-ERG gene fusion in prostate cancer. Neoplasia 2008;10(2):177-88.

126. Sun C, Dobi A, Mohamed A, *et al.* TMPRSS2-ERG fusion, a common genomic alteration in prostate cancer activates C-MYC and abrogates prostate epithelial differentiation. Oncogene 2008.
127. Cai C, Hsieh CL, Omwancha J, *et al.* ETV1 is a novel androgen receptor-regulated gene that mediates prostate cancer cell invasion. Mol Endocrinol 2007;21(8):1835-46.
128. Klezovitch O, Risk M, Coleman I, *et al.* A causal role for ERG in neoplastic transformation of prostate epithelium. Proc Natl Acad Sci U S A 2008;105(6):2105-10.

Chapter 2

ARRAY-BASED COMPARATIVE GENOMIC HYBRIDIZATION GUIDES IDENTIFICATION OF *N-COR* AS A NOVEL TUMOR SUPPRESSOR GENE IN PROSTATE CANCER

Karin G. Hermans[1], Hetty A. van der Korput[1], Anke A. Bressers[1], Wytske van Weerden[2], and Jan Trapman[1]
Departments of Pathology[1] and Urology[2], Josephine Nefkens Institute, Erasmus University Medical Center, Rotterdam, The Netherlands
In preparation

ABSTRACT

Prostate cancer is the most common malignancy in men in developed countries. Molecular mechanisms underlying prostate cancer development and progressive growth are not fully understood. Human prostate tumors propagated as xenografts on mice are perfect starting material to search for novel genes involved in prostate cancer. We analyzed genomic DNA of eleven xenografts by array-based comparative genomic hybridization. In eight xenografts eleven homozygous deletions were found: three on chromosome arm 10q, two on 13q, 16q, and 17p, and one on 2q and 8p. Part of these deleted regions contain genes previously implicated in tumorigenesis, including *PTEN* on 10q, *BRCA2* and *RB1* on 13q, and *ATBF1* on 16q. One of the two homozygous deletions on 17p showed deletion of *MKK4*, and the other had lost both copies of *N-COR*. Further analysis identified a second homozygous deletion of both genes in other xenografts. In two more xenograft DNAs one copy of *MMK4* was lost. Mutation or loss of one copy of *N-COR* was detected in four more xenografts. Downregulation of *N-COR*, using specific siRNA, demonstrated stimulated *in vitro* growth of LNCaP prostate cancer cells. These results strongly indicate *N-COR* as a novel tumor suppressor in prostate cancer.

INTRODUCTION

Prostate cancer is the most frequently diagnosed malignancy in men, and the second leading cause of cancer-related death in developed countries (Jemal et al., 2008). Locally confined prostate cancer can be cured by surgery or radiation therapy, however, for metastatic prostate cancer an adequate therapy is not available. Unraveling of the molecular mechanisms of prostate cancer development and progressive growth could provide novel targets for more effective therapies.

In tumor DNAs chromosomal gains indicate the localization of candidate oncogenes and chromosomal losses point to the localization of candidate tumor suppressor genes. Previous studies of chromosomal alterations in prostate cancer have identified multiple frequently affected regions (Saramaki et al., 2006; Sun et al., 2007). Commonly lost regions involve chromosome arms 6q, 8p, 13q, and 16q, less frequently lost regions are on 2q, 5q, 10q, 17p, and 18q. Frequently gained regions are on chromosome arms 7q, and 8q; less frequently gained regions involve 3q, 17q and Xq.

Comparative genomic hybridization (CGH) (Kallioniemi, 2008; Michels et al., 2007) on BAC arrays, cDNA microarrays, or oligonucleotide arrays allows a quantitative analysis of chromosomal copy-number changes at high resolution of the genome. Array CGH was recently used to study genomic alterations in clinical prostate cancer (Kim et al., 2007; Lapointe et al., 2007; Liu et al., 2006; Paris et al., 2004; Paris et al., 2007; Torring et al., 2007; van Dekken et al., 2004; Verhagen et al., 2006; Yano et al., 2004) and in xenografts and cell lines (Clark et al., 2003; Saramaki et al., 2006; Wolf et al., 2004).

Xenografts are powerful models to investigate genetic alterations, because they lack normal cells of human origin. This simplifies the detection of homozygous deletions, high-level amplifications and specific small regions of genomic losses. Previously, we described in xenograft DNAs frequent homozygous deletion of *PTEN* on 10q (Vlietstra *et al*., 1998; Hermans *et al*., 2004), and a homozygous deletion of *WRN* (Van Alewijk et al., 1999). In addition, we showed in three xenografts loss of a small region on 21q that linked *TMPRSS2* to *ERG* in the *TMPRSS2-ERG* fusion gene (Hermans et al., 2006).

In this study we screened the whole genome of prostate cancer xenografts by array CGH for genomic gains and losses, and, more specifically, for novel homozygous deletions. We identified eleven homozygous deletions. Most of these seem to contain genes relevant for tumorigenesis. Three are the previously described deletions of *PTEN* (Vlietstra *et al*., 1998; Hermans *et al*., 2004). The eight new homozygous deletions are on 2q, 8p, 13q (two deletions), 16q (two deletions) and 17p (2 deletions). Three of these homozygous deletions contain known tumor suppressor genes, including *BRCA2*, *RB1* and *ATBF1* (Agalliu *et al*., 2007; Kubota *et al*., 1995; Sun *et al*., 2005). The two homozygous deletions on 17p were subjected to further analysis, which resulted in the detection of additional homozygous deletions. This pointed to *MKK4* and *N-COR* as candidate tumor

suppressor genes. Further structural and functional analyses indicate *NCOR* as the more frequent novel tumor suppressor gene in prostate cancer.

RESULTS

Array CGH analysis of human prostate cancer xenografts

We used 1Mb-spaced genome-wide BAC arrays (Fiegler et al., 2003) to detect alterations in genomic DNA of eleven human prostate cancer xenografts: PCEW, PC82, PC133, PC135, PC295, PC310, PC324, PC329, PC339, PC346 and PC374. Figure 1 summarizes the frequencies of chromosomal regions of gains and losses found. In supplementary Table 1 the positions of the regions of gain and loss are indicated in detail. In total 332 candidate genomic alterations were detected (179 regions of loss and 153 regions of gain, with a log2 T/N <-0.3 or log2 T/N >0.3, respectively, of at least two consecutive BAC clones). The most frequent genomic alterations detected by array CGH, as found in six or more xenograft DNAs, were gains of parts of chromosomes 7 and 8q and losses of part of 8p, 10q, 13q and 16q, reflecting the genomic alterations described in clinical prostate cancers (Saramaki et al., 2006; Sun et al., 2007).

High level amplifications in prostate cancer xenograft DNAs

High-level amplifications (log2 T/N >1.2) were rare in xenograft DNAs. Previously described small, amplified regions on 8q in xenograft PC339 were confirmed (Van Duin

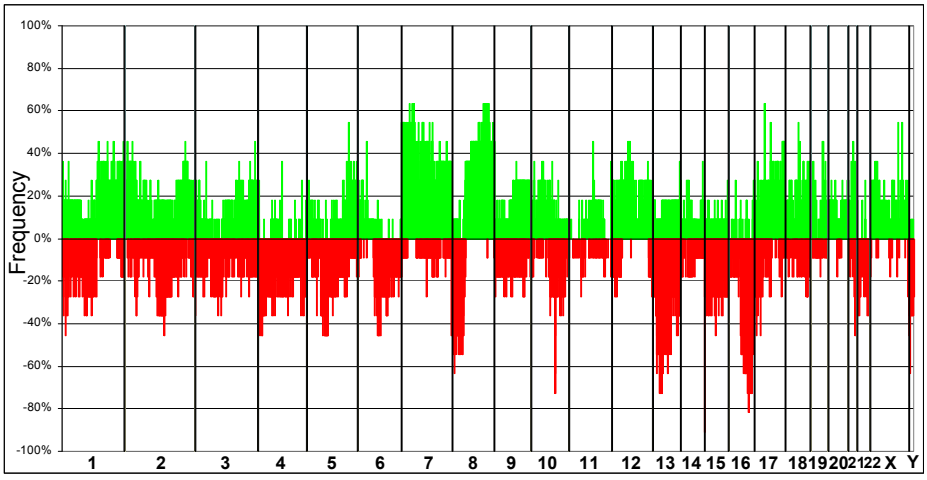

Figure 1. Overview of frequencies of chromosomal regions of gains (green) and losses (red) detected in eleven prostate cancer xenograft DNAs as plotted from 1p telomere to Yq telomere (Log2 T/N <-0.3 was taken as loss; Log2 T/N >0.3 was taken as gain).

Table 1. Characteristics of homozygous deleted regions detected in eleven prostate cancer xenografts

chromosome	HD	Size HD (Mbp)	Loss	Candidate genes
2q37.1	1/11	0.8	1/11	COPS7B, NPPC, ALPP, ALPPL2, ALPI, ECEL1, CHRND, CHRNG,TIGD1,EIF4EL3
8ptel	1/11	1.5	4/11	ZNF596, FBXO25, INMO1, LOC286161, LOC157697, DLGAP2
10q23.3	3/11	0.7-1.2	5/11	PTEN and 13 other genes
13q13.1-q13.2	1/11	1.4	6/11	BRCA2, CG018, PFAAF5, APRIN, KL, DLC2
13q14.2	1/11	0.9	7/11	ITM2B, RB1, P2RY5, CHC1L, CYSTRL2
16q22.2-q22.3	1/11	0.6	8/11	ATBF1
16q23.1	1/11	0.4	7/11	WWOX
17p11.2-p12	1/11	1.0	2/11	MKK4, MYOCD, KIAA0672
17p11.2-p12	1/11	0.8	2/11	DNAH9, ZNF18, MKK4
17p11.2-p12	1/11	1.8	3/11	N-COR and eleven other genes
17p11.2-p12	1/11	0.7	3/11	N-COR and six other genes

et al., 2005). Two small high-level amplifications (5-6 Mbp) were found in PCEW DNA on 3q22.1-q22.3 and 3q29, respectively. *PIK3CB* and *MRAS* are candidate oncogenes located in the 3q22.1-q22.3 interval, in the other amplified region a candidate oncogene cannot be defined.

Small regions of loss

The frequently lost regions of 8p, 13q and 16q mostly involve large parts of these chromosome arms. However, losses of chromosome 10q in some samples concern a small region of ~2 Mbp, spanning three BAC clones, where the tumor suppressor gene *PTEN* is located (Supplementary Table 1). Like for *PTEN* small regions of loss might indicate the positions of other tumor suppressor genes, particularly in those chromosomal regions that show frequent loss of large fragments in the other xenografts DNAs. These small regions of loss might also add information to that obtained from homozygous deletions. Moreover, the loss of exactly the same genomic region might be indicative of an interstitial deletion resulting in a fusion gene, as previously described in the xenograft DNAs for the *TMPRSS2-ERG* fusion gene on 21q (Hermans *et al*., 2006).

We found by array CGH 34 regions of loss that were smaller than 5 Mbp (two to five consecutive BACs with a Log2 T/N <-0.3) (Supplementary Table 1). Three of those involved loss of exactly the same four BACs, which fused the first part of *TMPRSS2* to the last part of *ERG* on 21q, as previously described (Hermans *et al.*, 2006). We could not detect another similar region of loss of exactly the same fragment in other parts of the genome of multiple xenografts. However, in two xenografts (PC82 and PC329) small partially overlapping regions of loss on 13q2.1-q22.2 were found. The common gene present in both genomic fragments was *KLF5*. Also, a small region of loss in PC82 that overlapped with a homozygous deletion in PC310 on 13q14 in the *BRCA2-DLC2*

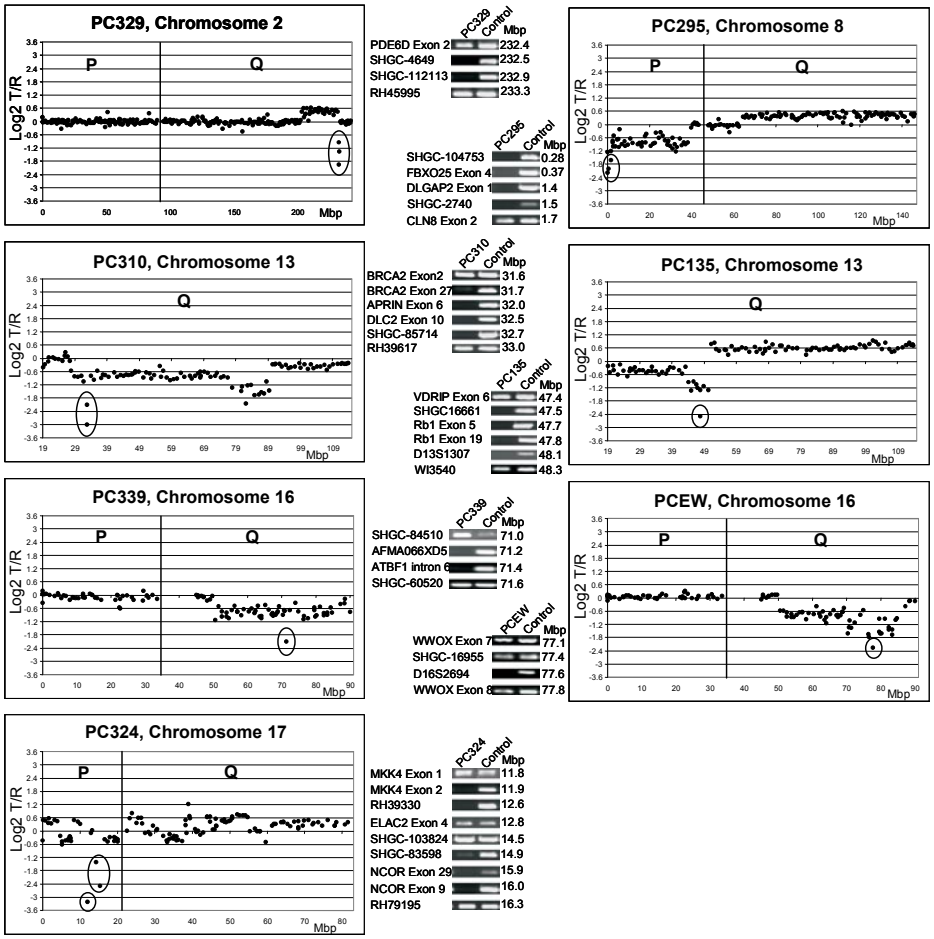

Figure 2. Mapping of eight novel homozygous deletions in the prostate cancer xenografts. Individual graphs of chromosomes with homozygous deletion (circled) are shown. Confirmation of the homozygous deleted region was by PCR analysis. PCR of xenograft DNA with homozygous deletion and a control are depicted.

region was detected (Supplementary Table 1 and Figure 2). A similar combination was found for a region of loss and a homozygous deletion on 16q22, in PC329 and PC339, including *ATBF1*. Many small regions of loss are not located on chromosomes that are frequently lost in prostate cancer. Most promising candidate tumor suppressor genes in these fragments are *MTSS1* (8q) (Loberg et al., 2005), *KAI1* (11p) (Bouras and Frauman, 1999), and *ATM* (11q) (Meyer et al., 2007).

Identification of homozygous deleted regions

We focused the analysis of the array CGH data on homozygous deletions as most reliable landmarks of tumor suppressor genes. Seventeen candidate regions with a log2

T/N ratio below -1.5, indicative of a homozygous deletion were detected. Eleven of these regions were confirmed as homozygous deletions by PCR with primers mapping in these genomic fragments. Graphs of the chromosomes with confirmed homozygous deletions and PCR data of eight homozygous deletions are depicted in Figure 2. More details of the homozygous deletions are given in Table 1. We excluded in the analyses three previously extensively described homozygous deletions of *PTEN* (Hermans *et al.*, 2004; Vlietstra *et al.*, 1998). One of the novel homozygous deletions was on 2q, one on 8p, two were on 13q, two on 16q, and two on 17p (Figure 2). Genes in the eight novel homozygous deletions were assayed by PCR in all other xenograft DNAs for overlapping homozygous deletions that were missed on the BAC arrays. However except for 17p, no additional overlapping homozygous deletions were found (see below). Moreover, all genes, except one-exon genes, located within the homozygous deleted regions were checked for mRNA expression in all xenografts to find substantial downregulation of candidate tumor suppressor genes by epigenomic mechanisms. Gene expressions were compared to mRNA expression in the normal prostate (Supplementary Table 2).

On 2q37.1 a homozygous deletion of ~800 kbp was detected in PC329 DNA. Ten genes map in this region (Table 1). The homozygous deletion is located adjacent to a region of gene copy number gain. Only two out of the ten genes in the homozygous deletion were expressed in xenografts. The other eight genes showed no expression, and were also not expressed in the normal prostate (Supplementary Table 2). In xenograft PC295 DNA a homozygous deletion of telomeric 8p was discovered (Figure 2). In this 1.5 Mbp region six genes are located (Table 1). Five genes were expressed in the prostate, but none of the genes was downregulated. None of the genes in the homozygous deletions on 2q and 8p seems a candidate tumor suppressor gene.

On 13q, two different homozygous deletions were found. The homozygous deletion on 13q13.1-q13.2 in PC310 DNA was ~1.4 Mbp, and was also part of large regions of genomic loss in six other xenograft DNAs. It contained seven genes (Figure 2 and Table 1) with *BRAC2*, *APRIN*, *KL* and *DLC2* as important candidate tumor suppressor genes. Except for *KL*, none of these genes was considerably downregulated in other xenografts (Supplementary Table 2).

A homozygous deletion of 0.9 Mbp on 13q14.2 in PC135 contained five genes (Figure 2). It was also part of a larger region of loss in seven other xenografts DNAs. *RB1* is the most important tumor suppressor gene in this fragment. None of the xenografts without a homozygous deletion for this region showed downregulation of the five genes.

Chromosome arm 16q contained two homozygous deletions. The first was on 16q22.2-q22.3 in PC339 DNA (Figure 2). This ~600 kbp genomic fragment harbored *ATBF1* as only gene. Loss of one copy of *ATBF1* was detected in eight other xenografts. In PC329 this region of loss is very small (~2 Mbp; see Supplementary Table 1). *ATBF1* contains a highly polymorphic polypyrimidine tract (poly(T)$_n$) in intron 8 near the splice acceptor

site of exon 9, which affects correct splicing (Sun et al., 2005). Sequencing of the poly(T)$_n$ tract in all xenograft DNAs detected shortened poly(T)$_n$, both 13Ts instead of 16Ts, in two xenografts (PC346 and PC374). This indeed resulted in alternative splicing of *ATBF1* mRNAs (data not shown). Both xenografts DNAs show also microsatellite instability and a defective mismatch repair system. Except for PC339, *ATBF1* mRNA expression was detected in all other xenografts.

A second homozygous deletion on 16q (~400 kbp) in PCEW was mapped on 16q23.1. This homozygous deletion is located in large intron 7 of the *WWOX* gene (Figure 2). Here also maps the fragile site FRA16D (Buttel et al., 2004; Palakodeti et al., 2004). In seven xenografts loss of one copy of *WWOX* was found. Expression analysis showed presence of *WWOX* mRNA in all xenografts (Supplementary Table 2).

Characterization of the homozygous deletions on chromosome 17p

In the genomic DNA of xenograft PC324 two homozygous deleted regions on 17p11.2-p12 were detected (Figures 2 and 3), one of ~1.0 Mb and the other of ~1.8 Mbp. PCR analysis of the first deleted DNA fragment identified in the other xenografts one more homozygous deletion in xenograft PC295 (Figure 3a,b). This homozygous deletion (~0.8 Mbp) was not detected by array CGH. One of the breakpoints of both homozygous deletions in xenografts PC295 and PC324 is in intron 1 of the *MKK4* gene, but the deletions do not overlap (Figure 3b). We detected loss of one copy of *MKK4* in two additional xenografts (PCEW and PC82). Because *MKK4* is the only gene deleted in both PC295 and PC324, we limited gene expression analysis to this gene. Expression analysis by QPCR confirmed absence of expression in the xenografts with the homozygous deletions, however, in all other xenografts *MKK4* mRNA was present (Figure 3c). The eleven exons of *MKK4* were sequenced in all xenograft DNAs, but no inactivating mutations were detected.

The second homozygous deletion in PC324 DNA on 17p11.2-p12 detected on the BAC arrays mapped very close to the first one. Again, PCR analysis of the DNAs of all xenografts resulted in the detection of an overlapping homozygous deletion, now in xenograft PC133 DNA (~0.7 Kbp, Figure 3b). This homozygous deletion, like the one in xenograft PC295 on 17p, was not detected by array CGH, because it was located between two BACs. The two homozygous deletions overlapped in *N-COR*. Three xenografts, PCEW, PC82 and PC295, showed loss of one copy of *N-COR*. mRNA expression analysis showed absence of expression in PC133 and PC324, however, in the other xenografts *N-COR* was expressed (Figure 3c).

Because the original clinical prostate tumor material of xenograft PC324 was available, we also performed array CGH on this DNA sample. We detected the homozygous deletion on 10q (*PTEN*) and both homozygous deletions on 17p (*MKK4* and *N-COR*) in this material (data not shown).

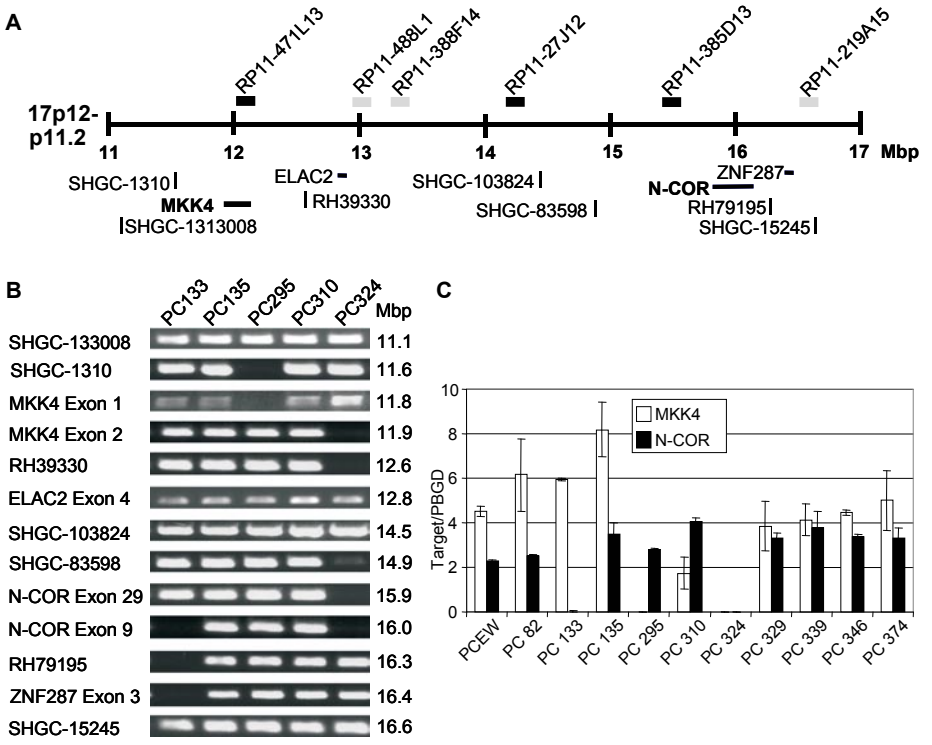

Figure 3. Characterization of two homozygous deleted regions on chromosome arm 17p. (A) Schematic representation of the genomic region where both homozygous deletions map. In black, BACs that are located in the homozygous deletions in DNA of PC324. (B) PCR analysis of the 17p region showing two homozygous deletions in PC324, one in PC295 and one in PC133. (C) Expression analysis of *MKK4* and *N-COR* as assessed by QPCR. Duplicate experiments relative to *PBGD* are presented; bars indicate standard deviations.

Structural and functional analysis of N-COR

We sequenced the DNA of all xenografts for exons 2-46 of *N-COR*, representing the coding region, complemented with five human prostate cancer cell lines: PC3, LNCaP, DU145, 22Rv1 and MDA Pca 2b. We detected one missense mutation in xenograft PC346 (GCA->GTA) in exon 13 that encodes the DAD domain of N-COR, and two frame-shift mutations, in xenograft PC346 (del A in exon 15) and in cell line MDA Pca 2b (del TC in exon 17). Both frame-shift mutations will result in the synthesis of a truncated N-COR protein. From sequencing of a cloned fragment of part of the *N-COR* cDNA (exons 12-16) of PC346 we deduced that the two mutations in *N-COR* were in the same allele, leaving expression of one wild type allele. MDA Pca 2b also expresses a wild type allele and a mutant allele.

Next, we investigated the effect of *N-COR* downregulation by siRNA on growth of the prostate cancer cell line LNCaP. Western blot analysis showed that LNCaP cells transfected

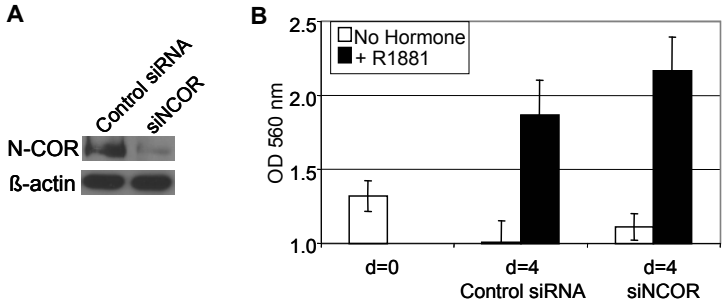

Figure 4. Effect of downregulation of N-COR protein by siRNA on proliferation of the prostate cancer cell line LNCaP. (A) Western blot of LNCaP cells transfected with N-COR siRNA or control siRNA showing N-COR expression. Actin is the loading control. (B) Proliferation of LNCaP cells transfected with N-COR siRNA or control siRNA as measured by MTT assay at day 0 and at day 4. Cells were cultured with or without the synthetic androgen R1881 (10^{-10}M). Bars indicate standard deviation. Statistical analysis was done with the Student's T-test; in the absence of R1881: p=0.11; in the presence of R1881: p=0.025.

with *N-COR* siRNA had downregulated N-COR protein expression (Figure 4a). Growth experiments indicated that *N-COR* downregulation had a small, but significant growth advantage on LNCaP cells in presence of the synthetic androgen R1881, compared to cells transfected with control siRNA (p=0.025, Figure 4b). In absence of hormone the difference in growth rate was not significant (p=0.11).

DISCUSSION

Molecular mechanisms underlying human prostate cancer development and progressive growth are only partially understood. For several of the chromosomal alterations detected in primary tumors and in late stage prostate cancer, the genes involved remain unknown. In the present study we investigated eleven human prostate cancer xenografts for chromosomal alterations. The xenografts represent a variety of clinical prostate cancer stages (van Weerden *et al.*, 1996). Xenografts are available in unlimited quantities and lack normal cells of human origin, which simplifies the detection and further characterization of genomic alterations, particularly homozygous deletions. Frequent genomic alterations detected by array CGH in the prostate cancer xenografts in this study coincided with alterations described in clinical prostate cancer specimens (Sun *et al*., 2007), confirming that the xenografts are powerful and representative models for studying molecular defects in prostate cancer.

Most of the eleven homozygous deletions described in this study were found on chromosomes that are frequently lost in prostate cancer (see Figures 1 and 2), which strengthens a possible role in tumorigenesis. Previously, we described the homozygous deletions on 10q, where *PTEN* maps (Hermans *et al.*, 2004; Vlietstra *et al.*, 1998). In the

array CGH experiments we missed two previously identified homozygous deletions, one on 8p in PC133, containing *WRN* (Van Alewijk *et al.*, 1999) and, not unexpected, a 30 kbp homozygous deletion containing exon 5 of *PTEN* in PC295 (Hermans *et al.*, 2004). In addition, we found out that we missed on the arrays two homozygous deletions on 17p, one containing *MKK4* and a second one containing *N-COR* (this study). Although it can be presumed that more, mainly small, homozygous deletions have been missed, it is likely that we have identified the majority of the most frequent genomic alterations.

Obviously, with as exception the unique small interstitial deletion of *TMPRSS2-ERG* on 21q (Hermans *et al.*, 2006), array CGH was not able to identify gene fusions or chromosomal translocations, genomic duplications or inversions. Identification of these specific genomic alterations needs more sophisticated technological approaches. Recently developed massive parallel sequencing of tumor DNAs compared to normal DNAs seems such a promising tool (Campbell *et al.*, 2008; Korbel *et al.*, 2007).

For both the homozygous deletion on 2q in PC329 and the telomeric homozygous deletion on 8p in PC295, we lack evidence that they play a role in prostate cancer. The positions of the breakpoints suggest that both deletions originated during chromosomal translocations. The absence of obvious candidate tumor suppressor genes in the deletions supports this hypothesis.

In clinical prostate cancer loss of 13q is frequently detected. Three separate regions on 13q14, 13q21-q22 and 13q33 have been suggested to harbor candidate tumor suppressor genes (Dong *et al*., 2001; Hyytinen *et al*., 1999; Wolf *et al*., 2004). We detected two different homozygous deletions, on 13q13.1-q13.2 and on 13q14.2, respectively. One of these might overlap with the previously described minimal lost fragment on 13q14. The 13q21-q22 region might contain *KLF5*, as also identified in the present study (see Results section). *KLF5* has previously been described as frequently deleted and downregulated in intestinal and prostate cancers (Bateman *et al*., 2004; Chen *et al*., 2003).

The genomic fragment on 13q13.1-q13.2 contains the *BRCA2* tumor suppressor gene, which previously has been indicated as a candidate susceptibility gene for hereditary prostate cancer (Edwards *et al*., 2003; Gayther *et al*., 2000; Latil *et al*., 1996). Carriers of *BRCA2* mutations have an elevated risk for developing prostate cancer with a more aggressive phenotype (Agalliu *et al.*, 2007; Narod *et al.*, 2008). Remarkably, the homozygous deletion on 13q13.1-q13.2 contains in addition to *BCRA2*, three more candidate tumor suppressor genes: *DLC2*, *APRIN* and *KL*. *DLC2* is downregulated in multiple tumors (Ullmannova *et al*., 2006). It encodes a Rho GTPase activating protein presumed to play a role in growth suppression (Ching *et al.*, 2003; Leung *et al*., 2005). *APRIN*, also known as *AS3*, has a critical role in proliferative arrest in the G0/G1 phase of the cell cycle (Geck *et al*., 2000; Maffini *et al*., 2002). More recently, it has been reported that *APRIN* may function as a regulator of chromatin architectural structure, and as a mediator of hormone-induced chromatin changes in differentiation and cancer (Maffini *et al*., 2008). The only

gene within this region that is downregulated in part of the other xenografts is *KL* or Klotho. *Klotho* knockout mice exhibit multiple phenotypes that resemble human aging. *KL* is also able to suppress the action of IGFs, which are associated with cancer, and can protect cells from oxidative stress. However, the exact mechanisms underlying these activities remain to be elucidated (Tsujikawa *et al.*, 2003; Kurosu *et al*., 2005, Wang *et al*., 2006). Obviously, this small genomic region with many candidate tumor suppressor genes can be very important for further study in clinical prostate cancer.

In the homozygous deletion on 13q14.2 the main candidate tumor suppressor gene is *RB1* (Konishi *et al*., 2002; Kubota *et al*., 1995; Latil *et al*., 1999). Loss of *RB1* has previously been associated with prostate cancer and might be an early event (Kubota *et al*., 1995; Phillips *et al*., 1994). Other candidate tumor suppressor genes that map in the same fragment are *ITMB2* (Latil *et al*., 2003) and *CHC1L* (Latil *et al*., 2002). These genes have been proposed as candidate tumor suppressor genes based on the finding that they have reduced mRNA expression in prostate tumors, but this was not clear from our data. More recently, *P2RY5* that maps in *RB1* intron 17 has been indicated as a novel candidate tumor suppressor gene (Kim *et al*., 2007, Crawford *et al*., 2008). However, further structural and functional analysis of this gene is needed to substantiate this observation.

On 16q we also identified two homozygous deleted regions. In the region on 16q22.2-q22.3 only *ATBF1* is located. The transcription factor *ATBF1* has first been indicated as a candidate tumor suppressor gene in gastric cancers and Hodgkin's lymphomas (Kataoka *et al*., 2001; Schwering *et al*., 2003) and more recently in breast and prostate cancers (Sun *et al*., 2005; Zhang *et al*., 2005). In the second region on 16q, the homozygous deletion consists of a large part of intron 7 of the putative tumor suppressor gene *WWOX* and spans the fragile site FRA16D (Bednarek *et al*., 2001; Paige *et al*., 2001). *WWOX* is frequently affected by translocation and homozygous deletion in multiple tumors. However, we observed normal mRNA expression in all the xenografts.

In two xenografts homozygous deletion of *MKK4* on 17p were detected. MKK4 is a stress activated protein kinase with as targets JNK and p38. *MKK4* has been described as a metastasis suppressor gene in prostate and ovarian cancer (Taylor *et al*., 2008, Whitmarsh *et al*., 2007). *MKK4* expression is inversely correlated with Gleason score in primary prostate cancer (Kim *et al*., 2001; Yoshida *et al*., 1999). *MKK4* was one of the two genes that we studied in more detail. However, besides the two homozygous deletions we did not detect inactivating *MKK4* mutations or *MKK4* downregulation. Loss of one copy of *MKK4* was observed in two xenografts (PCEW and PC82). We also carried out a preliminary study on *MKK4* inactivation in clinical prostate cancer. By array CGH we found in 4 out of 17 clinical samples loss of the part of 17p where *MKK4* maps (data not shown). Robinson *et al* reported absence of correlation between *MKK4* mutation or (homozygous) deletion and MKK4 protein expression (Robinson *et al*., 2007). They also showed that translational regulation is critical in determining MKK4 protein levels. Combined these data warrant

further analysis of *MKK4* in prostate cancer, including functional studies and expression analysis.

The other two overlapping homozygous deletions on 17q contained *N-COR* as candidate tumor suppressor gene. Further analysis showed frequent loss or mutation of one copy of *N-COR* in xenografts or cell lines. Preliminary analyses of clinical prostate cancer showed loss of one copy of *N-COR* in 4 out of 17 recurrent prostate tumors (data not shown). These findings are indicative for *N-COR* as the most frequent inactivated tumor suppressor gene in this part of 17p.

N-COR is a well-known co-repressor of nuclear receptors, including the AR (Jepsen and Rosenfeld, 2002). However, it has also been shown that N-COR can be recruited by many other transcription factors. N-COR is a component of a multiple protein complex containing histone deacetylases (HDACs), which inhibits gene expression (Jepsen and Rosenfeld, 2002).

We showed that downregulation of *N-COR* expression in LNCaP cells by siRNA transfection resulted in a growth advantage for these cells in presence of the synthetic androgen R1881 (Figure 4). So far, a role of *N-COR* in prostate cancer was unknown. A previous study revealed that decreased N-COR protein expression correlated with acquired tamoxifen resistance in a breast cancer mouse model (Lavinsky *et al*., 1998). Moreover, in breast cancer a low level of *N-COR* mRNA expression seems associated with shorter disease-free survival (Girault *et al*., 2003; Zhang *et al*., 2005).

In conclusion, in this study we showed that genome-wide analysis of xenograft DNAs by array CGH is an effective method to detect genomic alterations, including homozygous deletions, in prostate cancer. Our results support the importance of multiple tumor suppressor genes on 13q and of *MKK4* on 17p in prostate cancer. Moreover our findings indicate that *N-COR* is a novel candidate tumor suppressor gene in prostate cancer.

MATERIALS AND METHODS

Prostate cancer derived xenografts

The in vivo growing xenografts PCEW, PC82, PC133, PC135, PC295, PC310, PC324, PC329, PC339, PC346, and PC374 were propagated on male nude mice (Hoehn *et al*., 1980; Hoehn *et al*., 1984; van Weerden *et al*., 1996)

DNA and RNA preparation

Genomic DNA from xenografts and cell lines was isolated using the Puregene system from Gentra Systems (Minneapolis, MN) according to the procedure described by the manufacturer. Cell line RNA was isolated by the guanidium isothiocyanate procedure;

xenograft RNA was isolated according to the LiCl protocol (Sambrook and Russell, 2001). The mRNA from normal prostate tissue was purchased from Clontech (Palo Alto, CA)

Array-based CGH

Arrays were produced from the human 3600 BAC/PAC genomic clone set of the Welcome Trust Sanger Institute, covering the full genome at approximately 1 Mb-spacing. Degenerated oligonucleotide PCR-products were prepared for spotting on CodeLink® slides (Amersham Biosciences, Piscataway, NJ) according to published protocols (Fiegler *et al*., 2003) with some modifications (Knijnenburg *et al*., 2004). DNA labeling and hybridization were performed essentially as described (Fiegler *et al*., 2003) with minor modifications. After hybridization arrays were scanned in a ScanArray Express HT (Perkin Elmer, Freemont, CA). The resulting images were analyzed with GenePix Pro 5.0 software (Axon Instruments, Foster City, CA) and subsequently visualized with an excel macro (Knijnenburg *et al*., 2004).

PCR analysis of genomic DNA

Standard polymerase chain reaction (PCR) amplification utilizing Taq polymerase (Promega, Madison, WI) included 35 cycles of 1 min at 95°C, 1 min 55°C, and 1 min 72°C. PCR amplifications were performed in a 50µl reaction volume. The amplified fragments were separated on a 2% agarose gel. Primers used for homozygous deletion screening are available on request.

mRNA Expression

Analysis of mRNA expression was performed by semiquantitative RT-PCR or QPCR. cDNA was synthesized on 2 µg of RNA template using M-MLV RT (Invitrogen Life Technologies, Carlsbad, CA) and an oligo$(dT)_{12}$ primer. Specific cDNA fragments were amplified by standard PCR for 30 cycles and separated on a 2% agarose gel. QPCR was performed in Power Sybr green PCR master mix (Applied Biosystems, Foster City, CA) containing 0.33 µmol/L forward and reverse primer in an ABI 7700 Sequence Detection System. Amplified products were quantified relative to porphobilinogen deaminase (*PBGD*) by the standard curve method. Gene-specific RT-PCR/QPCR primers are available on request.

Sequence analysis

PCR products from exon 2-46 of *N-COR* and of exon 1-11 from *MKK4* were purified using SAP/ExoI (USB, Amersham Biosciences) according to the manufacturers' protocol. Fragments were sequenced using the ABI Prism BigDye terminator v3.1 ready reaction cycle sequencing kit (Applied Biosystems). Primers for PCR and sequencing are available on request. Sequence reactions were run on the ABI PRISM 3100 Genetic Analyzer (Applied Biosystems).

siRNA proliferation assay

Equal amounts of LNCaP cells grown on DMEM charcoal stripped FCS were on day 0 transfected with *N-COR* siRNA (SmartPool, Thermo Scientific, Lafayette, CO) or control siRNA using Dharmafect 3 (Thermo Scientific), according to the manufacturers' instruction. Cells were grown with or without 10^{-10} M R1881. At days 0 and 4 Thiazolyl blue tetrazolium bromide dissolved in PBS (MTT reagent; AppliChem, Darmstadt, Germany) was added and after 4h cells were harvested. Cells were suspended in DMSO-Sörensen buffer and OD 570 nm was measured. Statistical significance is calculated with a Student's T-test (SPSS, Chicago, IL).

Western blot analysis

For Western blot analysis LNCaP cells were transfected with *N-COR* siRNA or control siRNA using Dharmafect 3. Cells were harvested after 48h. Western blot analysis was carried out using standard procedures using N-COR (Santa Cruz, Santa Cruz, CA) and β-actin loading control (Sigma, Zwijndrecht, The Netherlands) antibodies. Protein bands were visualized by chemiluminesence (Pierce, Rockford, IL).

ACKNOWLEGDMENTS

The authors thank Hans Tanke (LeidenUniversity Medical Centre, Leiden, The Netherlands) for the 1 Mb spaced genome-wide BAC arrays.

REFERENCES

Agalliu I, Karlins E, Kwon EM, Iwasaki LM, Diamond A, Ostrander EA *et al* (2007). Rare germline mutations in the BRCA2 gene are associated with early-onset prostate cancer. *Br J Cancer* **97:** 826-31.

Bateman NW, Tan D, Pestell RG, Black JD, Black AR (2004). Intestinal tumor progression is associated with altered function of KLF5. *J Biol Chem* **279:** 12093-101.

Bednarek AK, Keck-Waggoner CL, Daniel RL, Laflin KJ, Bergsagel PL, Kiguchi K *et al* (2001). WWOX, the FRA16D gene, behaves as a suppressor of tumor growth. *Cancer Res* **61:** 8068-73.

Bouras T, Frauman AG (1999). Expression of the prostate cancer metastasis suppressor gene KAI1 in primary prostate cancers: a biphasic relationship with tumour grade. *J Pathol* **188:** 382-8.

Buttel I, Fechter A, Schwab M (2004). Common fragile sites and cancer: targeted cloning by insertional mutagenesis. *Ann N Y Acad Sci* **1028:** 14-27.

Campbell PJ, Stephens PJ, Pleasance ED, O'Meara S, Li H, Santarius T *et al* (2008). Identification of somatically acquired rearrangements in cancer using genome-wide massively parallel paired-end sequencing. *Nat Genet* **40:** 722-9.

Chen C, Bhalala HV, Vessella RL, Dong JT (2003). KLF5 is frequently deleted and down-regulated but rarely mutated in prostate cancer. *Prostate* **55:** 81-8.

Ching YP, Wong CM, Chan SF, Leung TH, Ng DC, Jin DY *et al* (2003). Deleted in liver cancer (DLC) 2 encodes a RhoGAP protein with growth suppressor function and is underexpressed in hepatocellular carcinoma. *J Biol Chem* **278:** 10824-30.

Clark J, Edwards S, Feber A, Flohr P, John M, Giddings I *et al* (2003). Genome-wide screening for complete genetic loss in prostate cancer by comparative hybridization onto cDNA microarrays. *Oncogene* **22:** 1247-52.

Dong JT, Boyd JC, Frierson HF, Jr. (2001). Loss of heterozygosity at 13q14 and 13q21 in high grade, high stage prostate cancer. *Prostate* **49:** 166-71.

Edwards SM, Kote-Jarai Z, Meitz J, Hamoudi R, Hope Q, Osin P *et al* (2003). Two percent of men with early-onset prostate cancer harbor germline mutations in the BRCA2 gene. *Am J Hum Genet* **72:** 1-12.

Fiegler H, Carr P, Douglas EJ, Burford DC, Hunt S, Scott CE *et al* (2003). DNA microarrays for comparative genomic hybridization based on DOP-PCR amplification of BAC and PAC clones. *Genes Chromosomes Cancer* **36:** 361-74.

Gayther SA, de Foy KA, Harrington P, Pharoah P, Dunsmuir WD, Edwards SM *et al* (2000). The frequency of germ-line mutations in the breast cancer predisposition genes BRCA1 and BRCA2 in familial prostate cancer. The Cancer Research Campaign/British Prostate Group United Kingdom Familial Prostate Cancer Study Collaborators. *Cancer Res* **60:** 4513-8.

Geck P, Maffini MV, Szelei J, Sonnenschein C, Soto AM (2000). Androgen-induced proliferative quiescence in prostate cancer cells: the role of AS3 as its mediator. *Proc Natl Acad Sci U S A* **97:** 10185-90.

Hermans KG, van Alewijk DC, Veltman JA, van Weerden W, van Kessel AG, Trapman J (2004). Loss of a small region around the PTEN locus is a major chromosome 10 alteration in prostate cancer xenografts and cell lines. *Genes Chromosomes Cancer* **39:** 171-84.

Hermans KG, van Marion R, van Dekken H, Jenster G, van Weerden WM, Trapman J (2006). TMPRSS2:ERG fusion by translocation or interstitial deletion is highly relevant in androgen-dependent prostate cancer, but is bypassed in late-stage androgen receptor-negative prostate cancer. *Cancer Res* **66:** 10658-63.

Hoehn W, Schroeder FH, Reimann JF, Joebsis AC, Hermanek P (1980). Human prostatic adenocarcinoma: some characteristics of a serially transplantable line in nude mice (PC 82). *Prostate* **1:** 95-104.

Hoehn W, Wagner M, Riemann JF, Hermanek P, Williams E, Walther R *et al* (1984). Prostatic adenocarcinoma PC EW, a new human tumor line transplantable in nude mice. *Prostate* **5:** 445-52.

Hyytinen ER, Frierson HF, Jr., Boyd JC, Chung LW, Dong JT (1999). Three distinct regions of allelic loss at 13q14, 13q21-22, and 13q33 in prostate cancer. *Genes Chromosomes Cancer* **25:** 108-14.

Jemal A, Siegel R, Ward E, Hao Y, Xu J, Murray T *et al* (2008). Cancer statistics, 2008. *CA Cancer J Clin* **58:** 71-96.

Jepsen K, Rosenfeld MG (2002). Biological roles and mechanistic actions of co-repressor complexes. *J Cell Sci* **115:** 689-98.

Kallioniemi A (2008). CGH microarrays and cancer. *Curr Opin Biotechnol* **19:** 36-40.

Kataoka H, Miura Y, Joh T, Seno K, Tada T, Tamaoki T *et al* (2001). Alpha-fetoprotein producing gastric cancer lacks transcription factor ATBF1. *Oncogene* **20:** 869-73.

Kim HL, Vander Griend DJ, Yang X, Benson DA, Dubauskas Z, Yoshida BA *et al* (2001). Mitogen-activated protein kinase kinase 4 metastasis suppressor gene expression is inversely related to histological pattern in advancing human prostatic cancers. *Cancer Res* **61:** 2833-7.

Kim JH, Dhanasekaran SM, Mehra R, Tomlins SA, Gu W, Yu J *et al* (2007). Integrative analysis of genomic aberrations associated with prostate cancer progression. *Cancer Res* **67:** 8229-39.

Knijnenburg J, Szuhai K, Giltay J, Molenaar L, Sloos W, Poot M *et al* (2004). Insights from genomic microarrays into structural chromosome rearrangements. *Am J Med Genet* **132A**:36-40

Konishi N, Nakamura M, Kishi M, Nishimine M, Ishida E, Shimada K (2002). Heterogeneous methylation and deletion patterns of the INK4a/ARF locus within prostate carcinomas. *Am J Pathol* **160:** 1207-14.

Korbel JO, Urban AE, Affourtit JP, Godwin B, Grubert F, Simons JF *et al* (2007). Paired-end mapping reveals extensive structural variation in the human genome. *Science* **318:** 420-6.

Kubota Y, Fujinami K, Uemura H, Dobashi Y, Miyamoto H, Iwasaki Y *et al* (1995). Retinoblastoma gene mutations in primary human prostate cancer. *Prostate* **27:** 314-20.

Lapointe J, Li C, Giacomini CP, Salari K, Huang S, Wang P *et al* (2007). Genomic profiling reveals alternative genetic pathways of prostate tumorigenesis. *Cancer Res* **67:** 8504-10.

Latil A, Bieche I, Pesche S, Volant A, Valeri A, Fournier G *et al* (1999). Loss of heterozygosity at chromosome arm 13q and RB1 status in human prostate cancer. *Hum Pathol* **30:** 809-15.

Latil A, Chene L, Mangin P, Fournier G, Berthon P, Cussenot O (2003). Extensive analysis of the 13q14 region in human prostate tumors: DNA analysis and quantitative expression of genes lying in the interval of deletion. *Prostate* **57:** 39-50.

Latil A, Cussenot O, Fournier G, Lidereau R (1996). The BRCA2 gene is not relevant to sporadic prostate tumours. *Int J Cancer* **66:** 282-3.

Latil A, Morant P, Fournier G, Mangin P, Berthon P, Cussenot O (2002). CHC1-L, a candidate gene for prostate carcinogenesis at 13q14.2, is frequently affected by loss of heterozygosity and underexpressed in human prostate cancer. *Int J Cancer* **99:** 689-96.

Leung TH, Ching YP, Yam JW, Wong CM, Yau TO, Jin DY *et al* (2005). Deleted in liver cancer 2 (DLC2) suppresses cell transformation by means of inhibition of RhoA activity. *Proc Natl Acad Sci USA* **102:** 15207-12.

Liu W, Chang B, Sauvageot J, Dimitrov L, Gielzak M, Li T *et al* (2006). Comprehensive assessment of DNA copy number alterations in human prostate cancers using Affymetrix 100K SNP mapping array. *Genes Chromosomes Cancer* **45:** 1018-32.

Loberg RD, Neeley CK, Adam-Day LL, Fridman Y, St John LN, Nixdorf S *et al* (2005). Differential expression analysis of MIM (MTSS1) splice variants and a functional role of MIM in prostate cancer cell biology. *Int J Oncol* **26:** 1699-705.

Maffini M, Denes V, Sonnenschein C, Soto A, Geck P (2008). APRIN is a unique Pds5 paralog with features of a chromatin regulator in hormonal differentiation. *J Steroid Biochem Mol Biol* **108:** 32-43.

Maffini MV, Geck P, Powell CE, Sonnenschein C, Soto AM (2002). Mechanism of androgen action on cell proliferation: AS3 protein as a mediator of proliferative arrest in the rat prostate. *Endocrinology* **143:** 2708-14.

Meyer A, Wilhelm B, Dork T, Bremer M, Baumann R, Karstens JH *et al* (2007). ATM missense variant P1054R predisposes to prostate cancer. *Radiother Oncol* **83:** 283-8.

Michels E, De Preter K, Van Roy N, Speleman F (2007). Detection of DNA copy number alterations in cancer by array comparative genomic hybridization. *Genet Med* **9:** 574-84.

Narod SA, Neuhausen S, Vichodez G, Armel S, Lynch HT, Ghadirian P *et al* (2008). Rapid progression of prostate cancer in men with a BRCA2 mutation. *Br J Cancer* **99:** 371-4.

Paige AJ, Taylor KJ, Taylor C, Hillier SG, Farrington S, Scott D *et al* (2001). WWOX: a candidate tumor suppressor gene involved in multiple tumor types. *Proc Natl Acad Sci U S A* **98:** 11417-22.

Palakodeti A, Han Y, Jiang Y, Le Beau MM (2004). The role of late/slow replication of the FRA16D in common fragile site induction. *Genes Chromosomes Cancer* **39:** 71-6.

Paris PL, Andaya A, Fridlyand J, Jain AN, Weinberg V, Kowbel D *et al* (2004). Whole genome scanning identifies genotypes associated with recurrence and metastasis in prostate tumors. *Hum Mol Genet* **13:** 1303-13.

Paris PL, Sridharan S, Scheffer A, Tsalenko A, Bruhn L, Collins C (2007). High resolution oligonucleotide CGH using DNA from archived prostate tissue. *Prostate* **67:** 1447-55.

Phillips SM, Barton CM, Lee SJ, Morton DG, Wallace DM, Lemoine NR *et al* (1994). Loss of the retinoblastoma susceptibility gene (RB1) is a frequent and early event in prostatic tumorigenesis. *Br J Cancer* **70:** 1252-7.

Saramaki OR, Porkka KP, Vessella RL, Visakorpi T (2006). Genetic aberrations in prostate cancer by microarray analysis. *Int J Cancer* **119:** 1322-9.

Schwering I, Brauninger A, Distler V, Jesdinsky J, Diehl V, Hansmann ML *et al* (2003). Profiling of Hodgkin's lymphoma cell line L1236 and germinal center B cells: identification of Hodgkin's lymphoma-specific genes. *Mol Med* **9:** 85-95.

Sun J, Liu W, Adams TS, Sun J, Li X, Turner AR *et al* (2007). DNA copy number alterations in prostate cancers: a combined analysis of published CGH studies. *Prostate* **67:** 692-700.

Sun X, Frierson HF, Chen C, Li C, Ran Q, Otto KB *et al* (2005). Frequent somatic mutations of the transcription factor ATBF1 in human prostate cancer. *Nat Genet* **37**: 407-12

Torring N, Borre M, Sorensen KD, Andersen CL, Wiuf C, Orntoft TF (2007). Genome-wide analysis of allelic imbalance in prostate cancer using the Affymetrix 50K SNP mapping array. *Br J Cancer* **96:** 499-506.

Tsujikawa H, Kurotaki Y, Fujimori T, Fukuda K, Nabeshima Y (2003). Klotho, a gene related to a syndrome resembling human premature aging, functions in a negative regulatory circuit of vitamin D endocrine system. *Mol Endocrinol* **17:** 2393-403.

Van Alewijk DC, Van der Weiden MM, Eussen BJ, Van Den Andel-Thijssen LD, Ehren-van Eekelen CC, Konig JJ *et al* (1999). Identification of a homozygous deletion at 8p12-21 in a human prostate cancer xenograft. *Genes Chromosomes Cancer* **24:** 119-26.

van Dekken H, Paris PL, Albertson DG, Alers JC, Andaya A, Kowbel D *et al* (2004). Evaluation of genetic patterns in different tumor areas of intermediate-grade prostatic adenocarcinomas by high-resolution genomic array analysis. *Genes Chromosomes Cancer* **39:** 249-56.

van Weerden WM, de Ridder CM, Verdaasdonk CL, Romijn JC, van der Kwast TH, Schroder FH *et al* (1996). Development of seven new human prostate tumor xenograft models and their histopathological characterization. *Am J Pathol* **149:** 1055-62.

Verhagen PC, van Duijn PW, Hermans KG, Looijenga LH, van Gurp RJ, Stoop H *et al* (2006). The PTEN gene in locally progressive prostate cancer is preferentially inactivated by bi-allelic gene deletion. *J Pathol* **208:** 699-707.

Vlietstra RJ, van Alewijk DC, Hermans KG, van Steenbrugge GJ, Trapman J (1998). Frequent inactivation of PTEN in prostate cancer cell lines and xenografts. *Cancer Res* **58:** 2720-3.

Wolf M, Mousses S, Hautaniemi S, Karhu R, Huusko P, Allinen M *et al* (2004). High-resolution analysis of gene copy number alterations in human prostate cancer using CGH on cDNA microarrays: impact of copy number on gene expression. *Neoplasia* **6:** 240-7.

Yano S, Matsuyama H, Matsuda K, Matsumoto H, Yoshihiro S, Naito K (2004). Accuracy of an array comparative genomic hybridization (CGH) technique in detecting DNA copy number aberrations: comparison with conventional CGH and loss of heterozygosity analysis in prostate cancer. *Cancer Genet Cytogenet* **150:** 122-7.

Yoshida BA, Dubauskas Z, Chekmareva MA, Christiano TR, Stadler WM, Rinker-Schaeffer CW (1999). Mitogen-activated protein kinase kinase 4/stress-activated protein/Erk kinase 1 (MKK4/SEK1), a prostate cancer metastasis suppressor gene encoded by human chromosome 17. *Cancer Res* **59:** 5483-7.

Zhang Z, Yamashita H, Toyama T, Sugiura H, Ando Y, Mita K *et al* (2005). ATBF1-a messenger RNA expression is correlated with better prognosis in breast cancer. *Clin Cancer Res* **11:** 193-8.

SUPPLEMENTARY INFORMATION

Table S1. Overview of regions of DNA loss and gain detected in the eleven xenografts by 1Mb spaced genome-wide array CGH

	loss (min. log2 T/R<-0.3))					gain (min. log2 T/R>0.3)				
	Begin (probe)	End (probe)	chr	Begin (bp)	End (bp)	Begin (probe)	End (probe)	chr	Begin (bp)	End (bp)
PCEW	GS-62-L8	RP3-365I19	1	1	141531879					
	RG-228-K22	RP11-91K8	3	1	134771767	RP11-91K8	RP11-397E9	3	134771767	140451436
	RP11-397E9	RP11-298A18	3	140451436	189918727	RP11-56C4	GS-196-F4	3	193863519	198471847
	RP11-575G10	CTD-2174D2	5	42897645	74970806	RP11-72L22	RP1-244J5	5	86340653	136366234
	RP11-114H21	CTD-2323H12	5	135915628	141198799	RP11-25F13	GS-240-G13	5	144610138	180756037
	RP1-234P15	RP1-84N20	6	75947919	125541230	RP11-104I20	RP5-1110E20	17	25071274	36373682
	RP11-295F4	RP11-448D5	6	132876727	137301607	RP11-220N20	RP11-481C4	17	42087499	46634200
	RP11-345K20	GS-137-E24	10	74954877	135313953	RP11-217N19	RP11-112J9	17	49753469	52172780
	RP11-44F24	GS-221-K18	12	120246686	133387831	RP11-19F16	RP11-342K2	17	52616475	57473353
	RP11-424K7	RP11-533D19	16	49618230	88643456					
	GS-202-L17	RP11-471L13	17	1	12108967					
	RP1-27J12	RP11-403E9	17	14364543	25693265					
	RP11-193B6	GS-2-H14	21	13462479	46900000					
	XX-p8708	RP3-515N1	22	15615802	30027385					
	CTA-397C4	GS-3018-K1	22	43154478	50100000					
PC82	GS-62-L8	RP4-631H13	1	1	53133031	RP11-292A20	RP11-111J6	2	4295218	18724913
	RP11-172I6	RP11-15G16	1	152762033	158660779	RP11-458J18	RP11-299C5	2	19386578	42576881
	RP4-768P8	RP11-440G22	1	181212687	188784525	RP11-519H15	RP11-378A13	2	106939463	219136043
	RP11-492K2	GS-167-K11	1	215864587	245100000	RP11-87G1	RP11-309H15	13	32842471	72777348

	loss (min. log2 T/R<-0.3))					gain (min. log2 T/R>0.3)				
	Begin (probe)	End (probe)	chr	Begin (bp)	End (bp)	Begin (probe)	End (probe)	chr	Begin (bp)	End (bp)
	RP11-262D22	RP11-17L8	2	17064501	20273684					
	RP11-478M12	RP11-19A8	2	41675898	49151272					
	RP11-260K8	RP11-52F10	2	59017517	62800899					
	RP11-434P11	RP11-548D17	2	73728655	83708878					
	RP11-154H23	RP11-220O14	3	71622997	77738883					
	RP11-432A10	CTD-2200O3	5	62010355	75734191					
	RP11-520O10	RP11-451H23	5	177813406	180060082					
	RP11-96B2	RP11-495D4	8	123525975	126798844					
	RP11-509D8	RP11-274B18	9	4911574	68528389					
	RP11-124O11	RP11-292F22	10	42660894	47159666					
	RP11-470J18	RP11-304I5	10	86226512	90615085					
	GS-124-K20	RP11-277E18	12	1	7919008					
	RP11-144O23	RP11-4N23	12	10845028	13642782					
	RP11-37E23	RP11-266E6	13	31703968	34159357					
	RP11-393H6	RP11-388E20	13	71078490	77997374					
	RP11-98N22	RP11-187E13	14	19570817	31601773					
	RP11-58E21	RP11-417P24	14	49608076	105437086					
	RP11-178D12	RP11-169M2	14	53411855	60895362					
	RP11-344L6	GS-191-P24	16	11124	90100000					
	GS-202-L17	RP11-220N20	17	1	42268621					
	RG-129-F16	CTD-3138B18	19	1	63516696					
PC133	RP11-12M5	RP5-936P19	1	176407505	183558585	RP5-916A15	RP4-667F15	1	106670439	109448052
	RP11-157C8	RP11-92H22	4	53206265	72179919	RP11-284N8	RP11-27K13	1	110807864	117317597
	RP11-473A17		8	30946131		RP11-418J17	RP11-46A10	1	119411930	177761286
	RP11-396M20	RP11-80H5	10	88054888	91463649	RP4-768P8	RP11-534L20	1	181212687	203144491
	RP11-359J14	RP11-460N10	12	22465615	33333489	RP11-359A17	GS-167-K11	1	235850850	245100000
	RP11-131F1	RP11-516G5	13	38450249	55883767	GS-8-L3	RP11-141H20	2	330	170070826
	RP11-232K22	GS-1-L16	13	106527433	114100000	RP11-65L3	RP11-556H17	2	179083644	241867426
	RP11-122K22	GS-191-P24	16	50431379	90100000	RG-228-K22	RP11-35C18	3	1	34655794
	RP11-385D13		17	15510169		RP11-474M18	RP11-23M2b	3	84623846	199163913
	GS-839-D20	RP11-418N20	x	1	3106255	GS-24-H17	RP11-192H6	5	1	25333169
	RP11-414C23	RP11-270H4	y	2828841	26727165	RP11-16A6	CTD-2052F19	5	31326937	35043272
						RP11-7M4	RP11-269M20	5	36988555	50093906
						RP11-97A19	RP3-444C7	6	12406236	20759036
						GS-164-D18	RP11-101N13	7	154219	94287000
						RP1-155L11	RP5-1056B24	8	35234984	146167102
						RP11-48L13	GS-135-I17	9	29493271	134300581
						GS-23-B11	RP11-399K21	10	1	76882526
						RP11-388G12	RP11-290I21	12	32552977	62854997
						RP11-76K19	RP11-95G6	13	19136604	27970943
						RP11-98N22	RP11-463C8	14	19570817	76654077
						GS-202-L17	RP11-135N5	17	1	2492162
						RP11-178C3	GS-50-C4	17	55350495	80827381
						GS-52-M11	GS-75-F20	18	1	78100000
						RP11-193B6	RP1-128M19	21	13462479	39702870

	loss (min. log2 T/R<-0.3))					gain (min. log2 T/R>0.3)				
	Begin (probe)	End (probe)	chr	Begin (bp)	End (bp)	Begin (probe)	End (probe)	chr	Begin (bp)	End (bp)
						RP1-265B9	GS-2-H14	21	41559383	46900000
						RP3-411B6	RP11-218L14	x	75792100	154392840
PC135	RP11-465B22	RP11-84A19	1	968368	32025999	RP11-418J17	RP11-206M24	1	11941193	154603342
	RP11-297N6	RP4-621B10	1	75758261	92371893	RP11-163L4	GS-167-K11	1	174439974	245100000
	RP11-206M24	RP5-990P15	1	154602575	175314382	GS-8-L3	RP11-24I5	2	330	44500654
	RP11-372A6	RP11-560C24	2	187527667	213464438	RG-228-K22	RP11-521J5	3	1	125434205
	RP11-9N20	RP11-59J16	3	124853438	128752049	RP11-321A2	RP11-223L18	3	127928382	155113468
	GS-24-H17	RP11-28I9	5	1	45708383	RP11-416A5	RP11-258N2	4	45754361	81811336
	RP11-767J14	GS-57-H24	6	63764613	170561549	RP11-400D2	GS-31-J3	4	135602222	191400000
	RP11-161I2	RP11-231D20	8	18447618	42333644	RP11-241J12	GS-240-G13	5	80045485	180756037
	RP11-172F7	RP11-8B23	9	85287618	89927994	RP11-449G3	GS-3-K23	7	54413839	158261821
	RP11-382A18	RP11-425A6	10	18260400	36004759	GS-77-L23	RP11-369E15	8	1	20890068
	RP11-396M20	RP13-238F13	10	88054888	126190348	RP1-198M21	RP5-1056B24	8	41516869	146167102
	RP11-11N15	CTD-3245B9	11	110352104	118395819	GS-43-N6	RP11-274B18	9	1	68528389
	RP11-76K19	RP11-327P2	13	19136604	51243933	GS-23-B11	RP11-2K17	10	1	15140784
	RP11-570N16	RP11-105D1	15	24960345	49085328	RP13-404M3	RP11-380G5	10	34543824	89798429
	RP11-282M16	GS-124-5	15	65872293	100100000	GS-8-M16	RP11-25J3	12	1	74333757
	RP11-394B2	RP4-597G12	16	69164308	88495411	RP11-410A13	GS-221-K18	12	94459564	133387831
	RP11-526H11	GS-75-F20	18	63881662	78100000	RP11-40A8	GS-1-L16	13	50328528	114100000
	RP5-914B9	RP5-1049G16	20	32566759	45732628	RP11-168D12	RP11-125H8	14	41341385	66870415
	RP11-414C23	RP11-270H4	y	2828841	26727165	RP11-79J20	GS-200-D12	14	88818864	105600000
						RP11-274A17	RP11-296I10	16	33544449	68870687
						GS-202-L17	GS-50-C4	17	1	80827381
						RP11-15A1	GS-325-I23	19	49045897	64100000
						GS-82-O2	RP5-1161H23	20	1	33049748
						RP5-1005L2	GS-81-F12	20	44219240	62892997
						RP11-304D2	GS-63-H24	21	18224008	46958137
						RP11-457M7	RP11-218L14	x	2773172	154392840
PC295	RP4-662P1	RP4-700A9	1	62070695	65399804	RP11-2A4	RP11-23M2b	3	138893138	199163913
	RP11-345J13	RP11-355H10	2	11155158	16164216	RP11-4O3	RP11-263F19	4	58332161	83487099
	RP11-94A14	RP11-305L22	3	10613350	15764879	RP11-515C16	RP11-451H23	5	139904062	180060082
	GS-36-P21	RP11-36B15	4	55628	37499323	GS-164-D18	RP4-612F12	7	154219	41152163
	RP11-140M23	RP11-301L8	4	174274371	186960518	RP4-715F13	GS-3-K23	7	68911602	158261821
	CTC-352M6	CTD-2323H12	5	127603123	141198799	RP11-227F6	RP5-1056B24	8	62411200	146167102
	GS-196-I5	RP11-97A19	6	1	12579760	RP11-384P5	RP11-269P11	9	80182461	125447742
	RP11-707H15	RP11-58A9	6	81474419	94898446	RP11-535A19	RP11-87N22	11	75107934	112764095
	RP5-1112D6	RP3-329H16	6	111684690	119707570	RP11-390F17	RP11-210L7	12	58234674	101460706
	GS-77-L23	RP11-51K12	8	1	40649244	RP11-414J4	GS-124-5	15	72737468	100100000
	RP11-428N21	RP11-373N18	10	68138624	106023281	RP11-383C19	GS-75-F20	18	32335236	78100000
	RP11-87C12	GS-221-K18	12	120771799	133387831	GS-839-D20	RP1-308O1	x	1	42143960
	RP11-550P23	RP11-478H12	13	29914797	88035241					
	RP11-178D12	RP11-64K10	15	53411855	68768604					
	RP11-424K7	GS-191-P24	16	49618230	90100000					
	GS-202-L17	RP11-524F11	17	1	17521462					
	RP3-469A13	RP4-600E6	20	34886009	37666045					

	loss (min. log2 T/R<-0.3))					gain (min. log2 T/R>0.3)				
	Begin (probe)	End (probe)	chr	Begin (bp)	End (bp)	Begin (probe)	End (probe)	chr	Begin (bp)	End (bp)
	RP11-164E1	RP11-113F1	21	38601021	42689289					
PC310	RP4-785P20	RP4-700A9	1	3247831	65399804	GS-8-L3	RP11-540E17	2	330	31641535
	RP5-940F7	GS-167-K11	1	232380898	245100000	RP11-260K8	RP11-21P18	2	59017517	88273126
	RP11-540E17	RP11-24I5	2	31441962	44500654	RP11-299N3	RP11-33E18	3	2181314	5696842
	RP11-519H15	RP11-81E19	2	106939463	189643781	RP11-484D18	RP11-14I2	3	178148602	185002170
	RP11-419H23	RP11-556H17	2	231905223	241867426	GS-164-D18	RP11-95J15	7	154219	46540919
	RP11-119E13	RP11-23M2b	3	188090395	199163913	RP11-200A13	RP11-71N3	8	106002673	133317994
	RP11-324I10	RP11-416A5	4	4242550	45926806	CTB-184C17	RP11-56J3	11	64626437	107646360
	RP11-373J21	RP11-63M2	4	73467553	138314464	GS-8-M16	RP11-333D23	12	1	37369589
	RP1-64M18	CTD-2052F19	5	12216435	35043272	RP11-96P3	RP11-293B1	12	51027859	76638486
	RP11-241J12	RP1-241C15	5	80045485	131577988	RP11-295A20	GS-221-K18	12	87539854	133387831
	RP11-506N21	RP11-538A16	6	62586405	93823810	RP11-463C8	RP11-417P24	14	76653370	105437086
	RP11-95J15	RP11-449G3	7	46360317	54591432	RP11-404G1	RP11-385D13	17	7563870	15510169
	RP11-506M12	RP11-384A20	7	99314269	121279367	GS-839-D20	RP4-639D23	x	1	32127544
	GS-77-L23	RP11-138J2	8	1	27462575					
	RP11-48L13	RP11-417A4	9	29493271	137871989					
	GS-23-B11	RP5-1194E14	10	1	15739245					
	RP11-152H18	RP11-131J4	11	8634965	55007563					
	RP11-125I23	GS-1-L16	13	26843897	114100000					
	RP11-98N22	RP11-61F4	14	19570817	77513223					
	RP11-289D12	RP11-178D12	15	20363717	53412638					
	RP11-2E17	RP11-266O8	15	78200185	91714417					
	RP11-405F3	GS-191-P24	16	56179405	90100000					
	RP11-4F24	RP11-404G1	17	1564767	8574309					
	GS-52-M11	GS-75-F20	18	1	78100000					
	RP11-164E1	GS-2-H14	21	38601021	46900000					
	XX-p8708	GS-3018-K1	22	15615802	50100000					
PC324	RP11-306I4	RP11-326G21	1	77716164	142392028	GS-232-B23	RP11-306I4	1	1	77883950
	RP11-451C2	RP11-12M21	2	102042560	139815008	RP11-418J17	GS-167-K11	1	119411930	245100000
	RP4-613B23	RP11-78O10	3	42599838	50006856	RG-228-K22	RP11-25C10	3	1	12590814
	RP11-122D19	RP11-12A13	3	54007388	96250469	GS-24-H17	RP11-269M20	5	1	50093906
	GS-118-B13	GS-31-J3	4	1	191400000	GS-164-D18	RP5-905H7	7	154219	62271685
	RP11-28I9	GS-240-G13	5	45570659	180756037	RP11-269P11	RP11-417A4	9	125271849	137871989
	RP5-905H7	RP11-5N18	7	62132326	107913946	GS1-756B1	RP11-79I23	10	8219578	60270663
	GS-77-L23	CTD-2115H11	8	1	43438715	RP11-166B18	RP11-165M8	10	61902228	89694968
	GS-43-N6	RP11-205K6	9	1	126460599	RP11-304I5	GS-137-E24	10	90435254	135313953
	GS-23-B11	RP1-249K20	10	1	9198070	RP11-125G9	GS-221-K18	12	20887518	133387831
	RP11-371O16	RP11-809M12	10	59005947	63041017	RP11-489A11	RP11-548B6	16	21304276	23756350
	RP11-396M20	RP11-304I5	10	88054888	90615085	RP11-283C7	RP11-357N13	16	45502891	52626428
	RP11-277E18	RP11-328P13	12	7918143	19281492	RP11-514D23	GS-191-P24	16	84749036	90100000
	RP11-289D12	GS-124-5	15	20363717	100100000	GS-68-F18	RP5-1050D4	17	150	4866267
	RG-191-K2	RP11-489A11	16	1	21473433	RP11-404G1	RP11-471L13	17	7563870	12108967
	RP11-207A10	RP11-523L20	16	22715683	46605357	RP11-121A13	RP11-474K4	17	20112029	27596064
	RP11-467J12	RP11-21B21	16	51466052	87260485	RP11-156E6	RP5-1169K15	17	37192625	40787106
	RP11-104O19	RP11-12H18	17	4001094	8574309	RP11-416K7	RP11-178C3	17	42875381	55498032

	loss (min. log2 T/R<-0.3))					gain (min. log2 T/R>0.3)				
	Begin (probe)	End (probe)	chr	Begin (bp)	End (bp)	Begin (probe)	End (probe)	chr	Begin (bp)	End (bp)
	RP11-401O9	RP11-488L1	17	10055064	13085706	RP11-89H15	GS-362-K4	17	59626448	81600000
	RP11-388F14	RP11-138P22	17	13211602	23308267	GS-52-M11	GS-75-F20	18	1	78100000
	RP11-47L3	RP11-506G7	17	30523581	38327610	RG-129-F16	GS-325-I23	19	1	64100000
	XX-p8708	GS-3018-K1	22	15615802	50100000	RP11-193B6	GS-2-H14	21	13462479	46900000
	RP11-414C23	RP11-270H4	y	2828841	26727165	RP11-457M7	RP11-218L14	x	2773172	154392840
PC329	RP11-45I3	RP4-540O3	1	16532955	19139464	RP11-309N8	RP11-52C8	2	202535825	232659128
	RP11-419H23	RP11-534J17	2	231905223	234218410	GS-196-I5	RP11-349P19	6	1	65280053
	RP11-767J14	GS-57-H24	6	63764613	170561549	GS-164-D18	GS-3-K23	7	154219	158261821
	GS-77-L23	RP11-197P20	8	1	37371241	RP11-98I12	RP5-1056B24	8	36363082	146167102
	RP11-108L12	RP11-164L18	11	42864060	46383009	RP11-166M16	GS-362-K4	17	67169020	81600000
	RP11-125A7	RP11-10M21	13	41262233	66421707					
	RP11-370A2	RP11-332E3	13	68180810	75439997					
	RP11-95C14	RP11-318K19	13	91284445	95498792					
	RP11-279D17	GS-1-L16	13	99118130	114100000					
	RP11-417N10	RP11-285K4	16	70269439	72453658					
	RP11-283E7	RP11-171G2	17	64281884	68366917					
	RP11-164E1	RP11-113F1	21	38601021	42689289					
PC339	RP11-566O4	RP11-141H20	2	109203303	170070826	GS-8-L3	RP11-245N4	2	330	70572498
	RP11-274J22	CTC-329H14	5	41662376	108180023	RP11-65L3	RP11-556H17	2	179083644	241867426
	GS-164-D18	RP11-71F18	7	154219	19394137	RP11-239J2	RP11-165B13	3	114747418	119243578
	RP11-354H2	RP11-437L1	7	115446926	129021533	RP11-71G7	RP11-23M2b	3	177684963	199163913
	RP11-8P6	GS-3-K23	7	136490854	158261821	RP11-434D11	RP11-420L4	5	126045881	169139510
	RP11-279I21	RP11-240L7	9	94473904	96229878	GS-62-L11	RP11-289M23	6	135997	23684090
	RP11-20H14	RP11-107P10	11	104950107	111973902	RP11-89N17	RP11-148A10	7	33525398	103891116
	RP11-37E23	RP11-394J19	13	31703968	74530080	RP11-353D5	RP11-24H3	8	92382762	99366374
	RP11-452G23	GS-191-P24	16	47238951	90100000	RP11-22A24	RP11-17E16	8	120711400	130702085
	RP11-164E1	RP11-113F1	21	38601021	42689289	RP11-160D19	RP11-417A4	9	95433765	137871989
	RP11-414C23	RP11-270H4	y	2828841	26727165	GS-23-B11	RP11-79I23	10	1	60270663
						RP11-765C10	RP11-80H5	10	89705200	91463649
						GS-8-M16	RP11-268A19	12	1	80392099
						RP11-76K19	RP11-141M1	13	19136604	32947408
						RP11-552M6	GS-163-C9	13	73124080	113376104
						RP11-99L13	RP11-78M2	15	22736020	74647142
						RP11-404G1	GS-362-K4	17	7563870	81600000
						RP11-51B9	RP11-178F10	18	7827406	20371175
						RP11-520K18	GS-75-F20	18	56874822	78100000
						RP11-25F24	RP1-128M19	21	23491444	39702870
						RP1-265B9	GS-63-H24	21	41559383	46958137
PC346	RP11-173C1	RP11-204D19	2	39065424	43756723	GS-232-B23	RP11-250D8	1	1	74512062
	RP11-16E8	RP11-2G22	3	21574294	27531253	RP5-963M5	RP11-80B9	1	76580261	237390561
	RP11-396M20	RP11-399O19	10	88054888	90783689	RP11-411G13	GS-167-K11	1	239599404	245100000
	RP11-76K19	GS-1-L16	13	19136604	114100000	RP11-296G16	RP11-211H6	4	1065447	5145322
						GS-164-D18	GS-3-K23	7	154219	158261821
						CTD-2115H11	RP5-1056B24	8	43315811	146167102
						GS-1061-L1	GS-81-F12	20	1	62892997

	loss (min. log2 T/R<-0.3))					gain (min. log2 T/R>0.3)				
	Begin (probe)	End (probe)	chr	Begin (bp)	End (bp)	Begin (probe)	End (probe)	chr	Begin (bp)	End (bp)
PC374	RP11-262D22	RP11-106G13	2	17064501	27048324	RP11-418J17	GS-167-K11	1	119411930	245100000
	RP11-540E17	RP11-391D19	2	31441962	51008795	RP11-51K12	RP11-503E24	8	40501073	42674285
	RP11-11G20	RP11-400O18	2	125735232	186543611	RP11-419L20	RP11-2K18	8	110436818	115915271
	RG-228-K22b	RP11-488M6	3	1	13656208	RP11-172F7	RP11-78H18	9	85287618	114805811
	GS-118-B13	GS-31-J3	4	1	191400000	RP3-432E18	RP11-173E19	12	46156911	72312988
	CTD-2276O24	RP11-667P13	5	50061472	78198544	RP11-565J15	RP11-559M6	14	45964782	62046831
	RP3-444C7	RP11-176J5	6	20630798	24421543	RP11-68I8	RP11-417P24	14	97835615	105437086
	GS-77-L23	RP1-198M21	8	1	41617043	RP11-500M22	GS-325-I23	19	4806367	64100000
	RP11-404K23	RP11-373J8	9	115288454	127499995					
	RP11-314J18	RP11-115N19	10	70288208	126760588					
	GS-8-M16	RP11-242B24	12	1	37489074					
	RP11-76K19	GS-1-L16	13	19136604	114100000					
	RP11-289D12	GS-124-5	15	20363717	100100000					
	XX-p8708	RP1-76B20	22	15615802	28545603					
	LL22NC01-132D12	GS-3018-K1	22	35473472	50100000					

Table S2. RT-PCR analysis of the genes in the eight novel homozygous deleted regions in 11 prostate cancer xenografts.

	PCEW	PC82	PC133	PC135	PC295	PC310	PC324	PC329	PC339	PC346	PC374	NP
genes on 2q37.1*												
COPS7B	++	++	++	++	++	++	++	–	++	++	++	++
NPPC*1	–	–	–	–	–	–	–	–	–	–	–	–
ALPP*1	–	–	–	–	–	–	–	–	–	–	–	–
ALPPL2*1	–	–	–	–	–	–	–	–	–	–	–	–
ALPI*1	–	–	–	–	–	–	–	–	–	–	–	–
ECEL1*1	–	–	–	–	–	–	–	–	–	–	–	–
CHRND*1	–	–	+/–	–	–	–	–	–	–	–	–	–
CHRNG*1	–	–	–	–	–	–	–	–	–	–	–	–
TIGD1*2	ND											
EIF4EL3	++	++	++	++	++	++	++	–	++	++	++	++
genes on 8p23.3 *												
ZNF596	+	+	++	++	–	+	++	++	++	++	++	+
FBXO25	++	++	++	++	+/–	++	++	++	++	++	++	++
INM01	++	++	++	++	+/––	++	++	++	+/–	++	++	++
LOC286161*2	ND											
LOC157697	++	++	++	++	–	+	++	++	+	++	++	++
DLGAP2 *1	–	–	–	–	–	–	–	–	–	–	–	–
genes on 13q13.1 *												
BRCA2	++	++	++	++	++	–	++	++	++	++	++	++
CG018	+	+	+	+/–	+	–	++	++	++	+	+/–	++

	PCEW	PC82	PC133	PC135	PC295	PC310	PC324	PC329	PC339	PC346	PC374	NP
LOC88523	++	++	++	++	++	–	+/–	++	++	++	++	++
PFAAF5	+	+	++	++	++	+	++	++	++	++	++	++
APRIN	++	++	++	++	++	–	++	++	++	++	++	++
KL	++	++	+/–	+/–	+/–	–	+	+	++	–	++	++
DLC2	++	++	++	++	++	–	++	++	++	++	++	++
genes on 13q14.2 *												
ITM2B	++	++	++	–	++	++	++	++	++	++	++	++
RB1	++	++	++	–	++	+	++	++	++	++	+	+/–
P2RY5	++	++	++	–	++	+	+	+/–	+	+	+	+
CHC1L	++	++	++	–	++	++	++	++	++	++	++	++
CYSTRL2 *2	ND											
gene on16q22.2-q22.3*												
ATBF1	+	++	++	++	++	++	++	++	–	++	++	++
gene on16q23.1*												
WWOX	+	+	+	+	+	+	+	+	+	+	++	+
genes on 17p12*												
MAP2K4	++	++	++	++	–	++	–	++	++	+	++	++
NCOR-1	++	++	–	++	++	++	–	++	++	++	++	++

*: According to the ref seq genes of UCSC Genome Browser, freeze may 2004

*1: no expression in prostate according to Unigene

*2: 1 exon gene

NP: Normal Prostate. ND: Not determined.

Chapter 3

LOSS OF A SMALL REGION AROUND THE *PTEN* LOCUS IS A MAJOR CHROMOSOME 10 ALTERATION IN PROSTATE CANCER XENOGRAFTS AND CELL LINES

Karin G. Hermans,[1,4] Dirk C. van Alewijk,[1,4] Joris A. Veltman,[3] Wytske van Weerden,[2] Ad Geurts van Kessel[3] and Jan Trapman[1*]

[1]Department of Pathology, Josephine Nefkens Institute, Erasmus Medical Center, Rotterdam, The Netherlands.

[2]Department of Urology, Josephine Nefkens Institute, Erasmus Medical Center, Rotterdam, The Netherlands.

[3]Department of Human Genetics, University Medical Center Nijmegen, Nijmegen, The Netherlands.

[4]K.G.H. and D.C.v.A. contributed equally to this work

Genes Chromosomes and Cancer 2004; 39: 171-184

ABSTRACT

We examined 11 prostate cancer xenografts and 4 cell lines for chromosome 10 alterations. Conventional Comparative Genomic Hybridization (CGH) and array-based CGH revealed a pattern of loss of distal 10p, gain of proximal 10p and 10q, and loss of distal 10q. In addition, array CGH identified 2 high-level amplifications in the cell line PC3, homozygous deletions around *PTEN* in the xenografts PCEW, PC133, PC324 and in PC3 and small single and double copy deletions around *PTEN* in PCEW, PC82, PC324, PC346 and LNCaP. Allelotype analysis confirmed all 10p deletions, 5/6 large 10q deletions, the homozygous deletions and the small regions of one copy loss. *MXI1*, *DMBT1* and *KLF6* were excluded as important tumor suppressor genes. Sizes of homozygous deletions around *PTEN* ranged from 1.2 Mbp (PC133) to <30 Kbp (*PTEN* exon 5 in PC295). The regions of small single or double copy loss around *PTEN* were all less than 4.5 Mbp. Loss of 1 or 2 copies *PTEN* was always accompanied by loss of the distal flanking gene *FLJ11218* and in most cases by loss of the proximal flanking genes *MINPP1*, *PAPSS2* and *FLJ14600*. Furthermore, differential expression was detected for *FLJ11218* and *PAPSS2*. Complete deletion or inactivating mutation of *PAPSS2* was found in at least 3 samples. Additional to 4 homozygous deletions, 1 missense mutation was detected in *FLJ11218*. In conclusion, our data provide evidence for a small region around *PTEN* as the major chromosome 10 alteration in prostate cancer xenografts and cell lines. *PTEN* inactivation is in part of the samples accompanied by loss of one *MINPP1* allele, loss of one copy, mutation or low expression of *PAPSS2,* and most frequently with loss of 1 or 2 copies or low expression of *FLJ11218*.

INTRODUCTION

Prostate cancer is the most frequently diagnosed cancer and the second leading cause of male cancer death in Western and Northern Europe, Northern America and Australia (Greenlee et al., 2001). At present, an adequate therapy of metastatic prostate cancer is not available. In order to identify novel therapeutic targets, knowledge of the major molecular alterations is urgently needed.

In prostate cancer, most frequent deletions were found for 6q, 8p, 13q and 16q, indicating the localization of tumor suppressor genes on these chromosomal arms (Visakorpi et al., 1995; Cher et al., 1996; Nupponen et al., 1998b; Alers et al., 2000). Less frequent chromosomal losses were found for 5q, 10q and 17p. The most frequently gained chromosome arm was 8q, followed by 7p, 7q and 20q.

Loss of 10q is generally considered as a late step in prostate cancer progression. Allelic imbalance studies indicated several separate regions at 10q22-q26 to be affected, suggesting the inactivation of more than one tumor suppressor gene (Gray et al., 1995; Ittmann, 1996; Komiya et al., 1996; Trybus et al., 1996; Cairns et al., 1997; Feilotter et al., 1998; Leube et al., 2002). Loss of 10q is not unique for prostate cancer. Frequent loss of distal 10q has also been described in renal cell carcinoma (Morita et al., 1991), non-Hodgkin's lymphoma (Speaks et al., 1992), glioblastoma (James et al., 1988; Fujimoto et al., 1989), meningioma (Rempel et al.,1993), malignant melanoma (Reifenberger et al., 1999), small lung cell cancer (Kim et al., 1998), bladder cancer (Cappellen et al., 1997), and endometrial carcinoma (Peiffer et al., 1995; Nagase et al., 1997).

The *PTEN* tumor suppressor gene at 10q23.3, which encodes a lipid and protein phosphatase, is frequently altered in prostate cancer (Cairns et al., 1997; Teng et al., 1997; Gray et al., 1998; Feilotter et al., 1998; Vlietstra et al., 1998; Whang et al., 1998; Wang et al., 1998; McMenamin et al., 1999). Complete *PTEN* inactivation was detected at varying frequency in primary tumors and in up to 60% of metastases, cell lines and xenografts. *PTEN* is even more frequently implicated in glioblastoma (Li et al., 1997; Steck et al, 1997; Wang et al., 1997; Rasheed et al., 1997; Teng et al., 1997) and endometrial carcinoma (Tashiro et al., 1997), and to a lesser extent in many other tumors. Additional to *PTEN*, 10q harbors the candidate tumor suppressor genes *MXI1* at 10q25.2 and *DMBT1* at 10q26.2. (Eagle et al., 1995; Mollenhauer et al., 1997).

Less is known about 10p alterations in prostate cancer. Variable frequencies of loss of distal 10p in prostate cancer have been found (Ittmann, 1996; Trybus et al., 1996, Fukuhara et al., 2001; Narla et al., 2001). Recently, mutation of *KLF6* on 10p15 in prostate cancer has been described (Narla et al., 2001; Chen et al., 2003).

Xenografts and cell lines are powerful tools in the search for genetic alterations in human cancer. They are available in unlimited quantities and, importantly, they lack normal cells of human origin, which simplifies the analysis of chromosomal alterations,

and the study of structural alterations and expression of individual genes. Previously, we described frequent *PTEN* inactivation in prostate cancer xenografts and cell lines (Vlietstra et al., 1998). In the present study we analyze the role of chromosome 10 in prostate cancer by conventional CGH, array-based CGH and allelotype analysis. Further, we present data on the expression and structure of the candidate tumor suppressor genes *MXI1*, *DMBT1* and *KLF6*. In addition, we describe the structure, deletion and expression of *PTEN* flanking genes, and we address the issue of *PTEN* haplo-insufficiency in prostate cancer.

MATERIALS AND METHODS

Prostate Cancer derived Cell Lines and Xenografts

The *in vitro* growing cell lines LNCaP, PC-3, DU-145 and TSU were cultured under standard conditions. The *in vivo* xenografts PC82, PCEW, PC133, PC135, PC295, PC310, PC324, PC329, PC339, PC346 and PC374 were propagated on male nude mice (Hoehn et al., 1980, 1984; van Weerden et al., 1996).

DNA and RNA preparation

Genomic DNA from cell lines and xenografts was isolated utilizing the Puregene system from Gentra Systems (Minneapolis, MN) according to the procedure described by the manufacturer.

Cell line RNA was isolated by the guanidium isothiocyanate procedure; xenograft RNA was isolated by the LiCl protocol (Sambrook and Russell 2001). mRNAs from fetal brain and normal prostate tissue were purchased from BD Biosciences Clontech (Palo Alto, CA).

Conventional Comparative Genomic Hybridization

Conventional CGH was performed essentially as described (Kallioniemi et al., 1992). In brief, tumor DNA and normal male reference DNA samples were labeled by nick translation (Nick translation system, Invitrogen Life Technologies, Carlsbad, CA) with bio-dUTP (Roche Diagnostics, Almere, The Netherlands) and digoxigenin (Roche Diagnostics), respectively. Labeled DNA samples (200 ng each) and 15µg COT-1 DNA was ethanol-precipitated and dissolved in 10 µl hybridization mix (50% formamid, 0.1% Tween-20, and 10% dextran sulfate in 2xSSC at pH7.0). The probe mixture was denatured (10 min, 72°C), pre-hybridized (30 min, 37°C) and hybridized to normal male chromosome spreads (72 h, 37°C). Next, slides were washed, and fluorescent detection of the biotin- and dioxigenin-labeled DNA probes was by fluorescein isothiocyanate (FITC)-conjugated avidin (Vector Labs, Burlingame, CA) and anti-digoxigenin-rhodamine (Roche Diagnostics) staining,

respectively. Chromosomes were DAPI counterstained (4'6'-diamidino-2-phenylindole) (Sigma, St. Louis, MO) in Vectashield anti-fade solution (Vector Labs).

Images were acquired with an epifluorescent microscope equipped with a cooled CCD camera (Photometrics Inc., Tuscon, AZ), a triple-band pass beamsplitter emission filters (P-1 filter set, Chroma Technology, Brattleboro, VT), and a Quips XL image analysis system (version 3.1 Vysis Inc., Downers Grove, IL). Chromosomal regions were scored as lost if the mean green to red ratio was below 0.85 and gained if this ratio was above 1.15. Eight or more metaphases were analyzed per sample.

Array CGH

Array CGH was performed essentially as described previously (Veltman et al., 2002 and 2003) with minor modifications, including the use of an automated hybridization station and advanced normalization procedures (Vissers et al., submitted). The chromosome 10 data presented here are part of a genome-wide array CGH study. Chromosome 10 is covered by 219 BAC clones, resulting in an average coverage of one clone per 620 Kbp. Mapping of BAC clones was derived from the April 2003 release of the UCSC human Genome database (http://genome. ucsc.edu). Clones were robotically spotted in triplicate onto CMT-GAPS coated glass slides (Ultragaps, Corning, Schiphol-Rijk, The Netherlands) using a Cartesian Prosys 5510TL arrayer (Genomic Solutions, Cambridgeshire, UK). The array CGH profiles were established through hybridization of 500 ng Cy3-dUTP labeled genomic DNA combined with 500 ng Cy5-dUTP labeled control genomic DNA using a GeneTac Hybridization Station (Genomic Solutions). After scanning, fluorescence test over reference ratios (T/R values) were determined for each clone, subsequently log2 transformed and normalized per array subgrid by applying Lowess curve fitting with a smoothing factor of 0.2. Thresholds for copy number gain and loss were set at log2 T/R values of +0.3 and –0.3, respectively, based on previous work (Vissers et al., submitted). Log2 T/R values below –1 were indications of homozygous deletions; ratios above +1 were interpreted as high-level amplification.

PCR and PCR-SSCP

Standard PCR amplifications utilizing *Taq* polymerase (Promega, Madison, WI) included 35 cycles of 1 min at 95°C, 1 min at 50°C or 55°C, and 1 min at 72°C. For allelotyping and PCR-SSCP, 1 µCi [alpha-^{32}P]dATP (Amersham Biosciences, Bucks, UK) was added to a 15 µl reaction mix. Amplified, radio-labeled polymorphic microsatellite markers were separated on a sequence gel. SSCP of radio-labeled gene specific PCR products were analyzed on a 6% non-denaturing polyacrylamide gel containing 10% glycerol. Gels were run at 7W, overnight at room temperature. For detection of homozygous deletions, PCR amplifications were performed in a 50 µl reaction volume. Amplified fragments were separated on a 2% agarose gel.

Allelotype analysis and screening for homozygous deletions

Polymorphic microsatellite markers applied for allelotype analysis and screening for homozygous deletions at 10p were: *D10S602*, *D10S1745*, CA237H5A, CA237H5B, *D10S591*, *D10S1729*, *D10S189*, *D10S547*, *D10S191*, *D10S595*, *D10S197*, *D10S193*, and at 10q: *D10S220*, *D10S581*, *D10S537*, *D10S1688*, *D10S1730*, *D10S1686*, *D10S1687*, CA163M19, *D10S579*, *D10S215*, *D10S1765*, *AFMa086WG9*, *D10S541*, CA13J3, CA80H5, *D10S1753*, *D10S583*, *D10S1680*, *D10S1726*, *D10S192*, *D10S187*, *D10S209*, *D10S217*. Most PCR primer sequences can be found in Genome Database (http://gdbwww.gdb.org). Additional primer sets are: CA237H5A: gcagagcagccttcagtaat and cacttggcaaactacagtgc; CA237H5B: caagagcatgagtcccattg and gaaccaatcagtcaccaagc; CA163M19: gttttgcccagttgaagtca and tcctcccccaactattctatc; CA13J3: gattagcacaacactgggtag and accctctggggaagtactat; CA80H5: accagattggatgtgcatgc and caaccagcagtatctgtcac. Positions of markers on chromosome 10 were derived from the April 2003 release of the UCSC human Genome database.

Primer sets utilized in screening for homozygous deletions of *KLF6*, *MINPP1*, *PAPSS2*, *FLJ14600*, *FLJ11218*, *LIPF*, *DKFZp761K1824*, *ACTA2*, *TNFRSF6*, *CH25H*, *LIPA*, *IFIT2*, *IFIT4*, *IFIT1*, *RI58*, *PANK*, *MPHOSPH1* and *MXI1* are available upon request.

The 74K, 36K, G14Ext, G14 and 60K primer sets for detection of homozygous deletions in *DMBT1* by PCR on genomic DNA have been published previously (Mollenhauer et al., 1997). For more detailed analysis of the homozygous deletion in *DMBT1* by PCR-SSCP the primers DMBTME39-F (5′-ACTTCAGAGGTAGGAGGGT-3′) and DMBTME39-R (5′-AGGTAGAGAGTGAGCCCTAG-3′) were utilized.

mRNA expression

Analysis of mRNA expression was performed by semi-quantitative RT-PCR. cDNA was synthesized on 1 µg RNA template utilizing 200 U M-MLV RT (Invitrogen Life Technologies) and a T_{12}-site primer (5′-GCATGCGAATTCGGATCCT$_{12}$-3′) in a buffer, containing 10 mM DTT, 1 mM dNTPs, and 40 U RNAsin (Promega) for 1 h at 37°C. RNA polymerase II was utilized as a control. Specific cDNA fragments were amplified by standard PCR. Gene specific RT-PCR primers are available upon request.

Structures of candidate tumor suppressor genes and *PTEN* flanking genes

For PCR-SSCP analysis, appropriate fragments of all exons of *MINPP1*, *PAPSS2*, *TNFRSF6*, *FLJ11218*, *MXI1* and *KLF6* were amplified. Primer sequences are available upon request. Selected amplified fragments were purified over QIAquick spin columns (Qiagen, Hilden, Germany), cloned into pGEM-T Easy (Promega), and sequenced according to the dideoxy chain termination method (Sambrook and Russell, 2001).

RESULTS

Alterations of chromosome 10 are among the most frequent chromosomal changes in prostate cancer as determined by allelotype analysis (Gray et al., 1995; Trybus et al., 1996; Ittmann, 1996; Komiya et al., 1998; Leube et al., 2002). However, conventional CGH studies show less frequent alterations (Nupponen et al., 1998; Alers et al., 2000). To increase our insight into the role of chromosome 10 in prostate cancer, we studied overall chromosome 10 alterations in prostate cancer xenografts and cell lines by conventional CGH, array CGH and allelotype analysis. In addition we investigated deletion, mutation and expression of individual candidate tumor suppressor genes.

Conventional Comparative Genomic Hybridization

In conventional CGH 8 out of 15 xenografts and cell lines showed gain or loss of specific parts of chromosome 10 (Figure 1). Loss of the distal region of 10p was found in PC310 (p13-pter), PC324 (p14-pter) and PC3 (p13-pter) (3/15). Small changes at the telomeres were not taken into account, because of limited reliability. The majority of gains were found around the centromere (5/15): PC135 (q11.2-q22), PC324 (p11.2-p12 and q21-

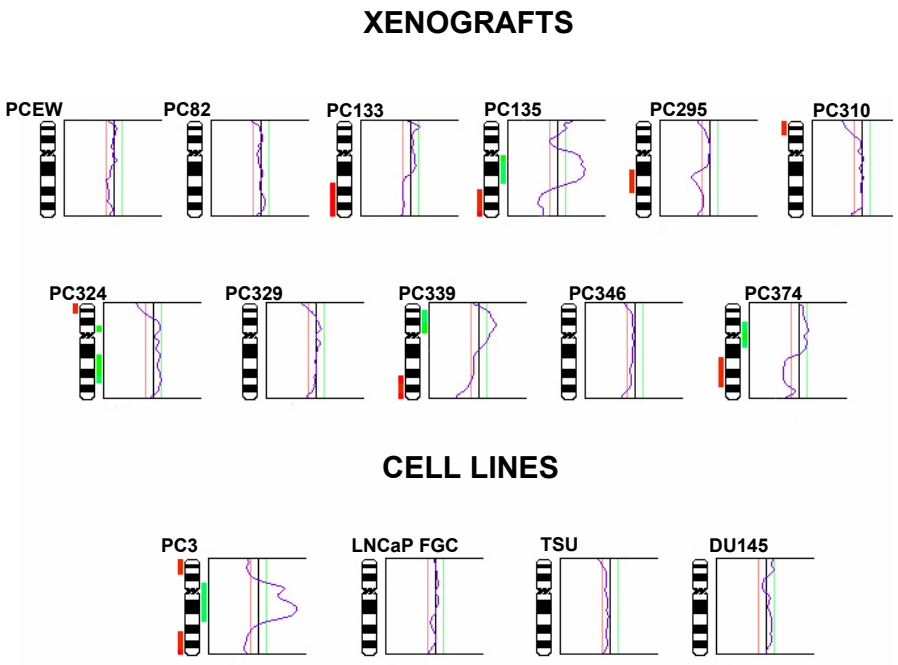

Figure 1. Chromosome 10 alterations identified by conventional CGH in prostate cancer xenografts and cell lines. CGH mean is 0.85-1.15; number of chromosomes analyzed was 12-16. A bar to the right of a chromosome ideogram indicates gain, a bar to the left indicates loss of the chromosomal region.

q24), PC339 (p11.2-p14), PC374 (p12-q21) and PC3 (p11.2-q22). Losses of 10q were most frequent (6/15). They were present in PC133 (q22-qter), PC135 (q23-qter), PC295 (q21-q23), PC339 (q23-qter), PC374 (q22-q25) and PC3 (q23-qter). In PCEW, PC82, PC329, PC346, LNCaP, TSU and DU145 clear chromosome 10 alterations were not detected. Summarizing, chromosome 10 alteration in prostate cancer xenografts and cell lines shows a characteristic pattern of loss of distal 10p, gain of proximal 10p and proximal 10q, and loss of distal 10q.

Array CGH

Array CGH has the advantage over conventional CGH that it detects smaller regions of chromosomal gains and losses, and most importantly high-level amplifications and homozygous deletions (Veltman et al., 2003). The chromosome 10 array that we utilized was composed of 219 BAC clones, covering the chromosome with an average spacing of one clone per 620 Kbp. Figure 2 shows representative examples of the profiles obtained. The positions of BAC clones are in Mbp form the top of 10p. Loss of telomeric 10p was clearly present in PC310 and in PC324; loss of a more proximal part of 10p was detected in PC135 (see Figure 2). Gain of large regions of both chromosome 10 arms was seen in PC135, PC324 and PC3 (Figure 2). Two small regions of high-level amplifications were identified in PC3, at 10p11.2 and 10q22.2, respectively. Losses of large 10q regions were detected in PC133, PC135, PC295 and PC374 (see PC135 as an example, Figure 2). Array CGH did not detect chromosome 10 alterations in xenograft PC329 and the cell lines TSU and DU145 (data not shown).

The BAC array contained 3 clones, RP11-57C13, RP11-79A15 and RP11-129G17, which directly flanked *PTEN* at 10q23.3 (89.8 Mbp) (see Figure 6A). The adjacent clones in the BAC array, RP11-9M11 and RP-11-67L13, map further away from *PTEN*. In the PCEW, PC133 and PC324 array, RP11-129G17 had a log2 T/R value of less than –1. In PC3 this value was -0.75 (see Figure 2 for PCEW, PC324 and PC3). All 4 DNA samples are known to contain a homozygous deletion of *PTEN* (Vlietstra et al., 1998). In PCEW, the log2 T/R value of RP11-57C13 and RP11-79A15 was also below –1, indicative of complete deletion of this region in PCEW and not in other samples (see also Figure 6A). Interestingly, the regions of loss around *PTEN* seem very small (<4.5 Mbp) in PC82, PC346 and LNCaP, which all contain a *PTEN* point mutation, and in PCEW and PC324 that carry a homozygous deletion (see Figure 2). PC82 also showed a small region of loss on 10q11.2 next to the centromere, a region difficult to study by conventional CGH.

Allelotype analysis of chromosome 10

To obtain more detailed information of chromosome 10 alterations, the 15 genomic DNA samples were also screened for 35 polymorphic microsatellite markers along both chromosomal arms. A high marker density was chosen in a small region around the *PTEN*

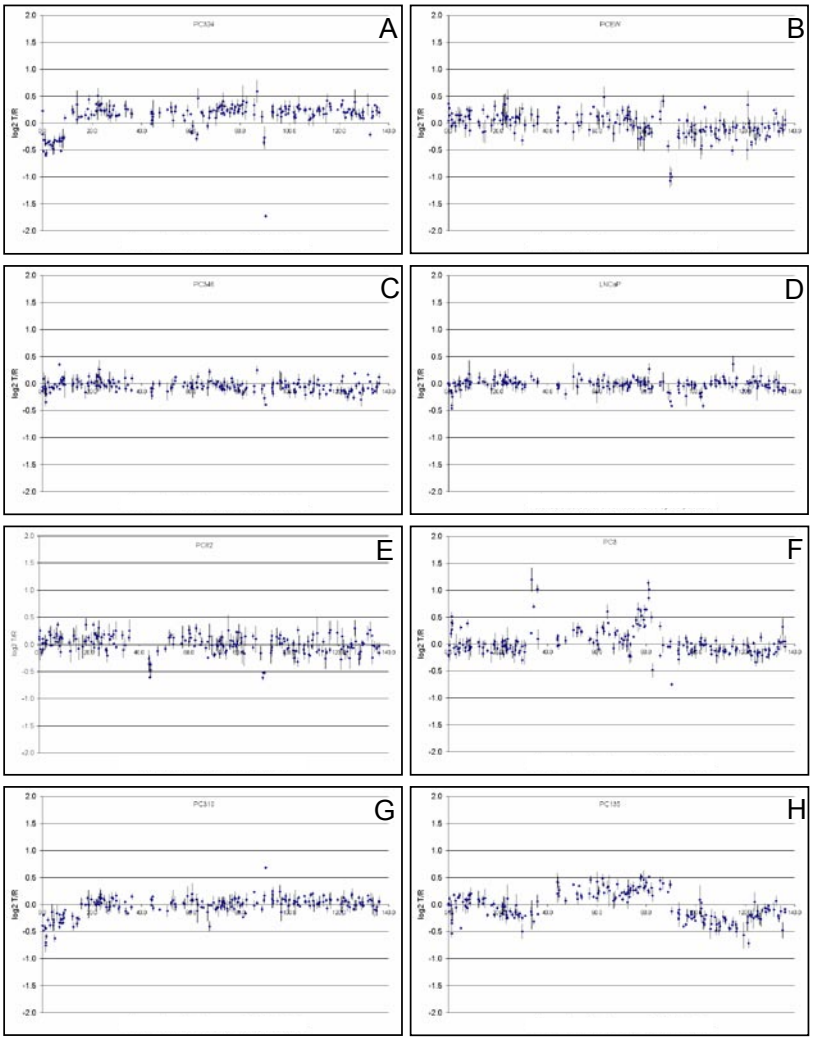

Figure 2. Chromosome 10 alterations as detected by array CGH of prostate cancer xenografts and cell lines. Panels A-H represent individual chromosome 10 profiles of 8 cases, with clones ordered within chromosome 10 from pter to qter on the basis of the physical mapping positions in the April 2003 release of the UCSC Genome database. Each small square represents the mean log2 transformed and Lowess normalized test over reference intensity ratio of an individual BAC. The standard deviation of each measurement is shown as a vertical bar. PC324 (A), PCEW (B), and PC3 (F) show a homozygous deletion of the *PTEN* region. A small single copy deletion of this region is shown for PC346 (C), LNCaP (D) and PC82 (F). Other regions with copy number alterations include loss of telomeric 10p in PC324 (A) and PC310 (G), high-level amplification at 10p11.2 and 10q22.2 in PC3 (F), and a complex pattern of copy number changes in PC135 (H).

locus, at 89.8 Mbp, and around *KLF6* at 3.9 Mbp. The results are summarized in Figure 3. Previously published *PTEN* alterations (Vlietstra et al., 1998) are indicated at the bottom of Figure 3.

Marker	Heterozygosity	band	Mbp (Santa Cruz*)	PCEW	PC82	PC133	PC135	PC295	PC310	PC324	PC329	PC339	PC346	PC374	PC3	LNCaP	TSU	DU145
D10S602	73	10p15.3	2.2	2	2	1	2	1	1	1	1	2	2	2	1	1	1	MSI
D10S1745	85	10p15.3	2.5	2	2	1	2	2	1	1	2	1	2	MSI	1	MSI	1	MSI
CA237H5A	-	10p15.1	3.9	1	2	1	1	2	1	1	1	2	2	1	1	2	1	2
CA237H5B	-	10p15.1	4.0	2	2	1	2	2	1	1	2	2	1	MSI	1	MSI	1	MSI
D10S591	71	10p15.1	4.5	1	1	2	1	2	1	1	2	2	1	2	1	MSI	1	1
D10S1729	72	10p15.1	4.9	2	2	1	1	2	1	1	2	1	2	MSI	1	2	1	MSI
D10S189	73	10p14	6.9	2	1	1	2	1	1	1	2	1	2	2	1	2	1	1
D10S547	74	10p14	10.7	1	1	2	2	1	1	2	2	2	2	2	1	2	1	1
D10S191	81	10p13	14.7	1	1	1	2	2	1	2	2	2	2	MSI	1	MSI	1	MSI
D10S595	85	10p12.31	20.8	2	2	2	2	2	2	2	2	2	2	2	1	MSI	1	MSI
D10S197	75	10p12.1	26.7	1	2	2	2	2	2	2	1	2	MSI	MSI	1	2	1	MSI
D10S193	81	10p11.23	30.7	2	1	2	2	2	2	2	2	1	2	2	1	2	1	MSI
D10S220	84	10q11.23	52.2	1	2	1	1	2	2	1	2	1	2	2	2	1	1	MSI
D10S581	80	10q21.3	65.7	2	1	1	1	2	1	1	1	1	1	2	1	2	1	MSI
D10S537	83	10q22.1	72.3	2	2	1	1	1	2	2	2	1	MSI	1	1	MSI	1	MSI
D10S1688	86	10q22.1	72.5	1	1	2	1	1	1	2	2	1	2	1	1	MSI	1	1
D10S1730	83	10q22.3	78.8	1	2	2	1	1	2	1	1	1	MSI	MSI	1	2	1	MSI
D10S1686	86	10q23.1	85.7	2	2	1	2	1	2	2	2	1	2	MSI	1	2	1	MSI
D10S1687	81	10q23.2	88.8	2	2	1	2	1	2	2	2	2	2	1	1	1	1	2
CA163M19	-	10q23.2	89.1	1	2	1	2	1	2	2	2	2	1	1	1	1	1	MSI
D10S579	59	10q23.31	89.5	0	1	1	1	1	1	1	1	2	1	1	1	1	1	1
D10S215	81	10q23.31	89.6	0	1	1	1	1	2	1	2	2	1	1	1	1	1	1
D10S1765	83	10q23.31	89.7	0	1	0	1	1	2	1	2	2	1	1	1	1	1	1
AFMa086WG9	-	10q23.31	89.8	0	1	0	1	1	1	0	1	1	1	1	0	1	1	1
D10S541	78	10q23.31	90.1	0	1	0	1	1	2	0	2	1	1	1	0	1	1	1
CA13J3	-	10q23.31	90.5	2	2	0	1	1	1	1	2	1	2	1	1	MSI	1	1
CA80H5	-	10q23.31	91.5	2	1	1	2	1	2	2	1	1	2	2	1	2	1	2
D10S1753	74	10q23.31	92.5	1	2	1	1	1	2	2	1	1	2	1	1	1	1	1
D10S583	84	10q23.33	94.5	1	2	1	2	1	2	1	1	1	2	1	1	1	1	1
D10S1680	82	10q23.33	95.7	2	2	1	1	2	2	1	2	1	MSI	1	1	1	1	MSI
D10S1726	76	10q24.2	100.8	2	1	1	2	2	2	1	1	1	MSI	MSI	1	MSI	1	MSI
D10S192	78	10q24.31	102.6	2	2	1	2	1	2	2	2	1	MSI	1	1	1	1	MSI
D10S187	84	10q25.3	118.8	2	2	1	1	2	2	2	2	1	2	MSI	1	MSI	1	MSI
D10S209	74	10q26.12	122.4	2	2	1	1	2	2	1	2	1	2	1	1	2	1	MSI
D10S217	81	10q26.2	129.5	1	2	1	1	2	2	2	2	1	MSI	MSI	1	2	1	MSI

*** April 2003 freeze Genome Browser UCSC**

PTEN

PTEN	10q23.31	89.8	-	-	-	+	-	+	-	+	+	-	-	-	-	+	+

Figure 3. Chromosome 10 alterations identified by allelotype analysis in prostate cancer xenografts and cell lines. If two bands of different lengths were detected, two allelic forms were retained in the DNA. One band indicates the presence of one allele or two alleles of identical length. The homozygous deletions in PCEW, PC133, PC295, PC324, and PC-3 are represented by "0". The status of the *PTEN* gene is shown at the bottom of the figure. (+) indicates wild-type *PTEN*; (-) indicates inactivated *PTEN*.

Because matching normal DNA samples were not available for comparison, 5 consecutive mono-allelic bands of highly polymorphic markers was taken as indicative for loss of one copy of the corresponding chromosomal region. According to this definition, complete loss of one copy of chromosome 10 was found for TSU. Loss of distal 10p, including *KLF6*, was detected in PC310, PC324 and PC3. Large regions of apparent loss at 10q were present in PC133, PC295, PC339, PC374 and PC3. As also indicated by array CGH, a remarkable large number of small regions of loss of 10q23.3 were detected in samples with (PCEW, PC82, PC324, PC346 and LNCaP) or without (PC135 and DU145) complete *PTEN* inactivation. Homozygous deletions and mutation of *PTEN* were found

both in small and large regions of allelic loss (PCEW, PC82, PC324, PC346 and LNCaP, and PC133, PC295, PC374 and PC3, respectively; see Figure 2). In PC346, PC374, LNCaP and DU145, several polymorphic markers showed microsatellite instability (MSI), which limited the accuracy of allelotype analysis. Gains, which might be scored by allelic imbalance, were not taken into account.

Analysis of candidate tumor suppressor genes

Previous allelotype analyses indicated that *PTEN* might not be the only tumor suppressor gene on chromosome 10q (Trybus et al., 1996; Ittmann, 1996; Komiya et al., 1998; Leube et al., 2002). Distal to *PTEN* the candidate tumor suppressor genes *MXI1* (10q25.2) and *DMBT1* (10q26.2) have been mapped (Edelhoff et al., 1994; Shapiro et al., 1994; Mollenhauer et al. 1997). MXI1 antagonizes MYC in modulation of gene expression and tumorigenesis (Lahoz et al., 1994). *DMBT1* is unstable in cancer cells and might play a role in immune defense and epithelial cell differentiation (Mollenhauer et al., 1997, 2000). We examined the expression and structure of both genes in the 15 prostate cancer cell lines and xenografts. No homozygous deletions or somatic mutations of *MXI1* were detected, and *MXI1* mRNA was present in all RNA samples (data not shown). In the *DMBT1* gene, an intragenic homozygous deletion of the markers G14EXT and G14 was found in PC135 (Figure 4A). This homozygous deletion was further examined by PCR-SSCP, utilizing a primer set, which amplified the repeat units in *DMBT1* (Figure 4B; Mollenhauer et al., 1999). Only in PC135 an aberrant PCR-SSCP pattern was visible. Sequencing of the amplified fragments combined with the presence of marker 36K (Figure 4A) indicated that the maximum size of the homozygous deletion in *DMBT1* was between exons 6 and 27 (Figure 4C). Semi-quantitative RT-PCR showed low DMBT1 expression in PC82 and PCEW (data not shown).

Recently, a variable frequency of inactivating mutations in *KLF6* on 10p15 has been described in prostate cancer (Narla et al., 2001; Chen et al., 2003). However, examination of *KLF6* in the 15 xenografts and cell lines revealed normal expression and absence of homozygous deletions or inactivating mutations (data not shown).

Loss of the *PTEN* flanking region at 10q23.3

In mouse prostate cancer models not only complete *PTEN* inactivation, but also *PTEN* haplo-insufficiency has been implicated in tumorigenisis (Di Cristofano et al., 2001; Kwabi-Addo et al., 2001; You et al., 2002; Kim et al., 2002). The role of *PTEN* haplo-insufficiency in human prostate cancer is not well defined. Investigation of the *PTEN* locus (Figure 3), compared with *PTEN* inactivation data (Figure 3, bottom; Vlietstra et al., 1998) learned that the xenografts PC310 and PC329 contain 2 wild-type *PTEN* alleles. In 9 DNA samples both *PTEN* alleles were inactivated by homozygous deletion (PCEW, PC133, PC295, PC324 and PC3) or deletion of one allele combined with a point mutation

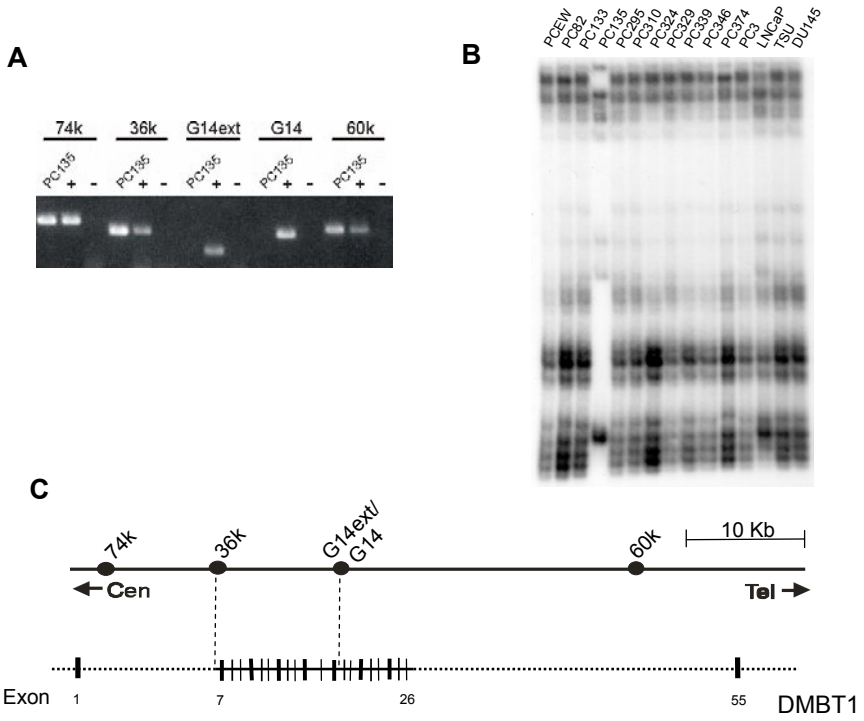

Figure 4. Characterization of the homozygous deletion in *DMBT1* in PC135. (A) Agarose gel analysis of the indicated amplified *DMBT1* gene fragments in PC135. (B) PCR-SSCP of the repeat units of *DMBT1* in prostate cancer xenografts and cell lines. (C) Schematic representation of the deleted segment in *DMBTl* in PC135.

(PC82, PC346, PC374 and LNCaP). Loss of 1 copy of *PTEN* might have occurred in PC135, PC339 and DU145 (Figure 3). TSU was not taken into account, because all chromosome 10 markers showed one allelic form. Array CGH did not confirm loss of *PTEN* in DU145 (data not shown). More detailed studies also excluded PC339 (see below). So, *PTEN* haplo-insufficiency seems only present in PC135.

PTEN flanking genes might be complementary or independent candidate genes involved in prostate cancer. We searched 16 genes flanking *PTEN* for homozygous deletions, and the borders of small regions of allelic loss or homozygous deletion were accurately mapped. The order of genes and candidate genes was taken from the UCSC Genome database (see also Figure 6A). Figure 5 illustrates the genes at 10q23.3, which were deleted in the xenografts and cell lines, as determined by PCR. The first distal *PTEN* flanking gene, *FLJ11218*, was completely or partially deleted in all samples containing *PTEN* deletion, except for PC295. *MINPP1*, *PAPSS2*, *FLJ14600* and *LIPF* were deleted in part of the samples. None of the DNA samples without complete deletion of *PTEN* contained a homozygous deletion of the 16 flanking genes (data not shown; see for genes investigated Materials and Methods and Figure 6A).

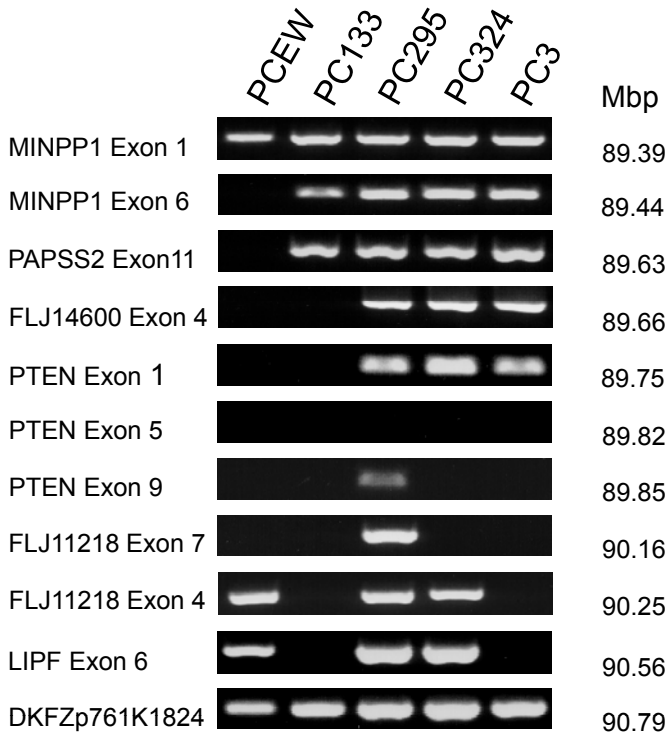

Figure 5. Genes at 10q23.3 inactivated by homozygous deletion in the prostate cancer xenografts PCEW, PC133, PC295 and PC324 and the cell line PC3. The figure shows agarose gel electrophoresis of amplified exons of the indicated genes. The positions of the genes on chromosome 10 in Mbp from the top of the p arm are indicated at the right.

Figure 6 summarizes the calculations of the lengths of homozygous deletions and mono-allelic regions in the *PTEN* region. These calculations not only took into account the outcome of microsatellite repeat analyses, but also single nucleotide polymorphisms in *MINPP1*, *PAPSS2*, *FLJ11218* and *TNFRSF6* genes (see Materials and Methods). The homozygous deletions in PCEW, PC133, PC295, PC324 and PC3 ranged in size from 1.2 Mbp (PC133) to <30 Kbp (PC295) (Figure 6B, see also Figures 3 and 5). In both PC324 and PCEW, the telomeric border of the deletion was in intron 5 of *FLJ11218*. In PCEW, the deletions in both 10q copies were small and almost identical in lengths. In PC324, the mono-allelic region around *PTEN* was less than 2 Mbp. The mono-allelic regions in PC82 and PC346, which both contain a *PTEN* point mutation, and in DU145 and PC135, which do not contain inactivated *PTEN* were less than 3 Mbp (Figures 3 and 6C,D). So, in many samples small mono-allelic regions around the *PTEN* locus could accurately be mapped. Most DNA samples did not only loose one or two copies of *PTEN*, but also one or two copies of *FLJ11218* and one copy of *MINPP1*, *PAPSS2* and *FLJ14600*. PC339 is an exception, because the mono-allelic region starts in *FLJ11218*, distal from *PTEN* to 10qtel.

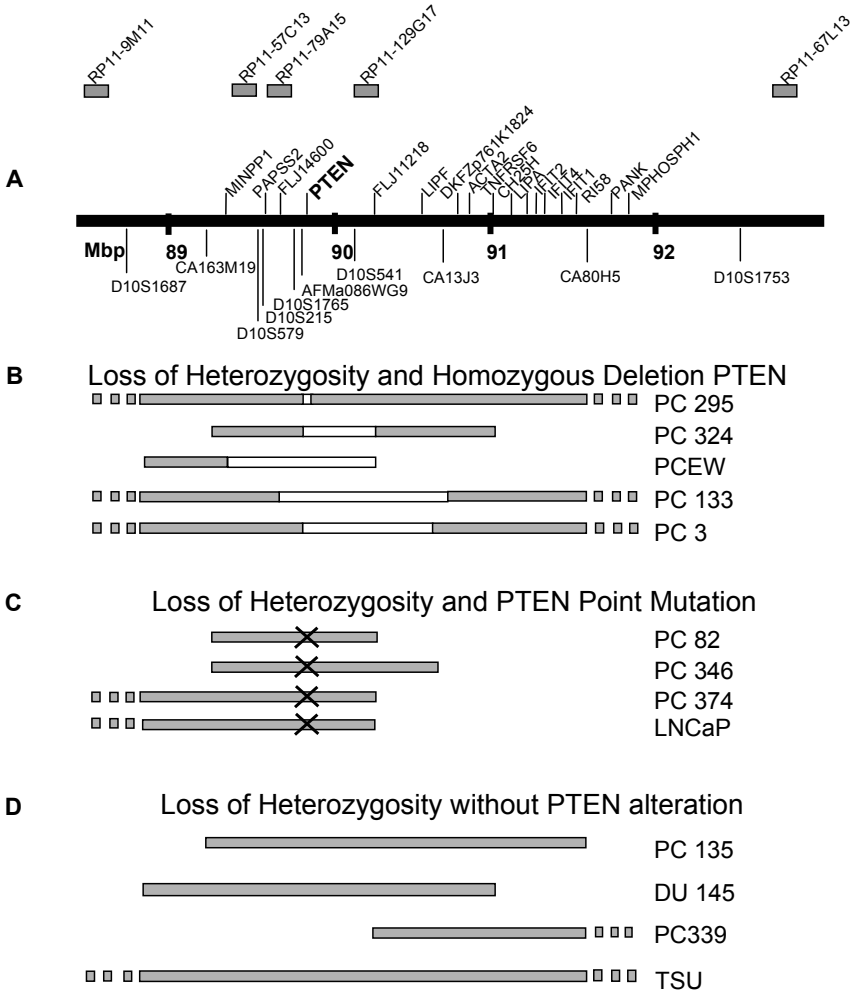

Figure 6. Schematic representation of the homozygous deletions and mono-allelic regions flanking the *PTEN* locus in prostate cancer xenografts and cell lines. (A) Genes mapping distal and proximal of *PTEN*. Data are from the April 2003 release of the UCSC gene map. (B) Homozygous deletions (open bars) and mono-allelic regions (gray bar) in PC295, PC324, PCEW, PC133 and PC3. Grey blocks indicate unknown border of loss (C) Mono-allelic regions (gray bars) in PC82, PC346, PC374 and LNCaP. A cross indicates *PTEN* inactivation by point mutation (see Vleitstra et al., 1998). (D) Mono-allelic regions in PC135, DU145, PC339 and TSU, which lack complete *PTEN* inactivation.

Expression and structure of genes flanking the *PTEN* locus

To investigate further a possible contribution of *PTEN* flanking genes in prostate cancer, the expression patterns of 14 genes in 3 Mbp flanking the *PTEN* locus, bordered by the polymorphic markers *D10S1687* and *D10S1753* (see Figure 6A) were analyzed by semi-quantitative RT-PCR The results are summarized in Table I. The 1 exon genes *DKFZp761K184* and *CH25H* were not included. *MINPP1*, *PAPSS2* and *FLJ11218* expressions

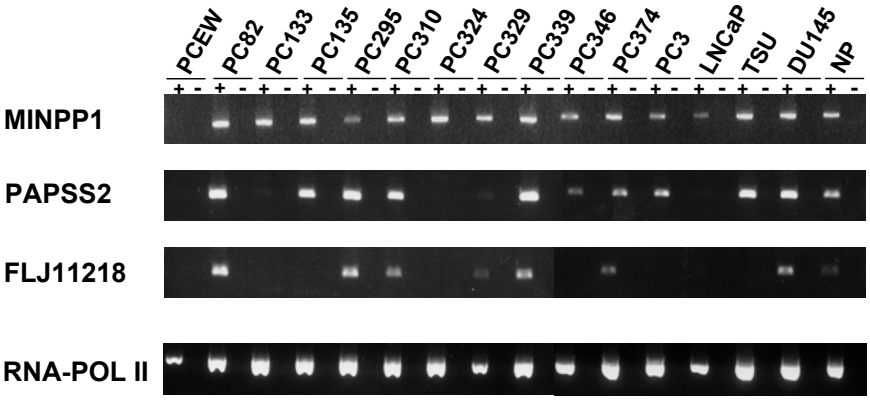

Figure 7. Expression of MINPP1, PAPSS2 and FLJ11218 mRNA in prostate cancer xenografts and cell lines. Expression was monitored by agarose gel electrophoresis of semi-quantitative RT-PCR products. RNA polymerase II was used as a control.

are shown as examples in Figure 7. A mixed pattern of expression profiles was found. Obviously, except for *PTEN* in PC295, homozygous deletion of a gene correlated with absence of expression. In the semi-quantitative RT-PCR no clear-cut correlation was found between the copy number and expression level of a gene, indicating gene-copy independent regulatory mechanisms to be more important. The stomach-specific gene *LIPF* was hardly expressed in the prostate tumor cells. Most other genes showed a rather stable expression level. Potentially interesting variable expression patterns were seen for *PAPSS2*, *FLJ11218*, and the interferon-regulated gene family *IFIT1,2,4*, *RI58*. High expression of the latter gene family almost perfectly correlated with androgen independence of a xenograft or cell line, PC82 is an exception (Table 1). *PAPSS2* not only showed absence of expression due to homozygous deletion of the gene (PCEW), but expression was also undetectable or very low in PC133, PC324, PC329 and LNCaP. *FLJ11218* expression was not only absent in the 4 samples, where the gene was completely deleted, but also absent or very low in PC135, PC346, LNCaP and TSU.

Four flanking genes, which were selected on the basis of frequent deletion and low expression (*FLJ11218*) or function, the phospholipid phosphatase *MINPP1*, the sulfatase *PAPSS2* and the tumor necrosis factor receptor *TNFRSF6*, were searched for point mutations. In *MINPP1* and *TNFRSF6* polymorphisms, but no somatic mutations were detected. In *PAPSS2* a polymorphism, which is presumed to decrease its function (Met295 in PC133; see Xu et al., 2002), one frame-shift (deletion C in codon 355 in LNCaP) and a missense mutation [GTG to ATG (V45M) in PC346] were found. In *FLJ11218* we frequently observed the polymorphism GAG/GAC (E37D) in exon 1, and polymorphisms in introns 4 and 6. In addition, we detected in PC374 the missense mutation ATT to AGT (N232S) in exon 5 in PC374.

Table I. Expression of the PTEN flanking genes in prostate cancer xenografts and cell lines

	PCEW	PC82	PC133	PC135	PC295	PC310	PC324	PC329	PC339	PC346	PC374	PC3	LNCaP	TSU	DU145
androgen dependend	+	+	-	-	+	+	-	+	-	+	+/-	-	+	-	-
mRNA															
MINPP1	-	+++	+++	+++	++	+++	+++	+++	+++	+++	+++	+++	++	+++	+++
PAPSS2	-	+++	+/-	+++	+++	+++	-	+	+++	+	++	++	+/-	+++	+++
FLJ14600	-	+++	+	+++	+++	+++	+++	+++	++	+++	+++	+++	+++	+++	+++
PTEN	-	+++	-	+	+++	+++	-	+++	++	+++	+++	-	+++	++	+++
FLJ11218	-	+++	-	-	+++	++	-	+	++	-	+	-	+/-	-	++
LIPF	+/-	+	-	-	+	-	-	-	-	-	+/-	-	-	-	-
ACTA2	++	++	-	++	++	++	++	++	++	-	++	++	++	++	++
TNFRSF6	+++	+++	+++	+++	+++	+++	+++	+++	+++	+	+++	+++	+++	+++	+++
LIPA	+++	+++	+++	+++	+++	+++	+++	+++	+++	+/-	+++	+++	+++	+++	+++
IFIT2	+/-	+	+	++	+/-	+	+++	+/-	+	+/-	+++	+++	+/-	+	++
IFIT4	-	++	++	++	-	+/-	+++	+/-	++	-	++	+++	-	+	+++
IFIT1	-	++	++	+++	-	+	+++	-	+++	+/-	+++	+++	+/-	+++	+++
RI58	-	++	++	++	-	+	+++	-	++	-	++	+++	+	++	++
PANK	++	++	++	++	++	++	++	++	++	++	++	++	++	++	++
MPHOSPH1	+++	+++	+++	+++	+++	+++	+++	+++	+++	+++	+++	+++	+++	+++	+++

Summarizing, low expression or inactivation of 1 or 2 copies of the telomeric flanking gene *FLJ11218* always paralleled *PTEN* inactivation. Less frequent alterations in *PAPSS2* copy number, structure or expression were detected. In approximately half of the DNA samples one copy of *MINPP1* was lost.

DISCUSSION

In this study, we characterized chromosome 10 alterations in xenografts and cell lines derived from human prostate cancer. Although it can be argued that xenografts and cell lines acquire extra genetic alterations during *in vivo* and *in vitro* culturing, as we were able to study for some xenografts, most genetic alterations are already present in the tumor tissue from which the xenografts derive. We choose for xenogafts and cell lines because they lack normal human cells, which enabled accurate study of homozygous deletions, regions of chromosomal loss and gene expression patterns.

The conventional CGH and array CGH data indicated a pattern of loss of distal 10p, gain of proximal 10p and 10q and loss of distal 10q. Previous conventional CGH studies of DNA from prostate cancer patients showed a similar pattern, although at a lower frequency (Cher et al., 1996; Nupponen et al., 1998b; Alers et al., 2000). Absence of chromosome 10 alterations in LNCaP and TSU, and the loss-gain-loss pattern in PC3 were in accordance with previous CGH data of these cell lines (Nupponen et al., 1998a). A recent CGH study on a different panel of xenografts also provided the overall picture of loss of distal 10p and distal 10q and gain of the middle part of chromosome 10 (Laitinen et al., 2002). In all studies loss of part of the q arm is the most frequent chromosome 10 alteration.

Array CGH data of chromosome 10 in prostate cancer xenografts and patient tissues are not yet available. In general, our conventional CGH and array CGH data showed the same large regions of loss and gain, although the 10p and 10q losses in the array CGH of PC3 are not very clear (compare Figures 1 and 2). Obviously, array CGH had the advantage to detect small homozygous deletions and high-level amplifications, not visible in conventional CGH. Except for the exon 5 deletion in PC295, all previously described *PTEN* homozygous deletions (Vlietstra et al., 1998) were detected by array CGH. Importantly, many regions of single copy loss around *PTEN* were also small. No doubt, a tilted BAC array, covering chromosome 10 completely should further increase the sensitivity of array CGH. It should also be instrumental in detection of homozygous deletions and *PTEN* haplo-insufficiency in DNA tissues from all stages of prostate cancer. From our findings it can be assumed that until now conventional CGH of prostate cancer tissues frequently missed loss of *PTEN*, underestimating its role in tumorigenesis.

Recently, cDNA arrays have been applied for the analysis of genomic DNA from LNCaP, PC3 and DU145 cell lines (Clark et al., 2003). The results indicated absence of alterations

in LNCaP and DU145, and amplification of the middle part of chromosome 10 in PC3. We confirmed by allelotype analysis the homozygous deletion of *SFTPA2* at 10q22 in PC3 described by Clark et al. (data not shown). However, we did not find the homozygous deletion by array CGH, due to the absence of a BAC that covers *SFTPA2*. Interestingly, three BACs (RP11-78F9, RP11-342M3 and RP11-31L4), which map directly proximal to *SFTPA2* at 10q22.3, showed high-level amplification in PC3 (see Figure 2). In PC3, chromosome 10 seems to be involved in several translocations (Pan et al., 1999). A frequently detected breakpoint in PC3 and other prostate cancer cell lines maps at band 10q22 (Pan et al., 2001). This knowledge combined with the abrupt transition from amplification to deletion at 10q22 in PC3, suggests that *SFTPA2* is at the border of a translocation. *SFTPA2* might be lost due to an unbalanced translocation. A breakpoint at 10q22, followed by amplification of proximal 10q and loss of distal 10q, might also be present in PC135 (Figure 2). The homozygous deletion of *PTEN* in PC3 was not detected in the cDNA array (Clark et al., 2003), which might be caused by cross-hybridization with the *PTEN* pseudogene, a drawback of the application of cDNA arrays for genomic analyses.

The two high-level amplifications in PC3, at 10p11.2 and 10q22.3 respectively, might provide a first clue to the most important amplified genes on proximal 10p and 10q in prostate cancer. However, many genes are located in the amplified region at 10p11.2, and an obvious candidate cannot be pinpointed as yet. *PPIF* (cyclophilin F) and the candidate gene *FLJ90798* map precisely in the high-level amplification at 10q22.3. Whether these genes or proximal flanking genes are most important for tumor growth remains to be established. The previously in PC3 observed amplified and over-expressed *uPA* gene (Helenius et al., 2001) maps approximately 5.5 Mbp centromeric of *PPIF* and *FLJ90798*. Further gene hunting should benefit from the identification of overlapping high-level amplifications in prostate cancer DNA samples.

Although in some DNA samples hampered by microsatellite instability, allelotype analysis was very informative. Many small regions of apparent chromosomal loss at the *PTEN* locus could easily be detected. In general, large regions of a mono-allelic band in allelotype analyses matched with 10q deletions as detected by CGH. However, allelotype analysis did not detect deletion of a large region of 10q in PC135. Further, chromosome 10 allelotype analysis did not match CGH in TSU. No chromosome copy changes were seen by CGH, but allelotype analysis showed one allelic form of all markers. This is strong evidence for isodisomy chromosome 10 in this cell line. A similar observation was made for chromosomes 6 and 8 (Verhagen et al., 2002, and Van Alewijk, unpublished data), suggesting defective chromosome segregation in TSU.

Allelotype analysis confirmed loss of distal 10p in PC310, PC324 and PC3. However, we did not find alterations in *KLF6* at 10p15, as previously reported in prostate cancer tissues (Narla et al., 2001; Chen et al., 2003). Although it can be argued that the number

of samples studied is small, our data indicate that the most frequently affected tumor suppressor gene on 10p remains to be identified.

Allelotype analysis of 10q23.3 in tumors from patients frequently showed a higher percentage of allelic loss at the *PTEN* locus than *PTEN* alterations (Feilotter et al., 1998; Pesche et al., 1998). There might be several explanations for this observation. First of all, complete inactivation of *PTEN* by point mutation or homozygous deletion might have been missed. Secondly, it has been proposed that in these samples not *PTEN*, but a more distal gene was inactivated. We could not find evidence for this argument. No alterations in *MXI1,* at 10q25.2, previously implicated at low frequency in prostate cancer were observed (Eagle et al., 1995; Prochownik et al., 1998). Neither did we detect at high-frequency deletions in the unstable *DMBT1* gene, which has been described as a candidate tumor suppressor gene in several other tumor types (Mollenhauer et al., 1999). We also could not find complete inactivation of one of the *PTEN* flanking genes in the absence of *PTEN* alteration. Therefore, an attractive alternative is *PTEN* haplo-insufficiency as the underlying molecular background of 10q loss in early stage prostate cancer. In general xenografts and cell lines should be considered as late stage prostate cancer, accordingly the high percentage of complete inactivation of *PTEN* is not surprising. *PTEN* haplo-insufficiency seems to be present in PC135 and possibly DU145 (Figure 3). Careful examination of DNA from micro-dissected prostate cancer samples with a variety of experimental approaches should be carried out to address the important issue of *PTEN* haplo-insufficiency in human prostate cancer. In favor of a role of *PTEN* haplo-insufficiency in human prostate cancer are mouse model studies. In four prostate cancer models, based on prostate specific SV40-Tag expression (TRAMP model), inactivation of *Ink4a/Arf*, *Cdkn1b* or *Nkx3.1, Pten* haplo-insufficiency stimulated tumor growth (Di Cristofano et al., 2001; Kwabi-Addo et al., 2001; You et al., 2002; Kim et al., 2002).

Although we could not find evidence for a *PTEN* independent role of flanking genes in prostate cancer, a complementary role cannot be excluded. Two observations are important in this regard: the high frequency of *PTEN* inactivation by homozygous deletion, and the remarkable small size of 10q losses that accompany many *PTEN* inactivations. The latter observation limits the candidate genes to those directly flanking *PTEN*. We did not study in detail *FLJ14600*, because it is clearly expressed in almost all xenografts and cell lines. *MINPP1* would have been an interesting candidate, because like *PTEN* it is able to affect phospholipid metabolism. However, the specificity of MINPP1 seems different from PTEN, and *MINPP1* is in only part of the samples affected by loss of one gene copy. The sulfatase gene *PAPSS2* shows more frequently loss of one copy. In addition, PAPPS2 is not expressed or expressed at a low level in several xenografts and cell lines. Interestingly, also 2 presumed inactivating mutations were detected, although both are in samples, which already show a low level of PAPSS2 expression (PC133 and LNCaP). Arguing against a role of *PAPSS2* deficiency in prostate cancer is the expression of the related

gene *PAPSS1* in all cell lines and xenografts (data not shown). The strongest candidate to complement *PTEN* in tumorigenesis is the candidate gene *FLJ11218*. It is inactivated by homozygous deletion in 4 DNA samples, and loss of one copy or low expression is found in many other samples (Figures 6 and 7). Unfortunately, so far the function of FLJ11218 is unknown. However, our data warrant further study of this candidate gene in prostate cancer.

ACKNOWLEDGMENTS

We thank Leen Blok, and Angelique Ziel-van der Made for RNA samples, Janneke Alers for conventional CGH advice, Irene Janssen for expert technical assistance and Jan Mollenhauer for making available *DMBT1* information prior to publication. This study was supported in part by a grant from the Dutch Cancer Society KWF.

REFERENCES

Alers JC, Rochat J, Krijtenburg PJ, Hop WC, Kranse R, Rosenberg C, Tanke HJ, Schroder FH, van Dekken H. 2000. Identification of genetic markers for prostatic cancer progression. Lab Invest 80:931-42.

Cairns P, Okami K, Halachmi S, Halachmi N, Esteller M, Herman JG, Jen J, Isaacs WB, Bova GS, Sidransky D. 1997. Frequent inactivation of PTEN/MMAC1 in primary prostate cancer. Cancer Res 57:4997-5000.

Cappellen D, Gil Diez de Medina S, Chopin D, Thiery JP, Radvanyi F. 1997. Frequent loss of heterozygosity on chromosome 10q in muscle-invasive transitional cell carcinomas of the bladder. Oncogene 14:3059-66.

Chen C, Hyytinen ER, Sun X, Helin HJ, Koivisto PA, Frierson HF, Jr., Vessella RL, Dong JT. 2003. Deletion, mutation, and loss of expression of KLF6 in human prostate cancer. Am J Pathol 162:1349-54.

Cher ML, Bova GS, Moore DH, Small EJ, Carroll PR, Pin SS, Epstein JI, Isaacs WB, Jensen RH. 1996. Genetic alterations in untreated metastases and androgen-independent prostate cancer detected by comparative genomic hybridization and allelotyping. Cancer Res 56:3091-102.

Clark J, Edwards S, Feber A, Flohr P, John M, Giddings I, Crossland S, Stratton MR, Wooster R, Campbell C, Cooper CS. 2003. Genome-wide screening for complete genetic loss in prostate cancer by comparative hybridization onto cDNA microarrays. Oncogene 22:1247-52..

Di Cristofano A, De Acetis M, Koff A, Cordon-Cardo C, Pandolfi PP. 2001. Pten and p27KIP1 cooperate in prostate cancer tumor suppression in the mouse. Nat Genet 27:222-4.

Eagle LR, Yin X, Brothman AR, Williams BJ, Atkin NB, Prochownik EV. 1995. Mutation of the MXI1 gene in prostate cancer. Nat Genet 9:249-55.

Edelhoff S, Ayer DE, Zervos AS, Steingrimsson E, Jenkins NA, Copeland NG, Eisenman RN, Brent R, Disteche CM. 1994. Mapping of two genes encoding members of a distinct subfamily of MAX interacting proteins: MAD to human chromosome 2 and mouse chromosome 6, and MXI1 to human chromosome 10 and mouse chromosome 19. Oncogene 9:665-8.

Feilotter HE, Nagai MA, Boag AH, Eng C, Mulligan LM. 1998. Analysis of PTEN and the 10q23 region in primary prostate carcinomas. Oncogene 16:1743-8.

Fujimoto M, Fults DW, Thomas GA, Nakamura Y, Heilbrun MP, White R, Story JL, Naylor SL, Kagan-Hallet KS, Sheridan PJ. 1989. Loss of heterozygosity on chromosome 10 in human glioblastoma multiforme. Genomics 4:210-4.

Fukuhara H, Maruyama T, Nomura S, Oshimura M, Kitamura T, Sekiya T, Murakami Y. 2001. Functional evidence for the presence of tumor suppressor gene on chromosome 10p15 in human prostate cancers. Oncogene 20:314-9.

Gray IC, Phillips SM, Lee SJ, Neoptolemos JP, Weissenbach J, Spurr NK. 1995. Loss of the chromosomal region 10q23-25 in prostate cancer. Cancer Res 55:4800-3.

Gray IC, Stewart LM, Phillips SM, Hamilton JA, Gray NE, Watson GJ, Spurr NK, Snary D. 1998. Mutation and expression analysis of the putative prostate tumour-suppressor gene PTEN. Br J Cancer 78:1296-300.

Greenlee RT, Hill-Harmon MB, Murray T, Thun M. 2001. Cancer statistics, 2001. CA Cancer J Clin 51:15-36.

Helenius MA, Saramaki OR, Linja MJ, Tammela TL, Visakorpi T. 2001. Amplification of urokinase gene in prostate cancer. Cancer Res 61:5340-4.

Hoehn W, Schroeder FH, Reimann JF, Joebsis AC, Hermanek P. 1980. Human prostatic adenocarcinoma: some characteristics of a serially transplantable line in nude mice (PC 82). Prostate 1:95-104.

Hoehn W, Wagner M, Riemann JF, Hermanek P, Williams E, Walther R, Schrueffer R. 1984. Prostatic adenocarcinoma PC EW, a new human tumor line transplantable in nude mice. Prostate 5:445-52.

Ittmann M. 1996. Allelic loss on chromosome 10 in prostate adenocarcinoma. Cancer Res 56:2143-7.

James CD, Carlbom E, Dumanski JP, Hansen M, Nordenskjold M, Collins VP, Cavenee WK. 1988. Clonal genomic alterations in glioma malignancy stages. Cancer Res 48:5546-51.

Kallioniemi A, Kallioniemi OP, Sudar D, Rutovitz D, Gray JW, Waldman F, Pinkel D. 1992. Comparative genomic hybridization for molecular cytogenetic analysis of solid tumors. Science 258:818-21.

Kim SK, Ro JY, Kemp BL, Lee JS, Kwon TJ, Hong WK, Mao L. 1998. Identification of two distinct tumor-suppressor loci on the long arm of chromosome 10 in small cell lung cancer. Oncogene 17:1749-53.

Kim MJ, Cardiff RD, Desai N, Banach-Petrosky WA, Parsons R, Shen MM, Abate-Shen C. 2002. Cooperativity of Nkx3.1 and Pten loss of function in a mouse model of prostate carcinogenesis. Proc Natl Acad Sci U S A 99:2884-9.

Komiya A, Suzuki H, Ueda T, Yatani R, Emi M, Ito H, Shimazaki J. 1996. Allelic losses at loci on chromosome 10 are associated with metastasis and progression of human prostate cancer. Genes Chromosomes Cancer 17:245-53.

Kwabi-Addo B, Giri D, Schmidt K, Podsypanina K, Parsons R, Greenberg N, Ittmann M. 2001. Haploinsufficiency of the Pten tumor suppressor gene promotes prostate cancer progression. Proc Natl Acad Sci U S A 98:11563-8.

Lahoz EG, Xu L, Schreiber-Agus N, DePinho RA. 1994. Suppression of Myc, but not E1a, transformation activity by Max-associated proteins, Mad and Mxi1. Proc Natl Acad Sci U S A 91:5503-7.

Laitinen S, Karhu R, Sawyers CL, Vessella RL, Visakorpi T. 2002. Chromosomal aberrations in prostate cancer xenografts detected by comparative genomic hybridization. Genes Chromosomes Cancer 35:66-73.

Leube B, Drechsler M, Muhlmann K, Schafer R, Schulz WA, Santourlidis S, Anastasiadis A, Ackermann R, Visakorpi T, Muller W, Royer-Pokora B. 2002. Refined mapping of allele loss at chromosome 10q23-26 in prostate cancer. Prostate 50:135-44.

Li J, Yen C, Liaw D, Podsypanina K, Bose S, Wang SI, Puc J, Miliaresis C, Rodgers L, McCombie R, Bigner SH, Giovanella BC, Ittmann M, Tycko B, Hibshoosh H, Wigler MH, Parsons R. 1997. PTEN, a putative protein tyrosine phosphatase gene mutated in human brain, breast, and prostate cancer. Science 275:1943-7.

McMenamin ME, Soung P, Perera S, Kaplan I, Loda M, Sellers WR. 1999. Loss of PTEN expression in paraffin-embedded primary prostate cancer correlates with high Gleason score and advanced stage. Cancer Res 59:4291-6.

Mollenhauer J, Wiemann S, Scheurlen W, Korn B, Hayashi Y, Wilgenbus KK, von Deimling A, Poustka A. 1997. DMBT1, a new member of the SRCR superfamily, on chromosome 10q25.3-26.1 is deleted in malignant brain tumours. Nat Genet 17:32-9.

Mollenhauer J, Holmskov U, Wiemann S, Krebs I, Herbertz S, Madsen J, Kioschis P, Coy JF, Poustka A. 1999. The genomic structure of the DMBT1 gene: evidence for a region with susceptibility to genomic instability. Oncogene 18:6233-40.

Mollenhauer J, Herbertz S, Holmskov U, Tolnay M, Krebs I, Merlo A, Schroder HD, Maier D, Breitling F, Wiemann S, Grone HJ, Poustka A. DMBT1 encodes a protein involved in the immune defense and in epithelial differentiation and is highly unstable in cancer. Cancer Res 60:1704-10.

Morita R, Saito S, Ishikawa J, Ogawa O, Yoshida O, Yamakawa K, Nakamura Y. 1991. Common regions of deletion on chromosomes 5q, 6q, and 10q in renal cell carcinoma. Cancer Res 51:5817-20.

Nagase S, Sato S, Tezuka F, Wada Y, Yajima A, Horii A. 1996. Deletion mapping on chromosome 10q25-q26 in human endometrial cancer. Br J Cancer 74:1979-83.

Narla G, Heath KE, Reeves HL, Li D, Giono LE, Kimmelman AC, Glucksman MJ, Narla J, Eng FJ, Chan AM, Ferrari AC, Martignetti JA, Friedman SL. 2001. KLF6, a candidate tumor suppressor gene mutated in prostate cancer. Science 294:2563-6.

Nupponen NN, Hyytinen ER, Kallioniemi AH, Visakorpi T. 1998a. Genetic alterations in prostate cancer cell lines detected by comparative genomic hybridization. Cancer Genet Cytogenet 101:53-7.

Nupponen NN, Kakkola L, Koivisto P, Visakorpi T. 1998b. Genetic alterations in hormone-refractory recurrent prostate carcinomas. Am J Pathol 153:141-8.

Pan Y, Kytola S, Farnebo F, Wang N, Lui WO, Nupponen N, Isola J, Visakorpi T, Bergerheim US, Larsson C. 1999. Characterization of chromosomal abnormalities in prostate cancer cell lines by spectral karyotyping. Cytogenet Cell Genet 87:225-32.

Pan Y, Lui WO, Nupponen N, Larsson C, Isola J, Visakorpi T, Bergerheim US, Kytola S. 2001. 5q11, 8p11, and 10q22 are recurrent chromosomal breakpoints in prostate cancer cell lines. Genes Chromosomes Cancer 30:187-95.

Peiffer SL, Herzog TJ, Tribune DJ, Mutch DG, Gersell DJ, Goodfellow PJ. 1995. Allelic loss of sequences from the long arm of chromosome 10 and replication errors in endometrial cancers. Cancer Res 55:1922-6.

Pesche S, Latil A, Muzeau F, Cussenot O, Fournier G, Longy M, Eng C, Lidereau R. 1998. PTEN/MMAC1/TEP1 involvement in primary prostate cancers. Oncogene 16:2879-83.

Prochownik EV, Eagle Grove L, Deubler D, Zhu XL, Stephenson RA, Rohr LR, Yin X, Brothman AR. 1998. Commonly occurring loss and mutation of the MXI1 gene in prostate cancer. Genes Chromosomes Cancer 22:295-304.

Rasheed BK, Stenzel TT, McLendon RE, Parsons R, Friedman AH, Friedman HS, Bigner DD, Bigner SH. 1997. PTEN gene mutations are seen in high-grade but not in low-grade gliomas. Cancer Res 57:4187-90.

Reifenberger J, Wolter M, Bostrom J, Buschges R, Schulte KW, Megahed M, Ruzicka T, Reifenberger G. 2000. Allelic losses on chromosome arm 10q and mutation of the PTEN (MMAC1) tumour suppressor gene in primary and metastatic malignant melanomas. Virchows Arch 436:487-93.

Rempel SA, Schwechheimer K, Davis RL, Cavenee WK, Rosenblum ML. 1993. Loss of heterozygosity for loci on chromosome 10 is associated with morphologically malignant meningioma progression. Cancer Res 53:2386-92.

Sambrook J, Russell DW. 2001. Molecular cloning A laboratory manual. Cold Spring Harbor, NY: Cold Spring Harbor Laboratory Press.

Shapiro DN, Valentine V, Eagle L, Yin X, Morris SW, Prochownik EV. 1994. Assignment of the human MAD and MXI1 genes to chromosomes 2p12-p13 and 10q24-q25. Genomics 23:282-5.

Speaks SL, Sanger WG, Masih AS, Harrington DS, Hess M, Armitage JO. 1992. Recurrent abnormalities of chromosome bands 10q23-25 in non-Hodgkin's lymphoma. Genes Chromosomes Cancer 5:239-43.

Steck PA, Pershouse MA, Jasser SA, Yung WK, Lin H, Ligon AH, Langford LA, Baumgard ML, Hattier T, Davis T, Frye C, Hu R, Swedlund B, Teng DH, Tavtigian SV. 1997. Identification of a candidate tumour suppressor gene, MMAC1, at chromosome 10q23.3 that is mutated in multiple advanced cancers. Nat Genet 15:356-62.

Tashiro H, Blazes MS, Wu R, Cho KR, Bose S, Wang SI, Li J, Parsons R, Ellenson LH. 1997. Mutations in PTEN are frequent in endometrial carcinoma but rare in other common gynecological malignancies. Cancer Res 57:3935-40.

Teng DH, Hu R, Lin H, Davis T, Iliev D, Frye C, Swedlund B, Hansen KL, Vinson VL, Gumpper KL, Ellis L, El-Nagger A, Frazier M, Jasser S, Langford LA, Lee J, Mills GB, Pershouse MA, Pollack RE, Tornos C,

Troncoso P, Yung WK, Fujii G, Berson A, Steck PA. 1997. MMAC1/PTEN mutations in primary tumor specimens and tumor cell lines. Cancer Res 57:5221-5.

Trybus TM, Burgess AC, Wojno KJ, Glover TW, Macoska JA. 1996. Distinct areas of allelic loss on chromosomal regions 10p and 10q in human prostate cancer. Cancer Res 56:2263-7.

van Weerden WM, de Ridder CM, Verdaasdonk CL, Romijn JC, van der Kwast TH, Schroder FH, van Steenbrugge GJ. 1996. Development of seven new human prostate tumor xenograft models and their histopathological characterization. Am J Pathol 149:1055-62.

Veltman JA, Schoenmakers EF, Eussen BH, Janssen I, Merkx G, van Cleef B, van Ravenswaaij CM, Brunner HG, Smeets D, van Kessel AG. 2002. High-throughput analysis of subtelomeric chromosome rearrangements by use of array-based comparative genomic hybridization. Am J Hum Genet 70:1269-76.

Veltman JA, Fridlyand J, Pejavar S, Olshen AB, Korkola JE, DeVries S, Carroll P, Kuo WL, Pinkel D, Albertson D, Cordon-Cardo C, Jain AN, Waldman FM. 2003. Array-based Comparative Genomic Hybridization for Genome-Wide Screening of DNA Copy Number in Bladder Tumors. Cancer Res 63:2872-80.

Verhagen PC, Hermans KG, Brok MO, van Weerden WM, Tilanus MG, de Weger RA, Boon TA, Trapman J. 2002. Deletion of chromosomal region 6q14-16 in prostate cancer. Int J Cancer 102:142-7.

Visakorpi T, Kallioniemi AH, Syvanen AC, Hyytinen ER, Karhu R, Tammela T, Isola JJ, Kallioniemi OP. 1995. Genetic changes in primary and recurrent prostate cancer by comparative genomic hybridization. Cancer Res 55:342-7.

Vlietstra RJ, van Alewijk DC, Hermans KG, van Steenbrugge GJ, Trapman J. 1998. Frequent inactivation of PTEN in prostate cancer cell lines and xenografts. Cancer Res 58:2720-3.

Wang SI, Parsons R, Ittmann M. 1998. Homozygous deletion of the PTEN tumor suppressor gene in a subset of prostate adenocarcinomas. Clin Cancer Res 4:811-5.

Wang SI, Puc J, Li J, Bruce JN, Cairns P, Sidransky D, Parsons R. 1997. Somatic mutations of PTEN in glioblastoma multiforme. Cancer Res 57:4183-6.

Whang YE, Wu X, Suzuki H, Reiter RE, Tran C, Vessella RL, Said JW, Isaacs WB, Sawyers CL. 1998. Inactivation of the tumor suppressor PTEN/MMAC1 in advanced human prostate cancer through loss of expression. Proc Natl Acad Sci U S A 95:5246-50.

Xu ZH, Freimuth RR, Eckloff B, Wieben E, Weinshilboum RM. 2002. Human 3'-phosphoadenosine 5'-phosphosulfate synthetase 2 (PAPSS2) pharmacogenetics: gene resequencing, genetic polymorphisms and functional characterization of variant allozymes. Pharmacogenetics 12:11-21.

You MJ, Castrillon DH, Bastian BC, O'Hagan RC, Bosenberg MW, Parsons R, Chin L, DePinho RA. 2002. Genetic analysis of Pten and Ink4a/Arf interactions in the suppression of tumorigenesis in mice. Proc Natl Acad Sci U S A 99:1455-60.

Chapter 4

TMPRSS2:ERG FUSION BY TRANSLOCATION OR INTERSTITIAL DELETION IS HIGHLY RELEVANT IN ANDROGEN-DEPENDENT PROSTATE CANCER, BUT IS BYPASSED IN LATE STAGE ANDROGEN RECEPTOR NEGATIVE PROSTATE CANCER

Karin G Hermans[1], Ronald van Marion[1], Herman van Dekken[1], Guido Jenster[2], Wytske M van Weerden[2] and Jan Trapman[1], Departments of [1]Pathology and [2]Urology, Josephine Nefkens Institute, Erasmus University Medical Center, Rotterdam, The Netherlands

Cancer Research 2006; 66: 10658-10663

ABSTRACT

Recently, a unique fusion between the prostate-specific, androgen-regulated *TMPRSS2* gene and the ETS genes *ERG*, *ETV1* or *ETV4* has been described in clinical prostate cancer. We investigated mechanisms of expression of four ETS genes, *ERG, ETV1*, *ETV4* and *FLI1*, in eleven xenografts representing different stages of prostate cancer. All five androgen-dependent xenografts showed as major transcripts over-expression of two splice variants of *TMPRSS2:ERG*, linking *TMPRSS2* exon 1 or 2 sequences to *ERG* exon 4. In one of two androgen-sensitive xenografts fusion transcripts of *TMPRSS2* and *ETV1* were detected. Array-based comparative genomic hybridization and interphase fluorescence *in situ* hybridization indicated both interstitial deletions and translocations as mechanisms of *TMPRSS2:ERG* gene fusion. Importantly, *TMPRSS2* to *ERG* fusions were also observed in three of four androgen-independent, androgen receptor negative xenografts and in two androgen receptor negative clinical prostate cancer specimens, however, the fusion gene was not expressed. In almost all androgen receptor negative tumor samples over-expression of wild type *ETV4* or *FLI1* was detected. Combined our observations indicate a key role of fusion of *TMPRSS2* and ETS genes in most androgen-regulated prostate cancers, which might be bypassed by androgen-independent expression of wild-type ETS factors in late stage disease.

INTRODUCTION

Prostate cancer is the most frequent cancer in men in countries with a western lifestyle and the second cause of male cancer death (1). Surgery and radiation are standard therapy of localized prostate cancer. Palliative therapy of metastatic prostate cancer aims at blocking androgen receptor (AR) function. A better understanding of the molecular mechanisms of tumorigenesis is essential for the development of novel therapies. Additionally, knowledge of the mechanism of prostate cancer development will improve prediction of the clinical course of the disease.

Recently, overexpression of the ETS gene *ERG* has been described in clinical prostate cancer (2). Subsequently, it was shown that overexpression of *ERG* and related *ETV1* was due to fusion of the *TMPRSS2* gene to either *ERG* or *ETV1* (3). This important finding adds gene fusion to the mechanisms of gene overexpression in epithelial tumors. At low frequency, *TMPRSS2* might also be fused to *ETV4* in prostate cancer (4). Expression of *TMPRSS2* that maps to 21q22 is androgen-regulated and prostate-specific (5). *ERG* is also located on 21q22, approximately 3 Mbp proximal to *TMPRSS2*. *ETV1* maps to 7p21 and *ETV4* to 17q21. Together with *FLI1*, modified *ERG*, *ETV1* and *ETV4* are well-known oncogenes involved in translocations in Ewing sarcoma and acute myeloid leukemia (6).

We investigated the ETS genes *ERG*, *ETV1*, *ETV4* and *FLI1* in human prostate cancers transplanted on nude mice. Xenografts are powerful models for dedicated genetic and molecular studies because they lack normal cells of human origin. The xenografts utilized represent a variety of clinical stages of prostate cancer, ranging from primary tumors and local metastases to recurrent disease and distant metastases, and from androgen-dependent to androgen-independent cancers (7-9). Our data reveal both interstitial deletion and gene translocation as mechanisms of fusion between *TMPRSS2* and *ERG*. Further our results show high overexpression of two splice variants of the *TMPRSS2:ERG* fusion gene in all androgen-dependent xenografts and absence of *ERG* overexpression in late stage, AR negative xenografts, even if they contain a *TMPRSS2:ERG* fusion gene. The latter observation was also made in AR negative clinical prostate cancer. In almost all late-stage, AR negative prostate cancer samples apparently androgen-independent expression of wild type *ETV4* and *FLI1* is detected. These findings show a key role of *TMPRSS2:ERG* in androgen-dependent prostate cancer, which might be bypassed by other ETS factors in late stage, AR negative disease.

MATERIALS AND METHODS

Prostate cancer samples.

The *in vivo* growing xenografts PCEW, PC82, PC133, PC135, PC295, PC310, PC324, PC329, PC339, PC346, and PC374 were propagated by serial transplantation on male nude mice as described (7-9). PCEW, PC82, PC295, PC310 and PC329, derived from primary tumors or local metastases, are androgen-dependent. PC133, PC324, PC339, PC346 and PC376 are derived from distant metastases or local progressive disease and are androgen-independent (PC133, PC324, PC339) or androgen-sensitive (PC346, PC374). PC135 is androgen-independent and derived from a lymph node metastasis (see Supplementary Table S1).

Clinical prostate tumor samples were obtained from recurrent disease by transurethral resection (TUR-P) after informed consent, following approval of the institutional ethical committee.

DNA and RNA preparation.

Genomic DNA was isolated utilizing the Puregene system from Gentra Systems (Minneapolis, MN) according to the procedure described by the manufacturer. Xenograft RNA was isolated according to the LiCl protocol (10). For isolation of RNA from clinical samples the Illustra mini RNA kit (General Electric Healthcare, Fairfield, CT) was utilized.

Array-based CGH.

Arrays were produced from the human 3600 BAC/PAC genomic clone set of the Welcome Trust Sanger Institute, covering the full genome at approximately 1 Mb-spacing. Degenerated oligonucleotide PCR-products were prepared for spotting on CodeLink® slides (General Electric Healthcare) according to published protocols (11) with some modifications (12). DNA labeling and hybridization were performed essentially as described (11) with minor modifications (13). After hybridization arrays were scanned in a ScanArray Express HT (Perkin Elmer, Freemont, CA). The resulting images were analyzed with GenePix Pro 5.0 software (Axon Instruments, Foster City, CA) and subsequently visualized with an excel macro (12).

Quantitative PCR.

Analysis of mRNA expression was performed by QPCR. Two µg RNA was reverse transcribed utilizing 400 U M-MLV RT (Invitrogen Life Technologies, Carlsbad, CA) and an oligo-dT12 primer. QPCR was performed in an ABI Prism 7700 Sequence Detection System (Applied Biosystems, Foster City, CA). QPCR reactions were performed in Power SYBR Green PCR Master Mix (Applied Biosystems) containing 330 nM forward and reverse primer in a total volume of 25 µl. Thermocycling conditions were according to

the recommendations of the manufacturer. Amounts of specific RNAs for each sample were determined relative to posphobilinogen deaminase (*PBDG*) by the Standard curve method (Applied Biosystems). Primer combinations used: PBGD-F: (5′-CATGTCTGGTAACGGCAATG-3′) and PBGD-R: (5′-GTACGAGGCTTTCAATGTTG-3′). PSA-4A: 5′-ACGTGTGTGCAAGTTCACC-3′ and PSA-5B: 5′- TGTACAGGGAAGGCCTTTCG-3′. TMPRSS2-F: 5′- CCTCTGGTCACTTCGAAGAAC-3′ and TMPRSS2-R: 5′-GTAAAACGACGTCAAGGACG-3′. AR-7/8A: 5′- TGACTCCGTGCAGCCTATTG-3′ and AR-8B: 5′- ATGGGAAGCAAAGTCTGAAG-3′. TMPRSS2-E1:ERG-E4F: 5′-AGCGCGGCAGGAAGCCTTA-3′ and ERG-E4/5R: 5′-CATCAGGAGAGTTCCTTGAG-3′. TMPRSS2-E2:ERG-E4F: 5′- GATGGCTTTGAACTCAGAAGC-3′ and ERG-E4/5R. TMPRSS2-E3F: 5′-CCACCAGCTATTGGACCTTA-3′ and ERG-E4/5R: 5′-CATCAGGAGAGTTCCTTGAG-3′. TMPRSS2–E1F: 5′-GAGCTAAGCAGGAGGCGGA-3′ and ETV1-E5R: 5′-TGACTGCAGGCAGAGCTGAT-3′. TMPRSS2-E2F: 5′-CCTATCACTCGATGCTGT-3′ and ETV1-E5R. ERG-F: 5′-TGCTCAACCATCTCCTTCCA-3′ and ERG-R: 5′-TGGGTTTGCTCTTCCGCTCT-3′. ETV1-F: 5′-CATACCAACGGCGAGGATCA-3′ and ETV1-R: 5′-TGGAGAAAAGGGCTTCTGGA-3′. ETV4-F: 5′-ACCGGCCAGCCATGAATTAC-3′ and ETV4-R: 5′-GAGAGCTGGACGCTGATTG-3′. FLI1-F: 5′-GAGGAGCTTGGGGCAATAAC-3′ and FLI1-R: 5′-AGAGCAGCTCCAGGAGGAAT-3′.

Interphase fluorescent *in situ* hybridization (FISH).

Nuclear suspensions of the prostate cancer xenografts were prepared essentially as described by Vindelov *et al* (14). Interphase FISH was performed as described (15). BAC clones RP11-164E1, RP5-1031F17 (both flanking *ERG*, see Figure 2A), RP11-113F1 (*TMPRSS2*, see Figure 2A), RP11-79G16 (*ETV1*), RP11-268E15 (*ETV4*) and RP11-44O2 (*FLI1*) were purchased from BacPac resources (Oakland, CA). Specificity of BACs is shown in Supplementary Figures S1 and S2. BAC DNA clones were biotin-16-dUTP or digoxigenin-11-dUTP labeled using a nick translation reagent kit (Vysis, Downers Grove, IL) according to the manufacturer's directions. Biotin-labeled probes were visualized with FITC-conjugated avidin (Vector Laboratory, Burlingame, CA) and digoxigenin labeled probes with rhodamine conjugated anti-digoxigenin antibody (Roche, Mannheim, Germany). Cells were DAPI counterstained. Images of the three fluorochromes were collected on an epifluorescence microscope (Leica DM, Rijswijk, The Netherlands) equipped with appropriate filter sets (Leica) and a CCD cooled camera (Photometrics, Tucson, AZ).

Sequence analysis.

PCR products were purified utilizing SAP/Exonuclease I (USB Corporation, Cleveland, OH) according to manufacturer's instruction. Purified PCR fragments were labeled utilizing the ABI BigDye Terminator Ready Reaction kit v3.1 (Applied Biosystems) according to manufacturer's instructions. In the sequence reactions the same primers were used as for fragment amplification. Sequence samples were run on the ABI 3100 genetic Analyzer (Applied Biosystems).

RESULTS AND DISCUSSION

Eleven xenografts derived from various stages of clinical prostate cancer (Supplementary Table S1; 7-9) were utilized to decipher the role of ETS genes. PCEW, PC82, PC295, PC310, PC329, PC346 and PC374 are AR positive. PCEW, PC82, PC295, PC310 and PC329 grow androgen-dependent on male nude mice; PC346 and PC374 are to a varying extent androgen-sensitive. PC133, PC135, PC324 and PC339 are androgen independent.

First, expression of *AR*, *PSA* and *TMPRSS2* in xenografts was assessed by QPCR. There is a good correlation between the expression of *AR* and the well-known androgen-regulated *PSA* and *TMPRSS2* genes in androgen-dependent and androgen-sensitive xenografts (Figure 1A) (5, 9, 16). An exception is PC310, which shows *AR* and *PSA* expression, but clearly is *TMPRSS2* negative (see below). All androgen-independent xenografts are AR negative or express an inactive AR, as deduced from lack of *PSA* and *TMPRSS2* expression (see also (17)).

Next, we investigated expression of *ERG* and *TMPRSS2:ERG* fusion transcripts utilizing an *ERG* specific primer set and primer sets spanning *TMPRSS2* exons 1, 2 or 3 and *ERG* exon 4, respectively, combined with an *ERG* exon 4/5 primer (Figure 1B). In all five androgen-dependent xenografts *ERG* overexpression corresponded with *AR* and *PSA* expression, linking *ERG* to a functional AR and to strict androgen-dependent tumor growth. Overexpression of *ERG* correlated with the presence of *TMPRSS2:ERG* fusion transcripts. As confirmed by sequencing, due to alternative splicing in all five xenografts two transcripts were present, one containing *TMPRSS2* exon 1 linked to *ERG* exon 4 and a second, linking *TMPRSS2* exons 1 and 2 to *ERG* exon 4, respectively (Figure 1D). PCEW contained a third transcript linking part of *TMPRSS2* exon 3 to *ERG* exon 4 due to use of a cryptic splice donor site in *TMPRSS2* exon 3. The open reading frame (ORF) of transcript 1 is predicted to start at an internal ATG in *ERG* exon 4. In transcripts 2 and 3 the ORF will begin at the start codon of *TMPRSS2* and continues in-frame with the indicated part of *ERG* (Figure 1D). The reason of the high frequency of alternative splicing is at present unclear. Possibly expression of a truncated ERG protein from the *TMPRSS2(exon 1):ERG(exon 4)* fusion transcript favors tumor growth.

Androgen-sensitive PC374 showed high *ETV1* overexpression (Figure 1C). High *ETV1* expression correlated with *TMPRSS2:ETV1* gene fusion, as shown by interphase fluorescent in situ hybridization (FISH) on nuclear suspensions utilizing *ETV1* and *TMPRSS2* specific BACs (Figure 1C), and the presence of two splice variants of *TMPRSS2:ETV1* (Figure 1C,D). *ERG* and *ETV1* were not overexpressed in PC346 or in late stage, AR negative prostate cancer xenografts. Interphase FISH indicated that low level *ETV1* expression in PC135 could not be correlated with *TMPRSS2* gene fusion (Figure 1C). 5'-RACE confirmed that *ETV1* expressed in PC135 was wild type (data not shown).

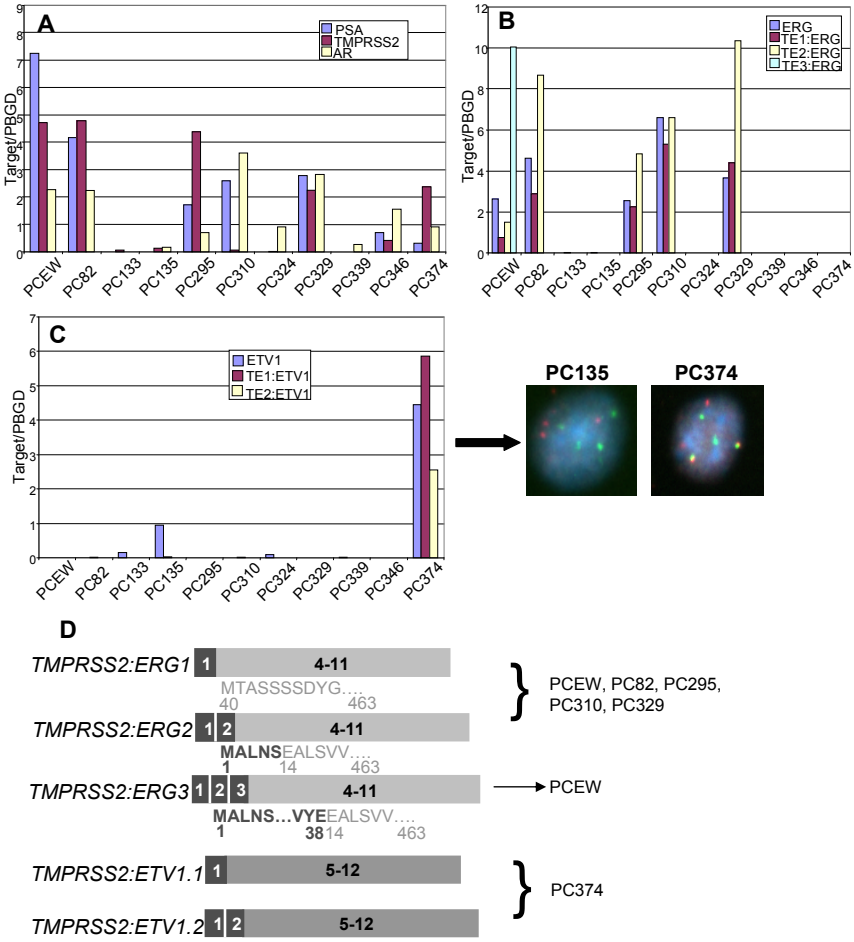

Figure 1. Expression of *AR*, *PSA*, *TMPRSS2* and *ERG* and *ETV1* fusion transcripts in prostate cancer xenografts. A, QPCR of *AR*, *PSA* and *TMPRSS2* mRNAs. B, QPCR of *ERG* and *TMPRSS2:ERG* fusion transcripts. C, QPCR of *ETV1* and *TMPRSS2:ETV1* fusion transcripts and interphase FISH with *TMPRSS2*(green spots) and *ETV1* (red spots) specific BACs of nuclei from PC135 and PC374. D, Composition of *TMPRSS2:ERG* and *TMPRSS2:ETV1* fusion transcripts. Details of methods, FISH BACs and QPCR primers are described in the Materials and Methods section. *PBGD* expression was utilized as a QPCR reference.

TMPRSS2 and *ERG* map in the same orientation at short distance on chromosome band 21q22.2-q22.3 (Figure 2A). To determine the mechanism of *TMPRSS2:ERG* gene fusion, genomic DNA from the five xenografts overexpressing the fusion gene was investigated by 1 Mbp spaced array-based comparative genomic hybridization (array-CGH). Two different representative array-CGH profiles of chromosome 21 are depicted in Figure 2B,C. In PC295 the region between *ERG* and *TMPRSS2* was lost, as indicated by the low T/R ratio of the four BACs mapping in this chromosomal region (Figure 2B). A similar profile was

present in PC329 (data not shown). Although PC82 contains the fusion transcript, the region between *ERG* and *TMPRSS2* was largely present (Figure 2C). A comparable profile was found in PCEW and PC310 (data not shown). In PC310 the profile was accompanied by a small homozygous deletion of the last exons of *TMPRSS2* (data not shown), explaining total absence of *TMPRSS2* transcripts in this xenograft. We extended the array-CGH data by interphase FISH of PC82, PC295 and PC310 nuclei. We utilized as hybridization probes BACs RP11-164E1 and RP5-1031P17, which map at a distance of approximately 1 Mbp, flanking *ERG* at positions indicated in Figure 2A. Both BACs exclusively stained

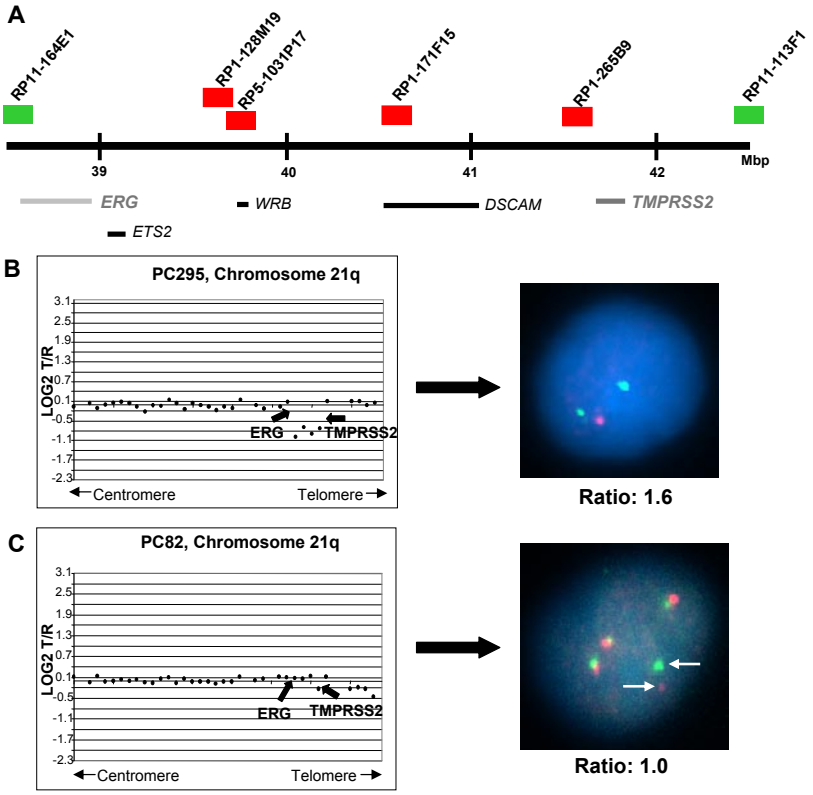

Figure 2. Array-based CGH analysis of chromosome 21 and interphase FISH of nuclei of prostate cancer xenografts PC295 and PC82. A, Chromosome 21 region indicating the position of *ERG, TMPRSS2* and flanking genes in Mbp from the top of the p arm. Positions of BAC clones in this region are indicated above the map. Genes mapping in this chromosomal region are indicated below the map. BACs utilized in interphase FISH are in red or green. B, PC295: Array CGH of 21q and representative interphase FISH (two green and one red spot) of a nucleus, utilizing BACs RP11-164E1 (green) and RP5-1031P17 (red). C, PC82: Array CGH of 21q and representative interphase FISH of a nucleus, utilizing the same BACs as above. Ratio's of green to red spots in interphase FISH, as calculated from over 30 nuclei, are indicated below the pictures. Separate spots in the PC82 nucleus are indicated by white arrows. Positions of *ERG* and *TMPRSS2* in the array CGH figures are indicated by black arrows. Vertical axis: Log2 ratio of normalized hybridization signal of tumor DNA versus reference DNA (T/R).

chromosome band 21q22.2 and showed two spots on interphase nuclei from normal cells (Supplementary Figure S1A,B). Representative nuclei of PC295 and PC82 are presented in Figure 2B,C, respectively. In nuclei from PC295 cells we found a higher number of green than red spots (average ratio 1.6), indicative of loss of the region between *ERG* and *TMPRSS2* in one copy of chromosome 21. In PC82 and PC310 we observed an identical number of green and red spots (average ratio's 1.0 and 1.1, respectively). In PC82 that contains four copies of chromosome 21, three pairs of red and green spots were always closely linked and one pair was clearly separated, as illustrated in Figure 2C. Both array-CGH and FISH data strongly suggest two different mechanisms of *TMPRSS2:ERG* fusion: one by an approximately 3 Mbp interstitial deletion of one copy of chromosome 21, and a second more complex mechanism by chromosomal translocation.

Array-CGH of genomic DNA from two of the six xenografts that did not over-express *TMPRSS2:ERG* showed a remarkable pattern. In the androgen-independent, AR negative xenografts PC133 and PC339 we detected a similar interstitial deletion as in PC295 and PC329. The chromosome 21 profile of PC339 is depicted in Figure 3A. Long range PCR followed by sequencing confirmed the fusion between *TMPRSS2* and *ERG* in PC133, mapping the chromosomal breakpoints in *ERG* intron 3 and in *TMPRSS2* intron 1, respectively (Figure 3B). Similarly, PCR plus sequencing identified *TMPRSS2:ERG* fusion in PC324 that does not show a 21q22 interstitial deletion. This adds a third AR negative xenograft to those with *TMPRSS2:ERG* gene fusion without expression of the fusion gene. Like in PC133 the breakpoint in PC324 is in *TMPRSS2* intron 1. We also mapped the breakpoints in AR positive PC82, PC295, PC310 and PC329 (Figure 3B). As expected from expression data (Figure 1B), these breakpoints were in intron 2 of *TMPRSS2* and in intron 3 of *ERG*. All six breakpoints in *ERG* were in the last part of intron 3, suggesting a preferred region of recombination in this part of the gene. It remains to be investigated whether the difference in *TMPRSS2* introns involved in *ERG* fusion between AR positive and AR negative xenografts, intron 2 and 1 respectively, is coincidental or of functional importance. The absence of *TMPRSS2:ERG* expression in PC133, PC324 and PC339 (Figure 1B) indicates that it is not involved in the androgen-independent growth of these xenografts. Importantly, however, the presence of *TMPRSS2:ERG* in genomic DNA strongly suggests that the fusion gene has been instrumental in an earlier androgen-dependent stage of tumor growth.

We postulated that in PC133, PC324 and PC339 androgen-regulated *ERG* expression is bypassed and subsequently downregulated by other mechanisms of progressive tumor growth. One mechanism to become independent of androgen-regulated *ERG* overexpression might be by androgen-independent increased expression of a member of the ETS transcription factor gene family. As shown in Figure 1, we had no evidence that this was the case for *ERG* or *ETV1*. Therefore we investigated in the xenografts expression of two other ETS transcription factors known to be involved in oncogenesis, *ETV4* and *FLI1*.

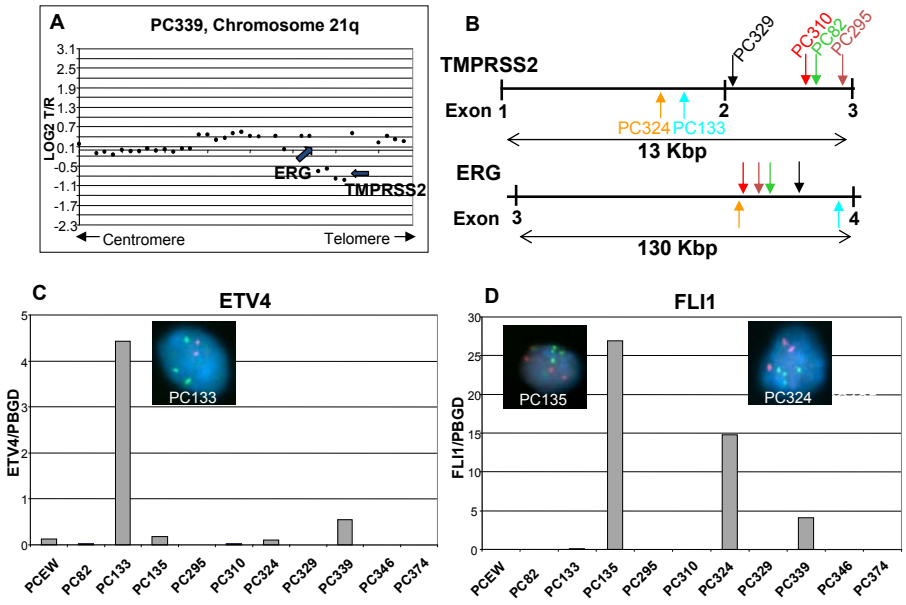

Figure 3. Genetic and expression analysis of AR negative prostate cancer xenografts. A, Array CGH of chromosome 21q of androgen-independent, AR negative xenograft PC339 (see for details Figure 2 and Materials and Methods). B, Positions of breakpoints in *ERG* and *TMPRSS2* in xenograft DNAs. Breakpoints were mapped by standard long range PCR utilizing a mixture of Taq and Proofstart DNA polymerase, as indicated by the manufacturer (Qiagen, Valencia, CA). Above the genes the positions of breakpoints in AR positive, androgen-dependent xenografts are shown, below the genes the breakpoints in AR negative xenografts are indicated. C, QPCR of *ETV4* expression in prostate cancer xenografts. D, QPCR of *FLI1* expression in prostate cancer xenografts. Details are described in the legend to Figure 1 and in Materials and Methods. Standard 5'-RACE, utilizing the Generacer kit from Invitrogen, indicated that *ETV4* and *FLI1* transcripts in AR negative PC133, PC135, PC324 or PC399 were wild type. Inserts in C and D show representative interphase FISH pictures of nuclei from indicated xenografts, showing the absence of fusion of *TMPRSS2* to *ETV4* or *FLI1*. In all pictures the green spots indicate *TMPRSS2*; in C, the red dots represent *ETV4;* in D, the red spots represent *FLI1*.

ETV4 was highly expressed in PC133 and *FLI1* in PC324 and PC135 (Figure 3C,D). Also in PC339 we observed expression of *FLI1*. *ETV4* and *FLI1* were not or hardly expressed in androgen-dependent or androgen-sensitive xenografts. Overexpression was not the result of fusion to *TMPRSS2* as illustrated by interphase FISH (Figure 3C,D). Additional 5'-RACE experiments confirmed that *ETV4* and *FLI1* mRNA in AR negative xenografts was wild type and not the result of fusion to other genes (data not shown).

In clinical prostate cancer many recurrent tumors still express a functional AR. However, a substantial proportion of recurrent tumors is heterogeneous for AR expression or is AR negative (18, 19). We investigated whether like in xenografts *TMPRSS2:ERG* gene fusion without expression of the fusion gene was present in clinical samples. Array CGH showed in four of eleven recurrent tumors the interstitial deletion at 21q22 indicative of *TMPRSS2:ERG* fusion (see Figure 4A,B for examples). From three of these

tumors (T1-1, T1-8 and T3-7) RNA was available. Importantly, we also had available DNA and RNA from recurrent tumor T1-7 of which AR negative xenograft PC324 was derived. These four tumors and a control recurrent tumor without *TMPRSS2:ERG* fusion (T6-9) were investigated by QPCR for specific gene expression patterns (Figure 4C,D). T1-1, T3-7 and T6-9 expressed *AR* and its target genes *PSA* and *TMPRSS2*, although expression in T1-1 was low. In contrast, T1-8 and, as expected, T1-7 showed hardly any *AR*, *PSA* and *TMPRSS2* expression. All tumor samples had a basal level of *ERG* expression. *ERG* overexpression combined with *TMPRSS2:ERG* fusion transcripts was clearly detected in T3-7, and absent in T1-8 and T1-7. T1-1 showed a low level of *TMPRSS2:ERG* expression, which might indicate tumor heterogeneity. The data confirm and extend the findings in xenografts showing that AR negative tumors can carry a *TMPRSS2:ERG* fusion gene without expression of the gene. Background expression levels and presumed heterogeneity of tumors hampered accurate investigation of *ETV4* and *FLI1* in the clinical samples (Supplementary Figure S3). *ETV4* expression was highest in AR negative T1-8 and T1-7, but differences with other tumor samples were small. Like in PC324, expression of *FLI1* was high in T1-7, but also T1-1 showed high expression of *FLI1*. The latter might be explained by tumor heterogeneity, as proposed previously (Figure 4C,D). Obviously, more

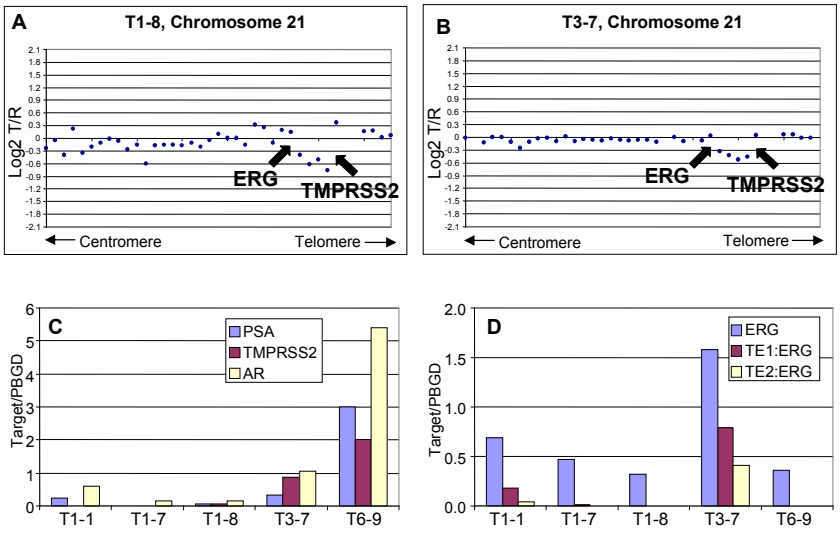

Figure 4. Array-based CGH of chromosome 21 and specific gene expression patterns of clinical recurrent prostate cancer specimens. A,B, Array CGH of chromosome 21 of recurrent tumors T1-8 and T3-7. Positions of *ERG* and *TMPRSS2* are indicated by black arrows. Vertical axis: Log2 ratio of normalized hybridization signal of tumor DNA versus reference DNA (T/R). C, QPCR of *AR*, *PSA* and *TMPRSS2* mRNAs. D, QPCR of *ERG* and *TMPRSS2:ERG* fusion transcripts. Details of methods and QPCR primers are described in the Materials and Methods section. *PBGD* expression was utilized as a QPCR reference.

detailed immunohistochemical studies, including AR and ETV4 or FLI1 double staining are needed to substantiate the latter observation.

In conclusion, our xenograft data extend previous observations in clinical prostate cancer (3, 4) and shed new light on the role of ETS transcription factors in prostate cancer. First, we detected two mechanisms of gene fusion between *ERG* and *TMPRSS2*. Secondly, we observed that *TMPRSS2:ERG* overexpression is functionally correlated with *AR* expression. Both in xenografts and clinical samples we showed that the *TMPRSS2:ERG* fusion gene can be present in absence expression of the gene in AR negative tumors. Furthermore, our data suggest that other members of the ETS family, possibly wild type *ETV4* or *FLI1*, might take over the role of androgen-regulated *TMPRSS2:ERG* in late stage AR negative prostate cancer.

ACKNOWLEDGMENTS

This study was supported by grants from the Erasmus University Medical Center and the Dutch Cancer Society KWF.

REFERENCES

1. Jemal A, Murray T, Ward E, et al. Cancer statistics, 2005. CA Cancer J Clin 2005; *55:* 10-30.
2. Petrovics G, Liu A, Shaheduzzaman S, et al. Frequent overexpression of ETS-related gene-1 (ERG1) in prostate cancer transcriptome. Oncogene 2005; *24:* 3847-52.
3. Tomlins SA, Rhodes DR, Perner S, et al. Recurrent fusion of TMPRSS2 and ETS transcription factor genes in prostate cancer. Science 2005; *310:* 644-8.
4. Tomlins SA, Mehra R, Rhodes DR, et al. TMPRSS2:ETV4 gene fusions define a third molecular subtype of prostate cancer. Cancer Res 2006; *66:* 3396-3400.
5. Lin B, Ferguson C, White JT, et al. Prostate-localized and androgen-regulated expression of the membrane-bound serine protease TMPRSS2. Cancer Res 1999; *59:* 4180-4.
6. Oikawa T. ETS transcription factors: possible targets for cancer therapy. Cancer Sci 2004; *95:* 626-33.
7. Hoehn W, Schroeder FH, Reimann JF, Joebis AC, Hermanek P. Human prostatic adenocarcinoma: some characteristics of a serially transplantable line in nude mice (PC 82). Prostate 1980; *1:* 95-104.
8. Hoehn W, Wagner M, Riemann JF, et al. Prostatic adenocarcinoma PC EW, a new human tumor line transplantable in nude mice. Prostate 1984; *5:* 445-52.
9. van Weerden WM, de Ridder CM, Verdaasdonk CL, et al. Development of seven new human prostate tumor xenograft models and their histopathological characterization. Am J Pathol 1996, *149:* 1055-62.
10. Sambrook J and Russell DW. Molecular Cloning. A laboratory manual, third edition, Vol. 1. Cold Spring Harbor, New York: Cold Spring Harbor Laboratory Press; 2001.p1.59-61.
11. Fiegler H, Carr P, Douglas EJ, et al. DNA microarrays for comparative genomic hybridization based on DOP-PCR amplification of BAC and PAC clones. Genes Chromosomes Cancer 2003; *36:* 361-74.
12. Knijnenburg J, Szuhai K, Giltay J, et al. Insights from genomic microarrays into structural chromosome rearrangements. Am J Med Genet A 2005; *132:* 36-40.
13. Verhagen P, van Duijn P, Hermans K, et al. The PTEN gene in locally progressive prostate cancer is preferentially inactivated by bi-allelic gene deletion. J Pathol 2006; *208:* 699-707.
14. Vindelov LL, Christensen IJ, and Nissen NI. A detergent-trypsin method for the preparation of nuclei for flow cytometric DNA analysis. Cytometry 1983; *3:* 323-7.
15. van Duin M, van Marion R, Vissers K, et al. High-resolution array comparative genomic hybridization of chromosome arm 8q: evaluation of genetic progression markers for prostate cancer. Genes Chromosomes Cancer 2005; *44:* 438-49.
16. Riegman PH, Vlietstra RJ, van der Korput JA, Brinkmann AO, Trapman J. The promoter of the prostate-specific antigen gene contains a functional androgen responsive element. Mol Endocrinol 1991; *5:* 1921-1930.
17. Hendriksen PJ, Dits NF, Kokame K, et al. Evolution of the Androgen Receptor Pathway during Progression of Prostate Cancer. Cancer Res 2006; *66:* 5012-20.
18. van der Kwast TH, Schalken J, Ruizeveld de Winter JA, et al. Androgen receptors in endocrine-therapy-resistant human prostate cancer. Int J Cancer 1991; *48:* 189-93.
19. Ruizeveld de Winter JA, Janssen PJ, Sleddens HM, et al. Androgen receptor status in localized and locally progressive hormone refractory human prostate cancer. Am J Pathol 1994; *144:* 735-46.

SUPPLEMENTARY INFORMATION

Interphase and metaphase FISH confirming specific hybridization signals of BAC clones in normal lymphocytes

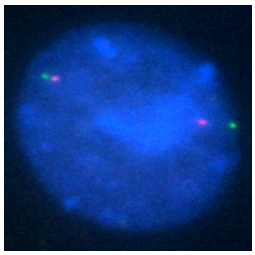

RP11-164E1 (green)
RP5-1031P17 (red)
both flanking *ERG*
See Fig 2A

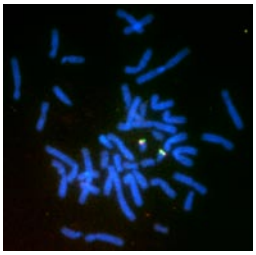

RP11-164E1 (green)
RP5-1031P17 (red)
both flanking *ERG*
See Fig 2A

Figure S1

Metaphase FISH confirming specific hybridization signals of BAC clones in normal lymphocytes

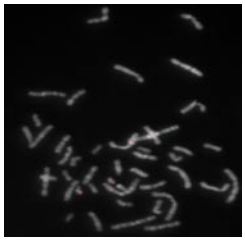

RP11-113F1
Chromosome 21q22.2
TMPRSS2

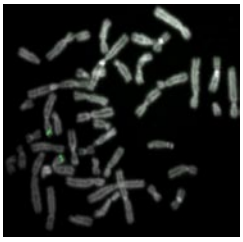

RP11-79G16
Chromosome 7p21
ETV1

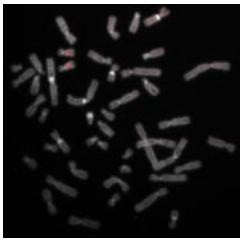

RP11-268E15
Chromosome 17q21
ETV4

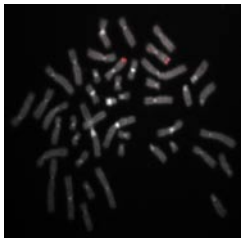

RP11-44O2
Chromosome 11q24
FLI1

Figure S2

QPCR of *ETV4* and *FLI1* transcripts in five recurrent tumors

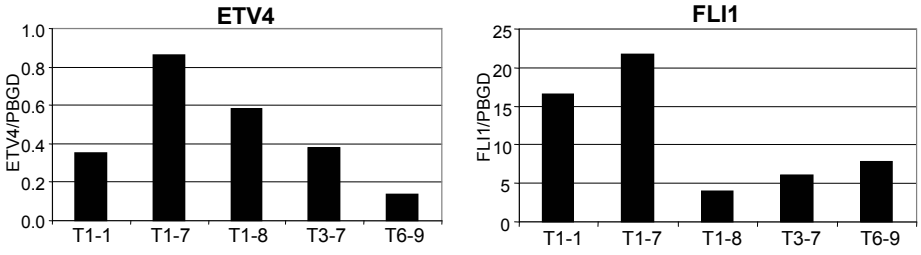

Figure S3

Chapter 5

OVEREXPRESSION OF PROSTATE-SPECIFIC *TMPRSS2(EXON 0)-ERG* FUSION TRANSCRIPTS CORRESPONDS WITH FAVORABLE PROGNOSIS OF PROSTATE CANCER

Karin G. Hermans[1,*], Joost L. Boormans[2,*], Delila Gasi[1], Geert J. van Leenders[1], Guido Jenster[2], Paul C.Verhagen[2] and Jan Trapman[1]

Departments of Pathology[1] and Urology[2], Josephine Nefkens Institute, Erasmus University Medical Center, Rotterdam, The Netherlands

** Equal contribution*

Submitted

ABSTRACT

TMPRSS2-ERG gene fusion is the most frequent genetic alteration in prostate cancer. *TMPRSS2* is an androgen-regulated gene that is preferentially expressed in the prostate. *TMPRSS2* transcripts can start at either exon 1 or at a more upstream and less well characterized exon 0. To gain insight in the mechanism of *TMPRSS2-ERG* expression we determined the specific characteristics of transcripts starting at exon 1 and exon 0. *TMPRSS2(exon 0)* and *TMPRSS2(exon 1)* transcripts were similarly androgen-regulated in prostate cancer cell lines, but the expression levels of *TMPRSS2(exon 1)* were much higher. Comparison of expression in different tissues showed *TMPRSS2(exon 0)* expression to be much more prostate-specific. In seven androgen-receptor-positive prostate cancer xenografts, *TMPRSS2(exon 1)* transcripts were expressed at similar levels, but *TMPRSS2(exon 0)* transcripts were expressed at very variable levels. The same phenomenon was observed for *TMPRSS2-ERG* fusion transcripts. In clinical prostate cancers, the expression of *TMPRSS2(exon 0)-ERG* was even more variable. Expression of *TMPRSS2(exon 0)-ERG* transcripts was detected in 55% (24 of 44) of gene-fusion-positive primary tumors, but only in 15% (4 of 27) of gene-fusion-positive recurrences and at much lower levels. Furthermore, in primary tumors, expression of *TMPRSS2(exon 0)-ERG* transcripts was an independent predictor of longer biochemical progression-free survival.

INTRODUCTION

Recently, recurrent fusions of prostate-specific and androgen-regulated *TMPRSS2* to the ETS genes *ERG*, *ETV1*, *ETV4* and *ETV5* have been reported as the most frequent genetic alterations in clinical prostate cancer (1-9). *TMPRSS2-ERG* fusion is detected in 40-70% of clinical prostate cancers. Fusion of *ETV1*, *ETV4* and *ETV5* to *TMPRSS2* are much less frequent, but *ETV1*, *ETV4* and *ETV5* have multiple fusion partners. Expression of most of these partner genes is prostate-specific and androgen-regulated (1-3, 5-9). Some clinical studies have shown an association between *TMPRSS2-ERG* and a more aggressive prostate cancer phenotype (10-14). However, other studies did not find a statistically significant association with recurrence-free survival (15), or even described *TMPRSS2-ERG* to be correlated with a more favorable outcome (16, 17).

TMPRSS2 has more than one first exon (UCSC Genome Browser, genome.ucsc.edu). Not only fusion transcripts starting at the well known *TMPRSS2* exon 1, but also transcripts that start from a more upstream and less well characterized alternative first exon, here denoted exon 0, have been identified (15, and Hermans, unpublished).

In the present study we determined the specific characteristics of *TMPRSS2* transcripts starting at exon 1 and exon 0 in benign prostatic tissue and in prostate cancer. Moreover, we investigated clinical prostate cancer samples (primary tumors and recurrences) for expression of *TMPRSS2(exon 0)-ERG* and *TMPRSS2(exon 1)-ERG* fusion transcripts. In the primary tumors we correlated fusion gene expression with time to biochemical progression after radical prostatectomy. Our data show different expression patterns of *TMPRSS2(exon 0)* and *TMPRSS2(exon 1)* transcripts. Further, our findings indicate a more favorable prognosis of tumors with *TMPRSS2(exon 0)-ERG* expression.

MATERIALS AND METHODS

Prostate cancer cell lines and xenografts.

Prostate cancer cell lines LNCaP and DuCaP were grown in RPMI-1640 supplemented with 5% fetal calf serum and antibiotics. Androgen receptor (AR) positive prostate cancer xenografts PCEW, PC82, PC295, PC310, PC329, PC346 and PC374, and AR-negative xenografts, PC133, PC135, PC324 and PC339, were propagated by serial transplantation on male nude mice as described (18).

Clinical samples.

Primary prostate tumors were obtained by radical prostatectomy and recurrent tumors by transuretheral resection of the prostate (TURP). Hematoxilin/eosin stained tissue sections were histologically evaluated by two pathologists (Van der Kwast, Van Leenders).

Only samples that contained at least 70% tumor cells were selected. The clinical and pathological demographics of the patients with primary prostate tumors included in the statistical analysis (N=67) are given in supplementary Table S1. Tissues were snap-frozen and stored in liquid nitrogen. Use of the samples for research purposes was approved by the Erasmus MC Medical Ethics Committee according to the Medical Research Involving Human Subjects Act (MEC-2004-261).

RNA isolation.

RNAs from the prostate cancer cell lines LNCaP and DuCaP cultured in the absence or the presence of 10^{-9}M R1881 were isolated using the RNeasy RNA extraction kit (Qiagen, Valencia, CA). RNA from clinical prostate cancer samples was isolated from frozen tissue sections using RNA-Bee (Campro Scientific, Berlin, Germany). Xenograft RNA was isolated according to the LiCl protocol.

Quantitative PCR (QPCR).

Total RNA was reverse transcribed using M-MLV reverse transcriptase (Invitrogen, Carlsbad, CA) and an oligo dT12 primer. cDNAs of 16 different tissues were purchased from Clontech (Mountain View, CA). QPCR reactions were performed in Power SYBR Green PCR Master Mix (25 µl), containing 0.33 µM forward and reverse primer in an ABI Prism 7700 Sequence Detection System (Applied Biosystems). Amplified products were quantified relative to Porphobilinogen Deaminase (*PBGD*). Primers are listed in supplementary Table S2.

Statistical analysis.

Associations between clinical and histopathological variables and expression of TMPRSS2-ERG transcripts were evaluated by the Pearson's Chi-square (X^2) test, the Mann-Whitney U test, or Kruskal-Wallis test, where appropriate. Expression of TMPRSS2-ERG transcripts was correlated with the primary end point: biochemical progression-free survival, defined as time from radical prostatectomy to date of biochemical recurrence. Biochemical recurrence was defined as: 1) a PSA-level higher than 0.2 ng/ml at two consecutive measurements with a three-month-interval if the PSA-nadir was < 0.1 ng/ml, or 2) a PSA-nadir of ≥ 0.2 ng/ml. Patients that died from other causes than prostate cancer, or that were lost to follow-up, were censored at the date of last PSA-test. Patients were routinely followed three-monthly the first year after radical prostatectomy, the second year semi-annually and subsequently at 12-month intervals. In case of progression, patients were again followed every three months. Kaplan-Meier curves were constructed to assess the probability of remaining free of biochemical recurrence as a function of time after surgery. The differences between the survival curves of the groups were tested using the log-rank test, or Breslow method if appropriate. A Cox propor-

tional regression analysis with forward stepwise elimination was performed to assess the impact of various parameters on time to recurrence. In the multivariate analysis the model included pathological T-stage, surgical margin status, the Gleason score of the primary tumor and expression of indicated TMPRSS2-ERG fusion transcripts. Patients with unknown parameters were excluded from the analysis. Statistical analyses were performed using the Statistical Package for Social Sciences, version 15.0 (SPSS, Chicago, IL), with a significance level of 0.05 (two-tailed probability).

RESULTS

TMPRSS2-ERG gene fusion is present in 40-70% of primary prostate tumors. *ERG* and *TMPRSS2* are located ~3 Mbp apart on chromosome 21q22.3 in the same orientation (Fig 1A). The most common *TMPRSS2-ERG* fusion transcripts are composed of *TMPRRS2* exon 1, or exons 1 and 2, linked to exon 4 of *ERG*. Less frequently, fusion of *TMPRSS2* exon 1 or 2 to other *ERG* exons have been detected (19). Genomic databases describe that *TMPRSS2* transcripts might also contain an alternative first exon, here denoted exon 0, that maps ~4 kbp upstream of exon 1 (Fig. 1A). *TMPRSS-ERG* fusion transcripts might also contain *TMPRSS2* exon 0 (15, and Hermans unpublished).

We determined the specific characteristics of transcripts starting at either exon 0 or exon 1 of *TMPRSS2*. First, we investigated the tissue-specificity of both transcripts on RNA from 16 different normal tissues. Although expression of *TMPRSS2(exon 1)* mRNA was highest in prostate, these transcripts were also detected in lung, kidney, pancreas and colon. In contrast, *TMPRSS2(exon 0)* mRNA had a prostate-specific expression pattern (Fig 1B). Subsequently, we performed QPCR analysis on RNA from prostate cancer cell lines DuCaP and LNCaP, cultured in absence or presence of the synthetic androgen R1881. Both *TMPRSS2* transcripts were induced by androgens (Fig. 1C). Notably, in the cell lines expression of *TMPRSS2(exon 0)* transcripts was very low compared with expression of *TMPRSS2(exon 1)*.

Testing of RNAs from eleven human prostate cancer xenografts for expression of *TMPRSS2* starting at either exon 0 or exon 1 showed that six AR-positive xenografts, PCEW, PC82, PC295, PC329, PC346 and PC374, expressed *TMPRSS2(exon 1)* at similar levels (Fig. 1D). Xenograft PC310 showed no expression of *TMPRSS2*, because of a homozygous deletion (8). Four xenografts expressed *TMPRSS2(exon 0)* with a much more variable level of expression. None of the AR-negative xenografts expressed *TMPRSS2*.

Previously we have shown that five androgen-dependent xenografts, PCEW, PC82, PC295, PC310 and PC329, contained *TMPRSS2(exon 1)-ERG* mRNA (8). Comparison of *TMPRSS2(exon 0)-ERG* and *TMPRSS2(exon 1)-ERG* expression by QPCR showed that three xenografts, PC82, PC295 and PC329, expressed *TMPRSS2(exon 0)-ERG* at different expres-

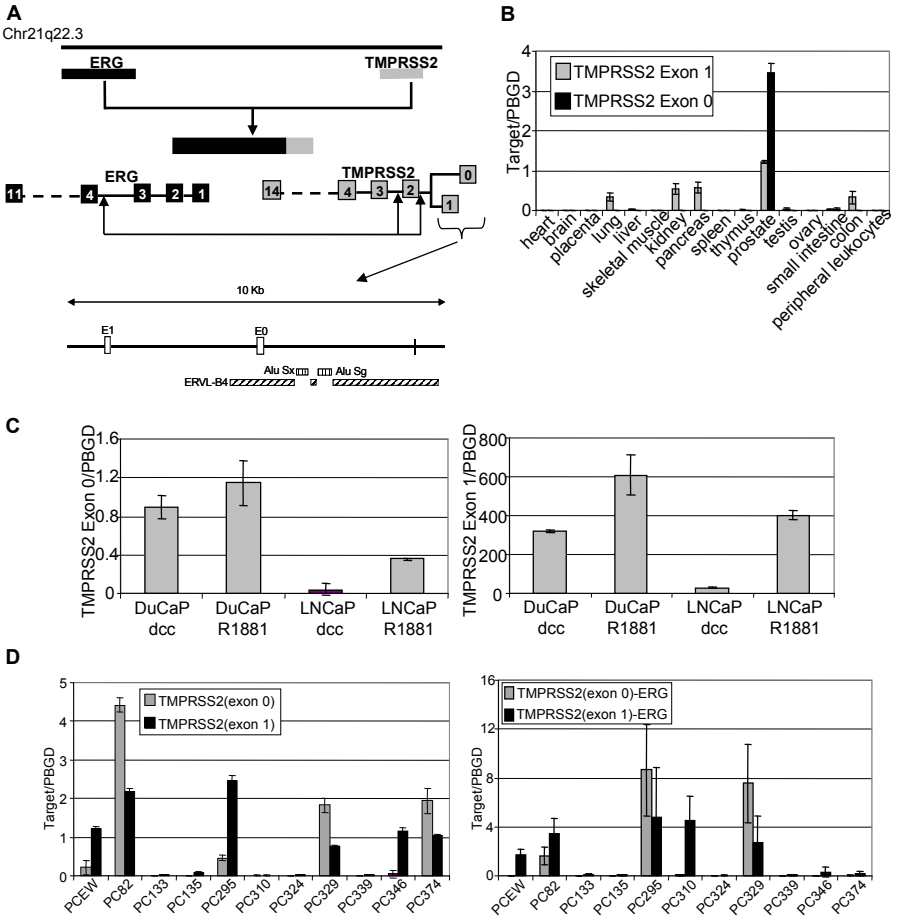

Figure 1. Characterization of *TMPRSS2* and *TMPRSS2-ERG* transcripts starting at exon 0 or exon 1. (A) Schematic representation of the *TMPRSS2-ERG* locus on chromosome band 21q22.3. The most frequent gene fusion events are indicated. The enlarged genomic region containing *TMPRSS2* shows exon 0 and exon 1 repeat sequences. (B) Tissue-specific expression of *TMPRSS2(exon 0)* and *TMPRSS2(exon 1)* mRNA assessed by QPCR analysis on a cDNA panel from 16 different normal tissues. Mean of duplicate experiment relative to *PBGD* with standard deviation (SD) is shown. (C) Androgen-regulated expression of *TMPRSS2(exon 0)* (left panel) and *TMPRSS2(exon 1)* (right panel) mRNA in AR-positive prostate cancer cell lines LNCaP and DuCaP. LNCaP and DuCaP cells were grown in absence and presence of synthetic androgen R1881 (10^{-9} M) for 24h. Mean of duplicate experiments relative to *PBGD* with SD are depicted. Note that the level of *TMPRSS2(exon 0*) expression is much lower in the cell lines than in the normal prostatic tissue (panel B). (D) QPCR analysis of *TMPRSS2(exon 0)* and *TMPRSS2(exon 1)* (left panel) and *TMPRSS2(exon 0)-ERG* and *TMPRSS2(exon 1)-ERG* (right panel) transcripts in eleven human prostate cancer xenografts. Mean of duplicate experiments relative to *PBGD* with SD are shown.

sion levels (Fig. 1D). However, the other two xenografts with *TMPRSS2-ERG* transcripts, PCEW and PC310, did not express *TMPRSS2(exon 0)-ERG* at all. No large variation in expression levels was seen for *TMPRSS2(exon 1)-ERG* transcripts in the five xenografts (Fig.

1D). This difference in expression level between *TMPRSS2(exon 0)-ERG* and *TMPRSS2(exon 1)-ERG* transcripts was similar as observed for wild type *TMPRSS2(exon 0)* and *(exon 1)* transcripts.

Next, we determined the expression of *TMPRSS2(exon 0)-ERG* and *TMPRSS2(exon 1)-ERG* transcripts in a cohort of 126 fresh-frozen clinical prostate cancer samples (81 primary tumors and 45 recurrent tumors) (Fig. 2A). *TMPRSS2-ERG* transcripts were detected in 54% (44/81) of the primary tumors and in 60% (27/45) of the recurrences. In the primary tumors, 20/81 (25%) of the cases exclusively expressed *TMPRSS2(exon 1)-ERG* transcripts, three samples (4%) exclusively expressed *TMPRSS2(exon 0)-ERG* and 21 (51%) expressed both transcript subtypes. In the recurrent tumors exclusive expression of *TMPRSS2(exon 1)-ERG* was detected in 23/45 (51%) of the cases, whereas none expressed exclusively *TMPRRS2(exon 0)-ERG* and only 4 cases (9%) expressed both subtypes. Expression levels of *TMPRSS2(exon 0)-ERG* transcripts were significantly higher in primary tumors than in recurrent tumors (p=0.015), and variation in expression was much larger in the primary tumors than in the recurrences (Fig. 2B). In contrast, the percentage of tumors expressing *TMPRSS2(exon 1)-ERG* transcripts was in the same range for primary and recurrent tumors and also the expression levels of these transcripts did not differ between both tumor types (p=0.74).

We correlated expression of *TMPRSS2(exon 0)-ERG* with clinical outcome in the primary prostate cancer cohort (N=81) to see whether it was of prognostic value. We excluded from the analysis 10 patients that were known to harbor fusion or overexpression of

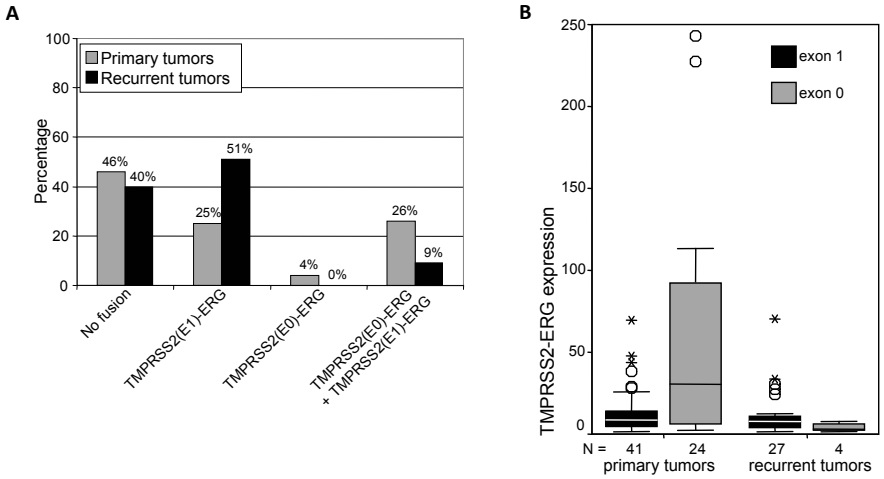

Figure 2. Expression of *TMPRSS2(exon 0)-ERG* and *TMPRSS2(exon 1)-ERG* transcripts in clinical prostate cancer samples. (A) Distribution of *TMPRSS2-ERG* transcript subtypes in primary tumors and in recurrences. Primary tumors: N=81; Recurrent tumors: N=45. (B) Box plot of *TMPRSS2(exon 0)-ERG* and *TMPRSS2(exon 1)-ERG* mRNA expression levels in primary tumors and recurrences. Outliers are depicted by an ° and extremes are depicted by an *.

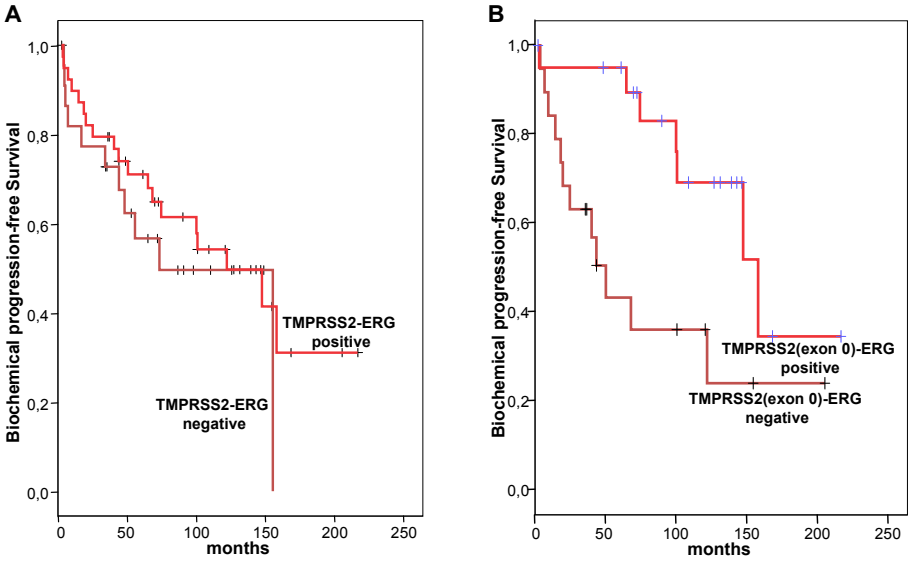

Figure 3. Kaplan-Meier curves showing biochemical progression-free survival of prostate cancer patients defined by *TMPRSS2-ERG* fusion transcript status and time to PSA progression after radical prostatectomy. (A) Biochemical progression-free survival curves for prostate cancer patients with or without expression of *TMPRSS2-ERG* transcripts. (B) Biochemical progression-free survival curves for the *TMPRSS2-ERG*-positive group, which was stratified in patients with and without expression of *TMPRSS2(exon 0)-ERG* transcripts.

other ETS genes, and 4 patients whose primary treatment was not a radical prostatectomy. Despite the very long follow-up available (median more than 10 years) only 11 out of the remaining 67 patients died from prostate cancer, precluding statistical analysis. Instead, we used time to PSA recurrence after radical prostatectomy as an end point. The patients' demographics are summarized in supplementary Table S1. No differences were seen in clinical and histopathological characteristics between patients expressing *TMPRSS2-ERG* and gene-fusion-negative patients, although *TMPRSS2-ERG*-negative patients had higher Gleason scores with borderline significance (p=0.053) (supplementary Table S3). The median time to PSA progression was not significantly different between the two groups: 73.2 versus 122.1 months (95% CI: 32.7-113.7 versus 70.6-173.6, p=0.45) (Fig. 3A).

Within the *TMPRSS2-ERG* positive population the only difference between patients that exclusively expressed *TMPRSS2(exon 1)-ERG* transcripts and patients that expressed the *TMPRSS2(exon 0)-ERG* subtype was that the former had higher pathological stages than the latter (p=0.009) (supplementary Table S4). The median time to PSA progression for patients expressing *TMPRSS2(exon 0)-ERG* transcripts was significantly longer than for patients that exclusively expressed *TMPRSS2(exon 1)-ERG* transcripts:158.2 versus 50.5 months (95% confidence interval (CI): 98.9-217.5 versus 32.6-68.4, p=0.012) (Fig. 3B).

Using a Cox proportional hazards model, positive surgical margins, Gleason score ≥ 7, pathological stage ≥ pT3a, and absence of *TMPRSS2(exon 0)-ERG* transcripts were all associated with a worse biochemical progression-free survival. Importantly, multivariate analysis with forward stepwise selection showed expression of *TMPRSS2(exon 0)-ERG* fusion transcripts to be an independent predictor of progression-free survival (HR = 0.34 (95% CI: 0.14-0.84, p=0.019)) (Table I).

DISCUSSION

This study addresses two important aspects of *TMPRSS2-ERG* expression in prostate cancer. First of all, a remarkable difference in expression characteristics was detected between *TMPRSS2(exon 1)* and *TMPRSS2(exon 1)-ERG* transcripts on the one hand, and *TMPRSS2(exon 0)* and *TMPRSS2(exon 0)-ERG* transcripts on the other hand. Secondly, the clinical data indicated a more favorable prognosis for prostate cancer patients expressing *TMPRSS2(exon 0)-ERG* transcripts.

Table 1. Results of univariate and multivariate analyses

		Univariate					Multivariate	
Variable	N	Median time to PSA recurrence (months)	95% CI	p-value	HR (95% CI)	p-value	HR (95% CI)	p-value
Surgical margins								
positive	30	43.9	31.0-56.8	< 0.001	7.5 (3.0-18.5)	< 0.001	7.7 (3.0-19.4)	0.001
negative	31	122.1	49.5-194.7		1.0			
Gleason Score								
≥ 7	26	68.2	41.5-94.9	0.037	2.1 (1.0-4.5)	0.041		
< 7	35	155.4	117.7-192.2		1.0			
pT-stage								
extraprostatic	43	65.0	37.4-92.5	< 0.001	5.7 (1.9-16.8)	0.002		
organconfined	18	158.2	146.7-169.7		1.0			
TMPRSS2(exon 0)-ERG expression								
Yes	2140	158.2	98.9-217.5	0.015	0.36 (0.15-0.85)	0.02	0.34 (0.14-0.84)	0.019
No		68.2	36.8-99.6		1.0			

Abbreviations:
CI = confidence interval
HR = hazard ratio
pT-stage = pathological stage

It is estimated that almost half of all genes in the human genome contain more than one first exon, as an important mechanism to regulate gene expression (20, 21). Here, we showed that *TMPRSS2* transcripts starting at exon 0 were much more prostate-specific than those starting at exon 1, and that the expression level of transcripts containing exon 0 was much more variable. Further, our xenograft data indicated that the fusion to *ERG* did not preferentially influence the use of *TMPRSS2* exon 0 or exon 1. *TMPRSS2* exon 0 is located in a retroviral repeat element, ERVL-B4 (Fig. 1A). This repeat does not contain a standard LTR promoter element, however, other retroviral repeat sequences might function as cryptic promoters (20). Within the same retroviral repeat the *TMPRSS2* sequence present in a *TMPRSS2-ETV4* fusion transcript is located (4). Although a different 5'-UTR might affect translation efficacy, the major protein translated from the fusion transcripts seems an identical N-truncated ERG protein, which is translated from an ATG in the *ERG* exon 4 part of the fusion transcripts.

It could be speculated that the prostate-specific *TMPRSS2(exon 0)* transcripts are expressed in tumors with a more differentiated phenotype. Recurrent tumors represent late stage prostate cancer that normally have a less differentiated phenotype. In our study, 55% of the recurrences had a Gleason score ≥ 8, compared with 15% of the primary tumors. An alternative explanation is that expression from exon 0 is stimulated by the stromal compartment, which will be different in primary tumors and recurrences. Obviously, there are no stromal cells present during *in vitro* culture of prostate cells, which had very low expression levels of *TMPRSS2(exon 0)* (Fig. 1).

The prognostic significance of *TMPRSS2-ERG* gene fusion remains subject of debate, although a growing number of studies has been published on this matter (10-17). Because technology used to investigate *TMPRSS2-ERG* varies (FISH or QPCR) and compositions of patient cohorts differ considerably, it is difficult to draw general conclusions from available data. In the present study on a well-defined patient cohort with a very long median follow-up, there was no difference in time to PSA recurrence after radical prostatectomy between patients that expressed *TMPRSS2-ERG* and patients without expression of the fusion gene.

In two studies on watchful waiting cohorts, it was shown that patients having *TMPRSS2-ERG* fusion had a higher incidence of metastases or cancer-specific death than gene-fusion-negative patients (10, 11). FISH analysis showed that patients with an interstitial deletion of genomic sequences between *TMPRSS2* and *ERG* (so called 'class Edel') had poorer cancer-specific and overall survival than gene-fusion-negative patients, or than patients with *TMPRSS2-ERG* fusion without loss of the genomic region between the two genes (10). Other studies have correlated *TMPRSS2-ERG* with biochemical progression after radical prostatectomy, like in the present study. Prior to the identification of the *TMPRSS2-ERG*, Petrovics et al. found that patients with high expression levels of *ERG* had longer PSA recurrence-free survival than patients without *ERG* overexpression (16).

Recently, similar results were reported by Saramaki et al. (17), using FISH-analysis of *TMPRSS2-ERG*. However, other studies claimed a negative correlation between *TMPRSS2-ERG* and PSA recurrence (12-14). Perner et al. indicated that patients with *TMPRSS2-ERG* rearrangement through deletion showed a trend for higher PSA recurrence rate than patients without fusion (13). Wang et al. provided evidence that specific *TMPRSS2-ERG* splice variants were associated with early PSA recurrence (14).

Information on *TMPRSS2(exon 0)-ERG* transcripts in prostate cancer is still scarce. So far, this transcript was only identified by Lapointe et al. (15). However, the clinical implications of this specific fusion transcript subtype were not investigated. The low expression frequency of *TMPRSS2(exon 0)-ERG* transcripts in late stage prostate cancer, and the favorable prognosis for patients expressing this fusion transcript in primary tumors, as shown in our study, urges further investigation of the heterogeneity of *TMPRSS2-ERG* in prostate cancer. More systematic identification of specific fusion transcripts like *TMPRSS2(exon 0)-ERG* or alternatively spliced mRNAs (14) might assist in a molecular classification of prostate cancers which can be integrated in therapeutic decision making in the future.

ACKNOWLEDGMENTS

The authors thank Theo van der Kwast for pathology, Wilma Teubel for collection of clinical samples, Wytske van Weerden for xenograft tissues, Anieta Siewerts for RNA isolation, Natasja Dits for cDNA samples of clinical prostate tumors, and Mark Wildhagen for support with statistical analysis.

REFERENCES

1. Helgeson BE, Tomlins SA, Shah N, et al. Characterization of TMPRSS2:ETV5 and SLC45A3:ETV5 gene fusions in prostate cancer. Cancer Res 2008;68:73-80.
2. Hermans KG, Bressers AA, van der Korput HA, Dits NF, Jenster G, Trapman J. Two unique novel prostate-specific and androgen-regulated fusion partners of ETV4 in prostate cancer. Cancer Res 2008;68:3094-8.
3. Tomlins SA, Laxman B, Dhanasekaran SM, et al. Distinct classes of chromosomal rearrangements create oncogenic ETS gene fusions in prostate cancer. Nature 2007;448:595-9.
4. Tomlins SA, Mehra R, Rhodes DR, et al. TMPRSS2:ETV4 gene fusions define a third molecular subtype of prostate cancer. Cancer Res 2006;66:3396-400.
5. Tomlins SA, Rhodes DR, Perner S, et al. Recurrent fusion of TMPRSS2 and ETS transcription factor genes in prostate cancer. Science 2005;310:644-8.
6. Attard G, Clark J, Ambroisine L, et al. Heterogeneity and clinical significance of ETV1 translocations in human prostate cancer. Br J Cancer 2008;99:314-20.
7. Hermans KG, van der Korput HA, van Marion R, et al. Truncated ETV1, fused to novel tissue-specific genes, and full length ETV1 in prostate cancer. Cancer Res 2008;68:7541-9.
8. Hermans KG, van Marion R, van Dekken H, Jenster G, van Weerden WM, Trapman J. TMPRSS2:ERG fusion by translocation or interstitial deletion is highly relevant in androgen-dependent prostate cancer, but is bypassed in late-stage androgen receptor-negative prostate cancer. Cancer Res 2006;66:10658-63.
9. Ham B, Mehra R, Dhanasekaran, SM et al. A fluorescence in situ hybridization screen for E26 transformation-specific aberrations: identification of DDX5-ETV4 fusion protein in prostate cancer. Cancer Res 2008;68:7629-37.
10. Attard G, Clark J, Ambroisine L, et al. Duplication of the fusion of TMPRSS2 to ERG sequences identifies fatal human prostate cancer. Oncogene 2008;27:253-63.
11. Demichelis F, Fall K, Perner S, et al. TMPRSS2:ERG gene fusion associated with lethal prostate cancer in a watchful waiting cohort. Oncogene 2007;26:4596-9.
12. Nam RK, Sugar L, Yang W, et al. Expression of the TMPRSS2:ERG fusion gene predicts cancer recurrence after surgery for localised prostate cancer. Br J Cancer 2007;97:1690-5.
13. Perner S, Mosquera JM, Demichelis F, et al. TMPRSS2-ERG fusion prostate cancer: an early molecular event associated with invasion. Am J Surg Pathol 2007;31:882-8.
14. Wang J, Cai Y, Ren C, Ittmann M. Expression of Variant TMPRSS2/ERG Fusion Messenger RNAs Is Associated with Aggressive Prostate Cancer. Cancer Res 2006;66:8347-51.
15. Lapointe J, Kim YH, Miller MA, et al. A variant TMPRSS2 isoform and ERG fusion product in prostate cancer with implications for molecular diagnosis. Mod Pathol 2007;20:467-73.
16. Petrovics G, Liu A, Shaheduzzaman S, et al. Frequent overexpression of ETS-related gene-1 (ERG1) in prostate cancer transcriptome. Oncogene 2005;24:3847-52.
17. Saramaki OR, Harjula AE, Martikainen PM, Vessella RL, Tammela TL, Visakorpi T. TMPRSS2:ERG Fusion Identifies a Subgroup of Prostate Cancers with a Favorable Prognosis. Clin Cancer Res 2008;14:3395-400.
18. van Weerden WM, de Ridder CM, Verdaasdonk CL, et al. Development of seven new human prostate tumor xenograft models and their histopathological characterization. Am J Pathol 1996;149:1055-62.
19. Clark J, Merson S, Jhavar S, et al. Diversity of TMPRSS2-ERG fusion transcripts in the human prostate. Oncogene 2007:26:2667-73.

20. Landry JR, Mager DL, Wilhelm BT. Complex controls: the role of alternative promoters in mammalian genomes. Trends Genet 2003;19:640-8.
21. Kimura K, Wakamatsu A, Suzuki Y, et al. Diversification of transcriptional modulation: large-scale identification and characterization of putative alternative promoters of human genes. Genome Res 2006; 16:55-65.

SUPPLEMENTARY INFORMATION

Table S1. Clinical and pathological characteristics of 67 patients with primary prostate cancer

Characteristic		
Mean age (± SD)	62.5	± 5.4 years
Median follow-up (± SD)	127.0	± 48.3 months
Mean PSA (± SD)	15.6	± 22.8 ng/ml
cT-stage		
organconfined	45	67.2%
extraprostatic	13	19.4%
unknown	9	13.4%
pT-stage		
pT2a	2	3.0%
pT2b	3	4.5%
pT2c	13	19.4%
pT2x	1	1.5%
pT3a	24	35.8%
pT3b	16	23.9%
pT4	5	7.5%
unknown	3	4.5%
Surgical margins		
positive	31	46.3%
negative	32	47.8%
unknown	4	6.0%
Gleason score		
< 7	38	56.7%
= 7	19	28.3%
> 7	10	15.0%
Occult metastases at RP		
Yes	7	10.4%
No	56	83.6%
unknown	4	6.0%
PSA recurrence		
Yes	33	49.3%
No	33	49.3%
Unknown	1	1.5%
Local recurrence		
Yes	9	13.4%
No	55	82.1%
Unknown	3	4.5%

Distant metastases during follow-up		
Yes	11	16.4%
No	55	82.1%
Unknown	1	1.5%
Death		
Yes	27	40.3%
No	40	59.7%
Prostate cancer death		
Yes	11	16.4%
No	54	80.6%
Unknown	2	3.0%

Abbreviations:
SD = standard deviation
cT-stage = clinical stage
pT-stage = pathological stage
RP = radical prostatectomy

Table S2. Primer sequences of primers used for QPCR analysis

Target	Forward 5'->3'	Reverse 5'->3'
PBGD	catgtctggtaacggcaatg	gtacgaggctttcaatgttg
TMPRSS2 E1-E3	gagctaagcaggaggcgga	aggggttttccggttggtatc
TMPRSS2 E0-E3	gactacttctactccaccag	aggggttttccggttggtatc
TMPRSS2(exon 0)-ERG	gactacttctactccaccag	catcaggagagttccttgag
TMPRSS2(exon 1)-ERG	gagctaagcaggaggcgga	catcaggagagttccttgag

Table S3. Clinical and pathological characteristics of patients expressing TMPRSS2-ERG versus patients not expressing TMPRSS2-ERG

	***TMPRSS2-ERG* positive (N=44)**	***TMPRSS2-ERG* negative (N=23)**	**p-value**	***Test***
Mean age (± SD)	62.2 (± 5.6)	63.0 (± 5.1)	0.57	MWU
Mean PSA (± SD)	16.1 (± 26.7)	14.8 (± 12.5)	0.30	MWU
Gleason Score				
< 7	29 (65.9%)	9 (40.9%)	0.053	Chi^2
≥ 7	15 (34.1%)	13 (59.1%)		
pT-stage				
extraprostatic	13 (31.0%)	6 (27.3%)	0.76	Chi^2
organconfined	29 (69.0%)	16 (72.7%)		
Surgical margins				
Positive	21 (50.0%)	10 (47.6%)	0.86	Chi^2
Negative	21 (50%0	11 (52.4%)		

Abbreviations:
SD = standard deviation
MWU = Mann-Whitney U test
pT-stage = pathological stage
*Patients with unknown parameters were not included in the analysis

Table S4. Clinical and pathological characteristics of patients expressing *TMPRSS2(exon 0)-ERG* fusion transcripts versus patients exclusively expressing *TMPRSS2(exon 1)-ERG* fusion transcripts

	***TMPRSS2(exon 0)-ERG* expression (N=24)**	**Exclusive *TMPRSS2(exon 1)-ERG* expression (N=20)**	**p-value**	**Test**
Mean age (± SD)	61.5 (± 4.8)	63.1 (± 6.4)	0.40	MWU
Mean PSA (± SD)	19.7 (± 35.2)	11.9 (± 10.3)	0.63	MWU
Gleason Score				
< 7	15 (62.5%)	14 (70.0%)	0.60	Chi^2
≥ 7	9 (37.5%)	6 (30.0%)		
pT-stage				
extraprostatic	11 (47.8%)	2 (10.5%)	0.009	Chi^2
organconfined	12 (52.2%)	17 (89.5%)		
Surgical margins				
Positive	9 (39.1%)	12 (63.2%)	0.12	Chi^2
Negative	14 (60.9%)	7 (36.8%)		

Abbreviations:

SD = standard deviation

MWU = Mann-Whitney U test

SD = standard deviation

pT-stage = pathological stage

*Patients with unknown parameters were not included in the analysis

Chapter 6

TWO UNIQUE NOVEL PROSTATE-SPECIFIC AND ANDROGEN-REGULATED FUSION PARTNERS OF *ETV4* IN PROSTATE CANCER

Karin G. Hermans[1], Anke A. Bressers[1], Hetty A. van der Korput[1], Natasja F. Dits[2], Guido Jenster[2] and Jan Trapman[1]
Departments of Pathology[1] and Urology[2], Josephine Nefkens Institute, Erasmus University Medical Center, Rotterdam, The Netherlands
Cancer Research 2008; 68: 3094-3098

ABSTRACT

Recently, fusion of *ERG* to the androgen-regulated, prostate-specific *TMPRSS2* gene has been identified as the most frequent genetic alteration in prostate cancer. At low frequency *TMPRSS2-ETV1* and *TMPRSS2-ETV4* fusion genes have been described. In this study we report two novel *ETV4* fusion genes in prostate cancer: *KLK2-ETV4* and *CANT1-ETV4*. Both gene fusions have important unique aspects. *KLK2* is a well-established androgen-induced and prostate-specific gene. Fusion of *KLK2* to *ETV4* results in the generation of an additional *ETV4* exon, denoted exon 4a. This novel exon delivers an ATG for the longest open reading frame, in this way avoiding translation start in *KLK2* exon 1. Although wild-type *CANT1* has two alternative first exons (exons 1 and 1a), only exon 1a was detected in *CANT1-ETV4* fusion transcripts. We show that *CANT1* transcripts starting at exon 1a have an androgen-induced and prostate-specific expression pattern, whereas *CANT1* transcripts starting at exon 1 are not prostate-specific. So, the two novel *ETV4* fusion partners possess as predominant common characteristics: androgen-induction and prostate-specific expression.

INTRODUCTION

Prostate cancer is the most common malignancy in men in Western countries (1). Growth of prostate tumors depends on androgen signalling, mediated by the androgen receptor (AR). Metastatic disease is treated by endocrine therapy, however, all tumors eventually become resistant to this therapy. The majority of resistant tumors still contain a functional active *AR* (2). In part of these tumors *AR* is overexpressed due to amplification of a small region of the X chromosome, where *AR* maps (3).

Most frequent genomic alterations in primary prostate cancers are losses of large fragments of chromosome arms 6q, 8p, 13q and 16q and gain of 8q (4, 5). In a subset of tumors a small region of loss of chromosome 21q22 has been detected. This genomic alteration is associated with recurrent fusion of prostate-specific and androgen-regulated *TMPRSS2* (6) to the ETS transcription factor gene *ERG*, which maps at a distance of 3 Mbp from *TMPRSS2* on 21q (7).

TMPRSS2-ERG fusion is present in 40-70% of clinical prostate cancers (7, 8, and Hermans unpublished). The gene fusion is an early event that has also been detected in a proportion of precursor lesions (9). Although in many tumors *TMPRSS2-ERG* overexpression is accompanied by loss of the region between *TMPRSS2* and *ERG*, in others this region has been retained, indicative of different mechanisms of gene fusion (10). At low frequency, fusion of *TMPRSS2* to a second ETS gene, *ETV1*, that maps to chromosome band 7p21, has been reported (7, 10). *TMPRSS2* seems the only fusion partner of *ERG*, but it has recently been shown that *ETV1* has more fusion partners (11, and Hermans unpublished).

For a third ETS gene, *ETV4*, only fusion to *TMPRSS2* has been described (12). In the present study we identified in clinical prostate cancer samples two unique novel *ETV4* fusion partners: Kallikrein 2 (*KLK2)* and Calcium Activated Nucleotidase 1 (*CANT1)*. KLK2, or hGK1, is a well-known prostate marker highly homologous to KLK3 or prostate-specific antigen (PSA) (13). Like *KLK3*, *KLK2* is prostate-specific and androgen-regulated expressed (13, 14). We show that *CANT1* expression is also androgen-regulated. *CANT1* possesses two alternative first exons, but only one of these is present in the *CANT1-ETV4* fusion transcript. In contrast to the majority of *CANT1* transcripts, this mRNA is preferentially expressed in the prostate. The novel fusion genes indicate prostate-specificity and androgen-regulation as important characteristics of *ETV4* fusion partners in prostate cancer.

MATERIALS AND METHODS

Samples.

Two series of clinical prostate cancer samples were obtained from the tissue bank of the Erasmus University Medical Center (Rotterdam, The Netherlands). Samples were snap-frozen and stored in liquid nitrogen. All samples contained at least 70% tumor cells. Collection of patient samples has been performed according to national legislation concerning ethical requirements. Use of these samples has been approved by the Erasmus MC Medical Ethics Committee according to the Medical Research Involving Human Subjects Act (MEC-2004-261). Prostate cancer xenografts were propagated by serial transplantation on male nude mice as described (10, 15).

DNA and RNA isolation.

RNA from clinical prostate cancer specimens was isolated using the RNA-Bee kit (Campro Scientific, Berlin, Germany). DNA was isolated using the DNeasy DNA extraction kit (Qiagen, Valencia, CA). Xenograft RNA was isolated according to the LiCl protocol. RNA from the prostate cancer cell line LNCaP cultured in the presence of 10^{-9}M R1881, or in the absence of hormone was isolated using the RNeasy RNA extraction kit (Qiagen).

mRNA expression analysis.

Analysis of mRNA expression was performed by RT-PCR or by QPCR. Two µg RNA was reverse transcribed using 400 U M-MLV RT (Invitrogen, Carlsbad, CA) and an oligo-dT12 primer. cDNA's of 16 different tissues were purchased from Clontech (Mountain View, CA). RT-PCR products were analyzed on a 1.5% agarose gel. QPCR was performed in an ABI Prism 7700 Sequence Detection System (Applied Biosystems, Foster City, CA), using Power SYBR Green PCR Master Mix (Applied Biosystems), containing 330 nM forward and reverse primer, in a total volume of 25 µl. Thermocycling conditions were according to the recommendations of the manufacturer. mRNA expression was determined relative to Porphobilinogen deaminase (*PBDG*) by the Standard curve method (Applied Biosystems). Primers are listed in supplementary Table S1.

RNA Ligase-Mediated Rapid Amplification of cDNA Ends (RLM-RACE).

5' RLM-RACE was performed using the GeneRacer kit from Invitrogen according to instructions of the manufacturer. To obtain the 5'-sequence, cDNA was amplified with Qiagen Taq (Qiagen) using the Generacer 5'-primer and an *ETV4* exon 6 primer. PCR products were separated over a 1.5% agarose gel, bands were excised, purified and sequenced on an ABI 3100 genetic analyser (Applied Biosystems).

Array Comparative Genomic Hybridization (array CGH).

Arrays were produced from the human 3600 BAC/PAC genomic clone set of the Welcome Trust Sanger Institute, covering the full genome at approx. 1 Mb-spacing. DNA labeling and hybridization were performed as previously described (10). After hybridization arrays were scanned in a ScanArray Express HT (Perkin Elmer, Freemont, CA). The resulting images were analyzed with GenePix Pro 5.0 software (Axon Instruments, Foster City, CA) and subsequently visualized with an excel macro.

Interphase fluorescent *in situ* hybridization (FISH).

Interphase FISH was done on 5 µm frozen tissue sections as described previously (10). BAC clones RP11-100E5 and RP11-209M4 (both flanking *ETV4*) were purchased from BacPac Resources (Oakland, CA). Specificity of BACs was confirmed on metaphase chromosome spreads. BAC DNA's were either Spectrum Orange or Spectrum Green labeled using a Nick Translation Reagent Kit (Vysis, Downers Grove, IL). Tissue sections were counterstained with DAPI in anti-fade solution (Vector Laboratories, Burlingame, CA). Images of the three fluorochromes were collected on an epifluorescence microscope (Leica DM, Rijswijk, The Netherlands) equipped with appropriate filter sets (Leica) and a CCD cooled camera (Photometrics, Tucson, AZ).

Breakpoint mapping.

Fusion points were mapped by standard long-range PCR on 200 ng genomic DNA in the presence of 0.5 µM of each forward (fusion partner) and reverse (*ETV4*) primer with Taq polymerase and Proofstart DNA polymerase (Qiagen). Primers are given in Supplementary Table 1. PCR products were separated on a 1% agarose gel. Specific amplified fragments were isolated and sequenced.

RESULTS AND DISCUSSION

ETV4 expression was studied by QPCR on two sets of clinical prostate cancer samples. Set 1 was composed of 84 clinical prostate cancer samples (49 primary prostate tumors, 11 lymph node metastases and 24 recurrent tumors) and set 2 of 36 primary prostate tumors and 29 recurrent tumors. In primary tumor 98, and in recurrent tumor 206, both from set 1, *ETV4* overexpression was detected (Fig 1A). In the second set we did not detect *ETV4* overexpression (data not shown), indicating that overexpression is a rare event, occurring in <2% clinical prostate cancers. Follow up experiments showed that *ETV4* overexpression was caused by fusions to two different genes with unique properties.

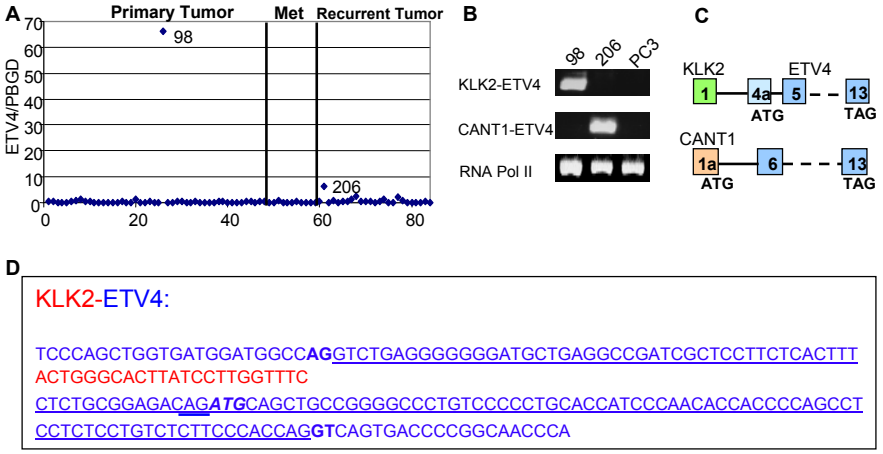

Figure 1 Expression of *ETV4* and characterization of *ETV4* fusion transcripts in clinical prostate cancer samples. (A) QPCR analysis of *ETV4* expression in clinical prostate cancer samples compared to *PBGD* expression. Overexpression of *ETV4* was detected in samples 98 and 206. Met: regional lymph node metastasis. (B) Confirmation of *KLK2-ETV4* (sample 98) and *CANT1-ETV4* (sample 206) fusion transcripts by RT-PCR, using *ETV4* and fusion partner specific primers. RNA from prostate cancer cell line PC3 was used as a negative control. An RNA Pol II amplified fragment is shown as a loading control. (C) Schematic representation of *KLK2-ETV4* and *CANT1-ETV4* fusion transcripts. Exons are indicated by colored boxes. In both transcripts ATG start codons and TAG stop codons of longest predicted open reading frames are indicated. (D) Sequence of *ETV4* exon 4a and flanking sequences. The *ETV4* exon 4a sequence is underlined. *KLK2* intron 1 sequence present in the fusion gene is in red. Splice sites are bold. The ATG start codon in *ETV4* exon 4a is depicted in bold and italic.

First, RT-PCR experiments with *TMPRSS2* and *ETV4* specific primers excluded *TMPRSS2* as fusion partner (data not shown). Next, we performed 5' RNA ligase-mediated rapid amplification of cDNA ends (RLM-RACE), using a reverse primer in *ETV4* exon 6. Sequencing of the amplified fragments showed *KLK2* (sample 98) and *CANT1* (sample 206) as novel *ETV4* fusion partners. The presence of *KLK2-ETV4* and *CANT1-ETV4* fusion transcripts in the individual samples was confirmed by RT-PCR (Fig 1B).

The *KLK2-ETV4* mRNA fragment detected by RLM-RACE, was composed of *KLK2* exon 1 linked to a new *ETV4* exon (here denoted exon 4a), followed by *ETV4* exon 5 and 6 sequences (Fig 1C). The novel *ETV4* exon 4a has a length of 133 bp and delivers the ATG start codon of the longest predicted open reading frame in the *KLK2-ETV4* fusion transcript (Fig 1D). *KLK2* maps to chromosome band 19q13 and *ETV4* on chromosome band 17q21. Because of the orientations of *KLK2* and *ETV4*, *KLK2-ETV4* gene fusion cannot be explained by a single chromosomal translocation.

The *CANT1-ETV4* fragment detected by RLM-RACE contained one of the two described exons 1 of *CANT1* (here denoted exon 1a). This exon maps approx. 4 Kbp downstream of the other first exon (here denoted exon 1) (Fig 1C). *CANT1* exon 1a delivers the ATG start codon of the predicted *ETV4* open reading frame. Remarkably, *CANT1-ETV4* fusion transcripts starting at *CANT1* exon 1 were not detected, although wild-type *CANT1* tran-

scripts starting either at exon 1 or 1a of the non-rearranged second allele were present in the tumor sample and in normal prostate (data not shown). *CANT1* and *ETV4* map in the same orientation on 17q, at a distance of approx. 35 Mbp. However, array-based CGH showed that the genomic region between *ETV4* and *CANT1* was not lost (data not shown), indicating that either an internal rearrangement of 17q had occurred or that this region was reintegrated in another part of the genome.

ETV4 rearrangements in samples 98 and 206 were confirmed by split signal FISH with probes flanking *ETV4* at both sites (Fig 2A). Next, the genomic fusion points were mapped by long-range PCR and sequencing (Fig 2B,C). As expected, the breakpoints of *CANT1-ETV4* were located in *CANT1* intron 1, downstream from exon 1a, and in *ETV4* intron 5, respectively. This latter breakpoint was located in a MER20 repeat, a low copy repetitive element known to be involved in unstable genomic regions prone to chromosomal rearrangement (16). Breakpoints in *KLK2* and *ETV4* in sample 98 were not in repetitive sequences. The breakpoint in *ETV4* intron 4 of the *KLK2-ETV4* rearrangement was 2 bp upstream of *ETV4* exon 4a (Fig 1D, 2C). Due to the gene fusion the purine-rich

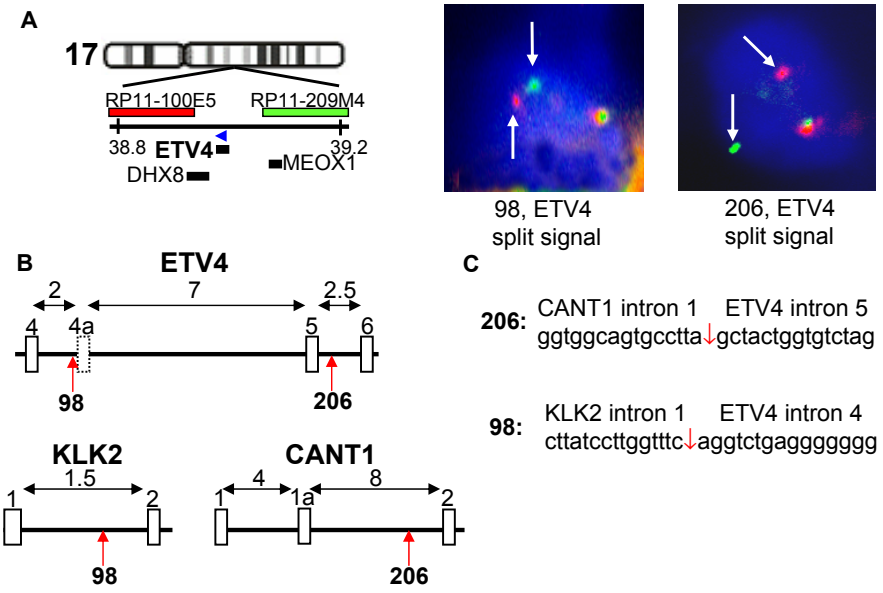

Figure 2 Characterization of *ETV4* fusion genes in clinical prostate cancer samples. (A) Schematic representation of the *ETV4* genomic region on chromosome 17. Distance from the top of chromosome is indicated in Mbp. Orientation of *ETV4* is indicated by blue arrowhead. BAC probes used in split signal FISH are indicated in colors corresponding to FISH staining. Split signal FISH on frozen tissue sections confirms *ETV4* rearrangements in samples 98 and 206 as indicated by arrows. Schematic representation of genomic breakpoints in *ETV4*, *KLK2*, and *CANT1* as found by long-range PCR and sequencing. Numbered exons are depicted as open boxes. Positions of genomic breakpoints are shown by red arrows. Distances in kbp between exons are indicated. (C) Sequences of *CANT1-ETV4* and *KLK2-ETV4* fusion points. Fusion point is indicated by red arrow.

ETV4 intron sequence was replaced by a more pyrimidine-rich sequence of *KLK2* intron 1, generating a novel splice acceptor sequence. To confirm that the rearrangement induced *ETV4* exon 4a, a splicing assay was performed (Fig S1). *ETV4* exon 4a was indeed retained if the *KLK2-ETV4* fusion sequence was used, but not if intron 4 sequence of wild-type *ETV4* was used in the assay (Fig S1).

KLK2 is a well-known androgen-regulated and prostate-specific gene (13, 14). To establish the specific characteristics of *CANT1* expression, QPCR analysis on cDNAs from eleven human prostate cancer xenografts derived from various stages of the disease and with different *AR* status was performed (10, 15). We compared expression of transcripts starting at *CANT1* exon 1 and transcripts starting at exon 1a to *KLK2* expression. *KLK2* mRNA expression was completely restricted to xenografts with highest *AR* expression (Fig 3A). *CANT1* transcripts starting at exon 1a showed highest expression in the more differentiated, androgen-dependent xenografts (Fig 3B). In contrast, transcripts starting at exon 1 were expressed at variable levels in all xenografts. Further analysis of RNA from LNCaP prostate cancer cells, which were *in vitro* cultured in the presence of the synthetic androgen R1881 or in the absence of hormone, showed that both transcripts starting at *CANT1* exon 1 and exon 1a are induced by androgens (Fig 3C). As expected *KLK2* expression was strongly induced by androgens. Next we tested the tissue-specificity of the *CANT1* and *KLK2* transcripts in a cDNA panel from 16 different normal tissue samples. *KLK2* showed an expected strictly prostate-specific expression pattern (Fig 3D). Remarkably, transcripts starting at *CANT1* exon 1 were ubiquitously expressed, but transcripts starting at exon 1a had a much more restricted expression pattern, with highest expression in the prostate (Fig 3E).

Both *KLK2-ETV4* and *CANT1-ETV4* have specific, unique characteristics. *KLK2-ETV4* because a novel *ETV4* exon is generated (exon 4a) and *CANT1-ETV4* because *CANT1* exon 1a is exclusively used in *CANT1-ETV4* fusion transcripts. A KLK2-ETV4 fusion protein containing the N-terminal KLK2 signal peptide would be secreted and could not function as a transcription factor. However, the start codon in the novel *ETV4* exon 4a, which is preceded by an in frame stop codon, prevents the generation of such a fusion protein. Instead, synthesis of a truncated ETV4 protein, starting in *ETV4* exon 4a can now be predicted (Fig 1D). Exclusive usage of *CANT1* exon 1a as first exon in *CANT1-ETV4* fusion transcripts might have various explanations, including the positions of breakpoints of the specific genomic rearrangement and the prostate-specific expression of transcripts starting at exon 1a.

In prostate cancer, *TMPRSS2* is the common fusion partner of the ETS family members *ERG*, *ETV1* and *ETV4*. Recently, several novel *ETV1* fusion partners have been identified: *SLC45A3*, *HERV-K_22q11.23*, *C15orf21*, *HNRPA2B1* (11), with different expression characteristics. Based on expression profiles the fusion partners were divided into distinct classes of *ETV1* rearrangements, separating prostate-specific, androgen upregulated genes and

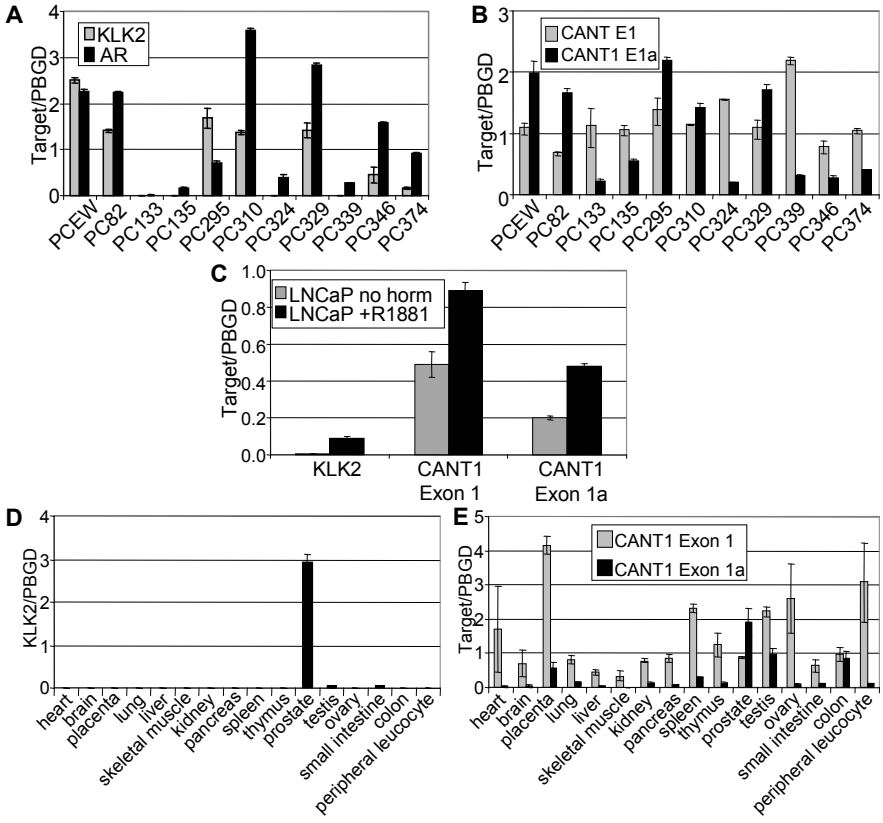

Figure 3 Characteristics of *KLK2* and *CANT1* mRNA expression. Expression of (A) *KLK2* and *AR* mRNA, and (B) of transcripts starting in *CANT1* exon 1 and *CANT1* exon 1a, respectively, in eleven human prostate cancer xenografts. *PBGD* expression is used as control. (C) Androgen-regulated expression of *KLK2* and *CANT1* transcripts assessed by QPCR analysis in LNCaP cells grown in the absence or in the presence of the synthetic androgen R1881 (1 nM). Expression relative to *PBGD* is presented. Tissue-specific expression of (D) *KLK2* and (E) *CANT1* transcripts. Tissue-specific expression was tested on a cDNA panel from 16 different normal tissues by QPCR analysis and is shown relative to *PBGD* expression. In all experiments, standard deviations, as indicated by vertical bars, are calculated from two independent experiments.

downregulated genes, and ubiquitously regulated genes. Recently, we identified three novel *ETV1* fusion partners: *FOXP1*, *HERVK17* and *EST14* (Hermans unpublished). Both *HERVK17* and *EST14* have a prostate-specific and androgen-induced expression pattern; *FOXP1* seems expressed in many tissues. The three *ETV4* partners identified, *TMPRSS2*, *KLK2* and *CANT1*, show identical expression profiles: upregulation by androgens and prostate-specificity.

The common expression pattern of *ETV4* fusion partners indicates a similar mechanism of gene fusion. It is tempting to speculate that the genomic region of prostate-specific genes is unstable in a specific cell type. Based on the stem cell/progenitor cell concept

of tumor development (17), progenitor cells of the luminal epithelial prostate cells, in which expression of the prostate-specific fusion partners is expected to be activated, are interesting candidates. In this regard, we could confirm *TMPRSS2* induction during development of the mouse prostate (Hermans, unpublished). Unfortunately, there are no appropriate mouse counterparts of *KLK2* and *CANT1*(exon 1a).

A second process that might play a role in a common mechanism of gene fusion includes the nuclear compartmentalization of gene expression. It might be proposed that prostate-specific genes are all expressed in a limited number of nuclear compartments, or so-called transcription factories (18, 19). Possibly, *ETV4* is expressed in the same compartments. In accordance with the latter hypothesis, it has recently been shown that *IGH* and *cMYC*, which are fusion partners in Burkitt lymphoma and plasmacytoma, are preferentially expressed in the same nuclear regions at *in vitro* B cell stimulation (20).

Taken together, the results from this study show that *ETV4* has multiple fusion partners and highlight the importance of meticulous examination of gene fusions. Importantly, key determinants of *ETV4* fusion partners are not chromosomal location or expression level, but their androgen-regulated and prostate-specific expression pattern.

ACKNOWLEDGEMENTS

The authors thank Theo van der Kwast and Arno van Leenders for pathology, Chris Bangma and Wilma Teubel for clinical samples, Wytske van Weerden for xenograft tissues and Anieta Siewerts for RNA isolation of clinical samples.

REFERENCES

1. Jemal A, Siegel R, Ward E, Murray T, Xu J, Thun MJ. Cancer statistics, 2007. CA Cancer J Clin 2007;57:43-66.
2. van der Kwast TH, Schalken J, Ruizeveld de Winter JA, *et al.* Androgen receptors in endocrine-therapy-resistant human prostate cancer. Int J Cancer 1991;48:189-93.
3. Visakorpi T, Hyytinen E, Koivisto P, *et al.* In vivo amplification of the androgen receptor gene and progression of human prostate cancer. Nat Genet 1995;9:401-6.
4. Cher ML, Bova GS, Moore DH, *et al.* Genetic alterations in untreated metastases and androgen-independent prostate cancer detected by comparative genomic hybridization and allelotyping. Cancer Res 1996;56:3091-102.
5. Visakorpi T, Kallioniemi AH, Syvanen AC, *et al.* Genetic changes in primary and recurrent prostate cancer by comparative genomic hybridization. Cancer Res 1995;55:342-7.
6. Lin B, Ferguson C, White JT, *et al.* Prostate-localized and androgen-regulated expression of the membrane-bound serine protease TMPRSS2. Cancer Res 1999;59:4180-4.
7. Tomlins SA, Rhodes DR, Perner S, *et al.* Recurrent fusion of TMPRSS2 and ETS transcription factor genes in prostate cancer. Science 2005;310:644-8.
8. Mehra R, Tomlins SA, Shen R, *et al.* Comprehensive assessment of TMPRSS2 and ETS family gene aberrations in clinically localized prostate cancer. Mod Pathol 2007;20:538-44.
9. Cerveira N, Ribeiro FR, Peixoto A, *et al.* TMPRSS2-ERG gene fusion causing ERG overexpression precedes chromosome copy number changes in prostate carcinomas and paired HGPIN lesions. Neoplasia 2006;8:826-32.
10. Hermans KG, van Marion R, van Dekken H, Jenster G, van Weerden WM, Trapman J. TMPRSS2: ERG fusion by translocation or interstitial deletion is highly relevant in androgen-dependent prostate cancer, but is bypassed in late-stage androgen receptor-negative prostate cancer. Cancer Research 2006;66:10658-63.
11. Tomlins SA, Laxman B, Dhanasekaran SM, *et al.* Distinct classes of chromosomal rearrangements create oncogenic ETS gene fusions in prostate cancer. Nature 2007;448:595-9.
12. Tomlins SA, Mehra R, Rhodes DR, *et al.* TMPRSS2: ETV4 gene fusions define a third molecular subtype of prostate cancer. Cancer Research 2006;66:3396-400.
13. Chapdelaine P, Paradis G, Tremblay RR, Dube JY. High level of expression in the prostate of a human glandular kallikrein mRNA related to prostate-specific antigen. FEBS Lett 1988;236:205-8.
14. Riegman PH, Vlietstra RJ, van der Korput HA, Romijn JC, Trapman J. Identification and androgen-regulated expression of two major human glandular kallikrein-1 (hGK-1) mRNA species. Mol Cell Endocrinol 1991;76:181-90.
15. van Weerden WM, de Ridder CM, Verdaasdonk CL, *et al.* Development of seven new human prostate tumor xenograft models and their histopathological characterization. Am J Pathol 1996;149:1055-62.
16. Shaw CJ, Lupski JR. Implications of human genome architecture for rearrangement-based disorders: the genomic basis of disease. Hum Mol Genet 2004;13:57-64.
17. Lawson DA, Witte ON. Stem cells in prostate cancer initiation and progression. J Clin Invest 2007;117:2044-50.
18. Fraser P, Bickmore W. Nuclear organization of the genome and the potential for gene regulation. Nature 2007;447:413-7.
19. Misteli T. Beyond the sequence: cellular organization of genome function. Cell 2007;128:787-800.
20. Osborne CS, Chakalova L, Mitchell JA, *et al.* Myc dynamically and preferentially relocates to a transcription factory occupied by Igh. PLoS Biol 2007;5:1763-72.

SUPPLEMENTARY INFORMATION

Supplementary Table S1 Primer sequences

Primer name	Forward (5'->3')	Reverse (5'->3')
QPCR and RACE		
ETV4 E12-13	accggccagccatgaattac	gagagctggacgctgattc
PBGD	catgtctggtaacggcaatg	gtacgaggctttcaatgttg
ETV4 E6		tccttcttgatcctggtggt
KLK2 E1	ttctctccatcgccttctct	
CANT1 E1a	gctggagaaacaaaccctct	
KLK2 E4-5	tccaatgacatgtgtgctag	caccattacagacaagtgga
CANT1 E1-2	ttagcccagccaagcccagc	agaacgtcaggatcaccttc
CANT1 E1a-2	gctggagaaacaaaccctct	agaacgtcaggatcaccttc
AR	tgactccgtgcagcctattg	atgggaagcaaagtctgaag
Splicing assay		
KLK2-ETV4	atactcgagctaaatccgcacccttttca	ataggatcccttcaaattggggctttgga
ETV4	atactcgagtacatgctgctgccctgtac	ataggatcccttcaaattggggctttgga
SD-SA	tctgagtcacctggacaacc	atctcagtggtatttgtgagc
Breakpoint mapping		
KLK2 E1	ttctctccatcgccttctct	
KLK2 I1	cagtcctaccacagtctact	
ETV4 I4		gagaaagtgagaaggagcga
CANT1 E1a	gctggagaaacaaaccctct	
CANT1 I1	tctgggagatagctggtttg	
ETV4 E6		tccttcttgatcctggtggt
ETV4 I5A		cggatcacaaggtcaggaat
ETV4 I5B		agcagcaaagagttggttcc
ETV4 I5C		tggtgaaaccctgtctctac
ETV4 I5D		gttggtctcaaactcctgac

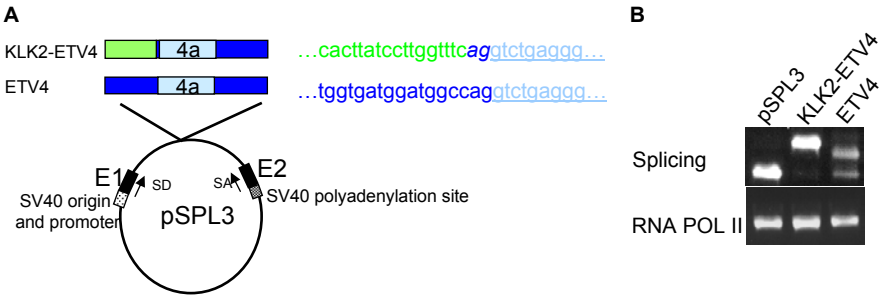

Figure S1. Detection of *ETV4* exon 4a in a splicing assay. (A) Schematic representation of the constructs used in the splicing assay. Appropriate *KLK2-ETV4* and *ETV4* genomic fragments, containing the *ETV4* exon 4a sequence were amplified and subsequently integrated in the multiple cloning site of splicing vector pSPL3 (Invitrogen). Primer sequences are given in Table S1. *KLK2* derived sequences are in green, *ETV4* sequences are in light or dark blue. LNCaP prostate cancer cells were transiently transfected with *KLK2-ETV4*, *ETV4* and control splicing constructs using the calcium phosphate precipitation method. Cells were harvested after 48 h and RNAs were isolated as described in Materials and Methods. Next, cDNAs were prepared and amplified with primers SD and SA in exons 1 and 2 of pSPL3, respectively. (B) Amplified fragments were analyzed over a 1.5% agarose gel, isolated and sequenced. An amplified RNA pol II fragment was used as a control. Control empty pSPL3 gave the expected E1/E2 fragment. pSPL3(KLK2-ETV4) cDNA contained E1 and E2 sequence and *ETV4* exon 4a. pSPL3(ETV4) cDNA contained the expected E1/E2 fragment and a larger fragment composed of E1 and E2 sequences, and the sequence of the last part of *ETV4* exon 4a, due to the usage of a cryptic splice acceptor site in exon 4a (double underlined in Fig 1D). This shortened exon is probably an artifact, because it was not observed if wild-type *ETV4* mRNA was analyzed by RT-PCR with *ETV4* exon 4 and exon 5 specific primers (data not shown).

Chapter 7

TRUNCATED ETV1, FUSED TO NOVEL TISSUE-SPECIFIC GENES, AND FULL LENGTH ETV1 IN PROSTATE CANCER

Karin G. Hermans[1], Hetty A. van der Korput[1], Ronald van Marion[1], Dennis J. van de Wijngaart[1], Angelique Ziel-van der Made[1], Natasja F. Dits[2], Joost L. Boormans[2], Theo H. van der Kwast[1], Herman van Dekken[1], Chris H. Bangma[2], Hanneke Korsten[1], Robert Kraaij[2], Guido Jenster[2] and Jan Trapman[1]

Departments of [1]Pathology and [2]Urology, Josephine Nefkens Institute, Erasmus University Medical Center, Rotterdam, The Netherlands

Cancer Research 2008; 68:7541-49

ABSTRACT

In this study we describe the properties of novel *ETV1* fusion genes, encoding N-truncated ETV1 (dETV1), and of full length ETV1, overexpressed in clinical prostate cancer. We detected overexpression of novel *ETV1* fusion genes or of full length *ETV1* in 10% of prostate cancers. Novel *ETV1* fusion partners included *FOXP1*, an EST (*EST14*) and an endogenous retroviral repeat sequence (*HERVK17*). Like *TMPRSS2*, *EST14* and *HERVK17* were prostate-specific and androgen-regulated expressed. This unique expression pattern of most *ETV1* fusion partners seems an important determinant in prostate cancer development. In transient reporter assays full length ETV1 was a strong transactivator, whereas dETV1 was not. However, several of the biological properties of dETV1 and full length ETV1 were identical. Upon stable-overexpression, both induced migration and invasion of immortalized non-tumorigenic PNT2C2 prostate epithelial cells. In contrast to dETV1, full length ETV1 also induced anchorage-independent growth of these cells. PNT2C2 cells stable-transfected with dETV1 or full length ETV1 expression constructs showed small differences in induced expression of target genes. Many genes involved in tumor invasion/metastasis, including *uPA/uPAR* and *MMP*s, were upregulated in both cell types. Integrinβ3 (*ITGB3*) was clearly upregulated by full length ETV1, but much less by dETV1. Based on the present data and on previous findings a novel concept of the role of dETV1 and of full length ETV1 overexpression in prostate cancer is proposed.

INTRODUCTION

The ETS transcription factor family is composed of 27 members (1-3). Depending on the cellular context they can function as transactivators or transrepressors. ETS transcription factors modulate many cellular functions, including proliferation, apoptosis, differentiation, tissue remodeling, migration, invasion and angiogenesis (1-3). Altered expression or properties of ETS transcription regulators affects the control of these processes.

Recurrent chromosomal rearrangements are well-defined in leukemias, lymphomas and sarcomas (4). These rearrangements result in fusion genes that express oncogenic proteins with altered properties or in overexpression of wild type oncogenes. In Ewing sarcoma and in acute myeloid leukemia, gene fusions of members of the ETS gene family have been found. At low frequency, gene fusions have also been described in solid tumors (4). However, recent analyses showed common gene fusions in prostate cancer, all involving members of the ETS transcription factor family (5-9).

In 40-70% of clinical prostate cancers, *ERG* (21q22.1) is directly linked to androgen-regulated, prostate-specific *TMPRSS2*, which is located 3 Mbp upstream of *ERG*. At low frequency, fusions of *TMPRSS2* to *ETV1*, *ETV4* and *ETV5*, which map on different chromosomes, have been described (5, 7, 8, 10).

Considering the complexity of fusion genes in haematological and mesenchymal malignancies, we questioned whether this would also be true for gene fusions in prostate cancer. Here we describe overexpression of *ETV1* in 8 out of 84 clinical prostate cancer samples. In four samples full length *ETV1* is overexpressed, but in the other four samples we detected novel *ETV1* fusion genes, which result in predicted N-truncated ETV1 proteins. Novel fusion partners include *FOXP1*, an EST (*EST14*) and an endogenous retroviral sequence (*HERVK17*, identified in two samples). Like *TMPRSS2* (11), both *EST14* and *HERVK17* are androgen-regulated and prostate-specific.

Transient reporter assays with full length ETV1 and N-truncated ETV1 (dETV1) showed that these proteins possess different transcription regulation functions. However, QPCR analysis of prostate epithelial cells with stable overexpression of full length ETV1 or dETV1 indicated less pronounced differences in expression of candidate target genes. Biological assays showed no significant difference in migration and invasion properties between full length ETV1 and dETV1 expressing cells. However, full length ETV1 is capable of inducing anchorage-independent growth, whereas dETV1 is not. We propose a different role of dETV1 and full length ETV1 in prostate cancer.

MATERIALS AND METHODS

Tissue samples.

Primary prostate cancer samples were obtained by radical prostatectomy, regional lymph node metastases were collected during surgery, recurrences were obtained by trans-urethral resection (TURP). Samples were snap-frozen and stored in liquid nitrogen. Use of the samples for research purposes was approved by the Erasmus MC Medical Ethics Committee according to the Medical Research Involving Human Subjects Act (MEC-2004-261).

Hematoxilin/eosin (HE) stained tissue sections were histologically evaluated by two pathologists (Van der Kwast, Van Leenders). All samples contained at least 70% tumor cells.

Balb/c mouse prostate tissues were collected at different developmental stages (16.5 and 18.5 embryonal day and postnatal days 3, 9, 15 and 50).

RNA and DNA preparations.

RNA from clinical prostate cancer specimens was isolated from frozen tissue sections using RNA-Bee (Campro Scientific, Berlin, Germany). DNA was isolated from frozen sections using the DNeasy DNA extraction kit (Qiagen, Valencia, CA). RNAs from the prostate cancer cell lines LNCaP and DuCaP cultured in the presence of 10^{-9}M of the synthetic androgen R1881, or in the absence of hormone, from PNT2C2 cells overexpressing full length *ETV1* or *dETV1*, and from mouse prostates of different developmental stages were isolated using the RNeasy RNA extraction kit (Qiagen).

Breakpoint mapping.

Positions of fusion points were mapped by standard long-range PCR on 200 ng genomic DNA in the presence of 0.5 µM of each forward (fusion partner) and reverse (*ETV1*) primer with Taq polymerase and Proofstart DNA polymerase (Qiagen). For primers see Supplementary Table 1. PCR products were separated on a 1% agarose gel. Specific amplified fragments were isolated and sequenced in an ABI 3100 genetic analyzer (Applied Biosystems, Foster City, CA).

mRNA expression.

mRNA expression was analyzed by RT-PCR or by QPCR. cDNA was prepared with M-MLV reverse transcriptase (Invitrogen Life Technologies, Carlsbad, CA) and an oligo-dT12 primer. cDNA's of 16 different tissues were purchased from Clontech (Mountain View, CA).

RT-PCR products were analyzed over a 1.5% agarose gel. QPCR was done in Power SYBR Green PCR Master Mix (25 µl), containing 0.33 µM forward and reverse primer in an

ABI Prism 7700 Sequence Detection System (Applied Biosystems). Amplified products were quantified relative to Porphobilinogen Deaminase (*PBGD*; human RNAs), or Hypoxanthine guanine phosphoribosyl transferase 1 (*Hprt*; mouse RNAs) by the Standard curve method (Applied Biosystems). For primers see Supplementary Table 1.

RNA Ligase-Mediated Rapid Amplification of cDNA Ends (RLM-RACE).

5'- RLM-RACE was performed using the GeneRacer kit (Invitrogen). cDNA was amplified with Taq polymerase (Qiagen) using the Generacer 5'-primer and a gene-specific primer (ETV1 exon 6 Reverse). RACE PCR products were analyzed on a 1.5% agarose gel, bands were excised, purified and sequenced.

Interphase fluorescent *in situ* hybridization (FISH).

Interphase FISH was done on 5 µm frozen tissue sections as described previously (5). BAC clones RP11-79G16 (*ETV1*), RP11-154H23 (*FOXP1*), RP11-460G19 (*EST14*), RP11-1099M24 and RP11-1B5 (both flanking *HERVK17*) (see Fig. 2A) were purchased from BacPac Resources (Oakland, CA). Specificity of BACs was confirmed on metaphase chromosome spreads. BAC DNA clones were either Spectrum Orange or Spectrum Green labeled using a Nick Translation Reagent Kit (Vysis, Downers Grove, IL). Tissue sections were counterstained with DAPI in anti-fade solution (Vector Laboratories, Burlingame, CA). Images of the three fluorochromes were collected on an epifluorescence microscope (Leica DM, Rijswijk, The Netherlands) equipped with appropriate filter sets (Leica) and a CCD cooled camera (Photometrics, Tucson, AZ).

Construction of expression plasmids.

cDNAs of full length *ETV1* and the different *ETV1* fusion transcripts were PCR amplified and cloned into pGEMT-easy (Promega, Madison, WI). For primers see Supplementary Table 1. Inserts were sequence verified and subsequently cloned into the Not1 site in the pcDNA3 expression vector (Invitrogen). Similarly, full length *ETV1* cDNA and *dETV1* cDNA were integrated in the expression vector pWPXLd (provided by Didier Trono).

Reporter assays.

LNCaP prostate tumor cells and immortalized non-tumorigenic PNT2C2 prostate epithelial cells (12) (provided by Norman Maitland) were grown in DMEM supplemented with 5% FCS and antibiotics. Cells were cotransfected with full length *ETV1* or truncated *ETV1* expression constructs and the ETS reporter PALx8-TK-Luc (provided by Boh Wasylyk) essentially as described (13). Cells were harvested after 24h and luciferase activity was measured in a LUMAC 2500 Biocounter (Lumac, Landgraaf, The Netherlands).

Western blot analysis.

For Western blot analysis, LNCaP cells were transfected with pcDNA3-ETV1 or pcDNA3-dETV1 expression construct or empty vector. PNT2C2 cells were transfected with pWPXLd-ETV1, pWPXLd-dETV1 expression vectors or control pWPXLd-GFP. Cells were harvested after 48h. Western blot analysis was carried out using standard procedure with ER81 (C-terminal, Santa Cruz Biotechnology, Santa Cruz, CA) and β-actin loading control (Sigma, St Louis, MO) antibodies. Bands were visualized by chemiluminescence (Pierce, Rockford, IL).

Infection with *ETV1* lentivirus.

To obtain lentiviruses, 293T cells were cotransfected with pWPXLd-ETV1, pWPXLd-dETV1 or pWPXLd-GFP (control) and pPAX2 and pMD2.G (Didier Trono) using the calcium-phosphate precipitation method. PNT2C2 cells were infected with lentiviruses expressing either full length ETV1 or dETV1, or with control virus. Pools of infected cells were propagated and used in the biological assays as described below.

Migration and Invasion Assays.

Migration and invasion assays of PNT2C2-ETV1, PNT2C2-dETV1 and control PNT2C2-GFP cells ($1x10^5$ cells/well) were performed according to the instructions of the manufacturer of the trans-wells (Chemicon, Bellerica, MA). The migration assay was stopped after 24 h incubation; the invasion assay was terminated after 48 h.

Proliferation Assay.

Equal amounts of PNT2C2-ETV1, PNT2C2-dETV1 and control PNT2C2-GFP cells were seeded in T25 culture flasks. At day 0, 2, 4, 6 and 8, Thiazolyl blue tetrazolium bromide dissolved in PBS (MTT reagent; AppliChem, Chesire, CT) was added and after 4 h cells were harvested. Cells were suspended in DMSO-Sörensen buffer and OD 570nm was measured.

Soft-Agar Assay.

A bottom layer of 0.6% low melting agarose in normal culture medium was prepared in six-well culture plates. On top, a layer of 0.3% agarose containing $1x10^4$ cells (PNT2C2-ETV1, PNT2C2-dETV1 or control PNT2C2-GFP) was plated. At day 14 cells were stained with crystal violet and numbers of colonies in representative microscope fields were counted.

RESULTS

We investigated 84 clinical prostate cancer samples (49 primary tumors, 11 lymph node metastases and 24 recurrent tumors) for *ETV1* overexpression. In eight samples, divided over each clinical subgroup, *ETV1* overexpression was found (Fig. 1A), however, QPCR failed to detect *TMPRSS2-ETV1* fusion transcripts (Fig. 1B). QPCR with two *ETV1* primer sets, one amplifying an exon 1-2 fragment and a second set amplifying an exon 11-12 fragment showed in four samples (37, 89, 308, 247) an ~1:1 signal ratio, indicative for full length *ETV1* expression (Fig. 1C). However, in four other samples (32, 104, 116, 342) a high exon 11-12 to exon 1-2 ratio, indicative for gene fusion was detected. 5'-Rapid Amplification of cDNA Ends (5'-RACE), followed by sequencing revealed that the four tumor samples with equal signal intensities for the two amplified *ETV1* fragments, indeed overexpressed full length *ETV1*. Novel fusion genes were present in samples

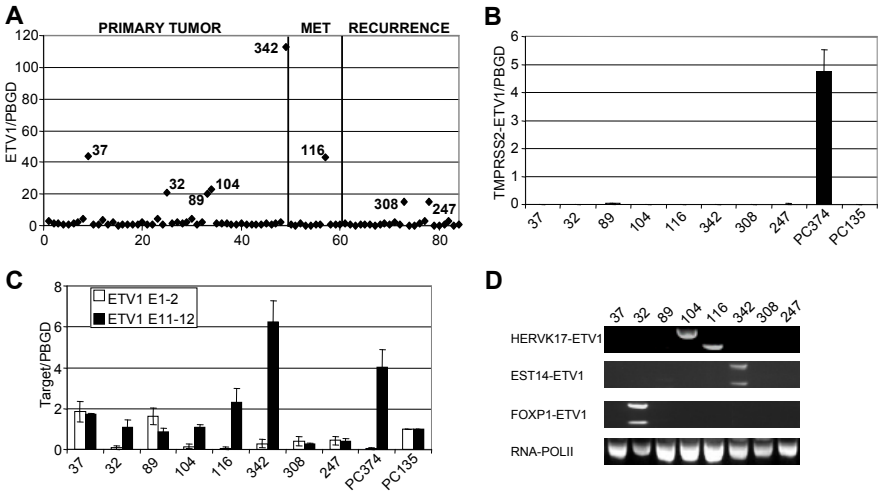

Figure 1 Expression of *ETV1* and characterization of *ETV1* fusion transcripts in clinical prostate cancer specimens. (A) Expression of *ETV1* compared to *PBGD* in clinical prostate cancer samples as assessed by QPCR. Overexpression of *ETV1* was detected in eight samples. MET: Regional Lymph Node Metastasis. (B) QPCR analysis for *TMPRSS2-ETV1* fusion gene expression in clinical samples with *ETV1* overexpression. Prostate cancer xenograft PC374 is the *TMPRSS2-ETV1* positive control, and xenograft PC135, overexpressing wild type *ETV1* is a negative control (5). Expression relative to *PBGD* plus Standard Deviations (SD) of a duplicate experiment is depicted. (C) Signal intensities of *ETV1* exon 1-2 QPCR compared to *ETV1* exon 11-12 QPCR. A reduced *ETV1* exon 1-2 to *ETV1* exon 11-12 ratio is indicative for *ETV1* gene fusion. Xenografts PC374 (*TMPRSS2-ETV1* fusion) and PC135 (wild type *ETV1*) are controls. Mean values plus SD of a duplicate experiment are presented. Samples 32, 104, 116, 342 and PC374 had a statistically significant higher exon 11-12 to exon 1-2 ratio ($p<0.05$, paired samples T-test). (D) Confirmation by RT-PCR with *ETV1* and fusion gene specific primers of the fusion transcripts found by 5'-RACE. *HERVK17-ETV1* specific fragments of different sizes are present in samples 104 and 116. Due to alternative splicing of *ETV1* exon 5, sample 342 shows two *EST14-ETV1* fragments, and sample 32 contains two *FOXP1-ETV1* fragments. RNA pol II amplification is shown as a loading control.

with high *ETV1* exon 11-12 to 1-2 ratio's. These novel *ETV1* fusion partners were *FOXP1*, a gene encoding a spliced EST (here denoted *EST14*), and an endogenous retroviral repeat sequence (denoted *HERVK17*; two samples). All fusion transcripts were confirmed by RT-PCR (Fig. 1D).

In contrast to *ERG* and *TMPRSS2*, *ETV1* and its three novel fusion partners all map to different chromosomes; *ETV1* is located on 7p, *FOXP1*, *EST14* and *HERVK17* on 3p, 14q and 17p, respectively (Fig. 2A). Chromosomal rearrangements in the four samples with fusion transcripts were confirmed by interphase fluorescent *in situ* hybridization (FISH) with specific BAC probes (Fig. 2A,B). *HERVK17* did not function as a retrotransposon (14), because in both sample 104 and 116 split signal FISH with flanking BACs showed separation of genomic fragments proximal and distal to one *HERVK17* copy (Fig. 2C). Their appropriate orientations (Fig. 2A) allow fusion of *ETV1* to *FOXP1* and *EST14* by standard recurrent chromosomal translocations. The *HERVK17-ETV1* fusion can most likely be explained by the integration of an *ETV1* genomic segment into the fusion chromosome (17p).

For fusions of *HERVK17* and *EST14* to *ETV1* we precisely mapped the fusion point by long range PCR followed by sequencing (Fig. 2D and Supplementary Fig.1). The breakpoints in *ETV1* are in intron 4 (104 and 342) and in intron 5 (116); the latter breakpoint is in an Alu repeat (Fig. 2D and Supplementary Fig. 1). The breakpoint in *EST14* is in its only intron, however, the genomic alteration turned out to be more complex (Fig. 2D). Additionally to the fusion to *ETV1*, a 117 kbp deletion from *EST14* to *C14orf25* (intron 4), removing *FOXA1*, was found. Both the interstitial deletion and the fusion to *ETV1* involve a LINE retroviral repeat, pointing to a role of this sequence in genomic instability (14, 15). *HERVK17* is a defective retroviral sequence (Fig. 2A, D). The two breakpoints in *HERVK17* mapped within 1 kbp from each other, both in a *HERVK* sequence flanking the 3'-*LTR*.

To increase our knowledge on properties and expression of fusion genes, we studied in detail the composition of fusion transcripts and the regulation of expression of the various *ETV1* fusion partners, including *TMPRSS2*. Figure 3A schematically summarizes the major *ETV1* fusion transcripts found by RT-PCR and sequencing. Note that part of the fusion transcripts lack *ETV1* exon 5, due to alternative splicing. Depending on the transcript, the ATG start codon is provided by *ETV1* exon 6 or by the fusion partner. In all cases the stop codon is in *ETV1* exon 12.

In the *FOXP1-ETV1* fusion transcript, part (154 bp) of *FOXP1* exon 11 is coupled to the *ETV1* sequence (Fig. 3A and Supplementary Fig. 2). The same part of this exon is present at the 5'-end of mRNA encoding the *FOXP1C* isoform (16). Unfortunately, the complex structure of the *FOXP1* locus, including several different first exons and extensive alternative splicing, prevented accurate detailed analyses of its expression.

EST14 maps between *MIPOL1* and *FOXA1* on 14q21.1. The *EST14-ETV1* fusion transcript contains part of the known exon 1 of this two exon EST (Unigene Hs.229997), linked to

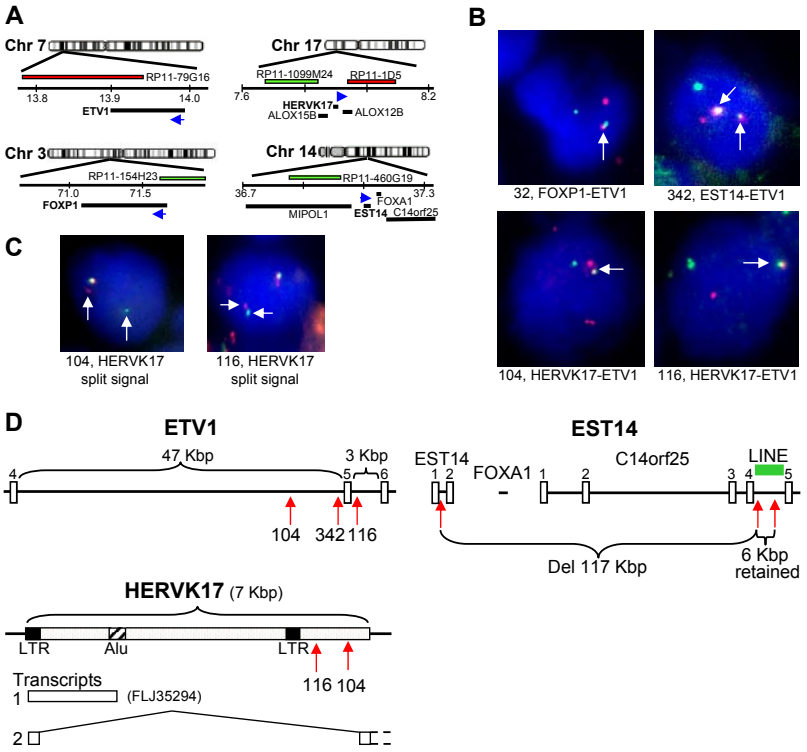

Figure 2 Characterization of *ETV1* fusion genes in clinical prostate cancer specimens. (A) Schematic representations of genomic regions of *ETV1*, *FOXP1*, *HERVK17* and *EST14* flanking genes on chromosomes 7, 3, 17 and 14, respectively. Distance from the top of chromosomes are indicated in Mbp. Directions of transcription are shown by blue arrowheads. BAC clones used in interphase FISH analysis are depicted in colors corresponding to FISH staining in b and c. (B) Interphase FISH on frozen tissue sections confirms *FOXP1-ETV1*, *EST14-ETV1* and *HERVK17-ETV1* gene fusions. *FOXP1-ETV1* fusion is indicated by a white arrow (upper left panel, sample 32); duplicated *EST14-ETV1* fusions are shown in the upper right panel (sample 342); *HERVK17-ETV1* fusions are depicted in the lower left and right panels. (C) Break apart FISH of *HERVK17* in samples 104 and 116. Both cases show separation of the yellow signal into red and green spots (white arrows). (D) Schematic representation of the breakpoints in *ETV1*, *EST14* and *HERVK17*. Exons in *ETV1, EST14* and *C14orf25*, and *HERVK17* are indicated by open boxes. Positions of breakpoints detected in fusion genes are indicated by red arrows. Speckled box indicates genomic *HERVK17* sequence. *LTR*s in *HERVK17* are shown in filled boxes. Breakpoints of the 117 Kbp deletion in *EST14/C140rf25* are in blue arrows. The LINE repeat in *C14orf25* containing two breakpoints is shown as a green bar. Breakpoints in *ETV1* are in large intron 4 (samples 104 and 342) or in small intron 5 (sample 116). Both breakpoints in defective *HERVK17* are in a *HERVK17* sequence flanking the 3′-*LTR*. Indicated below *HERVK17* are: Transcript 1 (present in databases as *FLJ35294*), and a novel spliced transcript detected in prostate cells, starting in the 5′-*LTR* (transcript 2).

ETV1 (Fig 3A and Supplementary Fig. 3). *EST14* is weakly androgen-regulated in LNCaP and DuCaP prostate cancer cells (Fig. 3B). *EST14* expression is highest in the prostate (Fig. 3C). Similarly, the flanking gene *FOXA1*, but not *MIPOL1*, is preferentially expressed in the prostate, indicating a common control region (Supplementary Fig. 4). Expression of the

mouse *Est14* ortholog (*mEst14*; Mm.387080) is also prostate-specific (data not shown). Like expression of *mTmprss2*, expression of *mEst14* increased during mouse prostate development, and is highest in the adult prostate (Fig. 3D).

HERVK17 maps between *ALOX15B* and *ALOX12B* on 17p13.1 (Fig. 2A). The 5'-*LTR* of this *HERV* has promoter activity, and several unspliced transcripts from this promoter are known (Hs.336697; transcript 1 in Fig. 2D). *HERVK17-ETV1* fusion transcripts are composed of 264 bp of the retroviral transcript linked to either *ETV1* exon 5 or 6 (Fig. 3A,

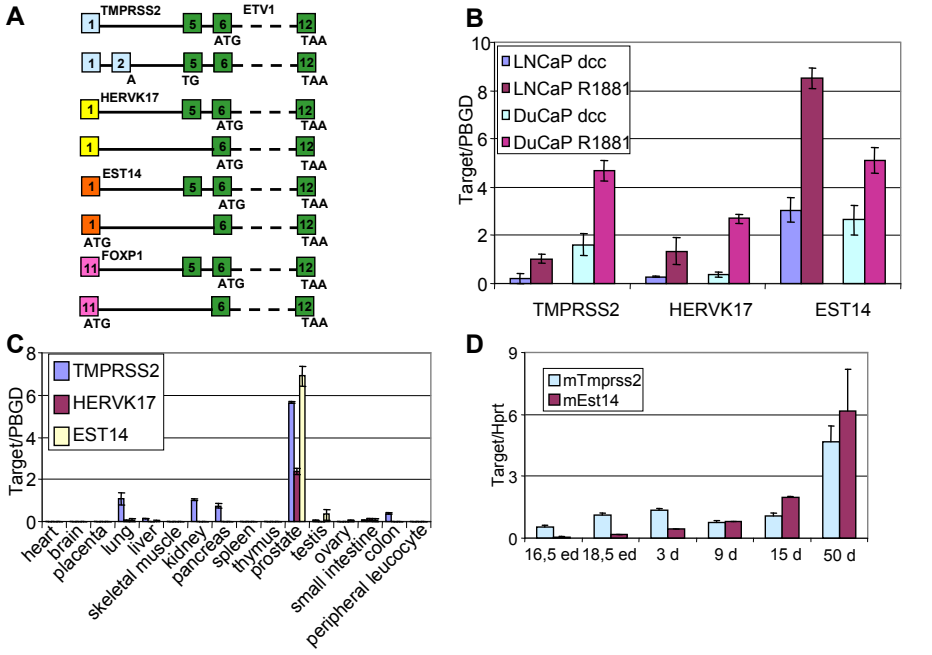

Figure 3 Properties of *ETV1* fusion transcripts and regulation of expression of *ETV1* fusion partners *HERVK17* and *EST14*. (A) Schematic representation of the different transcripts as detected by RT-PCR and sequencing. Exons are shown in colored boxes. ATG start codons and TAA stop codons of predicted long open reading frames are indicated in all transcripts. Almost all fusion transcripts are present in two forms, with or without *ETV1* exon 5. The *TMPRSS2-ETV1* fusion transcripts contain either exon 1 or exon 1 and 2 of *TMPRSS2* fused to *ETV1* exon 5 (5). Open reading frames start at an ATG in *ETV1* exon 6, or at an in frame ATG in the segment derived from the fusion partner. (B) Androgen-regulated *TMPRSS2*, *EST14* and *HERVK17* mRNA expression in androgen receptor positive LNCaP and DuCaP prostate cancer cells. LNCaP and DuCaP cells were grown in absence and presence of the synthetic androgen R1881 (10^{-9} M) for 24 h. mRNA expression was measured by QPCR and is presented relative to *PBGD* expression. Mean values and SD of a duplicate experiment are presented ($p<0.05$, paired samples T-test; except for *EST14* in LNCaP, p 0.07). (C) Tissue-specific expression of *EST14*, *HERVK17* and *TMPRSS2* mRNA. Transcript levels were assayed by QPCR on a cDNA panel from 16 different normal tissues and are presented relative to *PBGD* expression. Mean values plus SD of a duplicate experiment are depicted. *EST14*, *HERVK17* and *TMPRSS2* are higher expressed in prostate compared to all other tissues ($p<0.05$, paired samples T-test). (D) *mEst14* and *mTmprss2* mRNA expression during mouse prostate development. Time points of RNA isolation are indicated. QPCR data plus SD are presented relative to *Hprt* expression. Obviously, a mouse ortholog of *HERVK17* does not exist.

Supplementary Fig. 5). In wild type retroviruses the same splice donor site, as used here for *HERVK17-ETV1* transcripts, is used to remove the *gag* sequence, and produces mRNAs encoding *pol* and *env*. We detected by RT-PCR in prostate cells a novel *HERVK17* transcript, starting in the 5'-*LTR* (exon 1), followed by a second exon in the *HERV* sequence downstream of the 3'-*LTR* (transcript 2, Fig. 2D). The breakpoints are in the intron of this novel transcript. Expression of *HERVK17* is strongly androgen-regulated, and even more prostate-specific than *TMPRSS2* and *EST14* (Fig. 3B, C). *HERVK17* flanking *ALOX15B*, but not *ALOX12B*, is also preferentially expressed in the prostate (Supplementary Fig. 4).

Figures 3A and 4A summarize the different open reading frames and predicted translated proteins of the *ETV1* fusion transcripts. Wild type *ETV1* is composed of 12 exons, with the start codon in exon 1 and the stop in exon 12 (17). The DNA binding domain of ETV1, ETS domain, is located in the C-terminal half of the protein. In the N-terminal region, aa 42-73 is an acidic transactivation domain (TAD). In fusion transcripts, translation is predicted to start at an internal ATG in *ETV1* exon 6 (aa 132) or at an in frame ATG from the fusion partner followed by ETV1 fragments of different sizes (aa 80-477 or

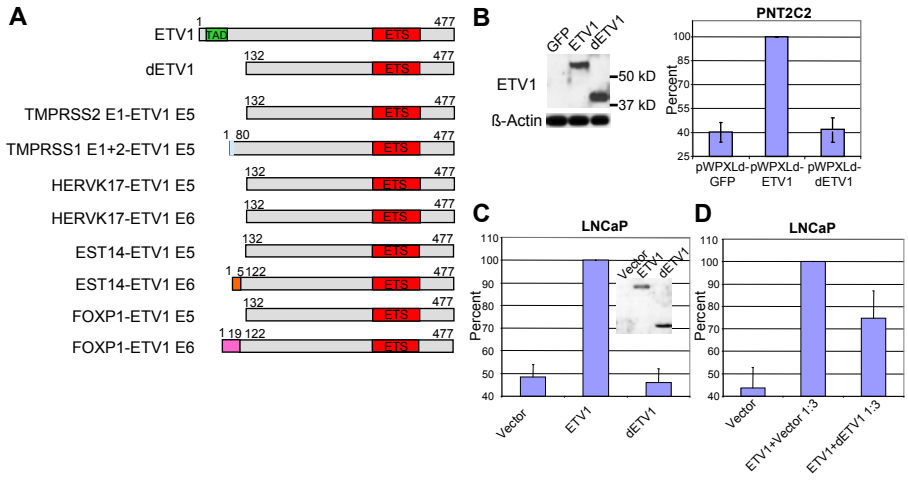

Figure 4 N-truncated ETV1 present in prostate cancer can inhibit transcription activation by full length ETV1. (A) Schematic representation of full length ETV1 and the predicted ETV1 truncated proteins and fusion proteins present in prostate cancer (compare Fig. 3a). TAD: Transactivation domain, ETS: ETS domain (DNA binding domain). (B) Transcription activation by ETV1 and dETV1. PNT2C2 cells were cotransfected with pWPXLd-ETV1, pWPXLd-dETV1 or pWPXLd-GFP and the PALx8-TKluc reporter construct. Luciferase activity relative to full length ETV1 is depicted. Expression of full length ETV1 and truncated ETV1 was visualized on Western blots. Actin is the loading control (C) LNCaP cells were cotransfected with pcDNA3-ETV1, pcDNA3-dETV1 or empty vector and the PALx8-TK-Luc reporter construct. The figure shows Luciferase activity relative to full length ETV1 activity. The insert shows a Western blot of full length ETV1 and N-truncated ETV1, expressed in transfected LNCaP cells. (D) dETV1 can decrease ETV1 activity. LNCaP cells were transfected with pcDNA3-ETV1 and pcDNA3-dETV1 in a 1:3 ratio, and the PALx8-TK-Luc reporter construct. Experiments were performed in quadruplicate. The figure shows the mean value plus Standard Error relative to ETV1 activity.

shorter) (Figs 3A and 4A). So, all fusion transcripts predict production of ETV1 lacking the N-terminal TAD.

To test the functional properties of ETV1 in prostate cells, expression constructs of full length ETV1 and truncated ETV1 (dETV1) were generated. The correct size of the proteins was verified by Western blotting in transiently transfected immortalized non-tumorigenic PNT2C2 prostate epithelial cells with low endogenous *ETV1* expression and in an LNCaP prostate cancer subline without *ETV1* expression (Fig. 4B,C). Transient transfection of PNT2C2 cells with ETV1 expression constructs and an ETS reporter gene clearly showed that full length ETV1 functioned as a transactivator, whereas dETV1 was not or hardly active (Fig. 4B) (see also (18)). Similar results were obtained in LNCaP cells (Fig. 4C) and in 3T3 cells (data not shown). Other dETV1 fusion transcripts (Fig. 3A) gave identical results in this assay (data not shown). In a competition assay, dETV1 diminished the activity of full length ETV1 (Fig. 4D). So, full length ETV1 and N-truncated ETV1 possess different transcription regulation functions, suggesting that prostate cancers overexpressing full length ETV1 and those expressing N-truncated ETV1 are not identical. dETV1 might compete with full length ETV1 for the ETS binding sites in the reporter construct or form heterodimers with full length ETV1, thereby weakening the much stronger transactivation of full length ETV1 (see also (18)).

Next we compared the properties of full length ETV1 and dETV1 in various *in vitro* biological assays. First, lentiviruses expressing either full length ETV1 or dETV1 were generated, and PNT2C2 cells were infected with these viruses. Pools of stable-transfected cells overexpressing ETV1 or dETV1, PNT2C2-ETV1 and PNT2C2-dETV1, respectively, were propagated and ETV1 protein expression was verified by Western blotting (Fig. 5A). PNT2C2 cells infected with a GFP-lentivirus were used as controls. Overexpression of full length ETV1 or truncated ETV1 had no effect on proliferation of PTN2C2 cells as determined in a standard MTT assay (data not shown). Compared to infected control cells (Fig. 5B, C) and uninfected parental cells (data not shown), both PTN2C2-ETV1 and PTN2C2-dETV1 showed increased migration and invasion (Fig. 5B, C). So, we did not observe a significant difference between both PNT2C2 sublines in these assays. However, overexpression of full length ETV1 strongly stimulated anchorage-independent growth of PTN2C2 cells, whereas dETV1 had no effect (Fig. 5D).

QPCR experiments were done to assess the expression of endogenous ETS target genes that are presumed to mediate migration, invasion or anchorage-independent growth (1-3). Genes studied encoded matrix metalloproteinases (*MMP*), *uPA*, *uPAR* and integrins (Fig. 6 and unpublished data). First, we confirmed overexpression of *ETV1* and *dETV1* mRNA in the PNT2C2-ETV1 and PNT2C2-dETV1 lines, respectively (Fig 6A). Next, we studied expression of members of the MMP family. Highest induction was detected for *MMP1* (Fig. 6B) and *MMP7* (data not shown). *MMP3* was also induced, but *MMP9* was not (data not shown). In none of the experiments a significant difference between

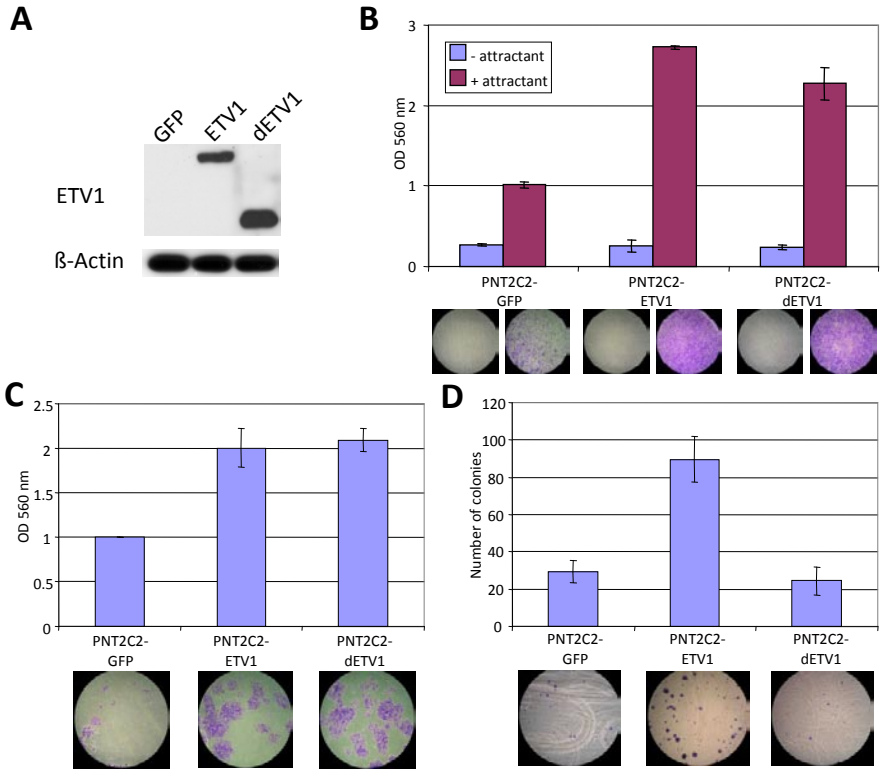

Figure 5 Biological properties of PNT2C2 epithelial prostate cells overexpressing full length ETV1 or N-truncated ETV1 (A) Western blot of PNT2C2 cells infected with lentiviruses expressing either full length ETV1, truncated ETV1 or GFP (control). Actin is shown as a loading control. (B) Migration of PNT2C2-ETV1 cells, PNT2C2-dETV1 cells and control PNT2C2-GFP cells was determined in a standard assay as described in Materials and Methods. 10% FCS was used as attractant. Pictures below the bar figure show migratory cells. (C) Invasion of PNT2C2-ETV1, PNT2C2-dETV1 and PNT2C2-GFP control cells. Experiments were done as described in Materials and Methods. Pictures of invaded cells are shown below the bar figure. (D) Anchorage-independent growth of PNT2C2-ETV1, PNT2C2-dETV1 and PNT2C2-GFP (control) cells, as assessed by a soft-agar assay. Representative pictures of colonies are shown. Bars show mean values plus SD of experiments in triplicate.

PNTC2-ETV1 and PNTC2-dETV1 was detected. Similarly, expression of *uPAR* was induced in both cell types, the effect of ETV1 and dETV1 on *uPA* expression was limited (Fig. 6C). *ITGAV* and *ITGB3* expression were induced in PTN2C2-ETV1 and PTN2C2-dETV1 cells (Fig. 6D). However, particularly the expression of *ITGB3* was strongly stimulated in PNT2C2-ETV1 cells, but much less in cells overexpressing dETV1. Neither ETV1 nor dETV1 affected the expression of *ITGB1* and *ITGB5* mRNA (data not shown).

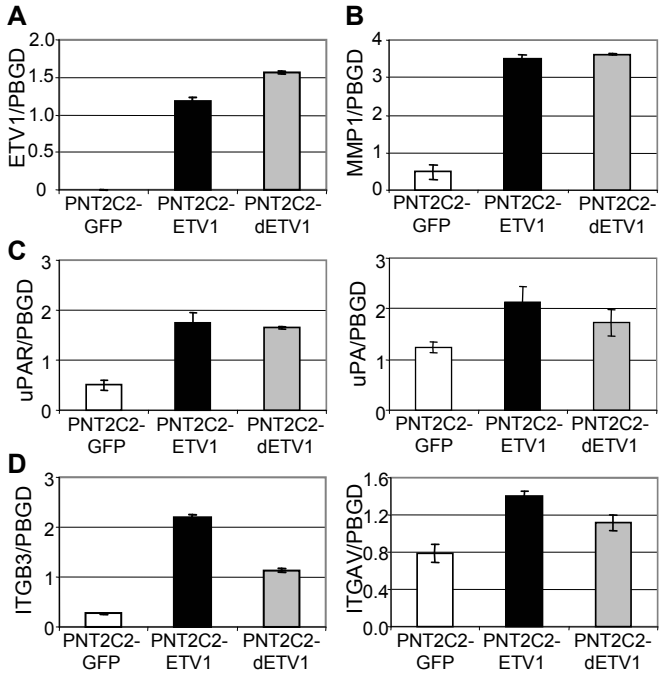

Figure 6 Expression of *ETV1* target genes. Expression of *ETV1* target genes was assayed by standard QPCR in PNT2C2-ETV1, PNT2C2-dETV1, and PNT2C2-GFP control cells. Bars represent mean QPCR data plus SD of duplicate experiments relative to *PBGD* expression. (A) *ETV1* and *dETV1* ($p<0.05$, paired samples T-test) (B) *MMP1* ($p< 0.05$) (C) *uPAR* ($p<0.05$) and *uPA* (D) *ITGB3* ($p<0.05$) and *ITGVA* .

DISCUSSION

The results presented in this study reveal several important aspects of prostate cancer. First, it is increasingly becoming clear that the prostate-specific and androgen-regulated expression of many *ETV1* fusion partners, as shown here for *EST14* and *HERVK17*, and previously for *TMPRSS2* (11) is an important determinant in fusion gene selection. In agreement with this observation, recently, for three other *ETV1* fusion partners, *SLC45A3*, *HERVK22q11.23* and *C15orf21*, preferential expression in prostate cancer has been documented (19). *SLC45A3* and *HERVK22q11.23* are upregulated by androgens, but *C15orf21* is downregulated. Similarly, prostate-specific and androgen-regulated *KLK2* and *CANT1* are novel *ETV4* fusion partners (20). An explanation for this remarkable selection would be a co-localization of prostate-specific genes in particular chromosome territories or prostate-specific transcription factories, favoring their selective interactions with partner oncogenes (21-23). Alternatively, it can be postulated that certain regions in the genome, involved in regulation of prostate-specific gene expression, are preferentially unstable at the shift in cellular programming from proliferation (DNA replication) to

differentiation (expression of prostate-specific genes) during development or at tissue renewal (24). These unstable regions could be targets for gene fusions and if fused to oncogenes, be involved in tumor development.

In the LNCaP prostate cancer cell line, the complete *ETV1* locus is translocated from chromosome 7 to chromosome 14, and integrated into the last intron of *MIPOL1* (19). Remarkably, *MIPOL1* is a directly flanking gene of *EST14*, which was found as *ETV1* fusion partner in this study. Also evidence exists that in the MDA-PC2A cell line, which shows a (7;14) chromosomal translocation, *ETV1* is linked to the same chromosome 14 region (19). Combined these findings indicate that chromosome 14 contains a small region that favours integrations and rearrangements of full length *ETV1* or *ETV1* fusion genes not only in cell lines, but also in clinical prostate cancer. It remains to be established whether or not overexpression of full length *ETV1* in other clinical samples is the result of genomic rearrangement of the complete *ETV1* locus. Elucidation of the chromatin structure of the chromosome 14 genomic region might shed more light on the mechanism of gene rearrangement in prostate cancer.

A further aspect of this study concerns the role of repeat sequences in prostate cancer. From the eight *ETV1* fusion partners ((8, 19), and this study) two are members of the *HERVK* subfamily of endogenous retroviral repeat sequences, *HERVK17* and *HERVK22q11.2*3. Previously, only one similar gene fusion has been reported, *HERVK19-FGFR1* in a myeloproliferative disorder (25). The finding of a role of common repeats, encoding apparently insignificant defective transcripts, in a frequent disease like prostate cancer urges to reconsider the role of such repeats in disease. In this regard, the *HERVK* retroviral subfamily is of particular interest, because many members possess active promoters (26, 27).

In transient reporter assays full length ETV1 is a strong transactivator, whereas dETV1 is not or hardly active (Fig. 4 and (18)). However, dETV1 can stimulate expression of endogenous target genes (Fig. 6). So, it seems that the acidic N-terminal region, which functions as a dominant TAD in transient transfections, is less important for activation of endogenous ETV1 target genes. This finding implies that ETV1 possesses additional TADs that remain to be defined in more detail. Moreover, it is of high interest to identify genes that are preferentially regulated by ETV1, and which are responsible for anchorage-independent growth of prostate cells overexpressing full length ETV1. In this regard, *ITGB3* is an attractive candidate.

The large family of ETS transcription factors displays a wide variety of biological activities, including cellular proliferation, apoptosis, differentiation, tissue remodeling, migration, invasion and angiogenesis (2, 28). The effects might depend on the cellular context and on the expression levels of the individual ETS factors. In most tumor types a role of overexpressed wild type ETS factors, including ETV1, has been described (2, 28). Although clinical prostate cancers can overexpress full length ETV1 (this study) most prostate cancers show overexpression of N-truncated ETS transcription regulators. It is

tempting to speculate that the combination of prostate-specificity and protein truncation is a unique prerequisite for initial oncogenic properties of a weaker, more specific ETS in prostate cancer.

Previously, the biological and molecular effects of overexpression of full length ETV1 in prostate cancer, as shown here, have not been studied. However, recently, the effects of dERG, as expressed from *TMPRSS2-ERG* (29, 30) and of dETV1, as expressed from *TMPRSS2-ETV1* (19), on cell growth, migration and invasion have been described. Some differences in proliferation and migration were found (this study and (29)), which might be due to differences between dERG and dETV1 or to the different cellular context. In agreement with our findings, in all studies the fusion proteins were able to stimulate invasion of the target cells. Like shown here, stimulation of invasive growth correlated with upregulation of genes known to stimulate tumor invasion and metastasis. The unique differences between full length ETV1 and dETV1 warrant further in depth investigation of the mechanism of prostate cancer growth.

We propose that overexpression of truncated ETV1 or other members of the ETS transcription family is most important in earlier stages of prostate cancer, whereas overexpression of wild type ETS transcription factors combined with downregulation of fusion gene expression comes into play at late stages of the disease (Supplementary Fig. 6). This hypothesis is supported by several observations. (i) The soft agar growth of PNT2C2-ETV1 cells indicates that full length ETV1 is more oncogenic than dETV1 (Fig. 5). (ii) In prostate cancer xenografts, overexpression of fusion genes is detected in hormone-dependent samples, whereas in hormone-independent xenografts fusion gene expression is shut off, and overexpression of a full length ETS factor is turned on (5). (iii) Our limited clinical data indicate that full length ETV1 is expressed in the two recurrent tumors (Fig 1A). Moreover, the two patients with overexpression of full length ETV1 in primary tumors had a remarkable short survival time (50 and 19 months), as compared to the three patients with primary tumors with ETV1 fusion gene expression (99, 141, >172 months, respectively), and with patients with *TMPRSS2-ERG* fusion or without gene fusion (data not shown). Obviously, these clinical data should be validated in a larger patient cohort.

In conclusion, the data presented in this study show that ETS genes play a pivotal role in prostate cancer, probably affecting many stages of tumor growth. Investigation of the mechanism of gene fusion and translocation, and the function of the various truncated and full length ETS transcription factors will contribute to a much broader knowledge of prostate tumor development and to the identification of novel therapeutic targets.

ACKNOWLEDGMENTS

The authors thank Arno van Leenders for pathology, Wilma Teubel for collection of clinical samples, Wytske van Weerden for xenograft tissues, Anieta Siewerts for RNA isolation, Boh Wasylyk for the ETS reporter, Norman Maitland for PNT2C2 cells, Didier Trono for cloning vectors and Erik Jan Dubbink for critical reading of the manuscript.

REFERENCES

1. Oikawa T. ETS transcription factors: possible targets for cancer therapy. Cancer Sci 2004;95:626-33.
2. Seth A, Watson DK. ETS transcription factors and their emerging roles in human cancer. Eur J Cancer 2005;41:2462-78.
3. Turner DP, Watson DK. ETS transcription factors: Oncogenes and tumor suppressor genes as therapeutic targets for prostate cancer. Expert Rev Anticancer Ther 2008;8:33-42.
4. Mitelman F, Johansson B, Mertens F. The impact of translocations and gene fusions on cancer causation. Nat Rev Cancer 2007;7:233-45.
5. Hermans KG, van Marion R, van Dekken H, Jenster G, van Weerden WM, Trapman J. TMPRSS2:ERG fusion by translocation or interstitial deletion is highly relevant in androgen-dependent prostate cancer, but is bypassed in late-stage androgen receptor-negative prostate cancer. Cancer Res 2006;66:10658-63.
6. Liu W, Ewing CM, Chang BL, *et al.* Multiple genomic alterations on 21q22 predict various TMPRSS2/ERG fusion transcripts in human prostate cancers. Genes Chromosomes Cancer 2007;46:972-80.
7. Laxman B, Tomlins SA, Mehra R, *et al.* Noninvasive detection of TMPRSS2:ERG fusion transcripts in the urine of men with prostate cancer. Neoplasia 2006;8:885-8.
8. Tomlins SA, Rhodes DR, Perner S, *et al.* Recurrent fusion of TMPRSS2 and ETS transcription factor genes in prostate cancer. Science 2005;310:644-8.
9. Wang J, Cai Y, Ren C, Ittmann M. Expression of variant TMPRSS2/ERG fusion messenger RNAs is associated with aggressive prostate cancer. Cancer Res 2006;66:8347-51.
10. Helgeson BE, Tomlins SA, Shah N, *et al.* Characterization of TMPRSS2:ETV5 and SLC45A3:ETV5 gene fusions in prostate cancer. Cancer Res 2008;68:73-80.
11. Lin B, Ferguson C, White JT, *et al.* Prostate-localized and androgen-regulated expression of the membrane-bound serine protease TMPRSS2. Cancer Res 1999;59:4180-4.
12. Berthon P, Cussenot O, Hopwood L, Le Duc A, Maitland NJ. Functional expression of SV40 in normal human prostatic epithelial and fibroblastic cells: Differentiation pattern of non-tumorigenic cell lines. Int J Cancer 1995;6:333-43.
13. Cleutjens KB, van der Korput HA, van Eekelen CC, van Rooij HC, Faber PW, Trapman J. An androgen response element in a far upstream enhancer region is essential for high, androgen-regulated activity of the prostate-specific antigen promoter. Mol Endocrinol 1997;11:148-61.
14. van de Lagemaat LN, Landry JR, Mager DL, Medstrand P. Transposable elements in mammals promote regulatory variation and diversification of genes with specialized functions. Trends Genet 2003;19:530-6.
15. Gasior SL, Wakeman TP, Xu B, Deininger PL. The human LINE-1 retrotransposon creates DNA double-strand breaks. J Mol Biol 2006;357:1383-93.
16. Wang B, Lin D, Li C, Tucker P. Multiple domains define the expression and regulatory properties of Foxp1 forkhead transcriptional repressors. J Biol Chem 2003;278:24259-68.
17. Monte D, Coutte L, Baert JL, Angeli I, Stehelin D, de Launoit Y. Molecular characterization of the ets-related human transcription factor ER81. Oncogene 1995;11:771-9.
18. Bosc DG, Janknecht R. Regulation of Her2/neu promoter activity by the ETS transcription factor, ER81. J Cell Biochem 2002;86:174-83.
19. Tomlins SA, Laxman B, Dhanasekaran SM, *et al.* Distinct classes of chromosomal rearrangements create oncogenic ETS gene fusions in prostate cancer. Nature 2007;448:595-9.

20. Hermans KG, Bressers AA, van der Korput HA, Dits NF, Jenster G, Trapman J. Two unique novel prostate-specific and androgen-regulated fusion partners of ETV4 in prostate cancer. Cancer Res 2008;68:3094-8.
21. Branco MR, Pombo A. Intermingling of chromosome territories in interphase suggests role in translocations and transcription-dependent associations. PLoS Biol 2006;4:780-8.
22. Meaburn KJ, Misteli T, Soutoglou E. Spatial genome organization in the formation of chromosomal translocations. Semin Cancer Biol 2007;17:80-90.
23. Osborne CS, Chakalova L, Mitchell JA, *et al.* Myc dynamically and preferentially relocates to a transcription factory occupied by Igh. PLoS Biol 2007;5:1763-72.
24. Zink D. The temporal program of DNA replication: new insights into old questions. Chromosoma 2006;115:273-87.
25. Guasch G, Popovici C, Mugneret F, *et al.* Endogenous retroviral sequence is fused to FGFR1 kinase in the 8p12 stem-cell myeloproliferative disorder with t(8;19)(p12;q13.3). Blood 2003;101:286-8.
26. Buzdin A, Kovalskaya-Alexandrova E, Gogvadze E, Sverdlov E. At least 50% of human-specific HERV-K (HML-2) long terminal repeats serve in vivo as active promoters for host nonrepetitive DNA transcription. J Virol 2006;80:10752-62.
27. Stauffer Y, Theiler G, Sperisen P, Lebedev Y, Jongeneel CV. Digital expression profiles of human endogenous retroviral families in normal and cancerous tissues. Cancer Immun 2004;4:2.
28. Kurpios NA, Sabolic NA, Shepherd TG, Fidalgo GM, Hassell JA. Function of PEA3 Ets transcription factors in mammary gland development and oncogenesis. J Mammary Gland Biol Neoplasia 2003;8:177-90.
29. Klezovitch O, Risk M, Coleman I, *et al.* A causal role for ERG in neoplastic transformation of prostate epithelium. Proc Natl Acad Sci U S A 2008;105:2105-10.
30. Tomlins SA, Laxman B, Varambally S, *et al.* Role of the TMPRSS2-ERG gene fusion in prostate cancer. Neoplasia 2008;10:177-88.

SUPPLEMENTARY INFORMATION

Supplementary Table S1. Primer sequences

	Forward (5'->3')	Reverse (5'->3')
RT-PCR, QPCR, RACE		
PBGD	CATGTCTGGTAACGGCAATG	GTACGAGGCTTTCAATGTTG
ETV1 E11-12	CATACCAACGGCGAGGATCA	TGGAGAAAAGGGCTTCTGGA
ETV1 E1-2	AGCTGAGATTTGCGAAGAGC	CTGCTCATCATTGTCAGGTAC
ETV1 E6		GGTTTCGGTGTATGAGTTGA
HERVK17	TGAAGTTACACCTGAGCGTG	
HERVK17 RT	CAGACAAACCTGGAGATGAG	AGGCTCCAAGCTACATTGCT
Chr 17 tr 2	TGAAGTTACACCTGAGCGTG	TCGCCATAAGCAACTTCCAC
EST14	AGAGGAGAAAGAGTGCTCTA	
EST14 RT	TCTCCAGGCTTTTTCATCTC	AGAGGAGAAAGAGTGCTCTA
FOXP1 E11	TCTGACCACGACATGTGTCT	
ALOX15B RT	CTCTCTGGTTGCTGAGCAAG	CTGGGATTTAGATGGAGACG

ALOX12B RT	GGAATCCACCGATTCAGACT	AGTGAATGTCCGGGAAGTGT
FOXA1 RT	ATGGAAGGGCATGAAACCAG	CATAGGACATGTTGAAGGAC
MIPOL1 RT	AGGAACTGGCTACTCAACTG	CAGATCACTGTCCTCATGGT
MMP1 RT	CTGCTTACGAATTTGCCGAC	GTTCTAGGGAAGCCAAAGGA
MMP7 RT	CCTCTGATCCTAATGCAGTG	GAATGGATGTTCTGCCTGAAG
MMP3 RT	GCTGAAGACTTTCCAGGGAT	TGGGTCAAACTCCAACTGTG
MMP9 RT	TTCGACGTGAAGGCGCAGAT	TCCACCTGGTTCAACTCACT
uPAR RT	GAAGAACAGTGCCTGGATGT	CGGCAGATTTTCAAGCTCCA
uPA RT	CACTACTACGGCTCTGAAGT	CCAGCTCACAATTCCAGTCA
ITGB3 RT	CTGGAAACTCCTCATCACCA	AGGTAGACGTGGCCTCTTTA
ITGAV RT	AGGATTGTTGCTACTGGCTG	CTTGTTCTTCTTGAGGTGGC
ITGB5 RT	TGGAAGCTGCTTGTCACCAT	CGTGGAGATAGGCTTTCTGT
ITGB1 RT	CATGACAGAAGGGAGTTTGC	CACAGTTGTTACGGCACTAT

Breakpoint mapping

ETV1 I4AR		AGCCAATTGAAGGGCAGGAG
ETV1 I4BR		GCATGATCCATGCTAGTGGA
ETV1 I4CR		ACAGCTTTGGTTGAGGGTAG
ETV1 I4C1R		CACACCTGGCTGAGAATATG
ETV1 I4DR		GACCTCAATTAGTGCTCAGT
ETV1 I4ER		CTGAAGGACTTCTGGTAAGC
ETV1 I4FR		ATATGCCTGTCATGGCTTTG
ETV1 I4GR		GTAACTAGGTAGCAGTGGTG
ETV1 I4HR		ACCACGGTTACCTGGTTATC
ETV1 I4IR		GACCCACAAATTAGGGTGTC
ETV1 I4JR		GGCTGTTGTGTTCATGAGGA
ETV1 I4KR		CATAAGCTCCATGATAGCAG
ETV1 I4LR		TGGGTCATCAATGCCTTGGC
ETV1 I4MR		TGGGACTTATGCACACTCCT
ETV1 I4NR		GGCTGAGAAAGACTTCAGTG
ETV1 I4OR		TGGTCAGTAGCAGCAGTTAG
ETV1 I5R		CTGTATAGCGATGGAAGTAC
EST14 E1F	GTTACTCAGTTCTTTACCCT	
EST14 I1AF	GAGCTTTACAGGTGATGAGA	
HERVK17 F	TGAAGTTACACCTGAGCGTG	

Mouse QPCR

Hprt	TCCCTGGTTAAGCAGTACAG	TTCCAGTTTCACTAATGACAC
mTmprss2	GAATGGGATCTGGTGGCTGA	GGGAGCACAGTCAAACAAGT
mEst14	ACCATCAGTGGACGGCATCA	CTTCTGCGGTAACAATGTAGA

ETV1 Expression constructs

ETV1	AGATTTGCGAAGAGCAGCAG	CCCTGCTTGACTGTCACTTG
dETV1	ATCAGAAGCCACAAGTGGGA	CCCTGCTTGACTGTCACTTG
HERVK17-ETV1	GCCTTTGCAATCTCCACGTTG	CCCTGCTTGACTGTCACTTG
EST14-ETV1	GATAGCACATCAGTGAAGAC	CCCTGCTTGACTGTCACTTG
FOXP1-ETV1	TCTGCACCTTCCAAGACCTC	CCCTGCTTGACTGTCACTTG

Breakpoints *HERVK17-ETV1*:

Fusion point

116: ...AGTATTACTTGGGGGAGGGG ↓ GCCTGGGCAACAAGAGCGAG…

CHR 17 (HERV-K) ETV1 intron 5 (Alu Sp)

Fusion point

104: …AGTTAGAAGATTTGAATCAA ↓ TGTTTTCAATGTAAGGATAC…

CHR17 (HERV-K) ETV1 intron 4

Breakpoint *EST14-ETV1*:

117kb deletion

342: …TAAAAAATATAGACAAGAAT ↓ CTATGCATTGATCTTGGACA…

EST14 intron 1 (L3) C14orf25 intron 4

Fusion point to ETV1

342: …GAAAAAGAAAACTACAGGCC ↓ AATGTGAATGACCTTTTTAA…

C14orf25 intron 4 (L1MA2) ETV1 intron 4

Figure S1. Sequences of genomic fusion points. Fusion points were mapped by long range PCR and sequencing in samples 116,104 and 342. The sequence of the fusionpoint formed by the 117 kbp deletion (sample 342) was determined by the same approach. PCR primers are given in Supplementary Table 1.

FOXP1 exon 11

accc ccct aaca ctag gctt tgtt tact gact cttt gatt taat tgct gttt gaag agga cgga atta gctg ttaa ttga ttta atta tcca attt gttt gttt cagG CATG ATTC CAAC AGAA CTGC AGCA GCTC TGGA AAGA AGTG ACAA GTGC TCAT ACTG CAGA AGAA ACCA CAGG CAAC AATC ACAG CAGT TTGG ATCT GACC ACGA CATG TGTC TCCT CCTC TGCA CCTT CCAA GACC TCCT TAAT AATG AACC CACA TGCC TCTA CCAA TGGA CAGC TCTC AGTC CACA CTCC CAAA AGGG AAAG gtag gaac cagc cact gaga tggg tcca aaac tgcc ttta acat gaga gggg tggg tggc cctg cctc gtca tatc tcag tgat ccct aatt ggat ccat gtga cttg aatg tgca tata atta ctga ggaa tgta tt

Figure S2. Sequence of the *FOXP1* exon in the *FOXP1-ETV1* fusion gene.

Sequence of *FOXP1* exon 11 is shown in capitals.

In grey: sequence present in *FOXP1C* transcripts and in *FOXP1-ETV1* fusion transcripts.

Italic: splice acceptor/donor site.

ATG translation initiation codon is underlined.

EST14 exon 1 (BF673302)

ctaa cagc ctgt agat ctag attt tttt ctct ctaa aaca tctt catt gacc atga ccat taat attt actc ataa atgg attt gtac acag gctc aacc ATAG CACA TCAG TGAA GACA AAAA GAGT TGTT ACTC AGTT CTTT ACCC TAGA ATAA ATCA AATC AACA AATA TTTA TTGA ATGT CTAC TATG TGCA AATA GCCC TGGA CTGT TCAG CTTT TAAA AGCC ATCC AACT TTTC ACAT TAAC AAAT CAAA GCAT TATT ATTT CAAG CATT GCAG AAGC TGCT TCCA TGTC CTTA AGGT GACA AAGC ATAT GAGG ACTT TGCA AGTA CTTG GAGT AAAG GAAG AGAA GAGA ATTC ACAG AGTG AAAA GAGG AGAA AGAG TGCT CTAA AATA TCAC CAAT GGAC TGCA ACAT gtat gtat gtac acat aagt ttat gtgt atgt gtct atat tatg tatg tgtt tata tatg tgta taca taca atga gaag aatg agtg aatt tgga gaga aata gcct tcgt taaa gtac aata ggaa tagg ca

Figure S3. Sequence of the *EST14* exon in the *EST14-ETV1* fusion gene.

Published sequence of *EST14* exon 1 is shown in capitals (Unigene Hs.229997).

In grey: *EST14* exon 1 sequence present in *EST14-ETV1* fusion transcripts.

TATA box is underlined.

Italic: splice donor site.

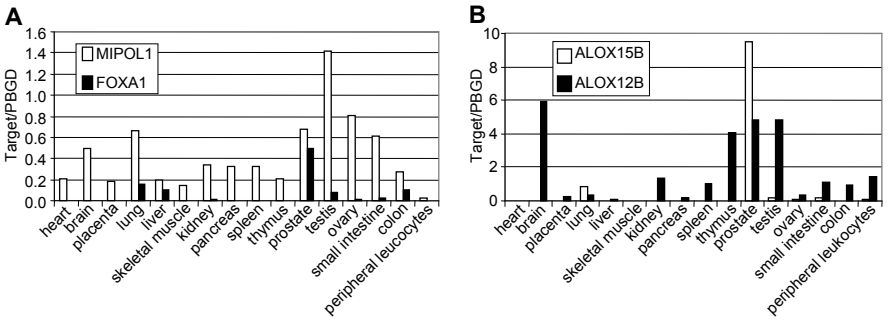

Figure S4. Tissue-specific expression of *EST14* and *HERVK17* flanking genes.

(A) Expression of *MIPOL1* and *FOXA1*, which flank *EST14* and (B) expression of *ALOX15B* and *ALOX12B*, flanking *HERVK17* as assessed by QPCR on a cDNA panel from 16 different normal tissues. QPCR data are presented relative to PBGD expression.

HERVK17

ctat gctc accc aatg atca cctc acca tcag ccca ccct cagc ctat agga tcaa agga actg tact caat aaat atca gtgg aacc caga gctc ctgg CCTT TGCA ATCT CCAC GTTG CGAT GGAT CCTT GGAC CCAC TTTT GTTA ACTC TTAA ACTT TGTG TCTT TGTC TTTA TTTC TTTT CTCA TTCC CTCG TCTC CACC GGGA AGGG GAGA GCCT GCGG GTGG TGTA TCAG GCAG GTTC CCCT ACAT CTTT GGCA CCCA ACAC GGTC TCCT TGAA CCCA GGTG AAGT TACA CCTG AGCG TGGT CGTT GTGA AGAA CGGT CTGT CCAG GAAC TCCC GAGA ACGT GTGG TCGG CCTT GCGG TAAG CTTG TGCA CTCG GAGC ATTC CAGG GACA CCAT GGGA CAAT CCAA AAGT AAAC ATTC TGCA TATT TACA TTTT ATTA AGCT CCTC TTAA AGAG GGCA GGAA TTAA GGCT AGCA CAGA AAAT TTGA TTAC TCTG TTTC CAAC AGTA GAGC AATA TCGT CCTT GGTT TCCT GAAC ATGG TACC ATGG ACTT CAAA GATT GGGA ACAG GTGG GAAT TGCC TTAA AACA AGTT TGTA……

Figure S5. *HERVK17* sequence present in *HERVK17-ETV1* fusion transcripts.

The 5'-region of *FLJ35294* is depicted in capitals.

In grey: exon 1 of *HERVK17* present in *HERVK17-ETV1* fusion transcripts.

TATA box is underlined.

Italic: splice donor site.

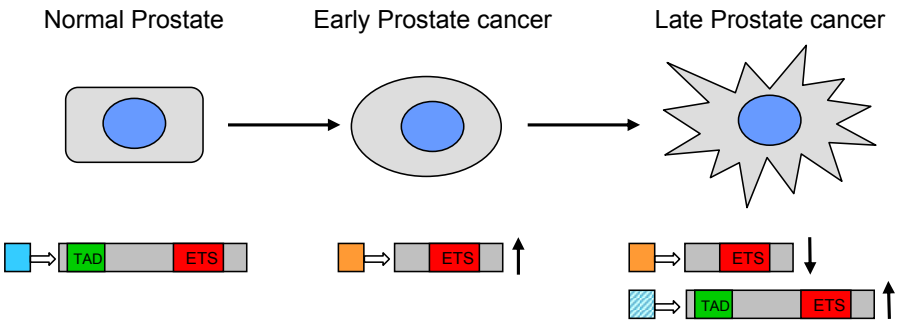

Figure S6. Model of sequential expression of ETS genes in prostate cancer.
In prostate cancer, first expression of prostate-specific truncated ETS is necessary for ncogenesis. In late stage prostate cancer fusion gene expression is down regulated. Instead, overexpression of wild type ETS is favored. Blue box indicates own promoter, orange box indicates prostate-specific promoter, hatched blue box indicates either own promoter and/or other promoter

Chapter 8

General Discussion

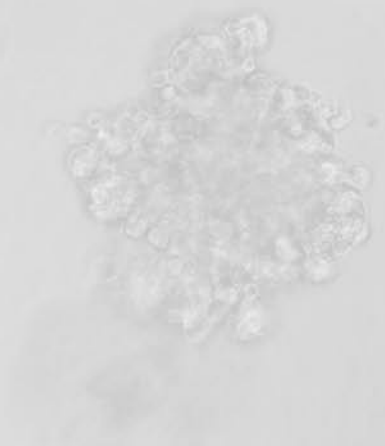

GENERAL DISCUSSION

Prostate cancer is the most frequently diagnosed tumor in men in countries with a Western lifestyle (1). Although our knowledge of molecular mechanisms underlying prostate cancer development and progression has rapidly increased over the past few years, there are still many questions that remain to be addressed. A better understanding of the molecular mechanisms is essential for the development of targeted therapies and for predicting the clinical course of the disease. The aim of this thesis was to unravel the major genetic alterations in prostate cancer. The main focus of this discussion will be on the recently identified ETS fusion genes in prostate cancer, which are the most frequent genetic alteration detected to date.

GENOME-WIDE STUDIES FOR IDENTIFICATION OF CANDIDATE ONCOGENES AND TUMOUR SUPPRESSOR GENES

Genome-wide array CGH studies can be used as a basis for the search of novel tumour suppressor genes and oncogenes in cancer (2, 3). Depending on the platform used, BAC, cDNA or oligonucleotide arrays, and on the distance between the probes, a high resolution can be reached. Nowadays, SNP arrays are frequently used to obtain detailed information on genetic alterations. An advantage of SNP arrays over BAC and cDNA arrays is that SNP arrays also provide allelotypic information. However, this information is not used to identify the classical tumour suppressor genes or oncogenes in sporadic cancer.

In our search for novel tumour suppressor genes we used 1 Mbp spaced genome-wide BAC arrays to identify genomic alterations in human prostate cancer xenografts. Xenografts are powerful tools to investigate genetic alterations. They lack contamination of normal cells and are available in unlimited quantities. This simplifies the identification of high-level amplifications and homozygous deletions. Moreover, they represent different stages of clinical disease, ranging from primary tumours to distant metastases and locally recurrent disease, and from androgen-dependent to androgen-independent tumours. However, one has to keep in mind that these xenografts may be biased in that they probably represent the more aggressive tumours and that they may have acquired additional genetic alterations during propagation on immuno-deficient mice.

Genomic alterations were characterized in eleven human prostate cancer xenografts (Chapters 2, 3 and 4) and eleven homozygous deletions were identified, one on chromosome 2q, one on 8p, three involving the tumour suppressor gene *PTEN* on 10q, two on 13q, two on 16q and two on 17p. The two homozygous deletions on 17p were further characterized. This led to the discovery of *N-COR* as a novel tumour suppressor gene

in prostate cancer. However, with the arrays used several homozygous deletions were missed: a small previously identified homozygous deletion of exon 5 of *PTEN* (4), one homozygous deletion on 8p involving *WRN* (5), and two homozygous deletions on 17p, one involving *MKK4* and the other involving *N-COR* (Chapter 2). All these homozygous deleted regions are located between two BACs. Use of a tilling path genome-wide BAC array or a high-density oligo array would have detected most of these alterations. The question remains how many more homozygous deleted regions were missed and whether they contain genes that are relevant in prostate cancer.

Very recently, genomic DNA from ten xenografts was investigated by oligonucleotide arrays containing over 1 million data points. Preliminary results showed overall the same genomic alterations as detected on the BAC arrays. However, on oligonucleotide arrays many additional small regions of (homozygous) loss and a few additional regions of gain were detected. The question can be raised whether all these alterations are relevant in tumorigenesis or whether they are an insignificant consequence of acquired genomic instability. Parts of these alterations were detected in multiple samples, including normal DNA. Most likely, many of the small regions of gain or loss are structural natural occurring copy number variations (6, 7). It remains to be investigated whether these structural variants contribute to disease, including cancer.

The homozygous deletions missed on the BAC arrays were detected on the oligonucleotide arrays. Also, in the DNA of the xenografts five larger specific homozygous deletions were detected, located on chromosome arms 4q, 5q, 10q, 13q (Figure 1), and 17q. The homozygous deleted region detected in xenograft PC339 on 4q (~310 kbp) contained seven genes, but none of these genes has been described as candidate tumour suppressor gene. A homozygous deleted region in DNA of xenograft PC339 was located on 5q (~300 kbp), *FBXL17* maps in this region. Whether this gene is a potential tumour suppressor gene needs to be established. In xenograft PC374 a homozygous deletion of ~100 kbp was detected on 10q. There are no known genes located in this fragment, however, this region is located between *BRWD2* and *FGFR2*, and it is a cancer-

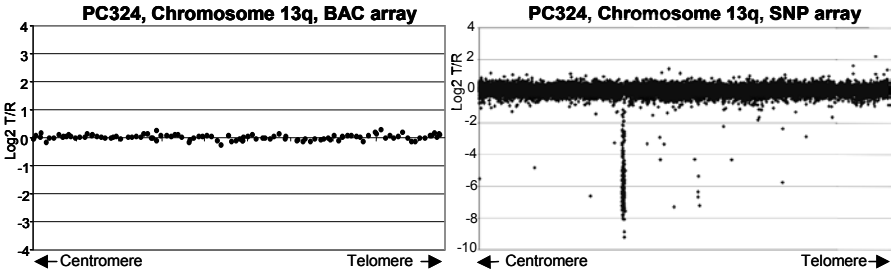

Figure 1. Comparison of the BAC array and SNP array data of chromosome 13q of DNA from xenograft PC324.

related recombination hot spot (8). On 13q a homozygous deletion of ~630 kbp in the DNA of xenograft PC324 was detected (Figure 1). In this region seven genes are located. Four of these, *ARL11*, *KPNA3*, *C13ORF1* and *KNCRG*, have been described as candidate tumour suppressor genes (9-12). In DNA of xenograft PC133 a ~130 kbp homozygous deleted region was detected on 17q. In this region kinase suppressor of RAS (*KSR1*) is located as candidate tumour suppressor gene (13). The most promising regions should be subjected to further study to identify true genes involved in prostate cancer.

In conclusion, oligonucleotide arrays detected many small additional alterations compared to the BAC arrays. However, many of these alterations were detected both in tumour and in normal DNA. Part of the homozygous deletions detected, overlapped with already known homozygous deletions, however, others were new. All new homozygous deletions were unique, which might indicate that genes that map in these fragments are of importance in a low percentage of tumours. Thus, high-density oligonucleotide arrays, although more sensitive, seem not essential in the search for frequently inactivated tumour suppressor genes. However, sensitive oligonucleotide arrays might be helpful in specific mapping of chromosomal breakpoints (see below).

SEARCH FOR NEW FUSION GENES IN CANCER

The first chromosomal translocation identified in human cancer was t(9;22), the Philadelphia chromosome (14). This translocation was discovered by classical cytogenetic techniques and led to the identification of the *BCR-ABL1* fusion gene in the early 1980's. Following this finding, many more fusion genes have been discovered, mainly in malignant haematological disorders and in childhood sarcomas (15), using molecular cytogenetic techniques as a tool to pinpoint gene rearrangements. In epithelial tumours fusion genes have hardly been detected, although many chromosomal aberrations have been identified. In a few rare subtype epithelial tumours fusion genes were described, including *ETV6-NTRK3* in secretory breast cancer, *PAX-PPARG* in follicular thyroid carcinoma, and *RET/NTRK1* rearrangements in papillary thyroid carcinomas (15). These fusion genes have been identified by cytogenetic techniques or by overexpression and subsequent gene walking.

As described in Chapter 2, we detected a unique situation of loss of a small region, encompassing four BACs on chromosome 21q in three human prostate cancer xenografts. The resolution of the BAC arrays did not allow precise mapping of the breakpoints. However, on the oligonucleotide arrays we could pinpoint the breakpoints to *ERG* and *TMPRSS2*, resulting in an interstitial deleting and the forming of the *TMPRSS2-ERG* fusion gene. The detection of this fusion gene by array CGH was only possible because of

the location of the fusion partners within 3 Mbp on the same chromosome. For direct detection of gene fusions array CGH is not suitable, but high-density oligo arrays can in some cases, where parts of chromosomes are gained or lost following chromosomal rearrangement, more precisely map chromosomal breakpoints. If such a breakpoint is in a gene, it might indicate the forming of a fusion gene. However, the partner, if there is one, remains to be identified. Also note that the initial discovery of the *TMPRSS2-ERG* fusion gene made use of a bio-informatics approach, denoted cancer outlier profile analysis (COPA) (16), searching for genes with marked overexpression in a subset of samples.

Recently, a functional approach resulted in the identification of a fusion gene in an epithelial cancer, making use of a retroviral cDNA library from a lung adenocarcinoma specimen. Infection of mouse 3T3 cells by the retroviral library led to the formation of many transformed foci (17). Sequencing of recovered cDNAs resulted in the identification of the *EML4-ALK* fusion transcript. *EML4-ALK* gene fusion turned out to be present in ~5% of non-small cell lung cancers (18, 19). Recently, genome-wide massive parallel paired-end sequencing has been developed as technological tool to characterize rearrangements in genomic DNA from healthy individuals and in cancer genomes (20, 21). Ruan *et al* used cDNA of cancer cell lines as template for massive parallel paired-end sequencing, denoted paired-end diTag analysis (22), allowing a comprehensive characterization of (cancer) transcriptomes, which is able to identify novel fusion transcripts. These novel genome-wide techniques seem very promising in the identification of previously unknown fusion genes, (fusion) transcripts and other rearrangements that underlie cancer development and progression.

TMPRSS2-ERG GENE FUSION AND PROGNOSIS OF CLINICAL PROSTATE CANCER

Several groups have attempted to correlate *TMPRSS2-ERG* fusion with clinical status of prostate cancer and tried to find out if *TMPRSS2-ERG* fusion is of prognostic value. This has resulted in confusing outcomes: no association with prognosis, association with good prognosis or with poor prognosis. These observations suggest that the role of *TMPRSS2-ERG* in prostate cancer is complex. However, it is not easy to compare the different studies because 1) Different techniques were used to determine *TMPRSS2-ERG* fusion status, i.e. FISH, RT-PCR or QPCR. 2) The origins of tumour materials, biopsies, radical prostatectomy samples, lymph node metastasis or transurethral resections of the prostate (TUR-Ps) were different. 3) Different patient cohorts; length of follow up; availability of clinical data; number of patient samples were included in the studies. This made it difficult to draw conclusions from the available data for the prognostic significance of *TMPRSS2-ERG* fusion in clinical prostate cancer.

Two studies (23, 24) reported on *TMPRSS2-ERG* fusion in watchful-waiting cohorts by FISH analysis on tissue microarrays constructed from TUR-Ps. Both studies concluded that presence of *TMPRSS2-ERG* fusion is associated with shorter cancer-specific survival. However, in one of the studies this was only true if the mechanism of fusion was by interstitial deletion. The percentage of *TMPRSS2-ERG* fusion gene positive specimens (Demichelis *et al* 15% and Attard *et al* 30%) was rather low in both studies, possibly because both cohorts consisted of patients with low-stage disease. Moreover, both studies used FISH analysis on paraffin-embedded material, which can be technically challenging on samples with low tumour volume. Perner *et al* and Attard *et al* found that *TMPRSS2-ERG* fusion by deletion in primary tumors was correlated with earlier biochemical recurrence (23, 25). Loss of one or more of the genes in the genomic fragment between *TMPRSS2* and *ERG* with tumour suppressor potential may influence oncogenic potential and might explain a worse clinical outcome. The best candidate gene that maps between *TMPRSS2* and *ERG* might be *HMGN1*. HMGN1 alters the compaction of chromatin and has previously been described as a candidate tumour suppressor gene (26). Interestingly, *ETS2*, an ETS family member, also maps between *TMPRSS2* and *ERG*. Recently, it has been reported that *ETS2* is downregulated in prostate cancer (27). It has also been shown that ERG competes with ETS2 in a transcriptional complex including c-FOS and c-JUN (28).

Not only the loss of the genomic region between *TMPRSS2* and *ERG* has been implicated in poor prognosis of prostate cancer, also the presence of specific *TMPRSS2-ERG* splice variants has been described in this regard. Wang *et al* reported that the presence of an in frame native ATG of either *TMPRSS2* or *ERG* in *TMPRSS2-ERG* fusion transcripts is correlated with more aggressive disease (29).

In contrast to manuscripts describing an association between *TMPRSS2-ERG* and poor prognosis, Petrovics *et al* associated high *ERG* mRNA expression levels with a favourable prognosis (30). Also Saramäki *et al* correlated *TMPRSS2-ERG* fusion with longer time to PSA progression (31). We found no difference in biochemical progression-free survival between the *TMPRSS2-ERG* fusion positive and fusion-gene negative patients (Chapter 5). However, by separation of the fusion-gene positive group in *TMPRSS2(exon 0)-ERG* transcript positive samples and *TMPRSS2(exon 0)-ERG* transcript negative samples we observed that patients with *TMPRSS2(exon 0)-ERG* expression had a better biochemical progression-free survival compared to patients not expressing this transcript.

Apparently, different aspects of *TMPRSS2-ERG* fusion are important in determining its prognostic value. It is clear that for accurate establishment of the prognostic value of the*TMPRSS2-ERG* fusion gene large well-defined patient cohorts with a long follow-up are needed. Fusion gene status should be determined both by QPCR and FISH analysis.

A next issue that remains to be addressed concerns the question whether patients with other ETS fusion genes have the same prognosis as patients harbouring *TMPRSS2-ERG* fusion genes. ERG on the one hand and ETV1, ETV4 and ETV5 on the other hand

are members of different subgroups of the ETS transcription factor family, with different structural and functional properties. So, at determining prognostic value of *TMPRSS2-ERG*, other ETS fusion genes should also be taken into account and considered as separate groups.

FUNCTION OF ETS FUSION GENES IN PROSTATE CANCER

ETS transcription factors are involved in multiple biological processes, like apoptosis, cellular proliferation, differentiation, angiogenesis, tissue remodelling, metastasis and transformation (32, 33). To determine the functional role of ETS factors in prostate and prostate cancer, recently several *in vitro* and *in vivo* studies have been performed (34-39). Translation from most ETS fusion transcripts will result in the synthesis of an N-truncated ETS protein (dETS), but sometimes also full length ETS proteins will be synthesized (see also above). We found overexpression of full length ETV1 and of dETV1 (Chapter 7). Full length ETV1 protein possesses an N-terminal transactivation domain (TAD) and in the C-terminal half the DNA binding ETS domain (ETS) (40). In dETV1 protein the TAD is absent. Two other fusion gene partners, ETV4 and ETV5, are members of the same ETS subfamily as ETV1. Most likely their function is closely related to that of ETV1. ERG is member of a different ETS subfamily and might have different properties (40-42). Because overexpression of both truncated and full length ETS factors has been found, it is important to investigate whether both proteins possess the same biological properties in prostate cancer. *In vitro* biological assays showed that both truncated and full length ETS factors are able to induce migration and invasion of immortalized, non-tumorigenic epithelial prostate cells. However, we also showed that full length ETV1 is capable of stimulating anchorage-independent growth in a soft agar assay, whereas dETV1 is not. It still needs to be established whether the other full length ETS factors have the same properties. Because ETV4 and ETV5 belong to the same ETS subfamily as ETV1 and share high homology in their structural domains it is to be expected that similar results will be obtained. ERG, on the other hand belongs to a different subfamily.

In Ewing sarcomas the same ETS genes are found in EWS-ETS fusion genes. In all these fusion genes the N-terminal TAD of the ETS factor is replaced by the more potent TAD of EWS. At first it was thought that all EWS-ETS fusion proteins would behave similarly as aberrant transcription factors. However, it has been shown that there are differences in oncogenic potential between the different EWS-ETS fusion proteins (43). Whether there are differences in oncogenic potential between the different ETS fusion genes detected in prostate cancer needs further research.

Many ETS target genes have been identified to date, including invasion-associated *matrix metalloproteinases* (*MMPs*) and *uPAR*/*uPA*. Expression analysis of ETS target genes

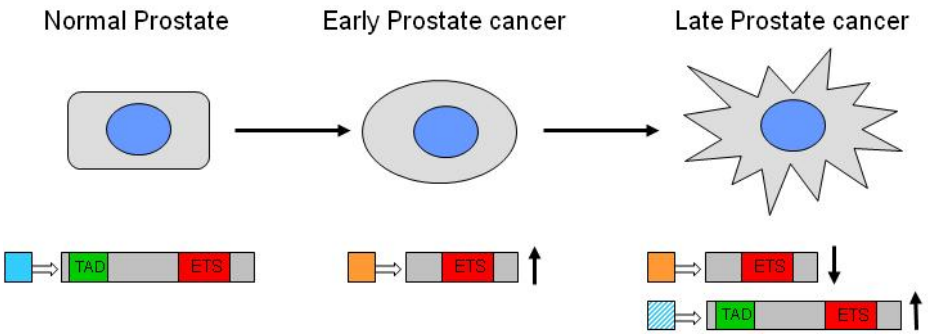

Figure 2. Model of the sequential expression of ETS genes in prostate cancer. The blue box indicates expression from the ETS promoter, the orange box a prostate-specific promoter and a hatched blue box ETS or prostate-specific promoter. TAD: transactivation domain. ETS: DNA binding domain.

has shown that *MMPs* and *uPAR*/*uPA* indeed are induced by full length ETS, but also by N-truncated ETS. However, we have shown a difference in stimulation of genes involved in integrin signalling (*ITGA3* and *ITGAV*) (35). Integrins are known to play a role in multiple processes, including metastasis, survival, proliferation and motility (44). Aberrant integrin signalling is thought to be involved in mediating the detachment of tumour cells from their neighbouring cells while providing enhanced survival and proliferative capabilities. This allows disseminating tumour cells to grow in a new, foreign, microenvironment

Thus, full-length ETS factors seem more oncogenic than truncated ETS factors in prostate cells (Chapter 7). In Chapter 4 we have shown that overexpression of full length ETS factors is detected in late stage AR negative disease, when expression of the *TMPRSS2-ERG* fusion gene is downregulated in these tumours. This indicates a role for truncated ETS factors in early stages of prostate cancer and that full length ETS factors are more important in late stages of prostate cancer progression. This hypothesis is summarized in the model depicted in Figure 2. Overexpression of full length ETS factors is also frequently detected in advanced stages and linked to metastasis of other type tumours (45, 46).

CHARACTERISTICS OF ETS FUSION PARTNERS

The most common fusion partner of ETS genes in prostate cancer is *TMPRSS2*. *TMPRSS2* is a prostate-specific and androgen-regulated gene (47). Recently, it has been shown that *ETV1*, *ETV4* and *ETV5* have, besides *TMPRSS2*, multiple fusion partners (34, 38, 48, 49) (Chapters 6 and 7). Most fusion partners have a prostate-specific and androgen-regulated expression pattern. It seems that prostate-specificity is a more important determinant

of the fusion partners than androgen upregulation, because some fusion partners are weakly induced by androgens (*EST14* and *CANT1*) or downregulated by androgens (*C15orf21*). Moreover, it is known that many prostate-specific genes are androgen-regulated, whereas many androgen-regulated genes are not prostate-specific.

Two ETS gene fusion partners, *HNRPA2B1* and *DDX5*, have a ubiquitous expression pattern (38, 50, 51). Especially the genomic locus between *HNRPA2B1* and the flanking gene, *CBX3*, is of interest. This locus contains a methylation-free CpG island, which encompasses the divergently transcribed promoters of *HNRPA2B1* and *CBX3* and possesses a dominant ubiquitously acting chromatin-opening element (52). This results in an open chromatin structure and a high and stable expression of the genes, because the promoters are resistant to transcriptional silencing. The genomic locus of *DDX5* and its flanking gene *CCDC45* seems structurally similar, containing closely spaced dual divergently transcribed promoters embedded within a large CpG island. Whether, this CpG island has the same properties as the *HNRPA2B1-CBX3* locus needs to be investigated. However, since both *DDX5* and *CCDC45* are ubiquitously expressed genes, it is tempting to speculate that this is the case.

MECHANISM OF ETS GENE FUSION

As stated above, the most important characteristics of the fusion partners of ETS genes in prostate cancer are prostate-specificity and androgen-regulation. This common expression pattern is suggestive for a similar mechanism of gene fusion. In the last few years accumulating evidence has been published that gene transcription is not random in the nucleus but that specific nuclear compartments are being formed, the so-called transcription factories (53-56). In these specific nuclear compartments genes might be expressed that are regulated by the same mechanisms. Possibly, there exist specialized prostate-specific, androgen-regulated transcription factories. Recently, it has been shown that the fusion partners in Burkitt lymphoma and plasmacytoma, *IgH* and *cMYC*, are preferentially expressed in the same nuclear regions upon *in vitro* B cell stimulation (57). In line with this observation, ETS transcription factors and the prostate-specific genes might also be preferentially expressed in the same nuclear compartments.

Because ETS fusion genes are detected in 40-70% of prostate cancer samples and in ~20% of high-grade PIN lesions (58, 59), they most likely occur early in prostate tumorigenesis and may even be an initiating event. Based on the stem cell/progenitor cell concept of tumour development (60, 61), a model for prostate cancer development is proposed (Figure 3).

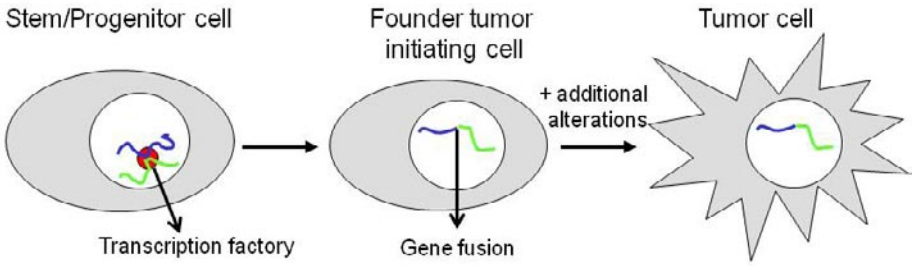

Figure 3. Model of formation of fusion genes and their role in prostate cancer development. Blue: prostate-specific gene; green: ETS gene. Red dot: transcription factory.

In this model, upon differentiation of stem/progenitor cells expression of prostate-specific genes is induced. This will lead to a more open chromatin structure of these genes, which might be more vulnerable to DNA damage. Aberrant repair of the damaged DNA can lead to gene fusions. If these fusions are with ETS genes an important step of prostate tumour development is initiated. An important issue in this model that remains to be addressed concerns the selection of ETS genes. Why are these genes selected as fusion partners? Are ETS genes selectively sensitive for DNA damage during certain stages of prostate development (renewal)? Are ETS genes indeed expressed in the same nuclear compartments as prostate-specific genes? Is fusion with ETS genes the only possibility for tumour development? Why are *ETV1*, *ETV4* and *ETV5* (and *ERG*) the fusion partners and not one of the other ETS family members?

Preliminary data obtained from transgenic mouse models indicate that overexpression of a (truncated) ETS protein is not sufficient for the formation of prostate tumours, although precursor stages are induced in some models (36, 38, 39). Additional alterations seem necessary for development of prostate carcinoma. This might also be true for human prostate cancer. An important next question that remains to be addressed is whether aberrant ETS signalling has preferential co-occurring genetic alterations in generation of prostate cancer.

REFERENCES

1. Jemal A, Siegel R, Ward E, *et al.* Cancer statistics, 2008. CA Cancer J Clin 2008;58(2):71-96.
2. Kallioniemi A. CGH microarrays and cancer. Curr Opin Biotechnol 2008;19(1):36-40.
3. Michels E, De Preter K, Van Roy N, Speleman F. Detection of DNA copy number alterations in cancer by array comparative genomic hybridization. Genet Med 2007;9(9):574-84.
4. Vlietstra RJ, van Alewijk DC, Hermans KG, van Steenbrugge GJ, Trapman J. Frequent inactivation of PTEN in prostate cancer cell lines and xenografts. Cancer Res 1998;58(13):2720-3.
5. Van Alewijk DC, Van der Weiden MM, Eussen BJ, *et al.* Identification of a homozygous deletion at 8p12-21 in a human prostate cancer xenograft. Genes Chromosomes Cancer 1999;24(2):119-26.
6. Liu W, Chang B, Li T, *et al.* Germline copy number polymorphisms involving larger than 100 kb are uncommon in normal subjects. Prostate 2007;67(3):227-33.
7. Redon R, Ishikawa S, Fitch KR, *et al.* Global variation in copy number in the human genome. Nature 2006;444(7118):444-54.
8. Katoh M, Katoh M. Recombination cluster around FGFR2-WDR11-HTPAPL locus on human chromosome 10q26. Int J Mol Med 2003;11(5):579-83.
9. Cho YG, Kim CJ, Song JH, *et al.* Genetic and expression analysis of the KCNRG gene in hepatocellular carcinomas. Exp Mol Med 2006;38(3):247-55.
10. Mertens D, Wolf S, Schroeter P, *et al.* Down-regulation of candidate tumor suppressor genes within chromosome band 13q14.3 is independent of the DNA methylation pattern in B-cell chronic lymphocytic leukemia. Blood 2002;99(11):4116-21.
11. van Everdink WJ, Baranova A, Lummen C, *et al.* RFP2, c13ORF1, and FAM10A4 are the most likely tumor suppressor gene candidates for B-cell chronic lymphocytic leukemia. Cancer Genet Cytogenet 2003;146(1):48-57.
12. Yendamuri S, Trapasso F, Calin GA. ARLTS1 - a novel tumor suppressor gene. Cancer Lett 2008;264(1):11-20.
13. Kortum RL, Johnson HJ, Costanzo DL, *et al.* The molecular scaffold kinase suppressor of Ras 1 is a modifier of RasV12-induced and replicative senescence. Mol Cell Biol 2006;26(6):2202-14.
14. Rowley JD. Letter: A new consistent chromosomal abnormality in chronic myelogenous leukaemia identified by quinacrine fluorescence and Giemsa staining. Nature 1973;243(5405):290-3.
15. Mitelman F, Johansson B, Mertens F. The impact of translocations and gene fusions on cancer causation. Nat Rev Cancer 2007;7(4):233-45.
16. Tomlins SA, Rhodes DR, Perner S, *et al.* Recurrent fusion of TMPRSS2 and ETS transcription factor genes in prostate cancer. Science 2005;310(5748):644-8.
17. Soda M, Choi YL, Enomoto M, *et al.* Identification of the transforming EML4-ALK fusion gene in non-small-cell lung cancer. Nature 2007;448(7153):561-6.
18. Choi YL, Takeuchi K, Soda M, *et al.* Identification of novel isoforms of the EML4-ALK transforming gene in non-small cell lung cancer. Cancer Res 2008;68(13):4971-6.
19. Perner S, Wagner PL, Demichelis F, *et al.* EML4-ALK fusion lung cancer: a rare acquired event. Neoplasia 2008;10(3):298-302.
20. Campbell PJ, Stephens PJ, Pleasance ED, *et al.* Identification of somatically acquired rearrangements in cancer using genome-wide massively parallel paired-end sequencing. Nat Genet 2008;40(6):722-9.
21. Korbel JO, Urban AE, Affourtit JP, *et al.* Paired-end mapping reveals extensive structural variation in the human genome. Science 2007;318(5849):420-6.

22. Ruan Y, Ooi HS, Choo SW, *et al.* Fusion transcripts and transcribed retrotransposed loci discovered through comprehensive transcriptome analysis using Paired-End diTags (PETs). Genome Res 2007;17(6):828-38.
23. Attard G, Clark J, Ambroisine L, *et al.* Duplication of the fusion of TMPRSS2 to ERG sequences identifies fatal human prostate cancer. Oncogene 2008;27(3):253-63.
24. Demichelis F, Fall K, Perner S, *et al.* TMPRSS2:ERG gene fusion associated with lethal prostate cancer in a watchful waiting cohort. Oncogene 2007;26(31):4596-9.
25. Perner S, Demichelis F, Beroukhim R, *et al.* TMPRSS2:ERG Fusion-Associated Deletions Provide Insight into the Heterogeneity of Prostate Cancer. Cancer Res 2006;66(17):8337-41.
26. Birger Y, Catez F, Furusawa T, *et al.* Increased tumorigenicity and sensitivity to ionizing radiation upon loss of chromosomal protein HMGN1. Cancer Res 2005;65(15):6711-8.
27. Rostad K, Mannelqvist M, Halvorsen OJ, *et al.* ERG upregulation and related ETS transcription factors in prostate cancer. Int J Oncol 2007;30(1):19-32.
28. Basuyaux JP, Ferreira E, Stehelin D, Buttice G. The Ets transcription factors interact with each other and with the c-Fos/c-Jun complex via distinct protein domains in a DNA-dependent and -independent manner. J Biol Chem 1997;272(42):26188-95.
29. Wang J, Cai Y, Ren C, Ittmann M. Expression of Variant TMPRSS2/ERG Fusion Messenger RNAs Is Associated with Aggressive Prostate Cancer. Cancer Res 2006;66(17):8347-51.
30. Petrovics G, Liu A, Shaheduzzaman S, *et al.* Frequent overexpression of ETS-related gene-1 (ERG1) in prostate cancer transcriptome. Oncogene 2005;24(23):3847-52.
31. Saramaki OR, Harjula AE, Martikainen PM, Vessella RL, Tammela TL, Visakorpi T. TMPRSS2:ERG Fusion Identifies a Subgroup of Prostate Cancers with a Favorable Prognosis. Clin Cancer Res 2008;14(11):3395-400.
32. Oikawa T, Yamada T. Molecular biology of the Ets family of transcription factors. Gene 2003;303:11-34.
33. Seth A, Watson DK. ETS transcription factors and their emerging roles in human cancer. Eur J Cancer 2005;41(16):2462-78.
34. Helgeson BE, Tomlins SA, Shah N, *et al.* Characterization of TMPRSS2:ETV5 and SLC45A3:ETV5 gene fusions in prostate cancer. Cancer Res 2008;68(1):73-80.
35. Hermans KG, van der Korput HA, van Marion R, *et al.* Truncated ETV1, fused to novel tissue-specific genes, and full length ETV1 in prostate cancer. Cancer Res 2008;68(18):7541-9.
36. Klezovitch O, Risk M, Coleman I, *et al.* A causal role for ERG in neoplastic transformation of prostate epithelium. Proc Natl Acad Sci U S A 2008;105(6):2105-10.
37. Sun C, Dobi A, Mohamed A, *et al.* TMPRSS2-ERG fusion, a common genomic alteration in prostate cancer activates C-MYC and abrogates prostate epithelial differentiation. Oncogene 2008.
38. Tomlins SA, Laxman B, Dhanasekaran SM, *et al.* Distinct classes of chromosomal rearrangements create oncogenic ETS gene fusions in prostate cancer. Nature 2007;448(7153):595-9.
39. Tomlins SA, Laxman B, Varambally S, *et al.* Role of the TMPRSS2-ERG gene fusion in prostate cancer. Neoplasia 2008;10(2):177-88.
40. Kurpios NA, Sabolic NA, Shepherd TG, Fidalgo GM, Hassell JA. Function of PEA3 Ets transcription factors in mammary gland development and oncogenesis. J Mammary Gland Biol Neoplasia 2003;8(2):177-90.
41. Bojovic BB, Hassell JA. The PEA3 Ets transcription factor comprises multiple domains that regulate transactivation and DNA binding. J Biol Chem 2001;276(6):4509-21.
42. Siddique HR, Rao VN, Lee L, Reddy ES. Characterization of the DNA binding and transcriptional activation domains of the erg protein. Oncogene 1993;8(7):1751-5.

43. Braunreiter CL, Hancock JD, Coffin CM, Boucher KM, Lessnick SL. Expression of EWS-ETS fusions in NIH3T3 cells reveals significant differences to Ewing's sarcoma. Cell Cycle 2006;5(23):2753-9.
44. Ramsay AG, Marshall JF, Hart IR. Integrin trafficking and its role in cancer metastasis. Cancer Metastasis Rev 2007;26(3-4):567-78.
45. Turner DP, Findlay VJ, Moussa O, Watson DK. Defining ETS transcription regulatory networks and their contribution to breast cancer progression. J Cell Biochem 2007;102(3):549-59.
46. de Launoit Y, Baert JL, Chotteau-Lelievre A, *et al.* The Ets transcription factors of the PEA3 group: transcriptional regulators in metastasis. Biochim Biophys Acta 2006;1766(1):79-87.
47. Lin B, Ferguson C, White JT, *et al.* Prostate-localized and androgen-regulated expression of the membrane-bound serine protease TMPRSS2. Cancer Res 1999;59(17):4180-4.
48. Attard G, Clark J, Ambroisine L, *et al.* Heterogeneity and clinical significance of ETV1 translocations in human prostate cancer. Br J Cancer 2008;99(2):314-20.
49. Hermans KG, Bressers AA, van der Korput HA, Dits NF, Jenster G, Trapman J. Two unique novel prostate-specific and androgen-regulated fusion partners of ETV4 in prostate cancer. Cancer Res 2008;68(9):3094-8.
50. Kumar-Sinha C, Tomlins SA, Chinnaiyan AM. Recurrent gene fusions in prostate cancer. Nat Rev Cancer 2008;8(7):497-511.
51. Han B, Mehra R, Dhanasekaran SM, *et al.* A fluorescence in situ hybridization screen for E26 transformation-specific aberrations: identification of DDX5-ETV4 fusion protein in prostate cancer. Cancer Res 2008;68(18):7629-37.
52. Lindahl Allen M, Antoniou M. Correlation of DNA methylation with histone modifications across the HNRPA2B1-CBX3 ubiquitously-acting chromatin open element (UCOE). Epigenetics 2007;2(4):227-36.
53. Branco MR, Pombo A. Intermingling of chromosome territories in interphase suggests role in translocations and transcription-dependent associations. PLoS Biol 2006;4(5):e138.
54. Meaburn KJ, Misteli T, Soutoglou E. Spatial genome organization in the formation of chromosomal translocations. Semin Cancer Biol 2007;17(1):80-90.
55. Misteli T. Beyond the sequence: cellular organization of genome function. Cell 2007;128(4):787-800.
56. Mitchell JA, Fraser P. Transcription factories are nuclear subcompartments that remain in the absence of transcription. Genes Dev 2008;22(1):20-5.
57. Osborne CS, Chakalova L, Mitchell JA, *et al.* Myc dynamically and preferentially relocates to a transcription factory occupied by Igh. PLoS Biol 2007;5(8):e192.
58. Cerveira N, Ribeiro FR, Peixoto A, *et al.* TMPRSS2-ERG gene fusion causing ERG overexpression precedes chromosome copy number changes in prostate carcinomas and paired HGPIN lesions. Neoplasia 2006;8(10):826-32.
59. Mosquera JM, Perner S, Genega EM, *et al.* Characterization of TMPRSS2-ERG Fusion High-Grade Prostatic Intraepithelial Neoplasia and Potential Clinical Implications. Clin Cancer Res 2008;14(11):3380-5.
60. Lawson DA, Witte ON. Stem cells in prostate cancer initiation and progression. J Clin Invest 2007;117(8):2044-50.
61. Maitland NJ, Collins AT. Inflammation as the primary aetiological agent of human prostate cancer: A stem cell connection? J Cell Biochem 2008.

Summary

Prostate cancer is the most common malignancy in men in countries with a Western lifestyle. Our knowledge of the molecular mechanisms underlying prostate cancer development and progression has rapidly increased over the past few years, however, many questions remain to be addressed. In this thesis the major genetic defects underlying prostate cancer development and progression are characterized.

In Chapter 1 a general introduction on genetic alterations in prostate cancer is given. By a genome-wide screen of the DNA of eleven human prostate cancer xenografts genomic alterations were identified (Chapter 2). The main focus was on the detection and characterization of novel homozygous deletions, because these are reliable landmarks of tumour suppressor genes. Eleven homozygous deletions were identified in eight xenografts, part of these deletions contain genes implicated in tumorigenesis, such as *PTEN*, *RB1* and *MKK4*. Moreover, further structural and functional analysis showed *N-COR* as a novel candidate tumor suppressor gene in prostate cancer.

In Chapter 3, chromosome 10 alterations were studied in more detail in eleven prostate cancer xenografts and four prostate cancer cell lines. We identified five homozygous deletions of the tumour suppressor gene *PTEN* and loss of one *PTEN* allele and mutation of the second allele in four samples. Loss of one copy of *PTEN* was observed in four samples. Loss of one or two copies of *PTEN* was always accompanied by loss of the distal flanking gene *FLJ11218* and often by loss of the proximal flanking genes *MINPP1*, *PAPSS2*, and *FLJ14600*.

One of the major discoveries in prostate cancer research during the last years was the detection of recurrent gene fusions. In Chapter 4, the identification and characterization of *TMPRSS2-ERG* and *TMPRSS2-ETV1* fusion genes in prostate cancer xenografts are described. *TMPRSS2-ERG* fusion transcripts were detected in five androgen-dependent xenografts and *TMPRSS2-ETV1* fusion transcripts were detected in one androgen-sensitive xenograft. *TMPRSS2-ERG* fusion was the result of an interstitial deletion or translocation as shown by array CGH and FISH analysis. Moreover, *TMPRSS2-ERG* gene fusion was detected in three androgen receptor negative xenografts, however, the fusion gene was not expressed. Instead overexpression of wild type *ETV4*, *ETV1* or *FLI1* was detected.

Transcription of *TMPRSS2* can start from two alternative first exons, exon 0 and exon 1. In Chapter 5, we determined the specific characteristics of transcripts starting at either *TMPRSS2* exon 0 or *TMPRSS2* exon 1. Both transcripts were regulated by androgens. However, *TMPRSS2* (exon 0) transcripts were more prostate-specific compared to *TMPRSS2(exon 1)* transcripts. Levels of *TMPRSS2(exon1)-ERG* transcripts in clinical prostate cancer samples were comparable, but *TMPRSS2(exon 0)-ERG* transcripts were present at very variable levels. Expression of *TMPRSS2(exon 0)-ERG* transcripts was detected in 55% of fusion-gene positive primary tumors, but, at a much lower level, in only 15% of fusion-

gene positive recurrences. In primary tumors, expression of *TMPRSS2(exon 0)-ERG* was an independent predictor of longer biochemical progression-free survival.

Besides the initial discovery of fusion of *TMPRSS2* to ETS genes, other fusion-gene combinations were discovered. In Chapter 6, the identification and characterization of unique novel *ETV4* fusion genes, *KLK2-ETV4* and *CANT1-ETV4*, is described. Both fusion partners showed androgen-regulated and prostate-specific characteristics. Overexpression of full length *ETV1* and novel *ETV1* fusion genes was detected in 10% of clinical prostate cancer samples (Chapter 7). Novel fusion partners identified were *FOXP1*, a spliced EST (*EST14*) and an endogenous retroviral repeat element (*HERVK17*). Both *EST14* and *HERVK17* had an androgen-regulated and prostate-specific expression pattern. Further functional characterization of full length ETV1 and N-truncated ETV1 (dETV1) protein revealed full length ETV1 as a strong transactivator, but dETV1 was not. Moreover, stable overexpression in immortalized non-tumorigenic prostate epithelial cells (PNT2C2) showed that both full length ETV1 and dETV1 were able to stimulate migration or invasion. However, full length ETV1 was able to induce anchorage-independent growth of PNT2C2 cells, whereas dETV1 was not. Furthermore, gene expression analysis showed upregulation of target genes involved in invasion/metastasis, like *uPa*/*uPAR* and *MMPs*, both by full length ETV1 and dETV1. In contrast, integrin β3 was clearly upregulated by full length ETV1, but much less by dETV1.

In Chapter 8 the results described in Chapters 2-7 are discussed in more detail and gaps in our knowledge are indicated. Moreover, novel concepts of molecular genetic mechanisms of prostate cancer development are proposed and future directions of research are suggested.

Samenvatting

Prostaatkanker is de meest voorkomende vorm van kanker bij mannen in landen met een westerse levensstijl. Onze kennis van de moleculaire mechanismen die ten grondslag liggen aan de ontwikkeling en progressieve groei van prostaatkanker is sinds de laatste paar jaar snel toegenomen, maar er zijn nog vele vragen die beantwoord moeten worden. In dit proefschrift zijn de meest belangrijke genetische veranderingen die een rol spelen bij prostaatkanker gekarakteriseerd.

In Hoofdstuk 1 wordt een algemene introductie gegeven van de genetische veranderingen die gevonden zijn in prostaatkanker. Door middel van een genoomwijde analyse zijn de veranderingen in het DNA van elf humane prostaatkankers, die gegroeid werden op immunodeficiënte muizen (zogenaamde xenografts), bepaald (Hoofdstuk 2). De focus was op het identificeren van nieuwe homozygote deleties in het DNA, omdat dit betrouwbare herkenningspunten voor tumor suppressor genen zijn. Er werden elf homozygote deleties gedetecteerd in acht xenografts, waarvan de meeste genen bevatten waarvan in meer of mindere mate duidelijk is dat ze een rol spelen in tumorigenese, zoals *PTEN*, *RB1* en *MKK4*. Verdere structurele en functionele analyses hebben *N-COR* als een nieuw kandidaat tumor suppressorgen in prostaatkanker geïdentificeerd.

In Hoofdstuk 3, werden veranderingen van chromosoom 10 in meer detail bestudeerd in elf prostaatkanker xenografts en in vier prostaatkanker cellijnen. We hebben vijf homozygote deleties van het tumorsuppressorgen *PTEN* geïdentificeerd. Verlies van een *PTEN* allel en mutatie van het tweede allel werd in vier monsters gevonden. Verlies van één kopie van *PTEN* in vier monsters gevonden. Verlies van een of twee kopieën van *PTEN* werd altijd gevonden in combinatie met verlies van het distaal flankerende gen *FLJ11218* en vaak ook met verlies van de proximaal flankerende genen *MINPP1*, *PAPSS2* en *FLJ14600*.

Een van de belangrijkste ontdekkingen van het genetisch onderzoek naar prostaatkanker van de laatste jaren is de detectie van fusiegenen. In Hoofdstuk 4, wordt de identificatie en karakterisering van *TMPRSS2-ERG* en *TMPRSS2-ETV1* fusiegenen in prostaatkanker xenografts beschreven. *TMPRSS2-ERG* fusietranscripten werden gedetecteerd in vijf xenografts, waarvan de groei afhankelijk is van androgenen, en *TMPRSS2-ETV1* fusietranscripten werden gevonden in een androgeen-gevoelig xenograft. Fusie van *TMPRSS2* met *ERG* is het gevolg van een interstitiële deletie of van een translocatie, zoals aangetoond door middel van array CGH en FISH analyse. Bovendien werd *TMPRSS2-ERG* fusie gedetecteerd in drie xenografts, die de androgeenreceptor niet tot expressie brachten, maar waarin het fusiegen niet tot expressie kwam. In plaats hiervan werd overexpressie van het nornale (wild type) *ETV4*, *ETV1* of *FLI1* gedetecteerd.

Transcriptie van *TMPRSS2* kan vanaf twee alternatieve eerste exonen, exon 0 en exon 1, beginnen. In Hoofdstuk 5 werden de specifieke karakteristieken van transcripten

beginnend vanaf of *TMPRSS2* exon 0 of exon 1 bepaald. Beide transcripten werden gereguleerd door androgenen, maar het niveau van expressie van transcripten, die *TMPRSS2* exon 1 bevatten, was veel hoger. *TMPRSS2(exon 0)* transcripten waren meer prostaatspecifiek vergeleken met *TMPRSS2(exon 1)* transcripten. Het niveau van transcripten van *TMPRSS2(exon 1)-ERG* was niet veel verschillend in klinische humane prostaatkanker monsters, maar *TMPRSS2(exon 0)-ERG* transcripten waren aanwezig in sterk variabele hoeveelheden. Expressie van *TMPRSS2(exon 0)-ERG* transcripten werd gedetecteerd in 55% van de primaire tumoren die het fusiegen bevatten en, met een veel lager expressieniveau, in 15% van de fusiegen positieve terugkerende tumoren, die resistent waren geworden tegen de hormonale therapie. Expressie van *TMPRSS2(exon 0)-ERG* in primaire tumoren voorspelde een langere overleving zonder biochemische progressie, onafhankelijk van andere parameters.

Naast de oorspronkelijke ontdekking van *TMPRSS2* fusie met ETS genen werden andere fusiegenen gevonden. In Hoofdstuk 6 wordt de identificatie en karakterisering van unieke, nieuwe *ETV4* fusiegenen, *KLK2-ETV4* en *CANT1-ETV4*, beschreven. Beide fusiepartners hebben net als *TMPRSS2* als eigenschappen dat ze androgeen-gereguleerde en prostaatspecifieke tot expressie komen. Overexpressie van het gehele *ETV1* gen of van nieuwe *ETV1* fusiegenen werd in 10% van klinische prostaatkanker monsters gevonden (Hoofdstuk 7). Als nieuwe fusiepartners van *ETV1* werden *FOXP1*, een twee exon EST (*EST14*) en een endogeen retroviraal repeat element (*HERVK17*) ontdekt. Zowel *EST14* als *HERVK17* vertoonden ook een androgeen-gereguleerd en prostaatspecifiek expressiepatroon. Verdere functionele karakterisering van het volledige ETV1 eiwit en het verkorte ETV1 (dETV1) eiwit toonde aan dat ETV1 een sterke activator van transcriptie was zoals gemeten met een reportergen, terwijl dat niet het geval was voor dETV1. Daarnaast liet stabiele overexpressie van het volledige ETV1 eiwit en het verkorte eiwit in geïmmortaliseerde niet-tumorigene epitheliale prostaatcellen (PNT2C2) geen verschil zien in de stimulering van migratie en invasie. ETV1 was echter in staat om "anchorage" onafhankelijke groei van PNT2C2 cellen te stimuleren, terwijl dETV1 dat niet kon. ETS doelwitgenen betrokken bij invasieve celgroei en metastase, zoals *uPa*/*uPAR* en *MMP's*, werden gestimuleerd door zowel ETV1 als dETV1. In tegenstelling hiermee werd een ander gen betrokken bij deze processen, *integrinβ3*, duidelijk opgereguleerd door ETV1, maar veel minder door dETV1.

In Hoofdstuk 8 worden de resultaten beschreven in hoofdstukken 2 tot en met 7 in meer detail bediscussieerd en lacunes in onze huidige kennis aangegeven. Daarnaast worden in dit hoofdstuk nieuwe modellen voor moleculaire mechanismen van prostaatkanker gepostuleerd en toekomstige richtingen van onderzoek aangegeven.

Curriculum Vitae

Karin Hermans werd geboren op 8 april 1976 te Boxmeer. In 1993 behaalde ze haar HAVO diploma aan het Elzendaal college te Boxmeer. Aansluitend begon ze aan de Hogeschool Venlo aan haar Hoger Laboratorium Opleiding, specialisatie technische microbiologie. Afstudeerproject werd uitgevoerd aan het VUMC in Amsterdam, afdeling pathologie onder supervisie van Marcel Jacobs en Dr. Jan Walboomers. In september 1997 begon ze haar werkzaamheden als research analiste in de groep van Prof. Dr. Jan Trapman, afdeling pathologie, Josephine Nefkens Instituut, Erasmus MC in Rotterdam. Vervolgens begon ze in juni 2004 begon ze aan haar promotie onderzoek binnen dezelfde onderzoeksgroep. De resultaten hiervan staan beschreven in dit proefschrift. Tijdens haar promotie onderzoek heeft ze een Scholar-in-training award van de American Association for Cancer Research en een travel award van de European Society for Urological Research gekregen. Vanaf september 2008 is ze werkzaam als postdoctoral fellow in de onderzoeksgroep van Prof. Dr. John Dick, University Health Network in Toronto, Canada.

List of Publications

Boormans, J.L., **Hermans, K.G.**, van Leenders, G.J., Trapman, J., Verhagen P.C. An activating mutation in AKT1 in human prostate cancer. (2008) *Int. J. Cancer.* 123, 2725-2726

Hermans, K.G., van der Korput, H.A., van Marion, R., van de Wijngaart, D.J., Ziel-van der Made, A., Dits, N.F., Boormans, J.L., van der Kwast, T.H., van Dekken, H., Bangma, C., Korsten, H., Kraaij, R., Jenster, G., Trapman, J. Truncated ETV1, fused to novel tissue-specific genes, and full length ETV1 in prostate cancer. (2008) *Cancer Res*. 68, 7541-7549

Hermans, K.G., Bressers, A.A., van der Korput, H.A., Dits, N.F., Jenster, G., Trapman, J. Two unique novel prostate-specific and androgen-regulated fusion partners of *ETV4* in prostate cancer. (2008) *Cancer Res*. 68, 3094-3098

Hermans, K.G., van Marion, R., van Dekken, H., Jenster, G., van Weerden, W., Trapman, J. *TMPRSS2:ERG* fusion by translocation or interstitial deletion is highly relevant in androgen-dependent prostate cancer, but is bypassed in late-stage androgen receptor-negative prostate cancer. (2006) *Cancer Res.* 66, 10658-10663

Verhagen, P.C., van Duijn, P.W., **Hermans, K.G.**, Looijenga, L., van Gurp, R., Stoop, H., van der Kwast, T., Trapman, J. The PTEN gene in locally progressive prostate cancer is preferentially inactivated by bi-allelic gene deletion. (2006) *J. Pathol.* 208: 699-707

Marques, R.B., Erkens-Schulze, S., de Ridder, C.M., **Hermans, K.G.**, Waltering, K., Visakorpi, T., Trapman, J., Romijn, J.C., van Weerden, W.M., Jenster, G. Androgen receptor modifications in prostate cancer cells upon long-term androgen ablation and antiandrogen treatment. (2005) *Int. J. Cancer*, 117, 221-229

Hermans, K.G., van Alewijk, D.C., Veltman, J.A., van Weerden, W., Geurts van Kessel, A., Trapman, J. Loss of a small region around the PTEN locus is a major chromosome 10 alteration in prostate cancer xenografts and cell lines. (2004) *Gene Chromosome Cancer*, 39, 171-184

Verhagen, P.C., **Hermans, K.G.**, Brok, M.O., van Weerden, W.M., Tilanus, M.G., de Weger, R.A., Boon, T.A., Trapman, J. Deletion of chromosomal region 6q14-16 in prostate cancer. (2002) *Int. J. Cancer*, 102, 142-147

Vlietstra, R.J., van Alewijk, D.C., **Hermans, K.G.**, van Steenbrugge, GJ, Trapman, J. Frequent inactivation of PTEN in prostate cancer cell lines and xenografts. (1998) *Cancer Res.* 58, 2720-2723

Dankwoord

De laatste loodjes….. het dankwoord. Een promotieonderzoek doe je niet alleen, daarom is dit het moment om iedereen te bedanken die hier op wat voor manier dan ook aan bijgedragen heeft. Ik wil beginnen met het bedanken van alle patiënten voor het afstaan van het weefsel voor onderzoek en natuurlijk alle mensen die er voor zorgen dat dit materiaal uiteindelijk ook netjes gedocumenteerd opgeslagen wordt. Want zonder dit materiaal kun je geen onderzoek doen. Dan wil ik nu een aantal mensen in het bijzonder bedanken.

In de eerste plaats wil ik graag mijn promotor, Prof. Dr. Ir. Jan Trapman bedanken. Beste Jan, bedankt voor alles wat je me de laatste 11 jaar geleerd hebt, eerst in de tijd als research analist en daarna in mijn tijd als aio. Ik wil je ook erg bedanken voor je inzet om mijn proefschrift leescommissie af te krijgen voor mijn vertrek naar Toronto. En ik weet heus wel dat ik eigenwijs ben….

Vervolgens wil ik ook Guido Jenster bedanken voor de prettige samenwerking en leerzame adviezen. Je overweldigende enthousiasme voor het onderzoek is een grote inspiratie.

Daarnaast wil ik natuurlijk alle leden van de leescommissie en grote commissie bedanken. Bedankt voor jullie interesse in mijn promotieonderzoek en voor al het advies en goed raad!

Joris Veltman, Ad Geurts van Kessel en de mensen in het lab in Nijmegen, bedankt dat jullie mij de ins en outs van array CGH bijgebracht hebben.

Hetty, bedankt dat je m'n paranimf wilt zijn, ondanks dat je altijd hebt geroepen dat je het niet meer doet. Verder, wil ik je enorm bedanken voor je hulp en steun zeker het laatste jaar! We waren een goed team.

Delila, tak! We have only been together in the lab for one year, but it was a fun time. Thanks for being my 'paranimf'. Good luck and I know you can do it!

Ook wil ik Angelique even noemen, na de 11 jaar die we samen in het lab 'rondgehangen' hebben. Bedankt voor de hulp en gezelligheid! Verder wil ik alle mensen van lab Be320, die ik door de jaren heen heb zien komen en gaan, bedanken voor alle hulp en gezelligheid.

Dan wil ik iedereen van het JNI bedanken. Bij veel van jullie ben ik wel eens langs geweest voor advies, hulp, of om iets te lenen/gebruiken. Dit geldt zelfs voor een aantal mensen uit de 'hoogbouw'. Waar zou ik zijn zonder jullie! Bedankt!

Ik wil mijn 'treinmaatjes' bedanken voor de gezellige treinritjes naar Rotterdam elke ochtend, geen tijd voor een ochtendhumeur. Helaas, geen treinritjes meer hier in Toronto....., maar een wandeling van vijf minuten naar het werk heeft ook z'n voordelen.

Vervolgens wil ik ook mijn familie en vrienden bedanken voor hun interesse in mijn promotieonderzoek. Hoewel, het meestal nogal moeilijk te begrijpen was wat ik nu precies deed. Ik hoop dat het nu jullie mijn boekje hebben, wat duidelijker is.

Tot slot wil ik mijn ouders en zusje in het bijzonder bedanken. Bedankt voor jullie steun en vertrouwen in mij. Ik weet dat Canada ver weg is, maar het is niet het eind van de wereld. En tot nu toe geniet ik met volle teugen van mijn nieuwe avontuur hier in Toronto!

Dus voor de laatste keer BEDANKT iedereen!!!!!

-x- Karin